Ontogeny of the enteric nervous system

Franck Boismoreau

PSL
UNIVERSITÉ PARIS

THÈSE DE DOCTORAT
DE L'UNIVERSITÉ PSL

Préparée à l'Ecole Normale Supérieure

Ontogénie du système nerveux entérique

Soutenue par
Franck BOISMOREAU
Le 30 Novembre 2020

Ecole doctorale n° 158
Cerveau, Cognition, Comportement

Spécialité
Biologie du développement

Composition du jury :

Jeanne, AMIEL PUPH, Institut Imagine	*Présidente*
Ulrika, MARKLUND DR, Karolinska Institutet	*Rapportrice*
Hermann, ROHRER PE, Center for Neuroscience Frankfurt	*Rapporteur*
Jean-François, BRUNET DR, IBENS	*Directeur de thèse*

ENS | PSL

Acknowledgments

Thank you to Jean-François for having welcomed me in your lab firstly for my master intership and then for these 4 years of PhD, for being present, for your advice, help and guidance through this long and complicated journey with the animals, the pandemic and the science.

Thank you Christo for your time and help at any moment and about any scientific topics.

Thank you Mamie Zouzou for your help, your presence, your conversations and your kindness in the lab.

Thank you Isa (aka Mama), it's been such a pleasure to meet and work with you. Thank you for your support in the lab, and thank you for still being present since you left, to keep on helping me and giving me advices. Nothing would have been the same without you. Muchas gracias Mama !

Thank you Fan Di, you've been my little sister in the lab even if you were older. Thank you for your kindness, your sweetness and for being always positive and supportive doesn't matter what happened. You've been a great example on how to be always cheerful. 謝謝 !

Thank you Orthis, we had each other's back for quite a long and we've had great moments.

Thank you Maïlys, you are as well my little sister in the lab, at least you're really younger than me. Hi Sisters! Thank you for being here in the happy moments but above all during the bad ones, the complicated ones, you've helped and supported me through winds and rains. I met someone as talkative as I am, with too many common interests and love. Thank you! Merci! Gracias! Danke!

Thank you to all the other current members of the lab, Renaud, Gilles, Selvee and Bowen; you've all helped me on your own way.

Thank you Esmee for working with me on my projects, I know now that it wasn't always good or motivating, but we've done it.

Thank you Maria for being my best intern I've ever had. You've certainly been singing and dancing too much in the lab, but you've helped me a lot as well.

Thank you Ioana, my forever friend. I wish I could invent a word greater than thank you to express everything you've meant and mean to me on this journey, you are an amazing woman and scientist. Thank you for the time talking, smoking, drinking tea/coffee, being on the phone, etc. This list is as long as the process to be French, and you're rocking it as well. Thanks a lot. Mulțumesc!

Thank you Gonzalo, my baby, my love. You've had too many nicknames in not enough years together. Nothing would have been the same without you. A minha comunidade e eu te amamos muito. Gracias.

Thank you to all the other past and present members of the 7th or 5th floor depending and when you joined: Kamal, Alciades, Rosette, Evelyn, Bridlance, Akinde, Hugues, Ludmilla, Morgane, Alexia, Olivier, Raphael, Marie, Nathalie S, Xavier, Sonia. It's been a pleasure to meet and talk with all of you.

Thank you Touzalinette, you've been such a pleasure to work with, my mice couldn't dream of a better person be assist them. You're a little woman with such a big heart.

Thank you Gwendoline for your help with the mice as well. I know I wasn't so easy to work with but we've adapted to each other and it's been efficient.

Thank you to all the other members of the Team Animalerie, Amandine, Dolores, Deborah, Abder and Matthieu ; you've each helped me at a moment.

Thank you to all the other members of IBENS for a few seconds/minutes/hours of conversation.

Thank you Sasha, my Husbie. You are the Trixie to my Katya and I think this sums up everything. You've never been aware of how importantly you've helped me doing this.

Thank you RuPaul for teaching me that I never dream too big and be proud of itself is the most important thing on Earth.

Thank you Cher for your unconditionnal presence by my sides from the first to the last day of this PhD. You've help me to Believe that I was Stron Enough. You are Eternal.

Thank you to my parents and my sister that supported me outside of the lab, I've been often absent but it was always good to go back home at any possible hour of the day or night. Thank you for pushing me to do what I wanted and be always proud of me, my choice and my thesis (that you may not understand, I'm sorry about it).

Thank you Bryan, you came at almost the end, aka the worst time; but you made it easier, brighter and so much better. Thank you for your love and your support. Thanks a lot for being my half.

Thank you to all the people who talked with me.

Thank you to all the people who laughed with (or at) me.

Table of contents

Introduction

1. GENERAL INTRODUCTION

The enteric nervous system (ENS) is the largest division of the autonomic nervous system, containing as much neurons as the spinal cord. It is capable of controlling the function of the gut (propulsion of the alimentary bolus and secretions of hormones), in isolation, even though the central nervous system can influence it. For this reason, and because it contains a large variety of neurotransmitter, like the central nervous system, including serotonergic and dopaminergic neurons, it was famously called the "second brain".

For some reason the study of this second brain has lagged behind that of the first, even though its study started in the XIXth century (Auerbach and Meissner, discoverers of the eponymous plexi, died in 1897 and 1905 respectively). One reason is that mouse as a model, and the genetic tools that were developed for it, have only slowly been adopted by the field, while guinea pig, a major original main model was still largely used during the 1990's to explore the structure of the ENS. Possibly the main reason however, is that the peripheral nervous system, unlike the central one, as little spatial organization. The main paradigm to explain the formation of the CNS, i.e. the patterning of the CNS anlage along a grid of cartesian coordinates, on the rostro-caudal and dorso-ventral axis, which has been so successful over the past 30 years, seems largely irrelevant in the ENS. The only spatial structure that can be detected there is the division in two plexi (myenteric and submucosal) and the grouping of neurons in ganglia, more or less regularly spaced. However, the size of these ganglia is varied, no ganglion is distinguished from others so far by its constituent cell type, and no spatial organization of the cell types in the ganglia is evident. This apparently random organization and the lack of groupings of cell types (as they are in the CNS in the form of nuclei), has probably played a role in delaying the description of the ENS in terms of constituent neuron types. The identification of neural-type specific transcription factors (which are not only markers but in many cases presumably determinants), which started for the CNS in the early 1990's (with to this day hundreds of transcription factors involved in neuron-type specification, most prominently in the spinal cord, hindbrain and cortex), has barely started for the ENS, helped by the advent of next generation sequencing and single cell transcriptomics.

My PhD has focused on the ontogeny of the ENS, except for a contribution to a study of the sacral autonomic outflow which established, on the basis of developmental genetics, that it is affiliated to the sympathetic rather than parasympathetic nervous system, as was though since the beginning of the XXth century. I contributed to describe gene expression in the preganglionic cells that project in the pelvic nerve, and show that they are indistinguishable from the thoracolumbar, i.e. sympathetic ones, in their expression of several transcription factors (**Article 1**). It is one the best

arguments to claim that the sacral outflow is sympathetic, even though most of the debate and controversy has subsequently focused on the targets of these neurons, the pelvic ganglion (e.g. (Horn, 2018; Neuhuber et al., 2017)). Unfortunately, preganglionic neurons are relatively rare and embedded in the spinal cord, thus difficult to study with a single cell transcriptomics approach, such as is currently used in the lab to further investigate the cell identities in the pelvic ganglion.

I then contributed to a revision of the way in which the neural crest invades the gut to form the ENS. The main neural crest source for the ENS has long thought to be the so-called "vagal crest", a more modest contribution being the sacral crest. We examined the "vagal crest" in more detail and found that this term is suited only for part of it: the crest that faces somites 1 and 2, thus the roots of the vagus nerve, and that this crest actually migrates along the vagal nerve (in the same way as parasympathetic precursors do along other cranial nerves) to invade exclusively the esophagus and antral stomach. On the other hand, the crest facing somites 3 to 7, classically lumped together with the vagal crest, has no relation to the vagal nerve and migrates ventrally directly into the foregut mesenchyme. On its way, it contributes to the superior-cervical ganglion, so that we called this crest "sympatho-enteric". This term was criticized by M. Gershon for "implying that the ENS may be considered to be a component of the sympathetic nervous system" (Rao & Gershon, 2018), in the same way that we claimed that the sacral autonomic outflow was sympathetic (see above), which was also criticized. But this is not the case. In our paper, the term "sympatho-enteric" refers to the neural crest, not the part of the nervous system that it forms, and means that collectively this crest has two fates, sympathetic and enteric (and no relationship with the vagus nerve, hence is not "vagal"). Possibly a better term would have been "trunk crest". My contribution was to examine the fate of the of S1-S2 and S3-S7 grafts from a GFP transgenic chicken onto a wild type one, to show the differential contribution to the gut.

Going further in the analysis of the development of the ENS, I then contributed, on the same paper, to establish the role of the ErbB3/Nrg1 signaling pathway in the development of the ENS showing that its absence leads to a gradient of depletion from the duodenum to the colon of respectively 75 to 50% (**Article 2**). After that, as Nrg1 was already known to be a co-factor of Ret in the human genetic of Hirschsprung disease, I wondered and tested if a similar mechanism could exist between ErbB3 and Ret where ErbB3 mutation would worsen Ret effects with a mouse model.

I then started studying the role of three transcription factors in the formation of the ENS. First *Hmx2* and *Hmx3*, which are markers of both the parasympathetic ganglia and the ENS. I engineered three knockouts (*Hmx2*, *Hmx3*, and *Hmx2/Hmx3* double KO) using CripsR:Cas9. I recount this experience, and how surprisingly difficult it actually was to get a clean knockout with this technology which just received the Nobel Prize, as a part of my results in this report. I found that even in the double *Hmx2/Hmx3* KO, the ENS and the parasympathetic ganglia are present, but I could

not characterize these lines in more detail so far, and I actually might have lost these three lines because of the pandemic.

I also created a conditional KO of *Tbx3*, using an existing *Tbx3*$^{lox/lox}$ allele combined with a *Phox2b::Cre* allele previously generated some time ago in the lab. The study of the ENS in these conditional knockouts makes up the main part of the result section of this report.

As an introduction, I will review the development of the ENS, emphasizing aspects that seem more relevant to the data I obtained.

2. DEVELOPMENT OF THE ENTERIC NERVOUS SYSTEM

I. Overview of the development of the ENS

The ENS ganglia are formed, just like sympathetic and parasympathetic ones, by neural crest cells (NCC) (Le Douarin et al., 1981; Nagy & Goldstein, 2017). Even if most of modern research is made on mice and zebrafish (Ganz, 2018; Obata & Pachnis, 2016), the original studies on the development of this system were made in chicken, originally by ablation experiments (Yntema & Hammond, 1954) and then by quail-chicken xenografts (Douarin & Teillet, 1973) to discover that the cells of the enteric nervous system are derived from neural crest cells at two rostro caudal levels: so called “vagal neural crest”, adjacent to somites 1-7, and the sacral crest ((derived from the neural tube posterior to somite 28). The concept of “vagal neural crest” was recently revisited (Isabel Espinosa-Medina et al., 2017) and it appeared that only NCC at the level of somites 1-2 deserve that denomination, because they are in register with the roots of the vagal nerve and migrate along the nerve itself, like precursors of the parasympathetic ganglia were previously shown to do ((I Espinosa-Medina et al., 2014), while NCC facing somites 3-7 have no relation to the vagal nerve, participate in the formation of the superior cervical ganglion (the rostral-most ganglion of the paravertebral sympathetic chain) and continue their ventral migration pathway beyond the dorsal aorta to enter the foregut: they are better viewed as post-vagal (i.e. cervical) or “sympatho-enteric” crest. The vagal crest proper invades only the esophagus and oral stomach, while the cervical or sympatho-enteric crest invades the entire length of the digestive tube.

The process of ENS formation starts at E8.5 in mouse, when the neural crest cells delaminate from the neural tube, and invasion of the digestive tube starts at E9.5 (Anderson et al., 2006). These cells migrate along the tube caudally (Allan & Newgreen, 1980; Young et al., 2004) and this migration, while the gut itself is still growing, is thought to be fueled by proliferation (Landman et al., 2007), at a speed which reaches 35µm/h (Young et al., 2004). At the level of the cecum, where the gut forms a loop, the mode of migration shifts from following the length of the gut to a trans-mesenteric short-cut that bypasses the cecum, and cells directly start to colonize the hindgut – from cecum to the rectum (Nishiyama et al., 2012). At least to the cecum itself, the migration of the NCC is guided by a gradient of Glia Cell Line-Derived Neurotrophic Factor (GDNF) with a maximum of expression in the cecum (Natarajan et al., 2002; Young et al., 2001). Its expression starts as soon as E9.5 in the stomach and at E10.5 in the cecum before establishing a gradient between both regions. In addition, GDNF has a role in increasing the proliferation rate of NCC, as shown in vitro where GDNF can double the proliferation rate (Hearn et al., 1998). This factor also help to maintain cells in

an undifferentiated condition: in the absence of GDNF the pool of progenitors is depleted by precocious differentiation and as a consequence the hindgut is not properly colonized (Gianino et al., 2003). GDNF acts through its receptor GFRα and the co-receptor Ret, a tyrosine kinase (Robertson & Mason, 1997), expressed at the surface of enteric NCC (Enomoto et al., 1998; Pachnis et al., 1993), while the ligand GDNF is expressed in the mesenchyme of the gut (Trupp et al., 1995). Inactivation of GDNF, GFRα or Ret leads to massive depletion of enteric ganglia, in most or all the length of the gut (Uesaka et al., 2008; Enomoto et al., 1998; Moore et al., 1996).

Other signaling pathways involved in ENS formation include G-protein coupled receptors (GPCR), and among them the endothelin receptor B (EDNRB) with its ligand endothelin-3 (EDN3), revealed by the study of knockout mice (Baynash et al., 1994; Hosoda et al., 1994) :these two mutants show an aganglionosis with an upstream formation of a megacolon. An interaction between the EDNRB and Ret pathways lead to a more severe phenotype, at least in a mouse model (McCallion et al., 2003). The receptor EDNRB is expressed by the NCC (Nataf et al., 1996), and its ligand, EDN3, is expressed in the mesenchyme (Leibl et al., 1999). EDN3 has a spatiotemporal specific expression appropriate to guide the NCC to their intermediate target organs one after the other, firstly the skin, then in the branchial arches and finally in the digestive tract (Nataf et al., 1998). This signaling pathways is also involved in survival, proliferation, migration and differentiation (Bondurand et al., 2018; Lahav et al., 1998; Wu et al., 1999).

Finally, a third signaling pathway has emerges as involved in the ENS development: the ErbB3/Neuregulin1 (Nrg1) pathway. Nrg1 belongs to the EGF-like signaling molecules. It was already known to be essential for the development of parasympathetic and sympathetic ganglia (Britsch et al., 1998; Dyachuk et al., 2014). The receptor ErbB3 is expressed by the NCC, while its ligand Nrg1 is expressed at the surface of the axons (Britsch et al., 2001; Perlin et al., 2011), as well has another source, likely to be the mesenchyme, which provide secreted isoforms of Nrg1 (Birchmeier, 2009; Birchmeier & Nave, 2008). Its absence leads to a gradient of atrophy along the ENS from to duodenum to the rectum with a loss from 75 to 50% (Isabel Espinosa-Medina et al., 2017b).

The second major source of cells of the ENS is the sacral neural crest, delaminating at the level of somite 28 and below, mostly responsible for colonizing the hindgut (Burns & Douarin, 1998). These sacral NCC first form the pelvic ganglia (Serbedzija et al., 1991), and then a sub-population continue to migrate along the pelvic nerve to reach the rectum at E13.5 (Wang et al., 2011) and start a rostral migration through the hindgut where they encounter and mix with the caudally migrating cervical (formally vagal) neural crest cells. These sacral neural crest cells never go further than the umbilicus (Burns & Douarin, 1998), even if in the absence of the caudally migrating cervical population (Burns et al., 2000). With the redefinition of the pelvic ganglia as sympathetic (I. Espinosa-Medina et al., 2016) (which means that there is no longer any reason to call the sacral crest

"parasympathetic"), the distinction of the "sympatho-enteric" neural crest (Isabel Espinosa-Medina et al., 2017) from the vagal, and the newly recognized contribution of trunk Schwann cell precursors to the ENS (Uesaka et al., 2015), it appears that from the cervical level to the sacral, the neural crest has a dual fate, sympathetic and enteric.

This whole process initially form the myenteric plexus of the ENS; later a portion of these cells start a second wave of migration, this time in the radial direction, to go deeper in the wall of the gut, toward the mucosa, and form the submucosal plexus (McKeown et al., 2001). Because of this delayed process, the differentiation of the neurons of this plexus is shifted in time: whereas the first differentiated neurons are visible at E10 in the myenteric plexus, they appear only at E14 in the submucosal plexus (Pham et al., 1991). An intriguing evolutionary complication is that in the hindgut of the chick, the neurons from a sacral origin firstly form the submucosal plexus and then effectuate a radial migration to form the myenteric one (Burns & Douarin, 1998). In zebrafish the submucosal plexus is missing altogether (Holmberg et al., 2003).

II. Regulation of neuron numbers in the ENS

II.A. Embryonic proliferation and death

The enteric neural crest probably represents one of the most proliferative cell populations during embryogenesis, since a small number of crest cells (albeit not precisely quantified to my knowledge) at vagal, cervical and sacral level gives rise to a number of neurons equivalent to that in the spinal cord (Furness et al., 2014). However, the exact extent and pattern of cell division during ENS formation is incompletely understood.

Initial size of the pre-enteric population is essential for ENCC migration as demonstrated after partial ablation of the neural crest that leads to reduced speed of the wavefront (Young et al., 2001) and distal agangliosis of the GI tract (Barlow et al., 2008; Burns et al., 2000; Druckenbrod & Epstein, 2005), which could be relevant to the common developmental defect observed in Hirschsprug disease (see below). An even more compelling demonstration that the number of pre-enteric neural crest cells is essential to generate a pool big enough to colonize the whole gut was obtained by back transplanting one-somite length of neural crest in chicken embryos where the crest facing somites 3-6 had been removed. Unexpectedly, this operation restored colonization of the entire gut even in cases where the graft itself could not participate in the colonization per se (i.e. if it was taken at thoracic level), but presumably restored an adequate population pressure in migrating neural crest prior to its entrance in the gut (Barlow et al., 2008).

Conversely, if apoptosis is blocked early on, by electroporation of an inhibitor, thus presumably in pre-enteric crest, the mature ENS is hypertrophic (Wallace et al., 2009), with an increase in the number of ganglia rather than of their size, in the midgut – from duodenum to the caecum – and hindgut. Incidentally, this study revealed an unexpected level of apoptosis in the early migrating crest.

The GDNF gradient also has a function in the regulation of neuronal numbers: it increases the proliferative capacities of cells, and in absence of GDNF the pool of precursors differentiate before reaching the caecum, the point of highest GDNF concentration in the gut (Gianino et al., 2003). The wavefront of migration is composed of progenitors that are dividing at the same time as migrating, but once a segment of the gut is colonized the proliferation occurs only in 4% of the cells, while the other cells are differentiating into neurons – expressing HuC/D – or even into mature neurons – expressing such specific neurotransmitter as Nitric Oxyde Synthase (NOS) (Young et al., 2005).

While the highly proliferative ENCC wavefront migrates into unpopulated gut regions, less proliferative rearguard cells populate already colonized regions by migrating non-directionally (Theveneau & Mayor, 2011). The previous studies mostly focused on the colonization of the distal bowel, but the early migration from the neural tube to the foregut is still poorly understood.

The first extensive study of the pattern of cell division in the ENS is very recent (Lasrado et al., 2017). It makes use of lineage analysis with the confetti reporter or the MADM complementation system. Recombination of these reporters were triggered at E12.5 to show the following: i) cells did not migrate extensively once they were behind the wave front; ii) they formed a mosaic of overlapping clones; iii) their degree of dispersion was proportional to the number of divisions and best explained by a model where neuronal progenitors intermingle with unrelated dividing cells of the mesenchyme; iv) cell fate decisions occurred at the last or penultimate division; v) formation of ganglia in the submucosal plexus was by descendants of myenteric precursors situated immediately radial to them; vi) Clonal analysis of Ret^{-} cells showed that decrease in Ret signaling cell-autonomously favors proliferation over neuronal differentiation (i.e. leads to larger clones containing fewer neurons and more glia).

A limitation of this study is that it was performed at a time when most of the gut is colonized, and a lot of proliferation has already occurred, and might thus explain the favored proliferation in absence of Ret. It would be interesting to repeat this analysis of clonal architecture of the ENS at earlier time points, to better understand the lineage of the ENS. However, image analysis of colored clones might be more challenging, if too many clones become intermingled.

II.B. Post-natal proliferation and death

The development of the ENS continues during post-natal life, including neurogenesis and neuronal differentiation, so that the birth of the animal might be considered as a somewhat arbitrary time point during ENS development. This is a debated topic however, and rather confusing in its details. I use the occasion of this report to try and clarify the literature on the subject. I will distinguish evidence concerning i) the number of neurons at different post-natal ages, ii) cell division and iii) cell death.

II.B.1. Evolution of the number of enteric neurons after birth

Gabella (1971), referring to the papers by Altman & Das (1965) and collaborators which famously put an end the "no new neuron" dogma in the central nervous system, sought evidence for the same phenomenon in the ENS. The author counted the density of neurons in the myenteric plexus of the small intestine of rats (i.e. the number of neurons per mm^2 of intestinal wall) in the newborn rat and the adult (6 months old) rat. After correction of this number by the enlargement of the gut wall during the same time window, an increase in neuronal numbers was estimated, from 420,000 to 1, 850,000, i.e. 4.4 fold. This would mean that around 75% of the enteric neurons found in the adult are born postnatally (during an unspecified time window between P0 and 6 months). This spectacular level of neurogenesis seems to have been neither contradicted nor confirmed by later studies and, to the best of my knowledge, the paper has not been cited for this piece of evidence in several decades.

In apparent contradiction Marese et al. (2007) found a stable number of neurons from 21 days-old rats to 60 days-old rats, albeit redistributed on a larger surface. However, this study leaves unexplored a time-window from P0 to P21, which is when the massive increase reported by Gabella could conceivably have taken place.

Liu et al. (2009) report an increase in neuronal density in the first 4 months after birth in wild type mice, by 20% (contrary to Gabella, who found that the surface of the gut increased more than the number of neurons, thus that there was a decrease in density). The total size of the intestine was not taken into account in that study and the Methods section is clear that the total number of neurons was not calculated. Thus, if the size of the gut wall increases between P0 and P120, which is

likely, it is possible that the increase in total cell numbers after P0 is much larger than 20% increase in density. In line with this possibility, the authors also report direct detection of neurogenesis (discussed below).

I could not find published evidence for the evolution of neuronal numbers during most of the adult life. Kulkarni et al. (2017) mention that the "numbers of enteric neurons in the healthy adult rat remain remarkably constant for most of adult life" with a reference to Gabella, which contains in fact only one sentence on that topic in the discussion: "*the number of nerve cells seems only slightly reduced, if at all, in rats more than 1 year old*", not illustrated by any data or reference.

On the other hand, a large literature has been devoted to enteric neuron loss in the aging animal by up to 50%. (Marese et al., 2007; Thrasivoulou et al., 2006) provide references for studies in the myenteric plexus of rats, mice, guinea pigs and humans, with evidence that cholinergic neurons are more affected than nitrergic ones. Thrasivoulou et al. (2006) show that caloric restriction, of the type that prolongs the life of rats by 40%, completely prevents this neuronal loss.

II.B.2. Evidence for ongoing neurogenesis

Early postnatal stages and juveniles

Gabella is probably the first to discuss this question, without providing original data, however. The author deduces a requirement for neurogenesis after birth from considering *i)* the need to generate new neurons in the young adult (i.e. to account for the massive increase in neuronal numbers during the first 6 months of life he reported, see above), *ii)* electron microscopy evidence of neuronal death (from the authors, but unpublished), despite *iii)* stability of the number of neurons in adults (with no data or no reference on the subject, see above). Speculations on the mechanism of neurogenesis are accompanied by ancient references (back to the 1920's and 1930's), with the underlying idea that a persisting pool of progenitors would explain the increase in neuronal numbers in juveniles and their stability in adults, while its exhaustion would explain neuronal loss in aged animals.

Pham et al. (1991), might be the first to report direct evidence for significant levels of neurogenesis until P30, mostly in the submucosal plexus, by administration of tritiated thymidine during 24 hours, at ages ranging from E8 to P21, and detection of the label at P30. Only the cells that are about to withdraw from the cell cycle at the time of labeling can retain the label by this method.

Detection of incorporated H^3 was combined with that of the neurotransmitter phenotype: serotonergic, cholinergic, and peptidergic (including *Vip*, *Enk*, *Npy* and *Cgrp*). Different dynamics of cell birth (i.e. withdrawal from the cell cycle) were detected for different phenotypes. Cholinergic and serotonergic neurons were all born before birth, as well as *Vip*, *Enk* and *Npy* neurons of the myenteric plexus. In contrast, a large fraction of *Vip*, *Npy* and *Cgrp* neurons of the submucosal plexus were born after birth. (These data were interpreted as arguing for an influence of early differentiating neurons on later ones, although they do not rule out the existence of separate lineages each with its intrinsic dynamic).

Two decades later, the same lab, (H. Wang et al., 2010), could detect BrdU incorporation (i.e. neuronal birth) a few hours after treatment, at stages ranging from P0 to P8, in different part of the digestive tube, accounting for a proportion of total PGP9.5+ cells (i.e. neurons) ranging from 16% in submucosal plexus of the colon at P8 to 2% for the myenteric plexus of the small intestine at P8.

By a completely different approach, Laranjeira et al. (2011) evaluated the number of neurons in an adult mouse that were born from *Sox10*$^{+}$ progenitors present at several embryonic and postnatal stages, using lineage tracing with a tamoxifen inducible Cre transgene driven by the *Sox10* promoter (*Sox10::Cre*^{ERT2}). The main finding was that, although large amounts of neurons in the adult ENS are born from progenitors present at E8.5 or E12.5, very few ((2.8%) are born from *Sox10*-positive progenitors present at P0, even fewer (1.6%) from progenitors present at P30 (those being presumably included in the former), and none from progenitors present at P84 (6 months). So that, for all practical purposes, no neurogenesis from *Sox10*$^{+}$ cells present at post-natal stages would contribute to make-up the adult myenteric plexus. These findings are hard to reconcile with the massive increase in neuronal numbers proposed by Gabella, or even the increase in cell density described in Liu et al. (2009), and are even substantially lower than those reported by Wang et al. (2010), but the different experimental designs prevent direct confrontation of the data. Possible caveats of the Laranjeira study are: *i*) the possibility that neurons generated postnatally would undergo a massive turnover, while those born in the embryo would last for the life of the animal, but this is unlikely. *ii)* the possibility that postnatal progenitors do not express *Sox10* (see below). *iii*) The possibility that the efficiency of recombination of the reporter transgene dramatically goes down with age (see below).

Finally, Uesaka et al. (2015), taking for proven the existence of a postnatal neurogenesis, with references to Pham et al. (1991), Wang et al. (2010) and Laranjeira et al. (2011) (despite the low level reported by the latter, see above), explore a possible mechanism for this neurogenesis. The

authors propose that one of its sources are Schwann Cell Precusrors (SCPs) of the extrinsic nerves of the gut. By lineage tracing SCPs with a *Cre* driven by the immature SCP marker *Desert Hedgehog* (*Dhh*) and a reporter gene for enteric neurons (a conditional knock-in of *GFP* in the *GFRα* locus), they show that about 5% of the submucosal ENS of the small intestine, and 20% of both myenteric and submucosal plexi of the colon are made of descendant of SCPs. Conversely, the destruction of these cells by a conditional mutation of *Ret* depletes the distal colon by about 30% of its neurons. Importantly for this discussion, SCP-derived neuronal precursors start acquiring neuronal features (expression of tyrosine kinase *Ret* and the neuronal marker *PGP9.5*) at P1 and all of them are Ret^+ and $PGP9.5^+$ at P21, so that neuronal differentiation from SCPs is post-natal. However, this observation cannot ascertain the birth date of these cells, so does not quite answer the question of postnatal neurogenesis per se, only of neuronal differentiation.

Adult animals

There is an abundant literature, spanning from 1913 to 1993, rather inconclusive in the aggregate, that documents the state of the myenteric plexus upstream of an experimentally induced stenosis, or after denervation by means of benzalkonium chloride (BAC) (reviewed in (Geuna et al., 2002)). Some authors have described addition of new neurons, others (like (Gabella & Trigg, 1984)) have denied it and found only an increase in the size of neurons, still others described DNA synthesis attributed to induction of polyploïdy but not followed by cell division, others yet have proposed the addition of new neurons without cell division, thus presumably by late induction of differentiation of post-mitotic precursors, in particular in the vicinity of the mesenteric nerves.

This line of research has been reactivated more recently, probably inspired by the revival of the question of postnatal neurogenesis in the central nervous system initiated by Altman et al. (see above) (although debate is ongoing on that subject) and also fueled by the hope that one could isolate stem cells from the ENS of adult animals that were earlier shown to generate neurons in vitro (Burns et al., 2004; Joseph et al., 2011; M. Kuwahara et al., 2004; Mosher et al., 2007; Takaki et al., 2006), and use them for cell replacement therapy of Hirschprung disease.

Liu et al. (2009) reported that they call “the first demonstration of adult enteric neurogenesis”, in wildtype animals treated with agonists of the 5-HT_4 receptor. BrdU was taken up by extra-ganglionic cells which, over the course of several weeks, integrated the myenteric ganglia.

The subject was then taken up by Joseph et al. (2011), whose study examines two topics: the in vivo source of the cells that are well-known, in vitro, to give rise to self-renewing enteric neural

crest stem cells (eNCSCs) (Kruger et al., 2002; Mosher et al., 2007); and the assessment of their actual progenitor role in vivo. The latter point is explored by several weeks-long pulses of BrdU, followed by chases ranging from 2 weeks to 6 months, at ages ranging from P30 to P120, in a broad — indeed extraordinary — variety of normal and pathological conditions: normal young adults, old adults, pregnant rats, hyperglycemic rats, rats undergoing dietary changes, mice undergoing voluntary exercise, mice with gut inflammation due to bacterial infection or chemical treatment, rodents with focal ablation of the myenteric plexus due to topical BAC treatment, *Gfap-tk* mice after ablation of enteric glia, and rats with osmotic minipumps that released growth factors into their peritoneum. The presence of labeled cells — that is, which were born during or shortly after the BrdU pulse — was assessed at various ages afterwards. Even though the exhaustiveness of this study was clearly driven by the hope of finding adult enteric neurogenesis, no BrdU+ cell was ever detected except in one animal during an injury scheme, in a non-reproducible fashion. A caveat of this experiment is that if newly born cells have very short life time and are constantly replaced they would not be detected weeks after their birth (see below).

Joseph et al. (2011) also addressed the old idea that neurogenesis could occur by neuronal differentiation of enteric glia, without cell division (i.e. impossible to detect by BrdU incorporation). For this, they employed a lineage tracing scheme with a *Cre* driven by the promoter of *Glial Fibrillary Acid Protein* (*GFAP*) and a *Cre*-dependent reporter gene. *GFAP* was chosen because the vast majority of enteric glia is *GFAP*-positive and because in vitro neurogenesis by isolated ENS cells occurs from $GFAP^+$ cells. A very limited proportion of YFP^+ neurons were found that corresponded to neuronal differentiation from $GFAP^+$ cells soon after birth, but no further additions of YFP^+ neurons occurred later. The same experiment with a Tamoxifen-inducible *GFAP::Cre* (*hGFAP-creERT2*) during adult life, with or without BAC induced injury, showed no detectable recombination in neurons.

The cautious conclusion of the article is that enteric glia are multipotent in culture but "primarily" form glia in the adult gut — in fact almost exclusively.

In line with this result, we already saw that Laranjeira et al. (2011) could not find any neuron born from $Sox10^+$ progenitors at P84, suggesting that none is born later either. A caveat though, is that recombination efficiency could go down with age, and this is exactly what Joseph et al. (2011) report with their *hGFAP-*Cre^{ERT2}, with a mere 5% recombination efficiency in glia of 4 to 8 months of mice. Concerning neurogenesis in the adult in response to injury, Lanrajeira et al. (2011), unlike Joseph et al (2011), find neurogenesis from glia in response to injury: up to 9% of neurons in enteric ganglia bordering a BAC-induced lesion of the enteric nervous system are derived from Sox10+ glia

months after the injury. Joseph et al. (2011) resolve their discrepancy with Laranjeira et al. (2011) (published back to back) by hypothesizing that there are Sox10^{+} cells, either too rare to be identified with *hGFAP-Cre^{ERT2}* or which altogether do not express GFAP, that would differentiate without cell division during an injury scheme.

This line of research recently took a striking and unexpected turn with Kulkarni et al. (2017) (cited 50 times to this day) who frontally contradicts the two previous studies. The paper first tries to establish that there is a great amount of cell death in the ENS, which would create a paradox with the stability of neuron numbers throughout life. The authors then proceed to show that cells not only disappear but are replaced at a high rate, which would solve the paradox. This is achieved, like in Joseph et al. (2011), by lineage tracing in adult animals with a tamoxifen inducible *Cre*, this time a *Nos1::Cre^{ERT2}* that targets nitrergic neurons. Tamoxifen was administered for a week and labeled cells were counted either immediately or 7 days after treatment. Over these 7 days, the authors find a striking 31% decrease in the number of double *tdT+*/*Nos1+* cells (thus already differentiated at the time of the treatment), and a concomitant appearance of *tdT-*/*Nos1+* cells, (thus born or differentiated after the treatment). An extrapolation would be that after 3 to 4 weeks most of the nitrergic cells present during the tamoxifen treatment should have disappeared. However, no time course is documented.

Since extraordinary claims require an extraordinary level of evidence, I shall review the evidence in more detail. The statistics of cell renewal are obtained by counting neurons per enteric ganglion: 6 *tdT+*/*Nos1+* double positive cells on average per myenteric ganglion on day 0, versus 4 cells on day 7, with the weakest p-value commonly accepted for "significance", $p<0.05$. Elsewhere in the paper the average size of ganglia is measured at 20.52 cells ±1.58. In my experience, the size of ganglia, which moreover are not always neatly separated from each other, is much more variable. At any rate, more convincing statistic could have been to count, on several hundred cells, the ratio of *tdT^{+}*/*Nos1^{+}* double positive cells (i.e. recombined *Nos1^{+}* cells that are still present) to all *Nos1^{+}* cells (= the latter + newly generated ones), which would directly measure the turnover, with a better chance of being statistically significant. One can also note that the images provided bear little relationship to the numbers in the text or the graph: day zero is illustrated by a field in which 7 Nos1+ cells are visible (all of them double positive for tdT), and day 7 by a field where only 3 Nos1+ cells are visible (1 double positive, and two single Nos1+), as if the vast majority of tdT+ cells had already disappeared and were replaced. The authors propose to reconcile their data with the negative finding of Laranjeira et al. (2011), by presenting evidence that the adult enteric neural stem cell is not *Sox10^{+}* (thus would not be traced by a *Sox10::Cre*), but *Nestin^{+}*.

In the second part of the paper, another tracing scheme is used whereby two base analogues are injected in succession, IdU for a week followed by CIdU for a week: 88% neurons retained one of the other label, i.e., were born during the two weeks span of IdU and CIdU injections, the vast majority of which being double labeled (i.e. born from progenitors that underwent one division during the IdU treatment and one more during the CIdU treatment). A striking aspect of the data is that if 18% of neurons are single labeled with IdU (i.e. were born from a neurogenic division that occurred during the first week of labeling), there should logically also be around 20% of neurons labeled with CIdU, (i.e. born from a division that occurred during the second week of labeling), some of them being double labeled, if their progenitor divided twice. However, the authors find 70% of single CIdU+ cells instead. One explanation could be that many IdU-labeled cells have already died at the time of analysis, i.e. a week after their birth. But that death would have to be higher than the 31% death in one week reported in *Nos1::Cre*^{ERT2} animals. Another way of analyzing these data is to say that if the number of neurons remains constant, and if 88% were born in the two weeks before counting (as shown by their incorporation of IdU and/or CIdU), 88% have died during the same time. Such an extremely high rate of turnover, i.e. of cell death, would make neurogenesis inherently difficult to detect by the previously used techniques. However, many studies report the detection, even in the adult, of large amounts of neurons labeled at various embryonic stages, using various methods, including incorporation of base analogs. This detection seems impossible to reconcile with the permanent renewal of all neurons on the scale of a few weeks proposed by Kulkarni et al., and is not discussed in the paper. One can also note that there is no example remotely approaching this level of cell replacement in any other part of the nervous system.

The above studies are difficult to reconcile with each other, even though the different experimental schemes prevent any single one from strictly contradicting the others.

3. NEURONAL DIVERSITY IN THE ENS

I. Introduction

The composition of the enteric nervous system in neuronal types has been studied, at the morphological level, since the XIXth century. In the XXth century, one of the main animal models for this study has been the guinea pig. Large mammals, like pig, have also been studied, and found to differ extensively from small mammals, both at gross neuroanatomical levels (for example with extra subdivisions of the submucosal plexus) and in term of cell types (see review by (Brookes, 2001)), from which it was concluded that the guinea pig does not necessarily model other species, including humans, whose diseases or malfunctions of the ENS motivate much of the field of enteric neuroscience. Unfortunately, mouse, which might not be a general model either, but at least provides a wealth of genetic tools for functional analysis of enteric circuits, has only slowly and recently emerged as a model animal in the field. This entails that even the most basic descriptive aspects of the enteric nervous system are sketchy in mouse. Finally, the topic is further complicated by the variation of cell types, and of their proportions, along the gut, from esophagus to the rectum (Mongardi Fantaguzzi et al., 2009; Qu et al., 2008), combined with the fact that most studies focus on a specific segment of the digestive tract.

II. Criteria for classification

Historically, the first criterion for classifying neurons has been the morphology of their cell bodies (according the original work by Dogiel in the XIXth century (Dogiel, 1895a, 1895b, 1896, 1899), which was later refined (Brehmer et al., 1999). The number of morphologically distinct neuron types ranges from 3 in mouse to 6 in pigs, not including some unclassified neurons (Brehmer et al., 1999). Figure 1 shows the classification proposed by Timmermans et al. (1997) for the guinea pig (modified from (Furness et al., 2009)):

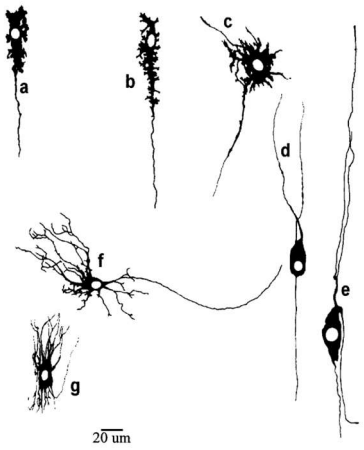

Figure 1: Morphological classification of enteric neurons on the basis of their shape. Drawings from whole mount preparations in guinea-pig small intestine. (a–c): multi (short, lamellar) dendritic uniaxonal type I neurons; (d,e): adendritic pseudouni- or multiaxonal type II neurons; (f): multi(long)dendritic uniaxonal type III neurons; (g): filamentous neuron.

This classification, although classical and still commonly referred to, is difficult to use in conventional histological analyses of the ENS since, most often, it implies the filling of individual neurons with biocytin and other dyes. Another limit to its use is that different functional classes of neurons can have the same morphology.

The second major criterion has progressively become the neurotransmitter phenotype, which can be inferred from the expression of biosynthetic enzymes or the presence of neurotransmitters: *Choline acetyl transferase* (ChAT) for cholinergic neurons, *GABA* for Gabaergic neurons, *5-HT* for serotonergic neurons, *Nitric oxide synthase* (NOS) for nitrergic neurons. In addition, enteric neurons, collectively, synthesize an impressive list of neuropeptides, which include (in alphabetical order): *a-neoendorphin* (a-NEOEND), *calcitonin gene-related peptide* (CGRP), *cholecystokinin* (CCK), *dynorphin* (DYN), *enkephalin* (ENK), *galanin* (GAL), *gastrin-releasing peptide* (GRP), *neuromedin U* (NMU), *neuropeptide Y* (NPY), *pituitary adenylate cyclase activating peptide* (PACAP), *peptide histidine isoleucine* (PHI), *somatostatin* (SOM), *substance P* (SP) and *vasoactive intestinal polypeptide* (VIP).

Finally, to this list of markers, one can add non-ubiquitous neural molecules such as *medium molecular weight neurofilament* (NF-M), or the calcium binding peptides *Calbindin* and *Calretinin* (also known as *Calbindin2*).

Most of these markers are expressed in complex combinations and few of them (or even combinations of two of them) allow for the unambiguous assignment of a neuron to a type, because they are shared by different types.

The third major criterion for classifying enteric neurons is electrophysiological, in two types: “S” (for synaptic”) and “AH” (for “After hyperpolarizing”). Obviously this criterion is never used in developmental studies.

It is only by combining molecular markers with the criteria of the plexus to which the neuron belongs (myenteric or submucosal) and the projections of its neurites (to different targets —

muscles, glands, or mucosa — and in different directions — rostral, caudal, etc…), that the type of a neuron can be uniquely identified. Combined with the fact that, as is generally the case in the peripheral nervous system, neuronal types do not occupy stereotypic positions, this situation makes it difficult to recognize neuron types by conventional histological methods.

Like in the central nervous system, it is likely that different neuronal types express distinct transcription factor signatures, at least transiently during development, but this line of study has only begun and lags far behind our knowledge in the central nervous system or in dorsal root ganglia, where transcription factors are among the best defining criteria for neuron types. Some indications of transcriptional codes can be found in Memic et al. (2018): for example *Meis2*, *FoxD1*, *EBF1* and *Pbx3* are co-expressed with *CGRP* and *Th*, thus presumably mark intrinsic primary afferents, and more recently in Morarach et al. (2020) (see below).

Most classes of neurons have been attributed functions, based on a variety of experimental evidence, including patterns of projections and physiological or pharmacological data (I will not review the latter).

III. Types of enteric neurons defined by classical studies

No complete code has yet been established in human (Anetsberger et al., 2018). I will restrict this review to rodents: guinea pig (the best studied model by far), and whatever is known about mouse (the model which is slowly becoming current, and on which I worked). The ENS is classically thought to be composed of 14 subtypes of neurons in mouse (J. B Furness, 2000) (but see later the recent single-cell RNA-Seq effort by Morarach et al. (2020)) and up to 18 in guinea pig (Brookes, 2001). I will treat separately the two anatomically distinguishable divisions of the ENS: the myenteric plexus and the submucosal plexus.

III.A. Myenteric plexus

III.A.1. Motor neurons

The ENS being in charge of the constant peristaltic movement of the digestive tract, a prominent class of neurons is predictably represented by motor neurons to the smooth muscle of the digestive tract. In small mammals, these motor neurons are located exclusively in the myenteric plexus and project either to the externally situated longitudinal muscles or to the internally situated circular muscles. Some motor neurons are excitatory, some are inhibitory, collectively ensuring the

propulsion of the alimentary bolus by upstream contraction and downstream relaxation. The main neurotransmitters for excitatory motor neurons are on one hand, acetylcholine and on the other hand, peptides of the Tachykinin family (mainly *Subtance P* and *Neurokinin A*, often collectively referred to as "tachykinins", TK, or sometimes as products of the *Tac1* gene) (Costa et al., 1982, 1985). The main neurotransmitters for the inhibitory motoneurons are Nitric Oxid (NO) and vaso-intestinal peptide (VIP). However, it is of note that animals in which the synthesis of NO is blocked by the knockout of its biosynthetic enzyme nitric-oxid synthase (*Nos*) have few motility problems apart from a slowing down of gastric emptying, due to piloric stenosis (Mashimo et al., 1996). Likewise for VIP, its role is verified by *Vip* knockouts, which have an impaired intestinal transit, although the effect (30%) is rather subtle and compatible with life (Lelievre et al., 2007). It could be that one neurotransmitter compensates for the other, but double knockouts have apparently not been analyzed.

Minor candidates as co-transmitters are ATP (Kenton M. Sanders, 2016), and peptides such as PACAP and PHI, encephalin (ENK) — at least in the guinea pig (Furness, Costa, & Miller, 1983)— and Neuropeptide Y (NPY) in the inhibitory motor neurons of the circular muscle (Holzer et al., 1987). Finally, Gamma-Aminobutyric Acid (GABA) is also found in several types of inhibitory neurons and, more surprisingly, excitatory motor neurons (Greg Baetge & Gershon, 1986; Jessen, 1981; Krantis, 2000) but its function is unclear.

Some neurons for the circular (internal) muscle project at long distance, others at short distance, and a few locally, these different projection patterns correlating with slightly different neurochemical or other genetic codes. Thus, by combining all these criteria, one can distinguish 5 types of motor neurons for the circular muscle and 2 for the longitudinal one. The situation for motor neurons of the circular muscle was clarified by Brookes et al. (1991), through the use of retrograde DiI labeling from the circular muscle, combined with immunofluorescence for various markers, and is summarized by the authors as follows:

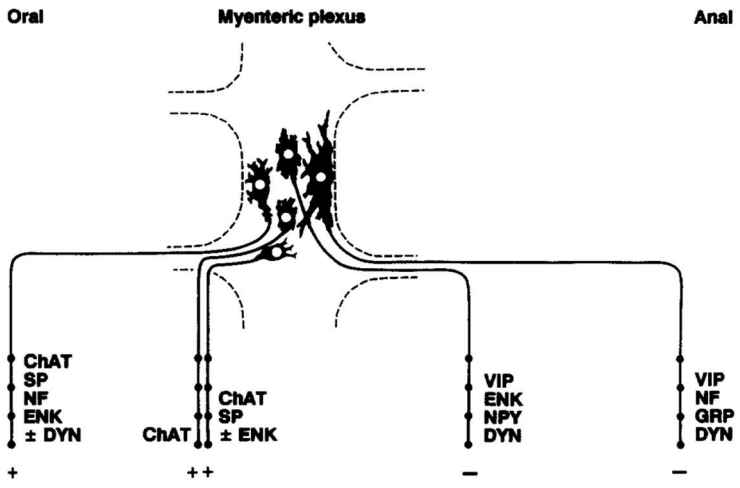

Figure 2: Schematic showing that motoneurons of the 5 types coexist in the same ganglia. This arrangement can explain, provided that the neurons of the same ganglion are activated together (for example by being targeted by the terminals of the same interneurons), that a local mechanical stimulus triggers relaxation downstream (anally) and contraction upstream (orally), thereby mediating a typical peristaltic movement.

Motoneurons represent 60% of the myenteric plexus (respectively 34% of excitatory motor neurons and 26% of inhibitory motor neurons). Because of the nature of their target, the projections of motor neurons are relatively easy to diagnose by histological techniques, as shown in **Figure 3:**

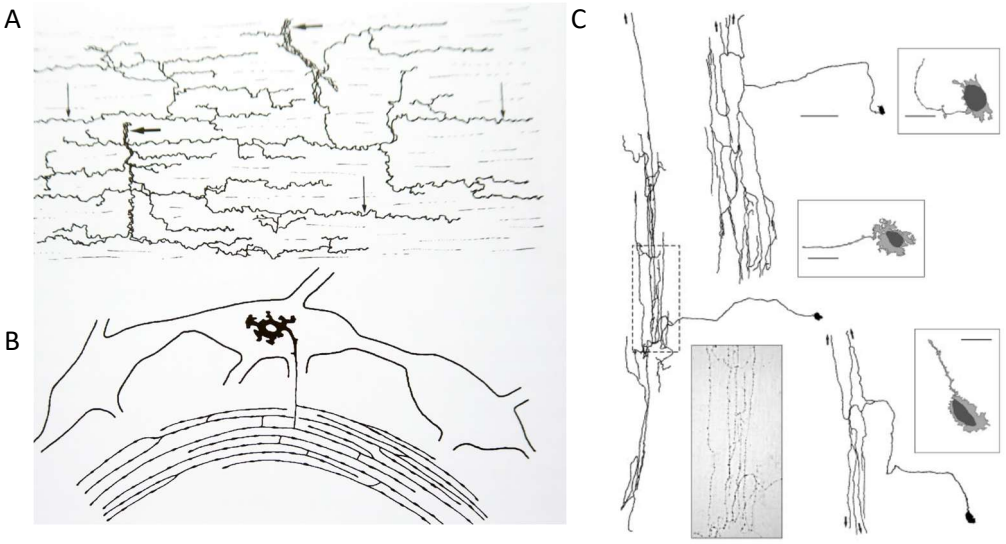

Figure 3: Various visualization of motoneurons: (A) Drawing of motor neurons made by Cajal (1895). (B) Drawing from Furness et al. (1991). (C) Appearance of a single circular muscle motor neuron filled with a marker dye via an intracellular microelectrode. Reproduced from Nurgali et al. (2004).

The inhibitor neurons to the circular muscle can be observed by immunohistology against NOS or by the NADPH diaphorase reaction which reveals this enzyme with a chromogenic substrate, and display the following typical pattern on the gut wall:s

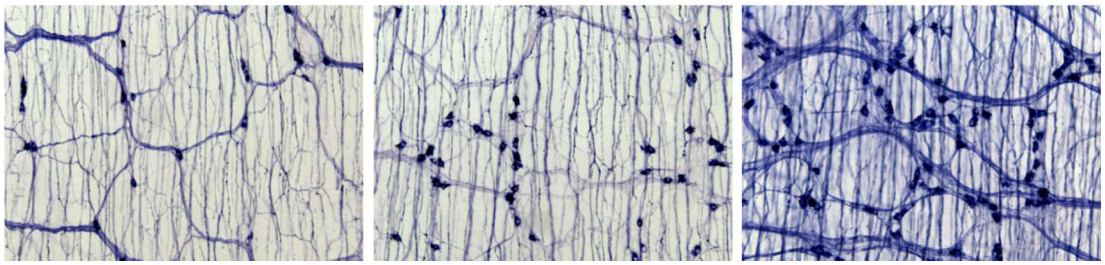

Figure 4: Projections of NoS+ neurons on flatmounts of the proximal, and distal small intestine and colon (from left ot right) by the NADPH-diaphorase reaction, from (Viader et al., 2011)

On the other hand, the motoneurons to the longitudinal muscle layer project in the tertiary plexus under this muscle layer:

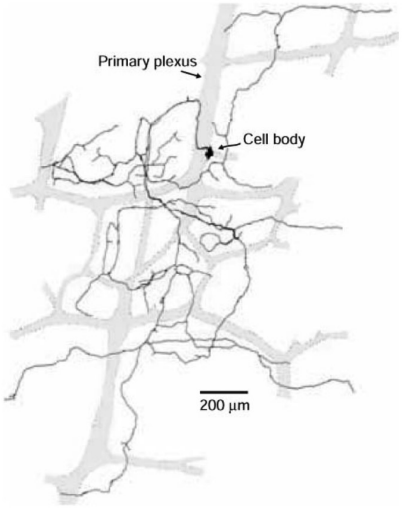

Figure 5: Drawing of the projection of a motoneuron for the longitudinal muscle. A single motor neuron was filled with a marker dye through an electrode (Furness, 2006). Note that the projections of the neuron do not follow the main strands of the plexus, but form the so-called “tertiary plexus”.

III.A.2. Sensory (afferent) neurons

After motor neurons, the second largest type of neurons are sensory neurons, called IPANs for *Intrinsic Primary Afferent Neurons*. The terminology "afferent" is preferred over "sensory" because these neurons do not convey conscious information (i.e. mostly pain, which is carried by spinal sensory neurons located in the dorsal root ganglia); and the term "intrinsic" distinguishes them from both, *extrinsic* afferents (which have cell bodies in the nodose ganglion and transmit visceral information from the gut to the central nervous system, more precisely, the nucleus of the solitary tract) (Langley & Magnus, 1905; Furness et al., 1995), and *intestinofugal* afferents (sometimes abbreviated as IFANS), which have cell bodies inside the ENS but project outside the gut, to the prevertebral sympathetic chain (see below). IPANs sense the composition of the alimentary bolus in the lumen, and mechanical deformation of the villi or intestinal wall, and participate in local, intestino-intestinal reflexes. They have been identified by a combination of projection patterns and electrophysiological recordings. They represent 26% of neurons of the myenteric plexus of the small intestine in both guinea pig (Furness, 2000) and mouse (Qu et al., 2008). They are the only neurons of the ENS which are unambiguously characterized by a morphology, that of Dogiel type II neurons (see **Figure 1**): an oblong soma with several axons, usually including a principal one which ramifies outside the ganglion into long and thin branches, and smaller ones (Grider, 1994; Nurgali et al., 2004). The neurotransmitter(s), which allows them to signal to interneurons or other IPANs, are not entirely elucidated. In the guinea pig, IPANs contain peptides of the tachykinin family (TK), and anti-tachykinin drugs blocks EPSPs in IPANs, presumably evoked from other IPANs. However, in mice IPANs do not express TK. In both guinea pigs and mouse, IPANs express *ChAT* but there is no published evidence that they are cholinergic. *CGRP* appears as another marker in mouse, and *calbindin* is a marker in guinea pig, but less constant in mouse. In conclusion, in mouse, histochemical identification of IPANs in the myenteric plexus mainly relies on *CGRP* immunoreactivity of cell bodies after colchicine treatment (without this treatment only fibers are detected, many of which come from extrinsic neurons).

III.A.3. Interneurons

The third class of neurons comprises interneurons (representing 12% of myenteric neurons in mouse), which relay information between IPANs and motor neurons, and also form chains of interconnected neurons (as determined in guinea pigs). They fall into two broad classes depending on the direction of their projection: descending (i.e. projecting anally) (8%) and ascending (i.e.

projecting orally) (4%). In both guinea pigs and mouse there are three types of descending interneurons and one type of ascending interneurons, all expressing ChAT, together with either *NOS*, 5-HT or *somatostatin* (for descending interneurons) and *calretinin* (for ascending ones).

III.A.4. Intestinofugal neurons

A small fraction of neurons have their cell bodies in the myenteric plexus and project outside of the ENS to synapse on prevertebral sympathetic ganglia (mainly the celiac ganglion) in order to inhibit secretory and motor neurons in another part of the gut or in the stomach, forming intersegmental reflexes (Furness, 2003). These intestinofugal neurons (IFANs) express ChAT and VIP and their proportion was not fully established but they are thought to be few. Finally, it was described that extremely rare neurons of the myenteric plexus project directly to the sacral spinal cord through the pelvic nerve (WI Neuhuber et al., 1993) or to the dorsal vagal complex through the vagal nerve (Holst et al., 1997).

III.B. Submucosal plexus

Concerning the submucosal plexus, much more is known about guinea pig than about mouse. Many neurons in the submucosal plexus project to the intestinal villi, including its blood vessels and secretory epithelium as schematized below.

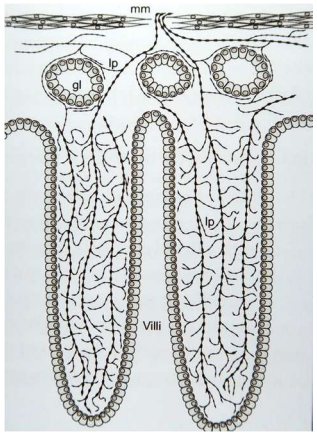

Figure 6: Schematic of projections of submucosal ganglia to the intestinal villi. Taken from (Furness, 2006)

III.B.1. Secretomotor/Vasodilator neurons

The dominant functional class (around 80% of the neurons) of submucosal neurons in both guinea pigs and mouse are secretomotor neurons and vasodilator neurons, which are sometimes the same neurons. Their presence was first evidenced by the demonstration in organotypic preparations that nerve stimulation activates a chloride current in the mucosa, followed by secretion of water and sodium, a phenomenon which is blocked by tetrodoxin (thus dependent on action potentials). Secretomotor/Vasolidator neurons were classified by Furness into three types:

VIP+ secremotor neurons

They are up 50% of the submucosal plexus (Kuwahara et al., 2019; Mourad et al., 2003; Furness, 2000). The demonstration of abundant VIP+ cell bodies and fibers in the gut (and in particular in the mucosa) of guinea pig was made by (Larsson et al., 1976), and extended to many species by (Keast et al., 1985).

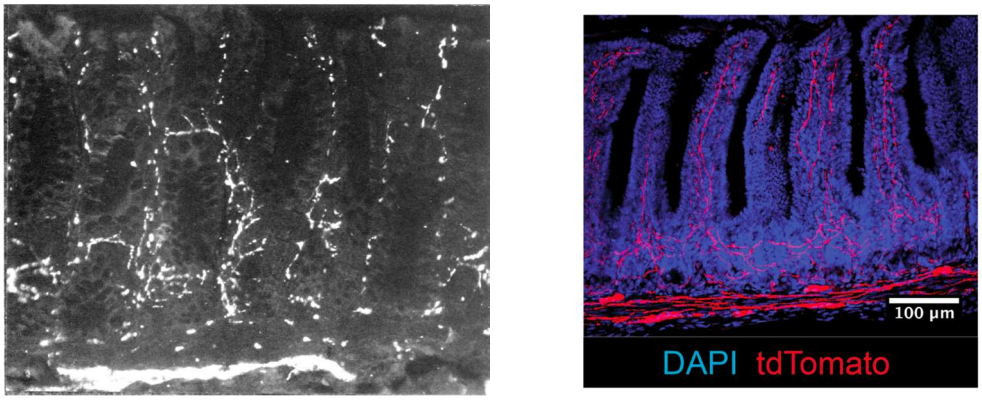

Figure 7: Two visualizations of VIP+ neurites in the intestinal villi, by immunofluorescence in cat (Larsson et al., 1976) (left) and in mouse in a VIP::Cre;tdTmoato transgenic mouse (Talbot et al., 2020) (right).

VIP innervation of the villi is preserved after sympathetic denervation, which proves that it comes from the submucosal plexus and not from the sympathetic chain (in which many neurons also synthesize VIP). The physiological “secretomotor” role of VIP neurons is suggested, or made likely, by the demonstration that VIP is a potent stimulant of secretion in the intestine.

Cholinergic secretomotor neurons

They representing 30% of the submucosal plexus and their presence was first suggested by an additional cholinergic component to the transmission to the mucosa. This class can be in turn subdivided into two types:

Calretinin+/ChAT secretomotor which are mentioned in (Furness, 2006) without any reference as to their innervation pattern. I did not find any bibliographic reference on these neurons.

NPY+/ChAT secretomotor which are non-vasodilator neurons and would represent a second cholinergic component. (Furness, Costa, Emson, et al., 1983) described NPY+ cell bodies in the submucosal ganglia (as well as in the myenteric ganglia), and NPY+ fibers inside the ganglia, along the blood vessels but also in the core of the villi, this morphological aspect being typical of "secretomotor" neurons (see VIP+ neurons above). The latter are said to be preserved after extrinsic denervation (sympathetic and vagal), in contrast to the perivascular ones, which disappear. The original figure actually shows only that NPY+ cell bodies in the submucosal ganglia are preserved after extrinsic denervation. Thus, strictly speaking, the claim that NPY+ cells of the submucosal plexus innervate the mucosa seems unsubstantiated (but likely).

In mouse, several markers for neurotransmitter phenotypes expressed in guinea pig submucosal plexus are also expressed, but in different combinations. For example, *VIP* is co-expressed with *NPY* and *Calretinin*, whereas it is mutually exclusive with them in guinea pig. In practice, it is next to impossible to relate the submucosal neuronal types of mouse with those of guinea pig, which is probably the reason why the Furness lab does not provide a table of correspondence (Mongardi Fantaguzzi et al., 2009), as they do for the myenteric plexus (Qu et al., 2008). By extrapolation from studies in guinea pig, one can only speculate that most neurons of the submucosal plexus of mouse are of the secretomotor/vasodilator type, and fall into 3 classes: VIP+ secretomotor (30%), VIP+ vasomotor (20%) (the two being distinguished by the fact that the latter but not the former co-expresses TH) (in total 50% VIP neurons), and cholinergic (ChAT+)/CGRP+ secretomotor (30%).

III.B.2. IPANs

IPANs make up 11% of the guinea pig submucosal plexus, but cannot be detected in mice on the basis of Dogiel morphology type II or immunoreactivity for NF-M.

III.B.3. Other types

Two other types of neurons are without identity or function: ChAT+/CGRP— (10%), and ChAT—/VIP— (8%) whose neurotransmitter identity (let alone function) is unknown.

III.C. Conclusion on the detection of enteric neuronal types

Since markers for neurotransmitter phenotype (enzymes, neurotansmitters and neuropeptides) are to this day the main tools to identify neuronal types in the ENS, it can be useful to keep in mind the full complement of neuronal types that are detected by a given marker. I will represent this summary as a table to clarify and simplify as possible the current knowledge on this field:

	Motorneurons		Sensory	Interneurons		Secretomotor	IFAN
	Excitatory	Inhibitory		Ascending	Descendig		
ChAT	X X		X X	X X	X X	X X	X
5HT					X X		
NOS		X X			X X		
CGRP			X				
SOM					X X		
Enk	?						
NPY		X X				X X	
SubP	X		X				
VIP		X X				X X	X
CalR				X X		X ?	
CalB			? X				
GABA	?	?					
ATP	?	?					
PACAP	?						

X = Proved **?** = unsure X = Mouse X = Guinea Pig

III.D. Glia

Enteric neurons are, like in the central nervous system, surrounded by several types of glia, four of them being described so far. Type-I glia cells display an astrocyte-like morphology and are present within the enteric ganglia of both plexi; Type-II glia has a fibrous morphology and are present along interganglionic fibers in each plexus; Type-III have multiple branches and are detected in the mucosa of the gut; Type-IV are bipolar and line the enteric fibers in the muscles layers (Gulbransen &

Sharkey, 2012). The four types have similar molecular signature, but no marker labels all of them, and no marker is specific to any of them (Boesmans et al., 2015; Grundmann et al., 2019).

IV. Types of enteric neurons newly defined by single cell transcriptomics

Recently, three studies from the same laboratory have reexamined the diversity of enteric neurons from scratch, by the method of single cell transcriptomics. A first glimpse of enteric neuron types was provided in the context of abroad assessment of the "molecular architecture of the mouse nervous system" (Zeisel et al., 2018), which found 9 neuron types:

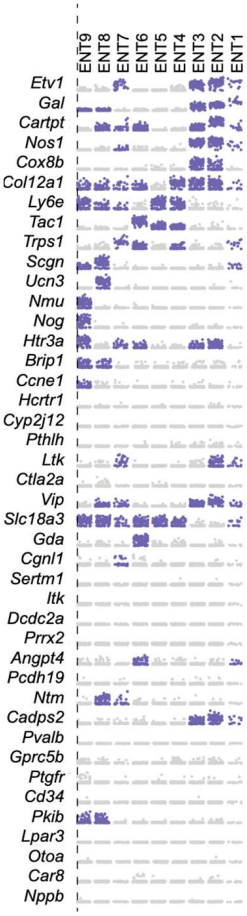

Figure 8: Marker gene expression in 9 enteric neuronal subtypes as determined by single cell transcriptomic. Adapted from supplementary Figure 4 of Zeisel et al. (2018)

More recently Morarach et al. (2020) analyzed 9141 cells sorted from juvenile (P21) mouse intestines by expression of reporter triggered by a neuron-specific Cre, reduced to 3468 neurons after several exclusion and quality check, which resolved themselves in 12 clusters numbered ENC1-ENC12. The authors attempted at relating this cell taxonomy to classical ones by using classical markers for broad categories mostly based on a combination of data from (Qu et al., 2008; Sang et al., 1997; Sang & Young, 1996):

IPANS marked by *Calca, Calcb, ChAT, Slc18a3, Nefm, Calb1, Calb2*

Excitatory motoneurons marked by *ChAT , Slc18a3, Calb2 (Calr), Tac1*

Inhibitory motoneurons marked by *Nos1, Gal, VIP, Npy*

Interneuron 1 marked by *ChAT, Slc18a3, Nos1,VIP*

Interneuron 2 marked by *ChAT, Slc18a3, Calb2, Sst*

Interneuron 3 marked by *ChAT, Slc18a3, Ddc, Slc6a4*

In that way, a tentative table of correspondence between the single cell Seq data and classical categories was proposed (no partition was proposed between the myenteric and submucous plexi):

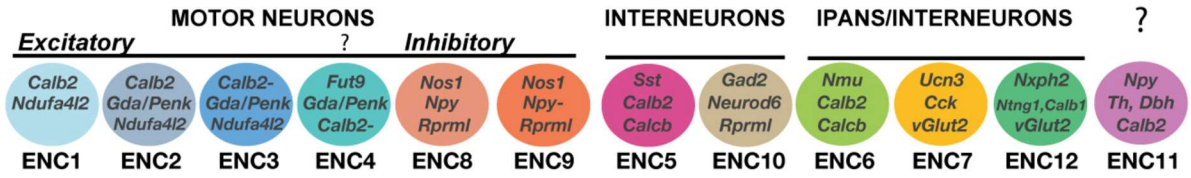

Figure 9: Types of enteric neurons, from Figure 1 of Morarach et al. (2020)

This classification cannot be matched entirely with that of (Zeisel et al., 2018) and few "top genes" allow for cross-correlation between the two studies, possibly because of the very different context in which the bioinformatic analysis was made (in the former study a cell purification technique applied to the entire embryo, that co-selected neurons and glia versus a pure population of enteric neurons in the more recent study). Some type-specific markers were discovered in the previous study such as *Nmu* (for former ENT9 which thus corresponds to current ENC6), *Ucn3* (for former ENT8 which thus corresponds to current ENC7), but, for example, *CCK* did not appear as a specific marker in the first study, possibly because it also marks many neurons of the central nervous system. Salient features of these new data are:

<u>IPANs (ENC6, ENC7, ENC12)</u>

They were identified by their expression of the classical markers (*CGRP*, *Calb*, and *NFm*) which collectively defined the global category "IPAN" in previous studies, although the new study reveals them to be differentially expressed among the 3 subcategories. Another argument, however, to label ENC6/7/12 as putative IPANS is that their projections are either local or to the mucosa but never to the muscle. On the other hand, the old notion that IPANS are all Dogiel Type II, has to be abandoned according to the new study: by labeling the cytoplasm with conditional transgenic or viral reporters driven by *Nmu::Cre* or *CCK::cre*, or with antibodies, it is revealed that putative IPANS have a variety of morphologies, included, but not limited to Dogiel type II (displayed only by ENC6). If this

identification is confirmed, IPANS, which were poorly resolved until now, now fall into 3 (possibly 4) classes, each with a single, or even two specific markers, respectively *Nmu*, *Ucn3*/*CCK*, and *Nxph2*.

Motoneurons

5 types are discovered: 3 (possibly 4) excitatory, and 2 inhibitory. It is not resolved how each related to the 4 excitatory and 3 inhibitory types previously described, distinguished from each other by target muscle (circular or longitudinal) and distance of projection

Interneurons

Three types are discovered (ENC5, ENC10 and possibly ENC12), all expressing *VAChT* (*Slc18a3*) (but one, ENC10, strangely devoid of *ChAT*) and the following codes: respectively *SSt*/*Chat*/*Calcb*, *Vip/Gal/Nos1*, and the serotonergic markers *Ddc* and *Slc18a2*, thus roughly corresponding to previous descriptions. One class of interneuron seems capable of synthesizing Gaba (ENC10).

One potential novel cell type (ENC11)

Expressing markers of the noradrenergic phenotype (*Th*, *Dbh*), previously undetected in the ENS.

This same dataset provides the beginnings of a transcriptional code for various neuron types, although the expression of any single transcription factor or even combination thereof is rarely restricted to a given neuron type or even to a coherent class of neuron types, except for *Neurod6* which is expressed in 100% ENC10 (but also 25% of ENC11). For example, no transcription factor or combination of transcription factor cleanly demarcates either motoneurons, or excitatory motoneurons or inhibitory motoneurons, as a group, as seen in Figure 10.

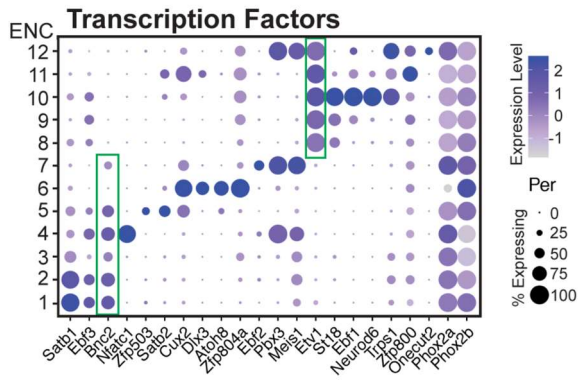

Figure 10: Expression of transcription factor in the 12 enteric neuron types, as determined by single cell transcriptomic, from figure 2 of Morarach et al. (2020).

V. Differentiation of enteric neurons into their different types

V.A. Timing of neuronal diversification

The migrating neural crest, which gives rise to all enteric neuronal types, invades the foregut at E9.5 and the first morphological neurons can be observed from E12 , even if expression of HuC/D and neurofilament starts as early as E10.5 (Bergner et al., 2014). From then on, birth (i.e. cell cycle exit) and differentiation of neuronal classes described above is progressive and occurs during a long time-window that spans the second half of gestation and the first post-natal weeks. The development of the submucous plexus is almost entirely post-natal (McKeown et al., 2001).

The time windows of birth of different neuronal types was studied by Bergner et al. (2014) and Pham et al. (1991), and I summarize the results in the following graph:

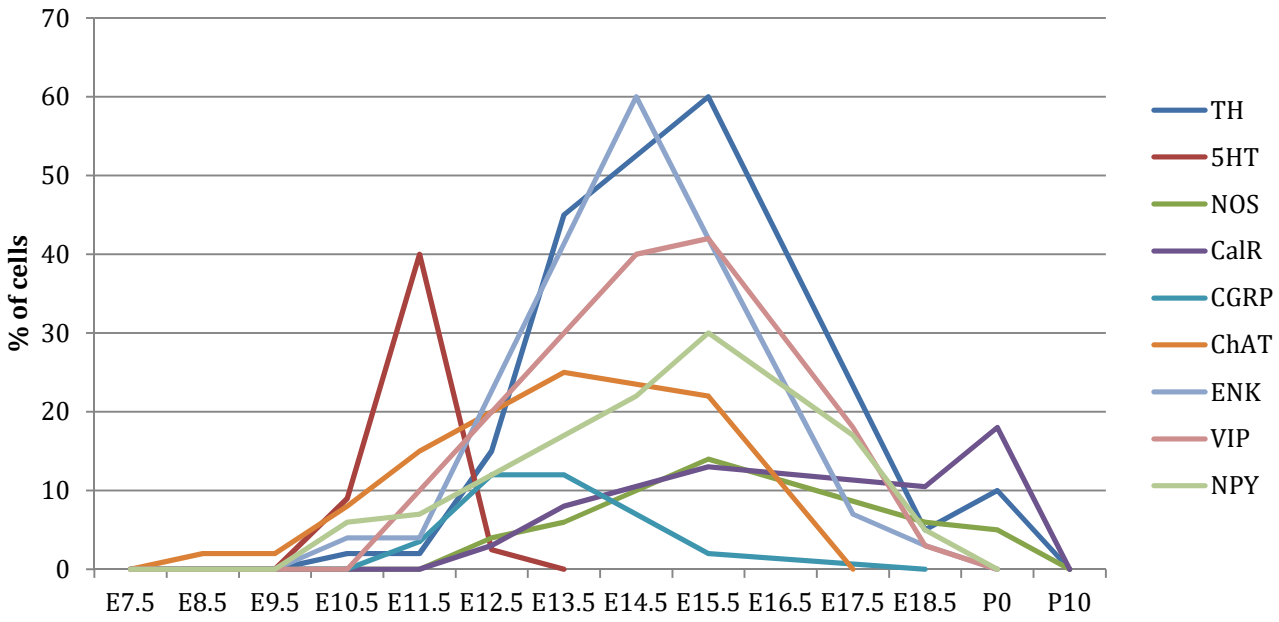

Figure 11: Time of birth of different neuron types as assessed by BrdU incorporation combined with immunofluorescence, according to Bergner et al. (2014) and Pham et al. (1991)

The protracted date of birth of neuronal types, and the fact that some are born earlier than others has prompted the speculation that early-born neurons could influence the birth (or differentiation) of later-born ones (Pham et al., 1991). The only evidence so far came much later from the same lab: Li et al. (2011) report that by genetic inactivation of the neuronal isoform of tryptophane hydroxylase, by definition expressed in the small fraction of serotonergic neurons, leads

to the complete loss of the (even smaller) population of dopaminergic neurons that differentiate after birth. Much more strikingly, however, it also leads to a loss of 50% of neurons in the ENS. This astounding non-cell autonomous defect of a neurotransmitter on the development of a part of the nervous system, without precedent to my knowledge, is strangely not discussed in the paper.

A limitation of the studies on the order of neuronal birth, however, is that neurotransmitter phenotypes were taken as proxies for neuronal types, but we now know that most neurotransmitter phenotypes are shared by different types of neurons. Possibly related to this, the neurotransmitter phenotype which has the narrowest time-window of birth (E10.5-E12.5) is the serotonergic phenotype, which is one of the rare neurotransmitters to represent a single neuron type: 5HT-descending interneurons (Sang et al., 1997; Sang & Young, 1996), and possibly for that reason one the most extensively studied neuronal type, despite its scarcity (about 1% of the mature myenteric plexus).

A distinct question from neuronal birth (i.e. cell cycle exit), is the timing of their acquisition of differentiation traits, in practice of detection of a handful of markers. Again, this dynamic has been assessed by immunohistology for the main markers of neurotransmitter phenotype (plus *calbindin*):

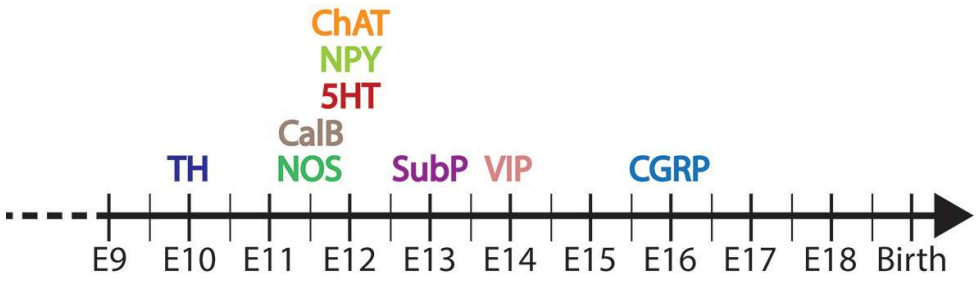

Figure 12: Schematic of the dates of detection of ENS markers, summarized from (G. Baetge & Gershon, 1989; Branchek & Gershon, 1989; Hao et al., 2010; Rothman et al., 1984)

The same limitation applies as before, and it could be, for example, that some classes of cholinergic neurons differentiate well after E12, the first day of *ChAT* detection. The first marker for a neurotransmitter phenotype that can be detected (as early as E10) is tyrosine hydroxylase (*Th*), but this phenotype is mostly transient and can in principle be expressed by several types for neurons, even if some *Th*+ neurons are still found in the mature ENS (Baetge & Gershon, 1989). Other early-differentiated neurons are *Nitric Oxide Synthase* (*Nos1*) expressing neurons (including inhibitory motor neurons (Sanders & Ward, 1992) and interneurons, and representing overall around 30% of

the neurons in the myenteric plexus). *Nos1* expression is detectable at E11.5 (Branchek & Gershon, 1989; Hao et al., 2010) but some *Nos1*+ neurons are still being born postnatally, up to P10, the peak of birth being at E15.5. Again, this protracted period of differentiation could reflect the heterogeneity of *Nos1*+ neurons.

Finally, these data might not all me reproducible. For example, in the case of NPY, it could be that the antibody used in the 1989 study is not specific or that the positive cells are not neurons, as for example in the following image, where immunoreactive cells are shown in the presumptive myenteric and submucosal plexi at E14.5 (there is, however, no submucosal plexus at E14.5 (McKeown et al., 2001)), and this study also reports NPY positive cells in the gut epithelium or mesenchyme):

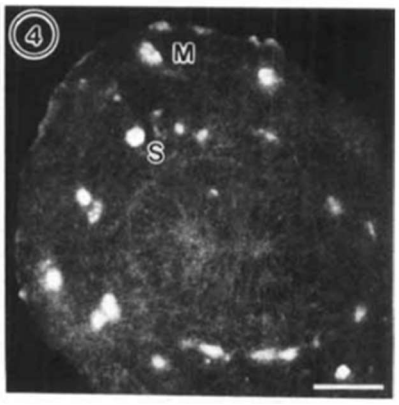

Figure 13: From figure 4 of Branchek & Gershon (1989), whose legend says: Day E14 jejunum; NPY-immunoreactive cell bodies were seen segregating into layers corresponding to the locations of the presumptive myenteric (M) and submucosal (S) plexuses.

On the other hand, a convincing NPY signal is reported at E18.5 in Memic et al. (2018):

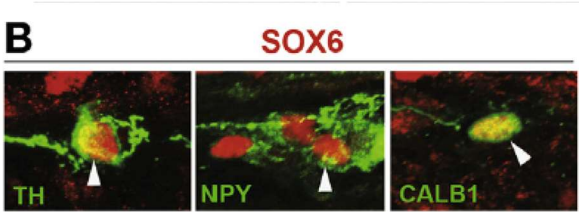

Figure 14: From Figure 4 in Memic et al. (2018). Immunofluorescence with the indicated markers on a E18.5 mouse embryo. NPY is co-expressed with Sox6.

It is thus could be that the onset of expression of *Npy* is at around birth.

V.B. Mechanisms of neuronal differentiation

A first attempt at describing the dynamic of neuronal differentiation in the developing ENS was accomplished in Memic et al. (2018) who compared the transcriptome of all ENS cells (sorted from a *Wnt::Cre;RosaYFP* embryos) to that of progenitors specifically (sorted from *Sox10Cre^{ERT2};RosaYFP* embryos) at two developmental stages, E11.5 and E15.5. In that way, many genes, including TFs could be classified as expressed in progenitors or post-mitotic precursors, and as "early" or "late". Moreover, in situ detection of many of markers for post-mitotic precursors showed that they were expressed in subpopulations of neurons. One of those, *Sox6*, was analyzed by knockout (see below).

A completely new layer of data and level of understanding was recently added to these notions, using single cell RNA-Seq analysis of enteric neurons at embryonic days E15.5 and E18.5 in Morarach et al. (2020) from which the next two figures are taken. Cells were displayed on UMAPs that show them to emerge from a pool of progenitors along two main directions or "branches" of differentiation, as shown below:

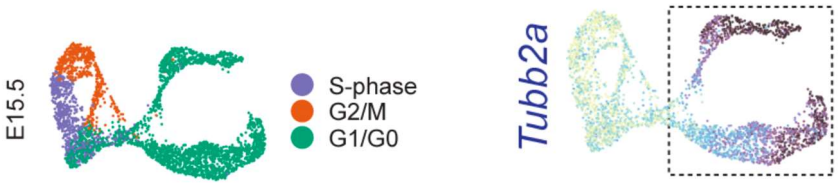

Figure 15: UMAP of enteric neurons in an E15.5 pup, with cell cycle genes (thus phase) mapped on the left, and the terminal differentiation marker Tbb2a mapped on the right.

Strikingly, 10 of the 12 ENCs defined at P21, mapped on this E15.5 UMAP by bioinformatically matching shared genetic signatures between the two stages, are arranged in a linear succession on the branches. For example, markers for ENC10-12 map distal to those of ENC8-10 along Branch2.

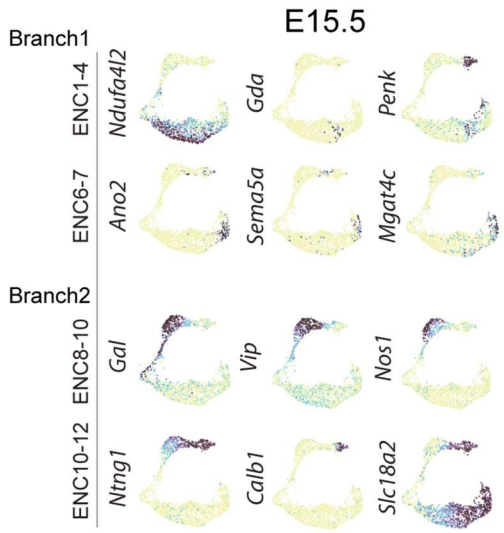

Figure 16: UMAP of enteric neurons in a E15.5 pups, with markers for neuro types mapped.

Collectively these data suggest that a binary fate split first gives rise to ENC1-4 and ENC8-10, but that most diversification events taking place later, among post-mitotic precursors. These data fit well with the protracted chronology of differentiation traits apparent from earlier studies, and in particular for markers 5-HT and CGRP, known to appear late, and fittingly map to the end of the UMAP branches. This mode of neuronal diversification differs from most of what we know about the central nervous system, whereby many categories of neurons are generated from distinct pools of progenitors. This difference in turn could result from the lack, in the ENS, of the spatial arrangement of progenitors of the CNS (see iontroduction), which would have favored a temporal rather than spatial logic of neuron specification. However, it is not excluded that such a temporal mode of differentiation of post-mitotic precursors is also used in the CNS, for example to produce the many interneuron types of the dorsal spinal cord (Häring et al., 2018), most of which cannot be accounted for by the 9 progenitor domains defined (Alaynick et al., 2011) and whose mechanism of generation is largely unknown.

VI. Transcriptional control of ENS development

Here I will briefly review our current knowledge of the role of transcription factors in the development of the ENS. A striking aspect of these studies is that so far, in the ENS unlike many other parts of the nervous system, very few transcription factors have emerged as a determinant of specific neuronal types. This, however could simply reflect our relatively poor knowledge of these types — the current markers being shared by several types (see above).

Several TFs are active in the pre-enteric neural crest (premigratory or migratory) and their inactivation impedes to various degrees the colonization of the digestive tract, leading to hypo- or aganglionosis, such as *Sox10* (Bondurand & Sham, 2013, bl 10), *Pax3* (Lang et al., 2000, bl 3), *SufU* (J. A.-J. Liu et al., 2015), *Foxd3* (Mundell et al., 2012, bl 3), etc… I will not review those here.

Other TFs are expressed in progenitors or post-mitotic precursors only once they have entered the wall of the gut. This is the case of 3 TFs that are expressed in all or the vast majority of enteric precursors as they enter the foregut mesenchyme: the bHLH ‘”proneural” TFs *Ascl1* and *Hand2* and the homeobox gene *Phox2b*.

Ascl1 is switched on in *Sox10*+ neural crest cells as they enter the foregut (Memic et al., 2016) and persists until early stages of differentiation (i.e. soon after onset of Hu), and lineage

tracing established that neurons of all the subtypes detectable at around birth with classical markers of neurotransmitter phenotypes, have expressed *Aslc1*.

The KO of *Aslc1* was shown to delay early neuronal differentiation in the ENS, with a late appearance of HUC/D+ cells. This is reminiscent of other observations of delayed neuronal differentiation in *Ascl1* mutants, in the nucleus of the solitary tract and in the sympathetic ganglia (Pattyn et al., 2006). In the esophagus, neurogenesis is almost completely blocked (Guillemot et al., 1993; Sang et al., 1999), while downstream of the stomach the mutation only partially depletes the ENS. These two situations, however, could be the consequence of the same phenomenon if, for some environmental reason, the time-window available for neuronal differentiation is shorter in the esophagus. Concerning terminal neuronal differentiation events, an early report claimed that 5-HT neurons were missing in *Aslc1* KO (Blaugrund et al., 1996), but a later report found them intact (Memic et al., 2016), the discrepancy probably explained by the fact that the early study detected 5-HT neurons indirectly (by uptake of tritiated 5-HT), which is possibly non-specific. On the other hand, several other subtypes of enteric neurons were reduced in the proportion they formed of a globally depleted ENS: those expressing *Calb1*, *VIP*, and *Th* but not those expressing *NPY*, *NOS* or *CGRP* (or 5-HT). It is important to note that these markers are still expressed, albeit in lower proportions (in 30 to 40% of the cells that should express them), which stands in contrast with, for instance the serotonergic phenotype of the hindbrain, which is all but abolished in *Ascl1* KO (Alexandre Pattyn et al., 2004). Thus, these data leave open the possibility that *Ascl1* acts in the progenitors of several classes of neurons, affecting for example their division or maturation rate, rather than in the specification of phenotypic traits per se (i.e. in the transcriptional control of marker, effector genes). On the other hand, *Ascl1* provides more than a generic proneural function since a knock-in of another proneural gene (*Neurog2*) in the *Ascl1* locus, rescues the total number of neurons produced but not the proportion of *Calb1+*, *VIP+*, and *Th+* cells (Memic et al., 2016).

Hand2. Two conditional knockouts of *Hand2* have been analyzed in the ENS, which both suffer from limitations: the *Wnt1::Cre;Hand2*$^{lox/lox}$ mice die from cardiovascular causes at E12.5 (because *Hand2* is also deleted in the cardiac crest) (D'Autréaux et al., 2007) and the *Nestin::Cre;Hand2*$^{lox/lox}$ inactivates the gene in only 80% of enteric precursors allowing for a degree of compensation from precursors which do not express *Nestin::Cre* (Lei & Howard, 2011). Nevertheless, collectively, these studies suggest that *Hand2* is required neither for colonization of the gut, proliferation, or early differentiation events (expression of *b-III tubulin*, *Gap-43* or *PGP9.5*) but for terminal neuronal differentiation (expression of *NOS* or *Dbh*), and the ontogeny of properly organized enteric ganglia. The *Nestin::Cre* animals die around P20 (i.e. soon after weaning) with a distended digestive tract.

Phox2b is a pan autonomic marker and determinant (Brunet & Pattyn, 2002). During formation of the ENS, it is switched on at around E10, in two populations of progenitors: Schwann Cell Precursors of the vagus nerve, that go on to colonize the esophagus and proximal stomach, and in the rostral sympathetic crest ("sympathetic" or rather sympatho-enteric in the sense that it also gives rise to the superior cervical ganglion and which is not in any way "vagal" despite its classical name) as soon as it penetrates the foregut mesenchyme and stay on until postnatal stages (Isabel Espinosa-Medina et al., 2017). In *Phox2b* KO, only the esophagus and proximal stomach are invaded by *Sox10*+ cells (most likely corresponding to the Schwann cell precursors population whose migration along the nerve does not depend on Phox2b, like it does not depend on this gene during the formation of parasympathetic ganglia (Coppola et al., 2010; I Espinosa-Medina et al., 2014) but not beyond the stomach (which is the place where the left vagus nerve ramifies terminally and where the right vagus leaves the digestive tract), and they fail to turn on Ret expression. These cells disappear later and the entire length of the gut is aganglionic (Pattyn et al., 1999). Dominant mutations in *Phox2b* can lead (in the larger context of Congenital Central Hypoventilation Syndrome) to partial distant agenesis of the ENS, i.e. to a Hirschprung syndrome (Amiel et al., 2003, 2009).

Five other homeobox genes have been claimed to be involved in ENS development:

Tlx2 (formerly known as *Enx* or *Ncx*) is widely expressed throughout the autonomic nervous system, including many enteric neurons (Hatano, Iitsuka, et al., 1997), at least from E13.5. Knockout mice display hyperganglionosis in the colon, i.e. an increase in the number of enteric ganglia and of neurons per ganglia (Hatano, Aoki, et al., 1997; Shirasawa et al., 2000), which was later attributed to an impairment of post-natal neuronal death (Aoki et al., 2007) (although there is no other report to our knowledge of massive normal cell death in the ENS). 50% of the animals die at around 5 weeks with a megacolon.

Hoxb5 A chimeric *Hoxb5* molecule, whose C-terminus was replaced by the repressor domain of *engrailed*, causes a defect in the migration of enteric neuronal precursors, hypoganglionosis, delay in intestinal transit and occasionally lethal megacolon. This phenotype was attributed to a down regulation of Ret (Lui et al., 2008). However, it is unclear to what extent this gain of repressive function is informative about the normal function of *Hoxb5* in enteric precursors, all the more because no defect in the ENS was reported in *Hoxb5* KO (Rancourt et al., 1995).

Dlx2, also expressed in enteric neurons was listed as having a role in ENS development (Qiu et al., 1995). However, the main "enteric" phenotypes of *Dlx2* KO was a distended stomach filled with air, combined with a massive remodeling of the first and second branchial arch mesenchymal

derivatives leading to a cleft palate, which could easily explain by itself the stomach phenotype. Thus, the case for a role of *Dlx2* in enteric neurons themselves can be considered open.

Sox6. The only subtype-specific TF which has been discovered so far by gene inactivation is *Sox6* (Memic et al., 2018), expressed in 2 gastric sub-populations of neurons, characterized respectively by late and strong expression of *Th* (thus presumably dopaminergic) or *Npy*/*Calb1* expression, thus presumably secremotor neurons (see **table 1** above). The conditional knockout of *Sox6* (in a *Wnt1::Cre;Sox6*$^{lox/lox}$ background) reduces by 70% the number of *Th+* neurons in the adult stomach, while leaving the other neuron types investigated (*Npy/Calb1+* or *Vip+*) intact. *Sox6* is thus the first transcription factor linked to the generation of a single neuronal subtype in the developing ENS. Strikingly, *Sox6* is also involved in the specification of dopaminergic neurons in the midbrain. Mutant mice have an enlarged stomach, with slower gastric emptying, and a weigh 20% less than wild types. These functional defects are reminiscent of gastrointestinal dysfunction of Parkinson disease (Fasano et al., 2015).

Other TFs have been shown to be expressed in the enteric neuronal precursors (Heanue & Pachnis, 2006) such as *Dlx1*, *Ebf3*, *Hmx2*, *Hmx3*, *Etv1*, *Tbx3*, but they not been examined yet for a developmental role in these neurons, with the exception of *Tbx3*, which I will treat in the second part of this introduction.

4. THE TRANSCRIPTION FACTOR *TBX3*

I. The T-Box family of TFs

Tbx3 is a TF of the T-box family that now counts around 20 members all sharing the "T-box" domain: a 180 amino acids DNA-binding domain. These TFs have various roles during development in metazoans, ranging from sponges to humans (Sebé-Pedrós & Ruiz-Trillo, 2017).

II. *Tbx3* in stem cells

During mouse embryogenesis, *Tbx3* is first expressed at the morula stage (Chapman et al., 1996), which inspired research on its roles in embryonic stem cells (ESC). One of the main characteristics of ESC is their capacity of self-renewal, i.e. that they can be kept in culture without losing their differentiating properties, provided by the presence of Leukemia inhibitory factor (LIF) in the medium (Burdon et al., 2002). To know if *Tbx3* could be an actor in this self-renewal capacity, derived-ESC were cultured in the absence of LIF but with a constitutive expression of *Tbx3*, and the cells could still renew themselves without any difference, and if LIF is added to the culture later and these cells are injected in a blastocyst of mouse, pups can be born from them (Niwa et al., 2009). A possible mechanism for this action of *Tbx3* is that it regulates the expression of *Nanog* (Zhao et al., 2014) and *Oct4* (Han et al., 2010) known factors of the pluripotency of ESC. Furthermore, when *Tbx3* is blocked in culture thanks to doxycycline-inducible expression of shRNAs, the self-renewal capacity of the cells is suppressed, and the expression of *Nanog* and *Oct4* switched off within 8 days, while early markers of mesoderm differentiation are up-regulated (Ivanova et al., 2006). This mesodermal differentiation is possible due to a direct inhibiton of the Wnt pathway by Tbx3 (Waghray et al., 2015). Thus, *Tbx3* can be considered as a promoter of ESC renewal and maintenance of their undifferentiated state, in parallel with the other major transcriptional determinants of the ESC state, *Oct4*, *Nanog*, *Sox2* and *Klf4*.

During development ESC eventually differentiate into various cell types, to do so switch off the key regulators of "stemness" is needed. To study this process microRNA (miRNA) became a very interesting target: they are short non-coding RNAs being able to modulate a gene's expression by binding the 3'UTR part of an mRNA, whose it possesses the complementary sequence (Bartel, 2004). A very interesting miRNA is miR-137 because its expression is regulated by *Nanog*, *Oct4* and *Sox2* and so leads ESC self-renewal and pluripotency (Boyer et al., 2005). Because of this, miR-137 was tested for its capacity to be regulated by *Tbx3* in a luciferase reporter assay, and it appears that miR-137 reduces the level of expression of *Tbx3* directly so *Tbx3* is a target of miR-137, thereby reducing the

proliferation and inducing the differentiation of the ESC (Jiang et al., 2013). This shows that more than having the same function than master genes of ESC regulation; Tbx3 is downstream of these masters genes because they regulated *Tbx3* regulators.

The master genes of ESC regulation (*Nanog*, *Sox2*, *Oct2*, *Klf4*) are also known for being able to reprogram differentiated cells into induced pluripotent stem cells (iPSC) which can be used as models of ESC (Takahashi & Yamanaka, 2006). Due to the shared functions of *Tbx3* with these genes, it was asked whether *Tbx3* could help inducing an iPSC state: when *Tbx3* is added to the cocktail of reprogramming genes, the efficacy of reprogramming is increased as calculated by the expression of a GFP-reporter under the control of the *Oct4* promoter. The first iPSC appear at 10 days of induction instead of 16 under the standard conditions. Moreover, when *Tbx3* is among the reprogramming genes, there is a better contribution of the iPSCs to the germ-line (Han et al., 2010).

Taken all together, these studies unveil a major role of *Tbx3* in the maintenance and renewal of stem cells, as well as for the reprogramming into artificial ESCs. All these data were obtained in mouse, but similar results were described using human ESC (Esmailpour & Huang, 2012).

III. Tbx3 in cancer

Aside of these role in the maintenance of undifferentiated state and being a promoter of proliferation in ESC, Tbx3 has also been reported as an actor in tumirogenesis, alongside other member of the Tbx family (Rowley et al., 2004; Wansleben et al., 2014).

Tbx3 is expressed in a various number of cancers in human such as breast, melanoma, pancreatic, lung, ovarian, liver, head and neck (Burgucu et al., 2012; Fan et al., 2004; Hoek et al., 2004; N. Liu et al., 2012; Lomnytska et al., 2006; Renard et al., 2007). The most common one being the breast cancer in which the expression of Tbx3 is up-regulated (Douglas & Papaioannou, 2013), with a proportional increase of its expression correlating with clinicopathological parameters allowing to use Tbx3 staining on biopsy as a diagnosis (Aliwaini et al., 2019).

To fight against cancer, many genes and their related proteins are involved among them p19ARF (or p14ARF in humans) which is an activator of senescence and so avoid cancer formation by replicating aging cells (Kamijo et al., 1997). This specific pathway is inhibited by Tbx3 by down-regulating p19ARF expression (Lingbeek et al., 2002) and thus disable senescence which leads to immortalization, at least in mouse embryonic fibroblast in culture (Brummelkamp et al., 2002). On a similar way, because they are related to each other, Tbx3 is also able to suppress the expression of p53 and p21, which are both as well known for their function in apoptosis and cell cycle arrest (Carlson et al., 2002; Willem M. H. Hoogaars et al., 2008), and in particular P21 which can be directly repressed by Tbx3 binding its promoter (Willmer et al., 2016). Finally, Tbx3 also represses the

expression of PTEN, an apoptosis activator, by direct interaction with its promoter as well (Burgucu et al., 2012). By this mechanism, Tbx3 is showing a major function as an activator of survival and proliferation of cells in cancer on a very specific pathway because p53 activate p21 and PTEN, while p19ARF inhibits p53's inhibitor MDM2 (Lowe, 1999; Nakanishi et al., 2014; Kulaberoglu et al., 2016).

Asides of this, Tbx3 is also involved in the ability of cancer cells to migrate, it has been tested in melanoma cells: if they are injected with a siRNA to repress Tbx3 then the cells do not migrate and either invade a culture plate, this process is due to the capacity of Tbx3 to repress the expression of E-Cadherin, which is in charge of cell-cell contact and so tissue stability, in a human melanoma cell line there are 4 times less E-Cadherin in the presence of Tbx3, because it directly binds E-Cadherin promoter to repress it (Rodriguez et al., 2008). Similar results have also been found in human breast cancer cells (Peres et al., 2010; Mowla et al., 2011), as well as bladder cancer cells (Du et al., 2014), and in head and neck squamous cell carcinoma (HNSCC) where the silencing of Tbx3 stops the invasion of the cells and even leads them to death (Humtsoe et al., 2012) showing that this mechanism is common to several cancer involving Tbx3. Furthermore, Tbx3 is actually more than essential to promote tumor because it is sufficient: when Tbx3 is artificially expressed in a non-tumorigenic melanoma cell lines, cells are then able to form tumorigenic melanoma and invade a culture plate (Peres & Prince, 2013).

Finally, during embryonic development as well as cancer development some similar mechanisms are used, among them the silencing of specific genes by methylation: the addition of methyl groups on a gene promoter or regulator leads to the impossibility of any transcriptase to bind it and therefore its silencing (Kulis & Esteller, 2010). Several studies have then performed genome wide analysis of comparative methylation in healthy and cancer cells, Tbx3 appeared methylated in bladder and gastric cancers (Kandimalla et al., 2012; Yamashita et al., 2006). Moreover, this methylation of Tbx3 was also observed in some glioblastoma, and the patients having this methylation, and so a silenced Tbx3, had a significantly lower survival rate then the other patients (Etcheverry et al., 2010). These results lead to an ambivalent role of Tbx3 which can promote cancer growth and migration or being a tumor repressor silenced by cancer cells.

IV. Developmental roles of *Tbx3*

The first indication that *Tbx3* plays multiple roles during embryogenesis at stages much later than in the inner cell mass or extraembryonic mesoderm, came when it was recognized that in humans, heterozygous mutations of *TBX3* cause the Ulnar Mammary Syndrome (UMS, OMIM 181450) (Bamshad et al., 1997), an autosomal dominant developmental disorder. Ulnar Mammary Syndrome has a highly variable clinical presentation and is characterized by a long list of

incompletely penetrant clinical features (Ramirez & Kozin, 2014) including upper limb defects, apocrine gland hypoplasia (mammary and sweat glands), hypogenitalism, orofacial dysmorphia and abnormal teeth. Several of these developmental defects, and more, are also observed in mice heterozygous or homozygous for a null allele of *Tbx3*. However, due to differences between the phenotypes of the mouse null alleles and of the truncated or otherwise mutated human ones, it has been questioned that the human disease results from mere haplo-insufficiency, and proposed that it could also reflect abnormal gain-of-functions, including in non-transcriptional roles, such as RNA splicing (Kumar P. et al., 2014).

Predictably, it turns out to be rather difficult, in fact impossible, to extract, among all the described developmental roles of *Tbx3*, a common theme at the cellular or molecular level, at least in the current stage of our mechanistic knowledge, except for the recurrent theme that *Tbx3* often acts as a transcriptional repressor. Thus, it is unlikely that exploring its role in the enteric nervous system can benefit much from the existing literature on other body parts. I will nevertheless summarize the most salient features below:

Mammary glands: *Tbx3* is expressed first in mesenchyme then in the epithelium of the mammary glands from E11.5 to E18.5 (Chapman et al., 1996; Davenport et al., 2003; Douglas & Papaioannou, 2013). Homozygous mutant mice have no mammary placode induction and heterozygous mutants have decreased ductal tree development and failed nipple formation. This phenotype is reminiscent of the aplasia or hypoplasia of the mammary glands and nipples of human UMS. Mechanistically, *Tbx3* has been implicated in feedforward loops with Wnt and Fgf signals, and a negative feedback loop with BMPs, and as being a direct upstream negative regulator of *Lef1* and *Wnt10b*.

Limbs: *Tbx3* is expressed early, widely and dynamically in the mesenchyme and the apical ectodermal ridge of the developing limb. In homozygous nulls (but not in heterozygotes) mouse mutants morphological anomalies of the limb range from deletions of the posterior skeletal elements (digits 4 /5, and ulna/fubula) to polydactyly (Tümpel et al., 2002; Sheeba & Logan, 2017). Mechanistically, a complex web of interactions link *Tbx3* (but also *Tbx2* and *Tbx5*) with the main players of limb morphogenesis. In particular, *Tbx3* is involved through its regulation of *Tbx5* in the maintenance of the posterior *Shh+* zone of polarizing activity and, through its upregulation of *Hand2*, in setting the posterior boundary of *Gli3* expression in the anterior limb (which can explain the polydactyly). Whereas in mouse both forelimbs and hindlimbs are affected, in humans the hindlimbs are spared for an unknown reason (although an extensive list of symptoms cites cases of “short, crooked and stiff terminal phalanges of fourth to fifth tows”(Chen, 2017)).

Pituitary gland: *Tbx3* is expressed in the ventral diencephalon, which then gives rise to the infundibulum, i.e. the anlage of the neurohypophysis. In the absence of *Tbx3* the infundibulum does

not form. The development of the neurohypophysis is integrated with that of the adenohypophysis or pituitary gland, which in *Tbx3* knockouts becomes hypoplastic in a non-cell autonomous fashion. This phenotype is most likely related to the delayed puberty and other signs of hypogonadism observed in many UMS patients. Mechanistically, *Tbx3* normally sequesters *Sox2* in the ventral diencephalon, away from an enhancer in *Shh*, with the effect of blocking the expression of *Shh* whose downregulation is required to form the neurohypophysis (Pontecorvi et al., 2008; Trowe et al., 2013). In the absence of *Tbx3*, the ventral diencephalon remains hyper-proliferative and acquires an abnormal cellular architecture.

In addition to these three organs, homozygous null mice have developmental defects which are not found in the human syndrome (either because one dose of *Tbx3*, or other co-expressed members of the *Tbx3* family, are sufficient to rescue these defects) but nevertheless unveil further developmental roles of *Tbx3*:

Heart: *Tbx3* null homozygotes die at around mid-gestation, a major cause of death being attributed to heart defects (W. M. H. Hoogaars et al., 2007; Mesbah et al., 2008). *Tbx3* is expressed early on in the "non-chamber myocardium" where it represses the program for myocardium formation and allows the formation of the atrioventricular canal, the cardiac conduction system, and the cardiac outflow tract. As a consequence, *Tbx3* inactivation disrupts early morphogenetic events and leads to ventricular septal defects, delays in heart looping and outflow tract malformations. In addition, *Tbx3* (together with *Tbx18* and *Sox2*) later directs the formation of the heart pacemaker, the sinoatrial node (Mohan et al., 2018). It does so in part by repressing the atrial differentiation program in the precursors of the sinoatrial node. As a consequence, a series of hypomorphic alleles of *Tbx3* lead to pre and post-natal arrhythmias (Frank et al., 2012).

The general lack of cardiac phenotype in humans (although two cases have been reported (Ramirez & Kozin, 2014)) could be explained by different dosage requirements, or redundancy among the 6 members of the T-box family reported to play a role in heart development (Willem M. H. Hoogaars et al., 2007; Plageman & Yutzey, 2005) especially *Tbx2*, *Tbx4* or *Tbx5* which, together with *Tbx3* form the *Tbx2* subfamily (Papaioannou, 2014) by virtue of coming from a common ancestor gene after two duplication (Agulnik et al., 1996).

Lungs: *Tbx3*, together with *Tbx2*, is expressed in the lung mesenchyme where they both play a key role in lung branching morphogenesis by maintaining the "mesenchymal signaling center" crucial to epithelial branching. They are activated by *Shh*, *Wnt* and other signaling molecules secreted by the overlying epithelium, and in the mesenchyme inhibit cell-cycle dependent kinases involved in cell cycle arrest, as well as *Shisa3* and *Frzb*, diffusible inhibitors of the pro-proliferative Wnt pathway. As a consequence, inactivation of *Tbx3* leads to hypomorphic lungs (Lüdtke et al., 2016).

Finally, and possibly more relevant to the topic of my thesis, *Tbx3* is expressed in several classes of neurons (Eriksson & Mignot, 2009; Heanue & Pachnis, 2006)'. Expression in the hypothalamus and in the enteric nervous system prompted the first studies of its neuronal function (López et al., 2018; Quarta et al., 2019). In the hypothalamus, *Tbx3* is specific for several types of neurons of the arcuate nucleus, previously defined by their neuropeptide content: pro-opiomelanocortin (*Pomc*) and Agouti-related protein (*Argp*) neurons. Based on a lineage tracing strategy, conditional inactivation of the gene (with a *Pomc*::*Cre* recombinase) either during embryogenesis or postnatally does not impede the production or survival of these neurons, at least until adulthood, but it downregulates several peptides (*Pomc*, *Npy* and *Carpt*) and makes their level of synthesis irresponsive to feeding patterns (which they normally respond to). In vitro evidence corroborates the fact that *Tbx3* transcriptionally regulates *Pomc*, *Npy* and *Carpt*. Collectively, the data implicate *Tbx3* in the peptide content of energy-responsive neurons during feeding and fasting, and hence the regulation of energy homeostasis. A caveat of this study though, which the authors do not discuss, is that the inactivation triggered after the initial expression of *Pomc*, thus of *Tbx3*, cannot rule out an additional and earlier role of *Tbx3*, i.e. in the generation or initial differentiation of these neurons.

The role of *Tbx3* in the development of enteric neurons has been the occasion of one publication so far (see below).

V. *Tbx3* and the enteric nervous system

Tbx3 expression in the ENS was first reported in (Heanue & Pachnis, 2006). In this paper, an RNA microarray differential screen on the mouse gut, in wild type versus Ret KO E15.5 embryos (the latter being a model of Hirschprung disease, and completely devoid of enteric neurons (Uesaka et al., 2008)) retrieved hundreds of differentially expressed genes, by definition candidate markers of enteric neurons. Among them were two transcription factors previously undescribed in the ENS, Etv1 and Tbx3. Expression of Tbx3 in the ENS was confirmed by in situ hybridization on sections of embryonic gut, where neuronal expression appears as a dotted pattern at the periphery of the gut wall, as seen in the figure below (Tbx3 in the lower left panel):

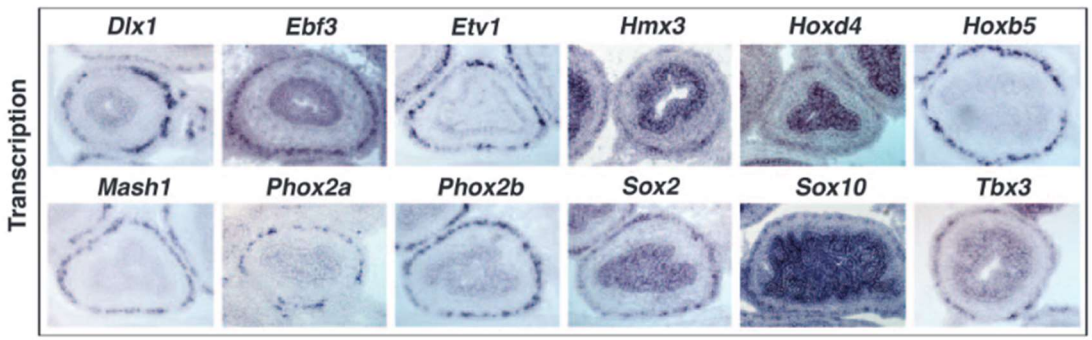

A similar approach was used by (López et al., 2018) who performed a microarray differential analysis between neuronal and non-neuronal cells of the gut, sorted thanks to a EYFP reporter driven by Wnt1 (a signaling factor expressed in neural crest precursors, from which all enteric neurons derive). Several transcription factors were found enriched in the EYFP+ versus the EYFP- cell fraction, including Tbx3, as summarized in the heatmap below:

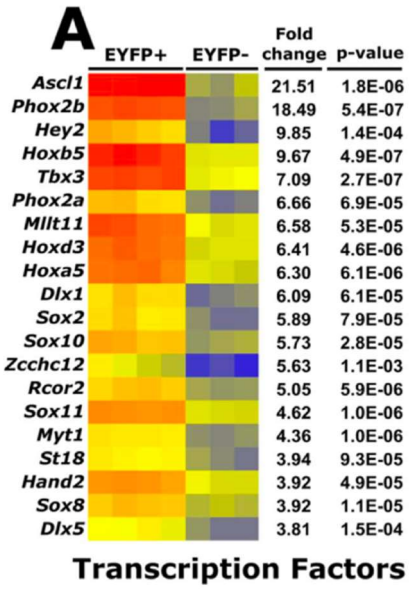

A more detailed transcriptomic analysis of gene expression in the murine ENS was published by (Memic et al., 2018), who performed multiple pairwise comparisons between 3 cell populations: ENS progenitors (marked by a YFP transgene driven by Sox10, a marker for dividing neural crest progenitors), ENS neural cells —including progenitors, glia and neurons — marked by a YFP transgene driven by Wnt1), and gut non-neural cells (YFP—) at two developmental stages, E11.5 and E15.5. Tbx3 was found enriched at both stages in both progenitors and total neural cells. Immunofluorescence on sections of embryonic gut confirmed the expression in progenitors and post-mitotic neurons from E11 to E19, at the level of both stomach and intestine. This expression was conserved in human embryos at developmental stages W5 and W10, as summarized in the following table:

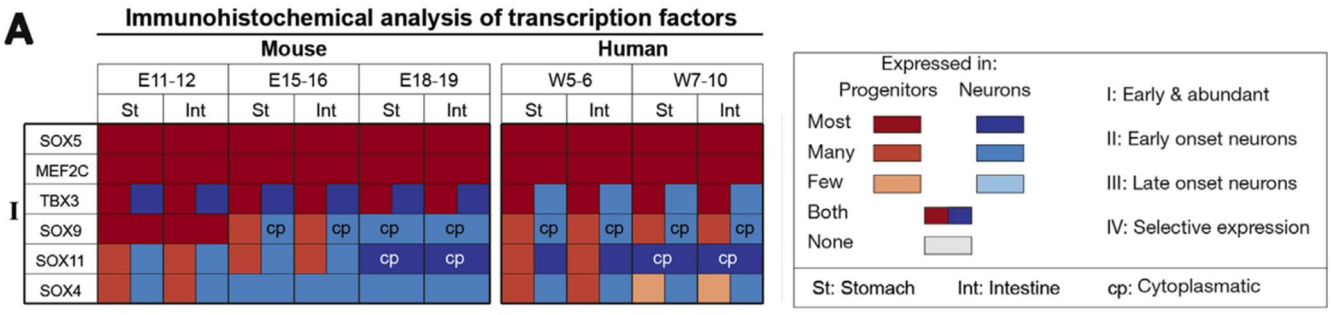

An example of immunofluorescence is shown (at an unspecified stage) where Tbx3 was detected in Sox10+ progenitors (yellow arrowheads) and in HUC/D+ neurons (white arrowheads):

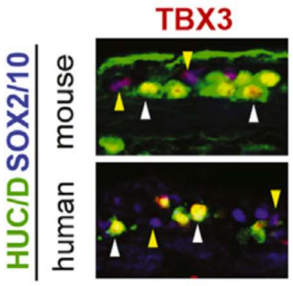

In mouse, the following chronology of expression was found:

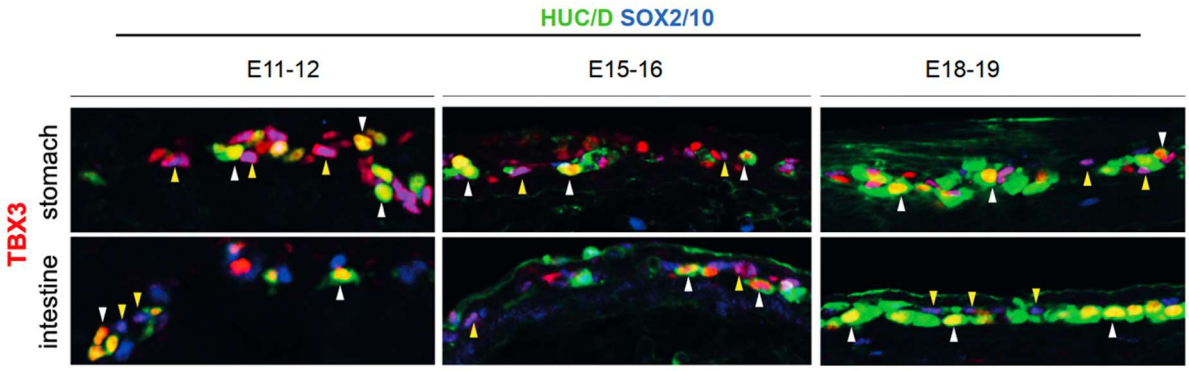

Although not commented in the paper, from the above picture it remains possible that, in the stomach, expression of Tbx3, while present in all neural cells from E11 to E16, is down regulated specifically in some neurons at E18-19 (but maintained in Sox10+ cells which, at this stage, could represent progenitors or glia). At the same stage, most neurons in the intestine are Tbx3+.

(López et al., 2018) went on to analyze the function of Tbx3 in the enteric nervous system, by crossing a floxed allele of Tbx3 (Frank et al., 2013) with a Wnt1::Cre allele, thus deleting Tbx3 in all neural crest cells and their derivatives. While this conditional inactivation scheme prevented the cardiovascular death at mid-gestation of constitutive knockouts (Frank et al., 2012), an unexpected consequence was that the pups died at birth with a cleft palate. The defect in palatal fusion (already partially described as requiring Tbx2 and/or Tbx3 (Zirzow et al., 2009), prevented feeding at birth, precluding postnatal analysis of digestive function. Analysis of embryos and newborns demonstrated a normal colonization of the entire gut by the neural crest, and a normal number of neurons at P0. The total number of Sox10+ cells — presumably representing both progenitors and glia at this stage — was slightly decreased in the “distal small intestine”, and the mature glia (marked by both Sox10

and S100β) was decreased in the small intestine, proximal and distal, by 24% and 48% respectively. This potential role of Tbx3 is glial differentiation, however, was attributed to an activity in early glial progenitors, because Tbx3 was switched off in both Sox10+ or S100+ cells (the latter being a subset of the former) at P0, as seen on panels P and Q of the following figure:

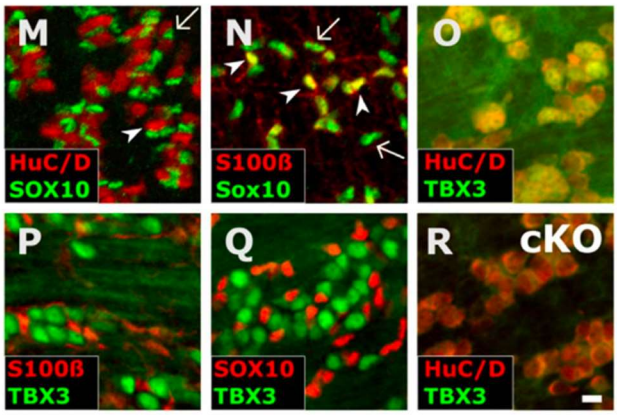

The *Tbx3* negativity of the Sox10-positive cells at P0 is surprising given the positivity reported by (Memic et al., 2018) at E19, which in practice represents P0 in most laboratory mouse strains.

In a functional test of intestinal transit at P0, the tracer fluorescein isothiocyanate (FITC)-dextran was fed to pups, and was transported at a normal rate in Wnt1::Cre;Tbx3lox/lox mutants compared to controls, all the way to the small intestine in 6 hours (the colon not being reached at this time point even in wild types). Thus, no disturbance of the intestinal function was detected in the narrow time window that could be explored.

5. *HMX2* AND *HMX3* IN DEVELOPMENT

I. *Hmx2* and *Hmx3* during embryonic development

Hmx2 and *Hmx3*, together with *Hmx1*, form the *Hmx* family of homeobox transcription factors. The literature concerning these genes is complicated by several changes of names and parallel work on different animal models. The first *Hmx* gene was called *H6* at its discovery (now *Hmx1*), when it was isolated from a cDNA library of the human craniofacial region, screened for homeobox genes (Stadler et al., 1992). Three years later, two novel homeobox genes were cloned in mouse and found to resemble the drosophila gene *Nk1* gene and, despite a slight sequence divergence from the NK family (and without recognizing that they formed a separate family), were called *Nkx5.1* and *Nkx5.2* (now respectively *Hmx3* and *Hmx2*), which are closely linked on the same chromosome (7 in mouse, and 10 in humans) (Bober et al., 1994; W. Wang & Lufkin, 1997). These three genes are likely present in all mammals (Stadler et al., 1995). Their homeodomain is very similar (although, with 5 amino acid differences between *Hmx2* and *Hmx3*, the conservation is less than for other pairs of paralogous homeodomains, such as *Phox2a* and *Phox2b* which have identical homeodomains).

The developmental expression of *Hmx2* and *Hmx3* overall has not been studied in great detail and mostly with now outdated techniques such as radioactive in situ hybridization, imprecise ones like wholemount in situ hybridization or indirect ones, like knock-ins of *LacZ* reporter genes (e.g. (Weidong Wang et al., 2000) or *Cre* recombinase (Niquille et al., 2018) and some interpretations should be taken with caution. For example *Hmx2* was found expressed in sympathetic ganglia at E12.4 (Wang et al., 2000), based on sections though a *Hmx2::LacZ* embryo, but no sympathetic expression was detected by in situ hybridization at E13.5 (I. Espinosa-Medina et al., 2016a) or by single cell transcriptomics at P5 (unpublished data from my lab). No antibody exists to our knowledge, and the Alllen Brain Atlas or Genepaint database do not provide a clear pattern for either gene.

The best studied expression (and the best studied loss-of-function phenotype) is by far in the inner ear where Hmx3 expression starts at E8.5 in otic placode and *Hmx2* expression 0.5 day later (Rinkwitz-Brandt et al., 1996; Wang et al., 2001). Mouse lacking *Hmx3* give birth to a decreased ratio of homozygous null mutants ($Hmx3^{-/-}$), display a reduced capacity of pregnancy in the females, and a highly abnormal locomotory behavior: they continuously locomote in circles, stopping only to groom, feed and sleep, suggesting a defect in the inner ear. Indeed, the mutants present a non-separation of the utricle and saccule during development of the inner ear, leading to a reduced sensory epithelial

area for both; aside from this, the horizontal semi-circular duct is not properly shaped, hence a non-properly working inner ear and a loss of equilibrium. The expression of *Hmx2* and *Hmx1* remain unchanged by the lack of *Hmx3* (Wang et al., 1998).

The case of *Hmx2* was examined some years later. Mice lacking *Hmx2* also present a circling behavior, in this case combined with head tilting. Unlike *Hmx3*, the loss of *Hmx2* leads to the complete absence of the 3 semi-circular ducts as well as a fused utricle and saccule, all of this entailing a general 60% decrease of the number of neurons in the inner ear at E18.5 (due to a decrease of cell proliferation during development, rather than premature cell death) (Wang et al., 2001).

The similar pattern of expression of *Hmx2* and *Hmx3* in the inner ear, and the fact that the expression of the later gene (*Hmx2*) does not depend on the earlier one (*Hmx3*) suggested the possibility of a partial redundancy and inspired the creation of a double mutant. This was not trivial since the two genes are separated by only 8kb (Wang et al., 2004), which in practice prevents recombination between the two loci. Thus, a third knockout line was created, with a 11 kb deletion encompassing the two genes. Animals lacking both *Hmx2* and *Hmx3* die at around 5 days after birth with a more severe loss of balance than either single knockout: starting at day 3 the *Hmx2*$^{-/-}$*;Hmx3*$^{-/-}$ pups show a fully penetrant loss of balance and are incapable of righting themselves. The inner ear of *Hmx2/3* knockouts develops normally until E12.5 but then starts to degenerate and the vestibular part of the inner ear is completely missing at E18.5. At the molecular level, the expression of a number of early markers of the otic vesicle is altered as early as E11.5, among them *Bmp4*, *FoxG1*, *Pax2*, and *Dlx5*. The double knockout also shows a complete absence of *Netrin1* around the otic vesicle, while its expression was not affected in either *Hmx2* or *Hmx3* simple knockout, showing shared redundant functions, for some aspects at least. At the moment of their death, pups lacking *Hmx2/3* present dwarfism which can be explained by a 40% reduction of circulating Growth Hormone, as well as a complete loss of Growth Hormone Releasing Hormone in the arcuate nucleus of the hypothalamus, attributed to the absence of expression of *Gsh1*, which is regulated by Hmx2/3 only in this specific nucleus (Wang et al., 2004).

Hmx genes are well conserved in evolution. Not only the homeodomain of the *Hmx* genes is very similar to that of the ancestral unique orthologue in Drosophila (Wang et al., 2000), but the latter can rescue a great part of the phenotype of *Hmx2/3* double mutants, in particular the lethality and growth deficit, the inner ear phenotype persisting albeit with a variable penetrance (Wang et al., 2004).

II. Expression of *Hmx2/3* in the Nervous system

In addition to the inner ear and the arcuate nucleus, *Hmx2* and *Hmx3* are expressed in other regions of the nervous system, without any clear function established yet. As early as E10.5, they are both expressed all along the spinal cord (probably in interneurons), as well as in dorsal root ganglia; later at E11.5 they can be detected in midbrain, hindbrain and trigeminal ganglia (Bober et al., 1994). Hmx3 is also expressed in the preoptic area from where are generated many neurons populating the striatum, olfactory bulb, septum, amygdala or GABAergic interneurons in the cortex (D. Gelman et al., 2011; D. M. Gelman et al., 2009). More precisely, *Hmx3* expressing progenitors were shown, by lineage tracing to give rise to the neurogliaform cortical interneurons, an important inhibitory interneuron type in the cortex (Niquille et al., 2018). The function of *Hmx3* in these neuronal types is however unexplored.

The expression of *Hmx2* and *Hmx3* was also reported in the peripheral nervous system (Bober et al., 1994) and more recently established as differential marker of parasympathetic ganglia versus sympathetic ones (Espinosa-Medina et al., 2016). These two genes are also found to be expressed in the enteric nervous system (Heanue & Pachnis, 2006), in the same study that uncovered *Tbx3*:

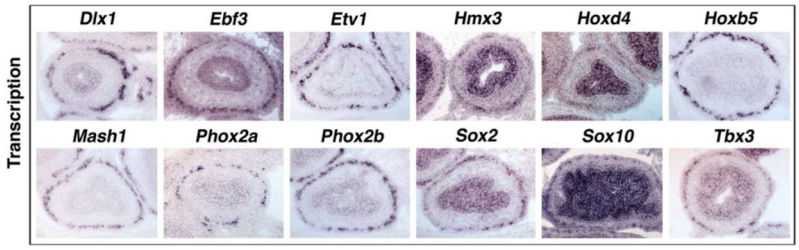

In situ hybridization of transcription factors in the enteric nervous system at E15.5.
Image reproduced from (Heanue & Pachnis, 2006)

Common expression of *Hmx3* in the ENS and parasympathetic ganglia might be considered as an additional trait shared by these two divisions of the autonomic nervous system. No functional study was made so far.

Results

Article 1

The Sacral Autonomic Outflow is Sympathetic

Espinosa-Medina I., Saha O., Boismoreau F., Chettouh Z., Rossi F., Richardson W.D., Brunet J.-F.

Science, 2016

conclude that the soluble UGT85B1 interacts with both CYP79A1 and CYP71E1, but that it is not necessary for CYP79A1-CYP71E1 complex formation (Fig. 4E). CYP79A1, CYP71E1, CYP98A1, and POR2b are situated very close together at the ER surface and have comparable pairwise FRET values (Fig. 4F and table S11). All microsomal P450s require electron donation from POR; therefore, it is not surprising that CYP98A1 is proximal to the dhurrin biosynthetic enzymes (Fig. 4, A, B, and D). UGT85B1 was situated close to the nonpartner ER membrane proteins, CYP98A1 and POR2b, when CYP79A1 and CYP71E1 were coexpressed (table S12).

A prerequisite to understanding how cells coordinate diverse metabolic activities is to understand how the enzyme systems catalyzing these reactions are organized and their possible enrollment as part of dynamic metabolons. Efforts to maximize product yield from genetically engineered pathways (*14*–*17*) would benefit from this information. In this study, we showed that the dhurrin pathway forms an efficient metabolon. CYP79A1 and CYP71E1 form homo- and hetero-oligomers, which enable recruitment of the cytosolic soluble UGT85B1 (Fig. 4G). UGT85B1 regulates the flux of L-tyrosine and stimulates channeling between CYP79A1 and CYP71E1. Efficient metabolic flux and channeling require an overall negatively charged lipid surface and may provide an additional means for regulating the dynamic assembly necessary to respond swiftly to environmental challenges. A similar organization may characterize the biosynthetic pathways of other specialized metabolites as well.

REFERENCES AND NOTES

1. R. M. Gleadow, B. L. Møller, *Annu. Rev. Plant Biol.* **65**, 155–185 (2014).
2. T. Laursen, B. L. Møller, J. E. Bassard, *Trends Plant Sci.* **20**, 20–32 (2015).
3. B. A. Halkier, B. L. Møller, *Plant Physiol.* **90**, 1552–1559 (1989).
4. O. Sibbesen, B. Koch, B. A. Halkier, B. L. Møller, *Proc. Natl. Acad. Sci. U.S.A.* **91**, 9740–9744 (1994).
5. B. L. Møller, *Science* **330**, 1328–1329 (2010).
6. K. Jørgensen *et al.*, *Curr. Opin. Plant Biol.* **8**, 280–291 (2005).
7. S. An, R. Kumar, E. D. Sheets, S. J. Benkovic, *Science* **320**, 103–106 (2008).
8. K. Mohr, E. Kostenis, *Nat. Chem. Biol.* **7**, 860–861 (2011).
9. S. C. Lee *et al.*, *Nat. Protoc.* **11**, 1149–1162 (2016).
10. T. Laursen *et al.*, *ACS Chem. Biol.* **9**, 630–634 (2014).
11. Materials and methods are available as supplementary materials on *Science* Online.
12. H. M. Ting *et al.*, *New Phytol.* **199**, 352–366 (2013).
13. J. E. Bassard *et al.*, *Plant Cell* **24**, 4465–4482 (2012).
14. I. Wheeldon *et al.*, *Nat. Chem.* **8**, 299–309 (2016).
15. C. Singleton, T. P. Howard, N. Smirnoff, *J. Exp. Bot.* **65**, 1947–1954 (2014).
16. G. Farré *et al.*, *Annu. Rev. Plant Biol.* **65**, 187–223 (2014).
17. J. E. Dueber *et al.*, *Nat. Biotechnol.* **27**, 753–759 (2009).

ACKNOWLEDGMENTS

This research was supported by the VILLUM Research Center for Plant Plasticity; by the bioSYNergy program of Center for Synthetic Biology (University of Copenhagen Excellence Program for Interdisciplinary Research); by a European Research Council Advanced Grant to B.L.M. (ERC-2012-ADG_20120314); and by funding from the VILLUM Foundation Young Investigator Programme to N.S.H. T.L. is recipient of a fellowship awarded by the VILLUM Foundation (project no. 95-300-73023). K.B. was supported by the P4FIFTY Marie Curie Initial Training Network (European Union's 7th Framework Programme). D.S. acknowledges funding from Innovation Fund Denmark (project no. 001-2011-4). F.T. and M.R.W. were supported by grants from the National Research Foundation of Singapore (NRFI2015-05) and a Biomedical Research Council–Science and Engineering Research Council joint grant (112 148 0006) from the Singapore Agency for Science, Technology and Research. T.R.D. acknowledges Biological and Biotechnology Science Research Council grants (BB/J017310/1 and BB/K004441/1). Imaging data were collected at the Center for Advanced Bioimaging, University of Copenhagen. We thank B. A. Halkier, C. Martin, A. Schulz, D. Werck-Reichhart, and anonymous reviewers for critical review of this manuscript. The supplementary materials contain additional data.

SUPPLEMENTARY MATERIALS

www.sciencemag.org/content/354/6314/890/suppl/DC1
Materials and Methods
Figs. S1 to S10
Tables S1 to S14
References (*18*–*30*)
Movies S1 and S2
Data S1 to S6

27 May 2016; accepted 4 October 2016
10.1126/science.aag2347

NEURODEVELOPMENT

The sacral autonomic outflow is sympathetic

I. Espinosa-Medina,[1]* O. Saha,[1]* F. Boismoreau,[1] Z. Chettouh,[1] F. Rossi,[1] W. D. Richardson,[2] J.-F. Brunet[1]†

A kinship between cranial and pelvic visceral nerves of vertebrates has been accepted for a century. Accordingly, sacral preganglionic neurons are considered parasympathetic, as are their targets in the pelvic ganglia that prominently control rectal, bladder, and genital functions. Here, we uncover 15 phenotypic and ontogenetic features that distinguish pre- and postganglionic neurons of the cranial parasympathetic outflow from those of the thoracolumbar sympathetic outflow in mice. By every single one, the sacral outflow is indistinguishable from the thoracolumbar outflow. Thus, the parasympathetic nervous system receives input from cranial nerves exclusively and the sympathetic nervous system from spinal nerves, thoracic to sacral inclusively. This simplified, bipartite architecture offers a new framework to understand pelvic neurophysiology as well as development and evolution of the autonomic nervous system.

The allocation of the sacral autonomic outflow to the parasympathetic division of the visceral nervous system—as the second tier of a "cranio-sacral outflow"—has an ancient origin, yet a simple history: It is rooted in the work of Gaskell (*1*), was formalized by Langley (*2*), and has been universally accepted ever since [as in (*3*)]. The argument derived from several similarities of the sacral outflow with the cranial outflow: (i) anatomical—a target territory less diffuse than that of the thoracolumbar outflow, a separation from it by a gap at limb levels, and a lack of projections to the paravertebral sympathetic chain (*1*); (ii) physiological—an influence on some organs opposite to that of the thoracolumbar outflow (*4*); and (iii) pharmacological—an overall sensitivity to muscarinic antagonists (*2*). However, analysis of cellular phenotype was lacking. Here, we define differential genetic signatures and dependencies for parasympathetic and sympathetic neurons, both pre- and postganglionic. When we reexamine the sacral autonomic outflow of mice in this light, we find that it is better characterized as sympathetic than parasympathetic.

[1]Institut de Biologie de l'École Normale Supérieure (IBENS), INSERM, CNRS, École Normale Supérieure, Paris Sciences et Lettres Research University, Paris, 75005 France. [2]Wolfson Institute for Biomedical Research, University College London, London, UK.
*These authors contributed equally to this work †Corresponding author. Email: jfbrunet@biologie.ens.fr

Cranial parasympathetic preganglionic neurons are born in the "pMNv" progenitor domain of the hindbrain (*5*) that expresses the homeogene *Phox2b* and produces, in addition, branchiomotor neurons (*6*). The postmitotic precursors migrate dorsally (*7*) to form nuclei (such as the dorsal motor nucleus of the vagus nerve) and project through dorsolateral exit points (*7*) in several branches of the cranial nerves to innervate parasympathetic and enteric ganglia. In contrast, thoracic and upper lumbar (hereafter "thoracic") preganglionic neurons, which are sympathetic, are thought to have a common origin with somatic motoneurons (*8*, *9*). By implication, they would be born in the pMN progenitor domain (just dorsal to p3)—thus from progenitors that express the basic helix-loop-helix (bHLH) transcription factor Olig2 (*10*). The sympathetic preganglionic precursors then segregate from somatic motoneurons to form the intermediolateral column in mammals (*11*), project in the ventral roots of spinal nerves together with axons of somatic motoneurons, and, via the white rami communicantes, synapse onto neurons of the paravertebral and prevertebral sympathetic ganglia.

We sought to compare the genetic makeup and dependencies of lower lumbar and sacral (hereafter "sacral") preganglionic neurons with that of cranial (parasympathetic) and thoracic (sympathetic) ones. As representative of cranial preganglionic neurons, we focused on the dorsal motor nucleus of the vagus nerve, a cluster of

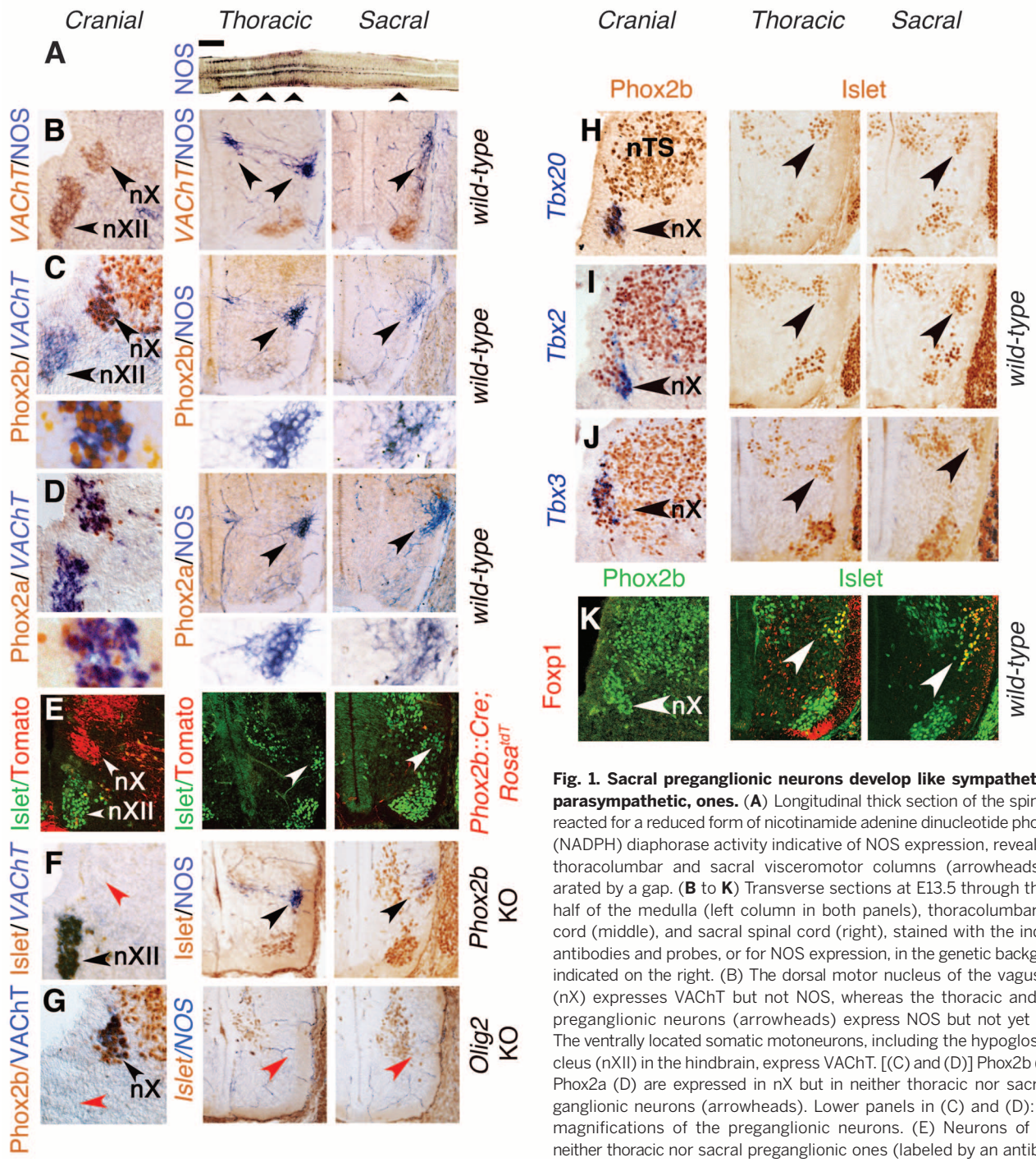

Fig. 1. Sacral preganglionic neurons develop like sympathetic, not parasympathetic, ones. (**A**) Longitudinal thick section of the spinal cord reacted for a reduced form of nicotinamide adenine dinucleotide phosphate (NADPH) diaphorase activity indicative of NOS expression, revealing the thoracolumbar and sacral visceromotor columns (arrowheads) separated by a gap. (**B** to **K**) Transverse sections at E13.5 through the right half of the medulla (left column in both panels), thoracolumbar spinal cord (middle), and sacral spinal cord (right), stained with the indicated antibodies and probes, or for NOS expression, in the genetic backgrounds indicated on the right. (B) The dorsal motor nucleus of the vagus nerve (nX) expresses VAChT but not NOS, whereas the thoracic and sacral preganglionic neurons (arrowheads) express NOS but not yet VAChT. The ventrally located somatic motoneurons, including the hypoglossal nucleus (nXII) in the hindbrain, express VAChT. [(C) and (D)] Phox2b (C) and Phox2a (D) are expressed in nX but in neither thoracic nor sacral preganglionic neurons (arrowheads). Lower panels in (C) and (D): higher magnifications of the preganglionic neurons. (E) Neurons of nX but neither thoracic nor sacral preganglionic ones (labeled by an antibody to Islet1/2, white arrowheads) derive from Phox2b^{+} precursors, permanently labeled in a Phox2b::Cre;Rosa^{tdT} background. (F) nX is missing in Phox2b knockouts (red arrowhead), but thoracic and sacral preganglionic neurons are spared (black arrowheads). (G) nX is spared in Olig2 knockouts (black arrowhead), but thoracic and sacral preganglionic neurons are missing (red arrowheads). nXII is also missing, as expected of a somatic motor nucleus (red arrowhead). [(H) to (J)] Tbx20, Tbx2, and Tbx3 are expressed in all or a subset of nX neurons (arrowheads in panels of the left column) but in no thoracic or sacral preganglionic neuron (arrowheads in panels of the middle and right columns). (K) Foxp1 is not expressed in the nX (arrowhead in left column) but is a marker of both thoracic and sacral preganglionic neurons (arrowheads in middle and right columns). nTS, nucleus of the solitary tract. Scale bars: 1 mm (A), 100 μm [(B) to (K)].

neurons already well delineated at 13.5 days of embryonic development (E13.5), that expresses the vesicular acetylcholine transporter (VAChT) (Fig. 1B). Thoracic and sacral preganglionic neurons, which both form a mediolateral column in the spinal cord, did not express VAChT at this stage despite their eventual cholinergic nature. To localize them, we thus used their common marker nitric oxide synthase (NOS) (*12*) (Fig. 1, A and B), which was absent from the dorsal motor nucleus of the vagus nerve at E13.5 (Fig. 1B) or later (fig. S1). Thus, NOS expression characterizes thoracic and sacral, but not cranial, preganglionic neurons.

In contrast to cranial (parasympathetic) preganglionic neurons, thoracic (sympathetic) ones

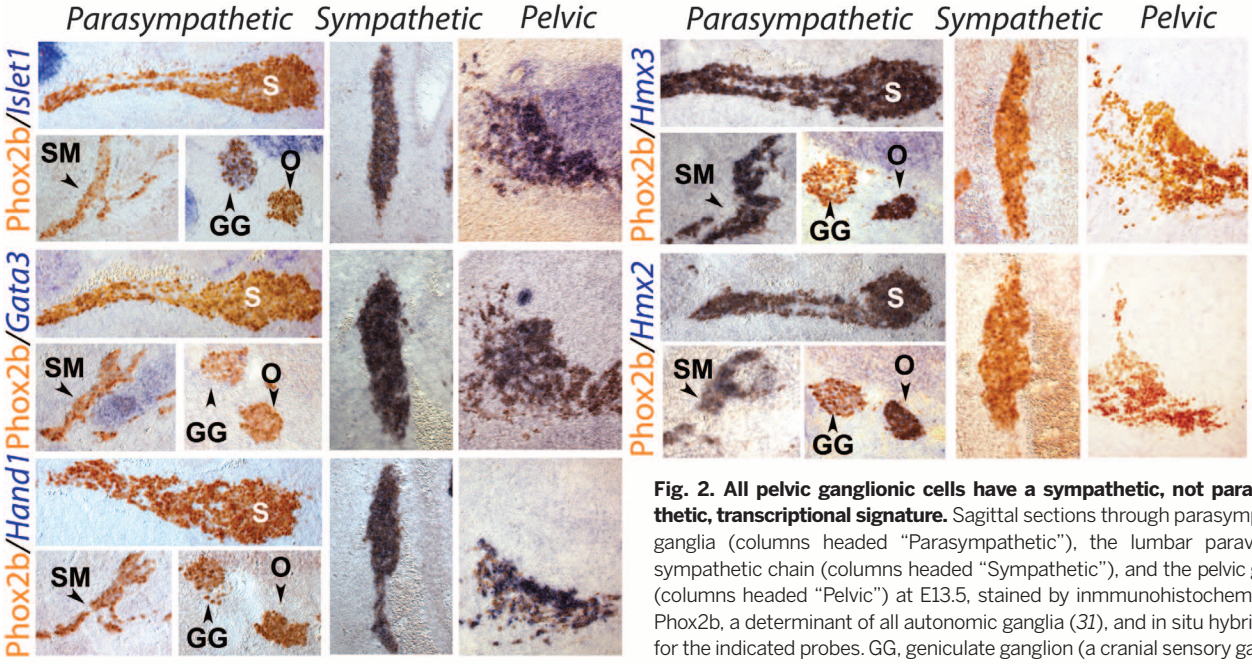

Fig. 2. All pelvic ganglionic cells have a sympathetic, not parasympathetic, transcriptional signature. Sagittal sections through parasympathetic ganglia (columns headed "Parasympathetic"), the lumbar paravertebral sympathetic chain (columns headed "Sympathetic"), and the pelvic ganglion (columns headed "Pelvic") at E13.5, stained by inmmunohistochemistry for Phox2b, a determinant of all autonomic ganglia (*31*), and in situ hybridization for the indicated probes. GG, geniculate ganglion (a cranial sensory ganglion); O, otic ganglion; S, sphenopalatine ganglion; SM, submandibular ganglion (all parasympathetic ganglia).

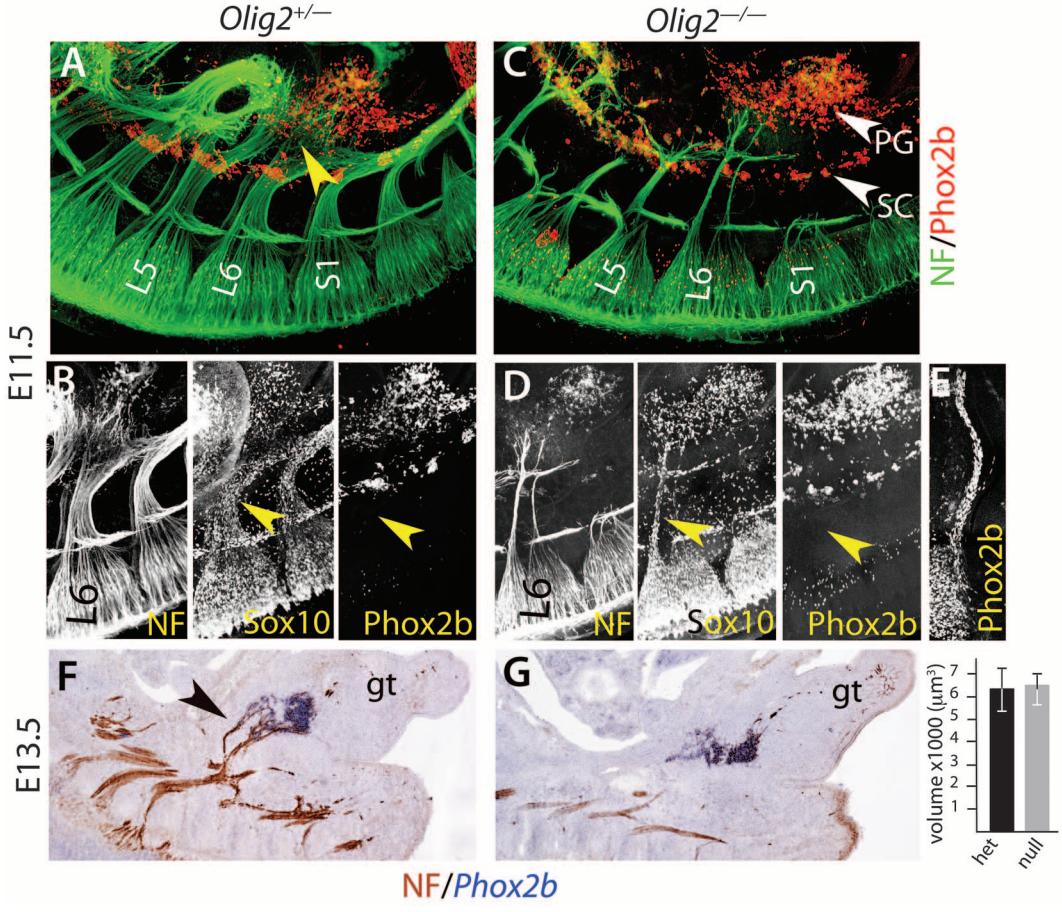

Fig. 3. The pelvic ganglion forms independently of its nerve, like sympathetic and unlike parasympathetic ones. (**A** and **C**). Whole-mount immunofluorescence with the indicated antibodies on E11.5 embryos either heterozygous (A) or homozygous (C) for an *Olig2* null mutation. The nascent pelvic nerves [yellow arrowhead in (A)] seem to derive mostly from the L6 nerve at that stage. The Olig2 null mutation (C) spares two thin sensory pelvic projections. The pelvic ganglion (PG) lies ahead of most fibers in both heterozygous and mutant background. (**B** and **D**). View of the L6 nerve, covered with Sox10^{+} cells but no Phox2b^{+} cells (yellow arrowheads), unlike cranial nerves that give rise to parasympathetic ganglia at the same stage [Jacobson's nerve in (**E**)]. (**F** and **G**) In situ hybridization for Phox2b and immunohistochemistry for neurofilament (NF) on heterozygous and homozygous Olig2 knockouts at E13.5, when parasympathetic ganglia have formed elsewhere in the body. Graph: the pelvic ganglion has the same volume whether its preganglionic nerve is present [black arrowhead in (F)] or not (6369 µm^3 ± 1066 versus 6441 µm^3 ± 919, $P = 0.96$, $n = 5$ embryos). gt, genital tubercle; L5 and L6, 5th and 6th lumbar roots; S1, 1st sacral root; SC, sympathetic chain.

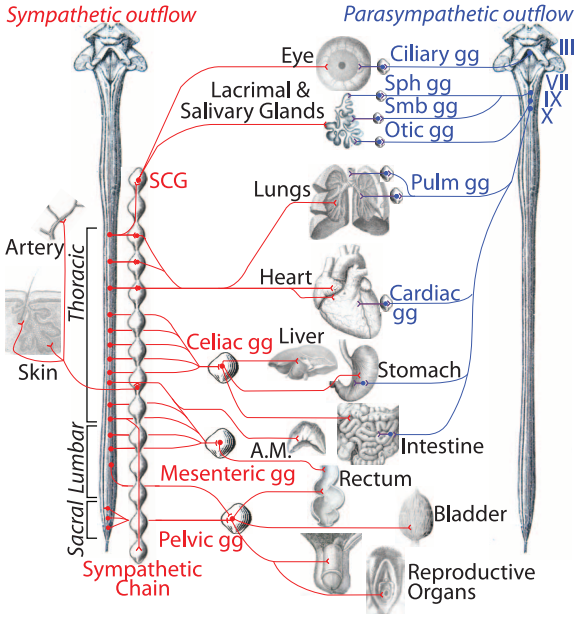

Fig. 4. Revised anatomy of the autonomic nervous system. The efferent path of the autonomic nervous system is made up of a spinal sympathetic outflow (left, in red) and a cranial parasympathetic outflow (right, in blue). Sympathetic targets in the skin other than arteries are piloerector muscles and sweat glands. III, oculomotor nerve; VII, facial nerve; IX, glossopharyngeal nerve; X, vagus nerve; A.M., adrenal medulla; gg, ganglion; Pulm, pulmonary; SCG, superior cervical ganglion; Sph, sphenopalatine; Smb, submandibular. For a larger version, see fig. S11.

not only failed to express Phox2b or its paralogue Phox2a at E13.5 but also arose from Phox2b-negative progenitors and did not depend on Phox2b for their differentiation (Fig. 1, C to F, left and middle columns) but instead depended on Olig2 (Fig. 1G). Sacral preganglionic neurons shared all these features with thoracic ones (Fig. 1, C to G, middle and right columns). At E13.5, the T-box transcription factors Tbx20, Tbx2, and Tbx3 were expressed by cranial (parasympathetic) neurons but by neither thoracic (sympathetic) nor sacral preganglionic ones (Fig. 1, H to J, and fig. S2). The F-box transcription factor Foxp1, a determinant of thoracic preganglionic neurons (*13*), was expressed by sacral but not cranial preganglionic neurons (Fig. 1K). Differential expression of Phox2b, Tbx20, and FoxP1 between cranial and all spinal preganglionic neurons, thoracic and sacral, was still observed at E16.5 (fig. S3). In sum, the ontogeny and transcriptional signature of sacral preganglionic neurons was indistinguishable from that of thoracic ones and therefore sympathetic as well.

Thoracic and sacral preganglionic neurons share a settling site in the mediolateral region of the spinal cord and a ventral exit point for their axons, whereas cranial preganglionics have a less systematized topography and a dorsal axonal exit point. These similarities of thoracic with sacral, and differences of both with cranial, are at odds with the notion of craniosacral outflow since its first description (*1*).

The targets of the sacral preganglionic neurons are in the pelvic plexus (figs. S4 and S5) and are considered, by definition, parasympathetic (*14*). Because a proportion of pelvic ganglionic neurons receive input from upper lumbar levels [half of them in rats (*15*)] and thus from sympathetic preganglionic neurons, the pelvic ganglion is considered mixed sympathetic and parasympathetic (*16*). This connectivity-based definition runs into a conundrum for cells that receive a dual lumbar/sacral input (*17*). The sympathetic identity of both thoracic and sacral preganglionic neurons that we unveil here makes the issue moot. Regardless, we looked for a cell-intrinsic criterion that would corroborate the sympathetic nature of all pelvic ganglionic cells in the form of genes differentially expressed in sympathetic versus parasympathetic ganglionic cells elsewhere in the autonomic nervous system. Neurotransmitter phenotypes do not map on the sympathetic/parasympathetic partition because cholinergic neurons in the pelvic ganglion comprise both "parasympathetic" and "sympathetic" ganglionic cells, as defined by connectivity (*14*), and bona fide sympathetic neurons of the paravertebral chain are cholinergic [reviewed in (*18*)]. However, we found that three transcription factors expressed and required in the sympathoadrenal lineage—Islet1 (*19*), Gata3 (*20*), and Hand1 (*21*)—were not expressed in parasympathetic ganglia such as the sphenopalatine, the submandibular, or the otic ganglia (Fig. 2 and fig. S6) [although Islet1 is expressed in ciliary ganglia (*22*) and Gata3 in cardiac ones (*20*), which thus diverge from the canonical parasympathetic molecular signature]. Conversely, we found that the two paralogous homeobox genes *Hmx2* and *Hmx3* are specific markers of all parasympathetic versus sympathetic ganglia and adrenal medulla (Fig. 2 and figs. S6 and S7). All cells of the pelvic ganglion were Islet1$^+$, Gata3$^+$, Hand1$^+$, Hmx3$^-$, and Hmx2$^-$ at E13.5 (Fig. 2) and at E16.5 (fig. S8), as were smaller scattered ganglia of the pelvic organs (fig. S8). Thus, all had a sympathetic transcriptional fingerprint. Similarly, the chicken ganglion of Remak, classically considered parasympathetic (*23*), displayed an Islet1$^+$, Hand1$^+$, Hmx3$^-$ signature, and thus is sympathetic (fig. S9).

Finally, we tested the pelvic ganglion for the contrasted modes of development of sympathetic and parasympathetic ganglia. Parasympathetic ganglia, unlike sympathetic ones, arise through the migration of Sox10$^+$/Phox2b$^+$ Schwann cell precursors along their future preganglionic nerve toward the site of ganglion formation and do not form if these nerves are absent (*24*, *25*). At E11.5, the lumbosacral plexus, which gives rise to the pelvic nerve, extended some fibers that reached the lateral and rostral edge of the pelvic ganglion anlagen, most of which was already situated well ahead of them (Fig. 3A and movie S1). These fibers were coated with Sox10$^+$ cells, none of which, though, expressed Phox2b (Fig. 3B), in contrast to the cranial nerves that produce parasympathetic ganglia at the same stage (Fig. 3E). Deletion of all motor fibers in Olig2$^{-/-}$ embryos spared only two thin, presumably sensory, projections from the lumbosacral plexus (Fig. 3C), also devoid of Phox2b$^+$ cells (Fig. 3D and fig. S10). Despite this massive atrophy, the pelvic ganglion appeared intact (Fig. 3C, fig. S10, and movie S2). This was verified quantitatively at E13.5 (Fig. 3, F and G). Thus, even though 50% of its cells are postganglionic to the pelvic nerve, the pelvic ganglion forms before and independently of it, as befits a sympathetic ganglion but contrary to parasympathetic ones.

Thus, the sacral visceral nervous system is the caudal outpost of the sympathetic outflow (Fig. 4 and fig. S11), the autonomic nervous system being divided in a cranial and a spinal autonomic system, in line with certain evolutionary speculations (*26*). This new understanding of the anatomy accounts for many data that were at odds with the previous one. For example, although schematics generally represent the sacral pathway to the rectum as disynaptic—i.e., vagal-like—[e.g., (*3*)], it is in fact predominantly (*27*) if not exclusively (*28*) trisynaptic—i.e., sympathetic-like (*29*). Despite the dogma of lumbosacral antagonism on the bladder detrusor muscle, the lumbar inhibition is experimentally absent (*4*) or of dubious functional relevance (*30*). The synergy of the lumbar and sacral pathway for vasodilatation in external sexual organs [reviewed in (*29*)] shows a continuity of action—rather than antagonism, as the old model suggested—across the gap between the thoracolumbar and sacral outflows.

The sympathetic identity of all sacral and pelvic autonomic neurons, which our data unveil, provides a new framework for discoveries on pelvic neuroanatomy and physiology.

REFERENCES AND NOTES

1. W. H. Gaskell, *J. Physiol.* **7**, 1–80.9 (1886).
2. J. N. Langley, *The Autonomic Nervous System: Part I* (W. Heffer, Cambridge, 1921).
3. E. Kandel, J. Schwartz, T. Jessell, S. Siegelbaum, A. J. Hudspeth, *Principles of Neural Science, Fifth Edition* (McGraw-Hill Professional, 2012).
4. J. N. Langley, H. K. Anderson, *J. Physiol.* **19**, 71–139 (1895).
5. J. Briscoe *et al.*, *Nature* **398**, 622–627 (1999).
6. A. Pattyn, M. Hirsch, C. Goridis, J. F. Brunet, *Development* **127**, 1349–1358 (2000).
7. S. Guthrie, *Nat. Rev. Neurosci.* **8**, 859–871 (2007).
8. A. Prasad, M. Hollyday, *J. Comp. Neurol.* **307**, 237–258 (1991).
9. J. A. Markham, J. E. Vaughn, *J. Neurobiol.* **22**, 811–822 (1991).
10. W. A. Alaynick, T. M. Jessell, S. L. Pfaff, *Cell* **146**, 178–178.e1 (2011).
11. P. E. Phelps, R. P. Barber, J. E. Vaughn, *J. Comp. Neurol.* **330**, 1–14 (1993).
12. C. R. Anderson, *Neurosci. Lett.* **139**, 280–284 (1992).

13. J. S. Dasen, A. De Camilli, B. Wang, P. W. Tucker, T. M. Jessell, *Cell* **134**, 304–316 (2008).
14. J. R. Keast, *Int. Rev. Cytol.* **248**, 141–208 (2006).
15. J. R. Keast, *Neuroscience* **66**, 655–662 (1995).
16. A. Kuntz, R. L. Moseley, *J. Comp. Neurol.* **64**, 63–75 (1936).
17. W. C. De Groat, A. M. Booth, J. Krier, in *Integrative Functions of the Autonomic Nervous System*, C. M. Brooks, K. Koizumi, A. Sato, Eds. (University of Tokyo Press, Tokyo, 1979), pp. 234–245.
18. U. Ernsberger, H. Rohrer, *Cell Tissue Res.* **297**, 339–361 (1999).
19. K. Huber *et al*., *Dev. Biol.* **380**, 286–298 (2013).
20. K. Tsarovina *et al*., *Development* **131**, 4775–4786 (2004).
21. E. Doxakis, L. Howard, H. Rohrer, A. M. Davies, *EMBO Rep.* **9**, 1041–1047 (2008).
22. L. Huber, M. Ferdin, J. Holzmann, J. Stubbusch, H. Rohrer, *Dev. Biol.* **363**, 219–233 (2012).
23. C. L. Yntema, W. S. Hammond, *J. Exp. Zool.* **129**, 375–413 (1955).
24. V. Dyachuk *et al*., *Science* **345**, 82–87 (2014).
25. I. Espinosa-Medina *et al*., *Science* **345**, 87–90 (2014).
26. S. Nilsson, in *Autonomic Nerve Function in the Vertebrates*, *Zoophysiology*, vol. 13, D. S. Farner, Ed. (Springer-Verlag, New York, 1983), chap. 2.
27. C. Olsson *et al*., *J. Comp. Neurol.* **496**, 787–801 (2006).
28. K. Fukai, H. Fukuda, *J. Physiol.* **362**, 69–78 (1985).
29. W. Jänig, *The Integrative Action of the Autonomic Nervous System: Neurobiology of Homeostatis* (Cambridge Univ. Press, Cambridge, UK, 2006).
30. W. C. de Groat, W. R. Saum, *J. Physiol.* **220**, 297–314 (1972).
31. A. Pattyn, X. Morin, H. Cremer, C. Goridis, J. F. Brunet, *Nature* **399**, 366–370 (1999).

ACKNOWLEDGMENTS

We thank the Imaging Facility of Institut de Biologie de l'École Normale Supérieure (IBENS), which is supported by grants from Fédération pour la Recherche sur le Cerveau, Région Ile-de-France DIM NeRF 2009 and 2011 and France-BioImaging. We thank A. Shihavuddin and A. Genovesio for help with image analysis, the animal facility of IBENS, C. Goridis for helpful comments on the manuscript, and all the members of the Brunet laboratory for discussions. This study was supported by the Centre National de la Recherche Scientifique, the Ecole Normale Supérieure, Institut National de la Santé et de la Recherche Médicale, Agence Nationale de la Recherche (ANR) award ANR-12-BSV4-0007-01 (to J.-F.B), Fondation pour la Recherche Médicale (FRM) award DEq. 2000326472 (to J.-F.B.), the Investissements d'Avenir program of the French government implemented by the ANR (referenced ANR-10-LABX-54 MEMO LIFE and ANR-11-IDEX-0001-02 Paris Sciences et Lettres Research University). I.E.-M. was supported by the French Ministry of Higher Education and Research and the FRM award FDT20160435297. Work in W.D.R.'s laboratory is supported by the European Research Council (grant agreement 293544) and Wellcome (100269/Z/12/Z). The supplementary materials contain additional data.

SUPPLEMENTARY MATERIALS

www.sciencemag.org/content/354/6314/893/suppl/DC1
Materials and Methods
Figs. S1 to S11
Movies S1 and S2
References (*32*–*43*)

12 July 2016; accepted 14 October 2016
10.1126/science.aah5454

PLANT SCIENCE

Phytochrome B integrates light and temperature signals in *Arabidopsis*

Martina Legris,[1] Cornelia Klose,[2]* E. Sethe Burgie,[3]* Cecilia Costigliolo Rojas,[1]* Maximiliano Neme,[1] Andreas Hiltbrunner,[2,4] Philip A. Wigge,[5] Eberhard Schäfer,[2,4]† Richard D. Vierstra,[3]† Jorge J. Casal[1,6]‡

Ambient temperature regulates many aspects of plant growth and development, but its sensors are unknown. Here, we demonstrate that the phytochrome B (phyB) photoreceptor participates in temperature perception through its temperature-dependent reversion from the active Pfr state to the inactive Pr state. Increased rates of thermal reversion upon exposing *Arabidopsis* seedlings to warm environments reduce both the abundance of the biologically active Pfr-Pfr dimer pool of phyB and the size of the associated nuclear bodies, even in daylight. Mathematical analysis of stem growth for seedlings expressing wild-type phyB or thermally stable variants under various combinations of light and temperature revealed that phyB is physiologically responsive to both signals. We therefore propose that in addition to its photoreceptor functions, phyB is a temperature sensor in plants.

Plants have the capacity to adjust their growth and development in response to light and temperature cues (*1*). Temperature-sensing helps plants determine when to germinate, adjust their body plan to protect themselves from adverse temperatures, and flower. Warm temperatures as well as reduced light resulting from vegetative shade promote stem growth, enabling seedlings to avoid heat stress and canopy shade from neighboring plants. Whereas light perception is driven by a collection of identified photoreceptors—including the red/far-red light-absorbing phytochromes; the blue/ultraviolet-A (UV-A) light–absorbing cryptochromes, phototropins, and members of the Zeitlupe family; and the UV-B–absorbing UVR8 (*2*)—temperature sensors remain to be established (*3*). Finding the identity (or identities) of temperature sensors would be of particular relevance in the context of climate change (*4*).

Phytochrome B (phyB) is the main photoreceptor controlling growth in *Arabidopsis* seedlings exposed to different shade conditions (*5*). Like others in the phytochrome family, phyB is a homodimeric chromoprotein, with each subunit harboring a covalently bound phytochromobilin chromophore. phyB exists in two photo-interconvertible forms: a red light–absorbing Pr state that is biologically inactive and a far-red light–absorbing Pfr state that is biologically active (*6*, *7*). Whereas Pr arises upon assembly with the bilin, formation of Pfr requires light, and its levels are strongly influenced by the red/far-red light ratio. Consequently, because red light is absorbed by photosynthetic pigments, shade light from neighboring vegetation has a strong impact on Pfr levels by reducing this ratio (*8*). phyB Pfr also spontaneously reverts back to Pr in a light-independent reaction called thermal reversion (*9*–*11*). Traditionally, thermal reversion was assumed to be too slow relative to the light reactions to affect the Pfr status of phyB, even under moderate irradiances found in natural environments, but two observations contradict this view. First, the formation of phyB nuclear bodies, which reflects the status of Pfr, is affected by light up to irradiances much higher than expected if thermal reversion were slow (*12*). Second, it is now clear that thermal reversion occurs in two steps. Although the first step, from the Pfr:Pfr homodimer (D2) to the Pfr:Pr heterodimer (D1), is slow (k_{r2}), the second step, from the Pfr:Pr heterodimer to the Pr:Pr homodimer (D0), is almost two orders of magnitude faster (k_{r1}) (Fig. 1A) (*11*).

Physiologically relevant temperatures could change the magnitude of k_{r1} and consequently affect Pfr and D2 levels, even under illumination (Fig. 1A). To test this hypothesis, we used in vitro and in vivo spectroscopy and analysis of phyB nuclear bodies by means of confocal microscopy. For the first of these approaches, we produced recombinant full-length phyB bearing its phytochromobilin chromophore. When irradiated under continuous red light, the in vitro absorbance at 725 nm reached lower values at higher temperatures, which is indicative of reduced steady-state levels of Pfr (Fig. 1, B and C). We calculated the differences between the steady-state absorbance spectra in darkness and continuous red light (Δ absorbance). The amplitude between the maximum and minimum peaks of Δ absorbance, which represents the amount of Pfr, strongly decreased between 10 and 30°C (Fig. 1, D and E). This characteristic of phyB differs from the typical behavior

[1]Fundación Instituto Leloir, Instituto de Investigaciones Bioquímicas de Buenos Aires–Consejo Nacional de Investigaciones Científicas y Técnicas (CONICET), 1405 Buenos Aires, Argentina. [2]Institut für Biologie II, University of Freiburg, Schaenzlestrasse 1, D-79104 Freiburg. [3]Department of Biology, Washington University in St. Louis, Campus Box 1137, One Brookings Drive, St. Louis, MO 63130, USA. [4]BIOSS Centre for Biological Signaling Studies, University of Freiburg, Schaenzlestrasse 18, 79104 Freiburg, Germany. [5]Sainsbury Laboratory, Cambridge University, 47 Bateman Street, Cambridge CB2 1LR, UK. [6]Instituto de Investigaciones Fisiológicas y Ecológicas Vinculadas a la Agricultura (IFEVA), Facultad de Agronomía, Universidad de Buenos Aires and CONICET, Avenida San Martín 4453, 1417 Buenos Aires, Argentina.
*These authors contributed equally to this work. †These authors contributed equally to this work. ‡**Corresponding author. Email: casal@ifeva.edu.ar**

Science

The sacral autonomic outflow is sympathetic

I. Espinosa-Medina, O. Saha, F. Boismoreau, Z. Chettouh, F. Rossi, W. D. Richardson and J.-F. Brunet

Science **354** (6314), 893-897.
DOI: 10.1126/science.aah5454

Sacral neurons reassigned

The autonomic nervous system regulates the function of internal organs such as the gut. The parasympathetic and sympathetic arms of this system tend to operate antagonistically. Espinosa-Medina *et al.* used anatomical and molecular analyses to reevaluate the assignment of neurons in the sacral autonomic nervous system (see the Perspective by Adameyko). Previously categorized as parasympathetic, these neurons are now identified as sympathetic. The results resolve a persistent confusion about how the two systems developed and open the avenue to more predictable outcomes in developing treatments targeted to the pelvic autonomic nervous system.

Science, this issue p. 893; see also p. 833

Science (print ISSN 0036-8075; online ISSN 1095-9203) is published by the American Association for the Advancement of Science, 1200 New York Avenue NW, Washington, DC 20005. The title *Science* is a registered trademark of AAAS.

www.sciencemag.org/content/354/6314/893/suppl/DC1

Supplementary Materials for

The sacral autonomic outflow is sympathetic

I. Espinosa-Medina, O. Saha, F. Boismoreau, Z. Chettouh,
F. Rossi, W. D. Richardson, J.-F. Brunet*

*Corresponding author. Email: jfbrunet@biologie.ens.fr

Published 18 November 2016, *Science* **354**, 893 (2016)
DOI: 10.1126/science.aah5454

This PDF file includes:

Other Supplementary Material for this manuscript includes the following:
(available at www.sciencemag.org/cgi/content/full/354/6314/893/DC1)

Movies S1 and S2

Materials and Methods

Histology.

-In situ hybridization and immunochemistry have been described in ref *(32)*.

-Diaphorase staining on cryostat sections was performed as described in ref *(33)*.

-Immunofluorescence on cryostat or vibratome sections was performed as previously described *(25)*. Whole-processed embryos where fixed overnight in 4% paraformaldehyde (in PBS) and dissected spinal cords were fixed for 2 hours at room temperature. Antigen retrieval, by boiling for 10 minutes in sodium citrate (10mM) was needed for optimal labeling with the α-Islet antibody.

Wholemount immunofluorescent staining using the 3DISCO method was adapted from ref *(34)*. All steps up to the imaging of the embryos were performed under nutation. Embryos at stage E11.5 were fixed overnight in 4% paraformaldehyde (in PBS), serially dehydrated in graded methanol (in PBS) up to 100% methanol and then bleached using Dent's bleach overnight at 4°C. Following serial washes in 100% methanol, the embryos were incubated in Dent's fixative overnight at 4°C. The embryos were then serially rehydrated in graded methanol (in PBS) up until re-immersion in PBS. Embryos were further subjected to incubation at 70°C to optimize antigen recognition by the anti-Phox2b antibody. Following washes in PBS-Tween (0.1%), tiny superficial perforations were made in the embryo with a minutien pin to facilitate antibody penetration. The embryos were then incubated with primary antibodies in blocking buffer (20% DMSO, 5% FCS in PBS) for 5 days at room temperature. Following washes in PBS-Tween (0.1%) at room temperature, secondary antibodies in blocking buffer were then applied for 4 days at room temperature. Finally, embryos were cleared following the 3DISCO protocol subsequent to washes in PBS-Tween (0.1%) at room temperature, Embryos were imaged using a SP8 confocal microscope (Leica). 3D reconstructions and videos were obtained using the IMARIS imaging software.

Antibodies

The following primary antibodies were used for immunochemistry and immunofluorescent staining:

α-2H3 (NF), Mouse, 1:500, Hybridoma Bank (#2H3)
α-bIII Tubulin (Tuj1), Mouse, 1:500, Covance (#MMS-435P)
α-dsRed, Rabbit, 1:500, Clontech (#632496)
α-Tomato, Goat, 1:1000, Sicgen (#AB0040-200)
α-Islet1:2, Mouse, 1:400 (40.2D6 and 39.4D5, Hybridoma Bank)
α-Phox2b, Rabbit, 1:500 *(35)*
α-Phox2b, Guinea Pig, 1:500 *(36)*
α-Phox2a, Rabbit, 1:500 *(37)*
α-Sox10, Goat, 1:250, Santa Cruz (#SC-17342)
α-FoxP1, Rabbit, Abcam,1:200 (#AB-16645)

The following secondary antibodies were used:

α-rabbit Cy3, 1:500, Jackson Immunoresearch Laboratories (#711-165-152)
α-rabbit A488, 1:500, Jackson Immunoresearch Laboratories (#711-545-152)
α-goat Cy3, 1:500, Jackson Immunoresearch Laboratories (#705-166-147)
α-goat A647, 1:500, Jackson Immunoresearch Laboratories (#705-606-147)
α-rabbit Cy3, 1:500, Jackson Immunoresearch Laboratories (#711-165-152)
α-mouse Cy3, 1:500, Jackson Immunoresearch Laboratories (#715-165-150)
α-mouse A488, 1:500, Invitrogen (#A-21202)
α-mouse Cy5, 1:500, Jackson Immunoresearch Laboratories (#715-175-150)

Immunohistochemical reactions were processed with the Vectastain Elite ABC kits (PK-6101 and PK-6012; Vector Laboratories) as per manufacturer's guidelines followed by colour development using DAB (3,3'-Diaminobenzidine).

Probes

For the Phox2b riboprobe, primers containing SP6 and T7 overhangs were used to amplify a 635 bp region (nucleotides 123 – 757) from a plasmid containing the full-length Phox2b cDNA sequence. The purified amplicon was then used as the template for antisense probe synthesis using T7 RNA polymerase.

Forward Primer: 5'-CCGTCTCCACATCCATCTTT-3'

Reverse Primer: 5'-TCAGTGCTCTTGGCCTCTTT-3'

The other probes were: Gata3 (gift of JD Engel), Hand1 (Stratagene), Hmx2 (gift of E.E. Turner), Hmx3 (gift of S. Mansour), Islet1 *(37)*, Tbx2 (gift of A. Kispert), Tbx3 (gift of V.M Christoffels), Tbx20 *(38)*, VAChT (Source BioScience, UK, 40129421 (CK3-a14) IMAGE clone).

Transgenic Mouse Lines:

-*Phox2b::Cre (39)*: BAC transgenic line expressing Cre under the control of the Phox2b promoter.

-*Rosa*$^{lox\text{-}stop\text{-}lox\text{-}tdTomato}$ (*Rosa*^{tdT}) *(40)*: Knock in line expressing the reporter gene tdTomato from the Rosa locus in a Cre-dependent manner.

-*Phox2b*$^{LacZ/+}$ line *(31)*: Knock in line expressing the reporter gene *LacZ* from the second exon of the *Phox2b* locus, which is disrupted and lead to a null phenotype in *Phox2b*$^{LacZ/LacZ}$ embryos.

-*Olig2Cre* line *(41)*: Knock in of Cre in the *Olig2* locus (Jackson Laboratories, Stock #25567).

All animal studies were done in accordance with the guidelines issued by the French Ministry of Agriculture and have been approved by the Direction Départementale des Services Vétérinaires de Paris.

Image Analyses.

To measure the size of the pelvic ganglion on cryosections from E13.5 *Olig2*$^{+/—}$ and *Olig2*$^{—/—}$ embryos hybridized for Phox2b and immunostained for neurofilament, we used the open source image analyses tool ilastik *(42)*. Pixels were segmented by a Random Forest Classifier into signal (corresponding to the pelvic ganglion) and background (corresponding to surrounding tissues and nerve fibers). Segmentation on one section was

optimized through an iterative training procedure based on color/intensity, edge and texture, and subsequently applied to the batch processing of all sections passing through one pelvic ganglion. Local neighborhoods for calculating edge and texture were defined as 3 X 3 pixels and 5 X 5 pixels. Finally, scattered signal areas smaller than 0.2μm2 were removed on FIJI. The remaining signal area corresponded to the pelvic ganglion and was measured on 5 to 6 consecutive sections, depending on ganglia. The volume of the ganglion was deduced by multiplying the surface by the thickness of the sections (20μm). Wild-type and mutant ganglia were compared by a paired two-tailed Student's t-test.

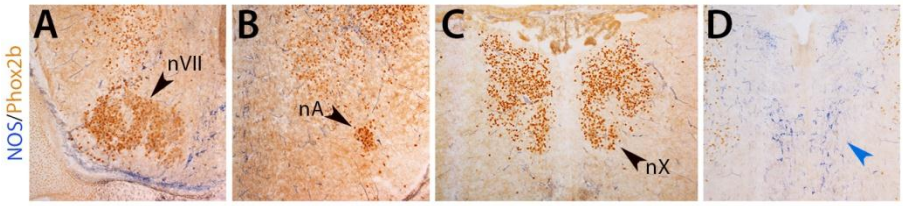

Figure S1

NOS is not expressed neither in branchiomotor neurons nor in hindbrain preganglionic neurons. Transverse sections of the hindbrain at E17.5 stained for diaphorase activity and Phox2b immunohistochemisty and passing through: (A) the facial nucleus (nVII); (B) the nucleus ambiguus (nA); (C) the dorsal nucleus of the vagus nerve (nX); (D) the pons, showing NOS+ neurons of the raphe (blue arrowhead). No double Phox2b+/NOS+ neurons were found in the hindbrain.

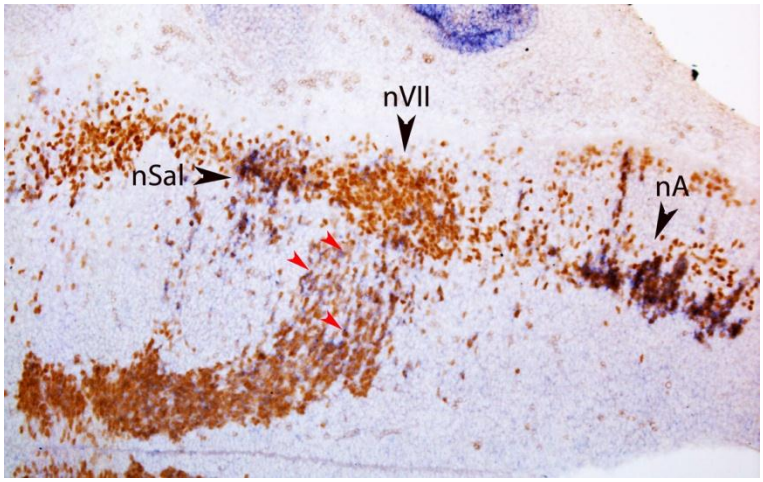

Figure S2

Expression of Tbx3 in all branchial and visceral motoneurons of the hindbrain. Longitudinal section though an E11.5 medulla, stained by combined Phox2b immunohostochemistry and *Tbx3* in situ hybridization. In addition to nX (Fig. 2), *Tbx3* is expressed in salivatory motoneurons (nSal) and the nucleus ambiguus (nA). Expression is also found in a subset of migrating facial motoneuronal precursors (red arrowheads). nVII: facial motor nucleus.

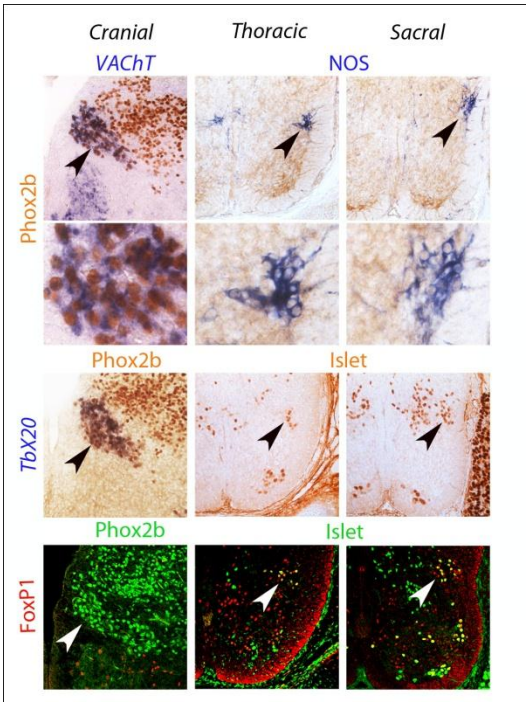

Figure S3

Maintenance at E16.5 of a parasympathetic genetic signature by cranial preganglionics and of a sympathetic genetic signature by both thoracic and sacral preganglionics. Transverse sections at E16.5 through the right half of the medulla (left column), thoracolumbar spinal cord (middle column) and sacral spinal cord (right column), stained with the indicated antibodies and probes. Arrowheads point to the nX in the left column and to spinal preganglionics in the middle and right columns.

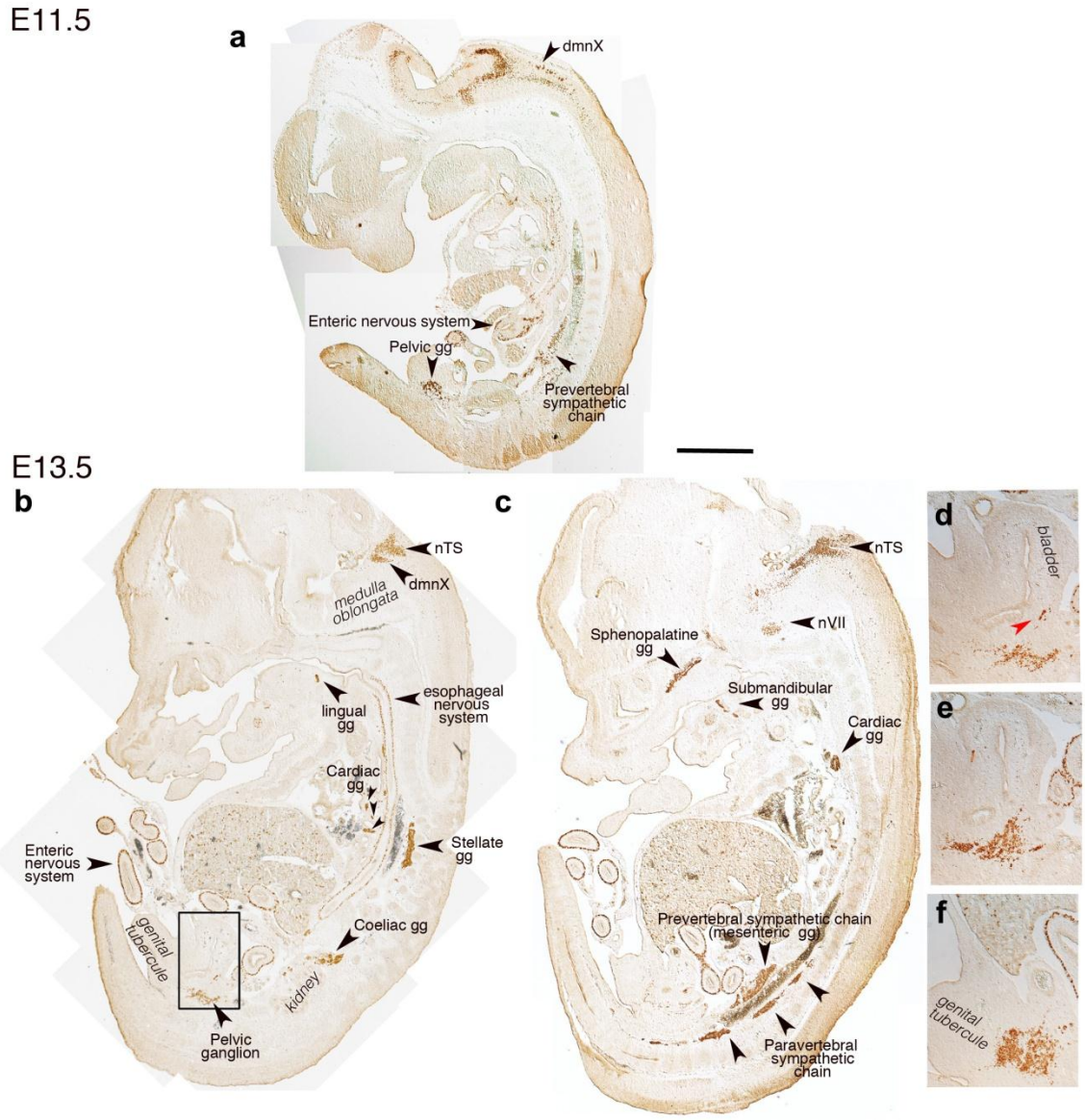

Figure S4

Anatomical location of sympathetic and parasympathetic ganglia in mouse embryos at E11.5 and E13.5. (**a**-**c**) Parasagittal sections through a whole mouse embryo at E11.5 (**a**) or E13.5 (**b**,**c**), stained by immunohistochemistry for Phox2b. (**d**-**f**) Parasagittal sections through the urogenital region of an E13.5 embryo, showing different aspects of the pelvic ganglion. (**d**) is a higher magnification of the area boxed in (**b**). Red arrow: an intramural ganglion of the bladder. gg: ganglion; dmnX: dorsal motor nucleus of the vagus nerve; nTS: nucleus of the solitary tract. Scale bar: **a**-**c**, 1mm; **d**-**f**, 0.5mm.

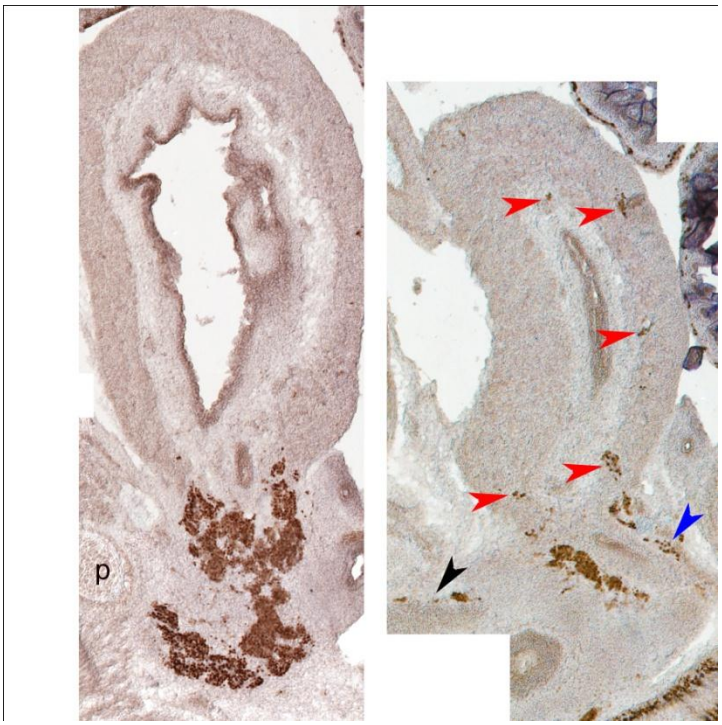

Figure S5

Pelvic and accessory ganglia at E16.5. Two parasagittal sections through the bladder and the pelvic ganglion at E16.5 stained by immunohistochemistry for Phox2b. The main ganglion appears split in a number of lobes. As previously described (*43*), small ganglia or isolated Phox2b+ neurons can be seen in the wall of the bladder (red arrowheads), along the urethra (black arrowhead) and along the ureter (blue arrowhead).

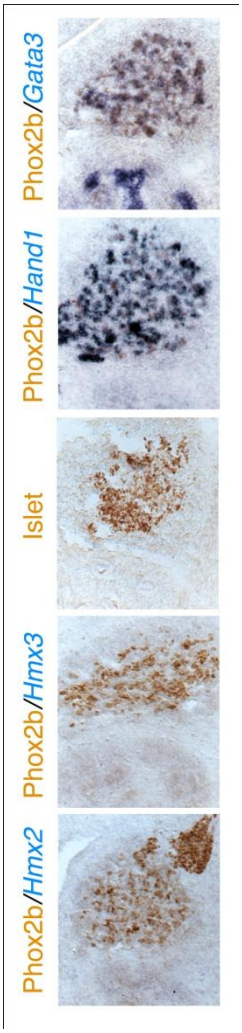

Figure S6

Sympathetic genetic signature of the adrenal medulla. Parasagittal sections through the adrenal medulla at E13.5 stained with the indicated probes or antibodies. The transcriptional signature is Phox2b+/Gata3+/Hand1+/Islet+/Hmx2-/Hmx3-, thus sympathetic.

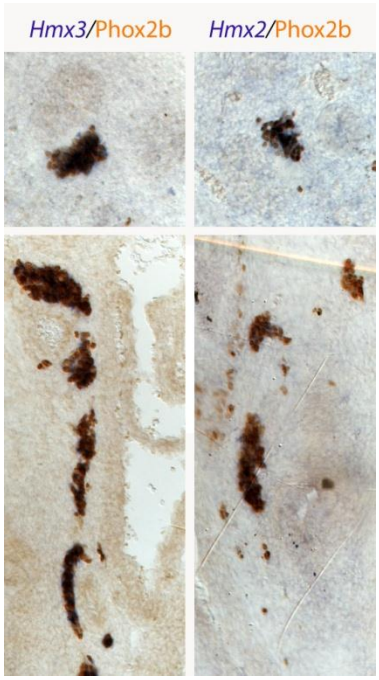

Figure S7

Expression of *Hmx2* and *Hmx3* in cardiac and ciliary ganglia. Parasagittal sections in an E13.5 embryo stained for immunhistochemistry against Phox2b and Hmx3 (left) or Hmx2 (right) in situ hybridization, showing expression of all three genes in the ciliary ganglion (upper panels) and the cardiac ganglia (lower panels).

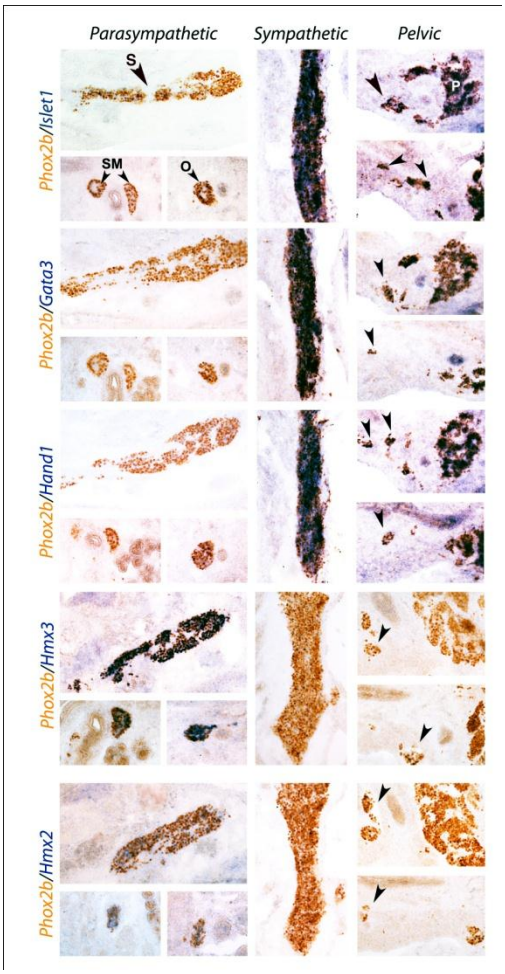

Figure S8

Pelvic and bladder intramural ganglia retain a sympathetic signature at E16.5. Sagittal sections through parasympathetic ganglia (left), the lumbar paravertebral sympathetic chain (middle) and the pelvic ganglion (right) and intramural ganglia of the bladder (arrowheads in the right panels) at E16.5, stained by inmmunohistochemistry for Phox2b, a determinant of all autonomic ganglia (*31*), and in situ hybridization for the indicated probes. O: otic ganglion; S: sphenopalatine ganglion; SM: submandibular ganglion (all parasympathetic ganglia). By this stage *Hmx2* expression has been partially downregulated in parasympathetic ganglia. Note that some intramural ganglia of the bladder have been previously shown to contain noradrenalin (*43*), in line with their sympathetic nature demonstrated here.

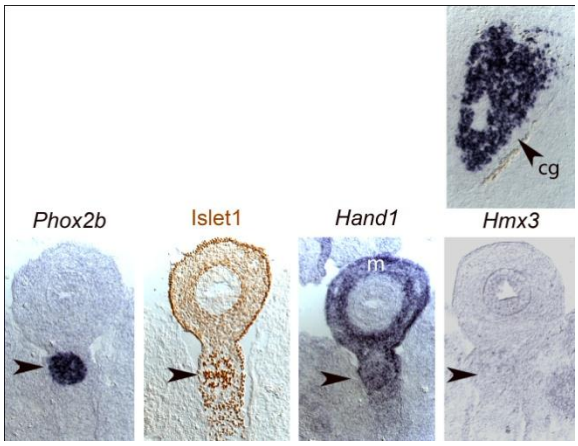

Figure S9

The ganglion of Remak has a sympathetic genetic identity. Transverse sections through a chicken embryo at 5 days post fertilization, passing through the hindgut. The ganglion of Remak (arrowhead) coexpresses Phox2b with the sympathetic markers Islet (detected by an Islet1-2 antibody) and *Hand1*, but not the parasympathetic marker *Hmx3*, which is expressed at the same stage in the ciliary ganglion (cg). Islet and *Hand1* are also expressed in the mesenchymal wall of the gut (m).

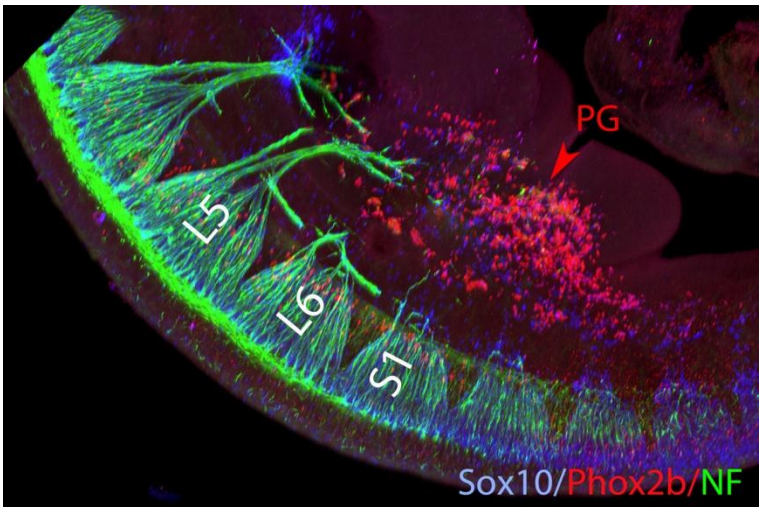

Figure S10

The pelvic ganglion forms in the absence of the pelvic nerve. Wholemount immunofluorescence with the indicated antibodies on an *Olig2*$^{-/-}$ littermate of the E11.5 embryo shown in Fig. 3. In this embryo, no nerve projection is seen at all towards the pelvic ganglion, which nevertheless is present and indistinguishable from its counterpart in heterozygotes (see Fig. 3). L5, L6 and S1: fifth and sixth lumbar and first sacral roots. PG: pelvic ganglion.

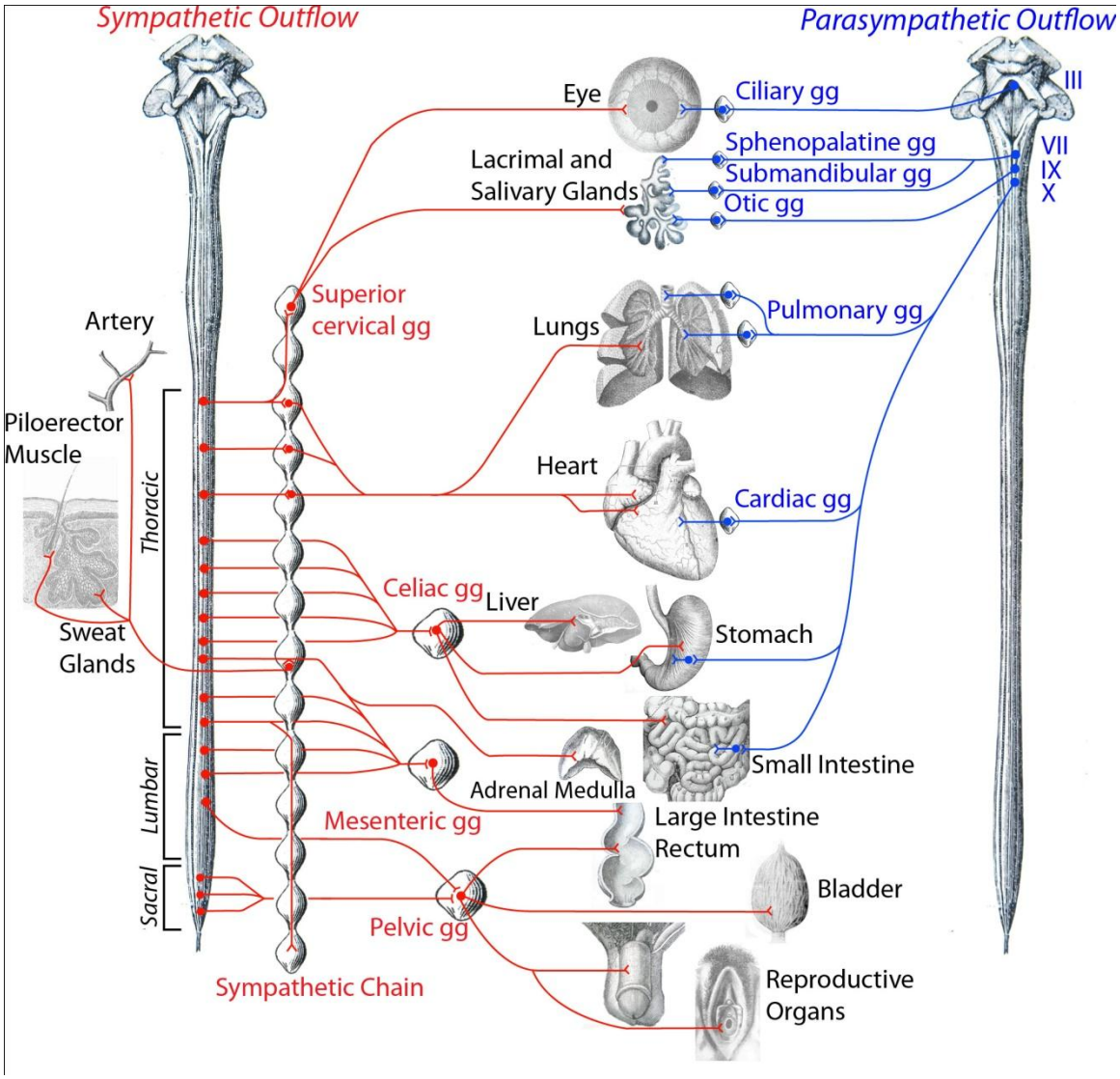

Figure S11. Revised anatomy of the autonomic nervous system. The efferent path of the autonomic nervous system is made up of a spinal sympathetic outflow (in red) and a cranial parasympathetic outflow (in blue). III: occulumotor nerve; VII: facial nerve; IX: glossopharyngeal nerve; X: vagus nerve; gg: ganglion.

Movie S1

The pelvic ganglion at E11.5 in a wild type. The pelvic nerve (in green) reaches the rostral dorsal and lateral edge of the pelvic ganglion (that expresses Phox2b, in red), whose cells lie for the most part distal and medial to them.

Movie S2

The pelvic ganglion at E11.5 in an *Olig2* null mutant. When all motoneurons are deleted, a vestigial pelvic nerve, made up exclusively of sensory fibers, barely touches the pelvic ganglion (that expresses Phox2b, in red), which has the same appearance and size than in wild type embryos (see Movie S1).

References

1. W. H. Gaskell, On the structure, distribution and function of the nerves which innervate the visceral and vascular systems. *J. Physiol.* **7**, 1–80.9 (1886). Medline doi:10.1113/jphysiol.1886.sp000207

2. J. N. Langley, *The Autonomic Nervous System: Part I* (W. Heffer, Cambridge, 1921).

3. E. Kandel, J. Schwartz, T. Jessell, S. Siegelbaum, A. J. Hudspeth, *Principles of Neural Science, Fifth Edition* (McGraw Hill Professional, 2012).

4. J. N. Langley, H. K. Anderson, The innervation of the pelvic and adjoining viscera: Parts II–V. *J. Physiol.* **19**, 71–139 (1895). Medline doi:10.1113/jphysiol.1895.sp000587

5. J. Briscoe, L. Sussel, P. Serup, D. Hartigan-O'Connor, T. M. Jessell, J. L. Rubenstein, J. Ericson, Homeobox gene Nkx2.2 and specification of neuronal identity by graded Sonic hedgehog signalling. *Nature* **398**, 622–627 (1999). Medline doi:10.1038/19315

6. A. Pattyn, M. Hirsch, C. Goridis, J. F. Brunet, Control of hindbrain motor neuron differentiation by the homeobox gene Phox2b. *Development* **127**, 1349–1358 (2000). Medline

7. S. Guthrie, Patterning and axon guidance of cranial motor neurons. *Nat. Rev. Neurosci.* **8**, 859–871 (2007). Medline doi:10.1038/nrn2254

8. A. Prasad, M. Hollyday, Development and migration of avian sympathetic preganglionic neurons. *J. Comp. Neurol.* **307**, 237–258 (1991). Medline doi:10.1002/cne.903070207

9. J. A. Markham, J. E. Vaughn, Migration patterns of sympathetic preganglionic neurons in embryonic rat spinal cord. *J. Neurobiol.* **22**, 811–822 (1991). Medline doi:10.1002/neu.480220803

10. W. A. Alaynick, T. M. Jessell, S. L. Pfaff, SnapShot: Spinal cord development. *Cell* **146**, 178–178.e1 (2011). Medline doi:10.1016/j.cell.2011.06.038

11. P. E. Phelps, R. P. Barber, J. E. Vaughn, Embryonic development of rat sympathetic preganglionic neurons: Possible migratory substrates. *J. Comp. Neurol.* **330**, 1–14 (1993). Medline doi:10.1002/cne.903300102

12. C. R. Anderson, NADPH diaphorase-positive neurons in the rat spinal cord include a subpopulation of autonomic preganglionic neurons. *Neurosci. Lett.* **139**, 280–284 (1992). Medline doi:10.1016/0304-3940(92)90571-N

13. J. S. Dasen, A. De Camilli, B. Wang, P. W. Tucker, T. M. Jessell, Hox repertoires for motor neuron diversity and connectivity gated by a single accessory factor, FoxP1. *Cell* **134**, 304–316 (2008). Medline doi:10.1016/j.cell.2008.06.019

14. J. R. Keast, Plasticity of pelvic autonomic ganglia and urogenital innervation. *Int. Rev. Cytol.* **248**, 141–208 (2006). Medline doi:10.1016/S0074-7696(06)48003-7

15. J. R. Keast, Visualization and immunohistochemical characterization of sympathetic and parasympathetic neurons in the male rat major pelvic ganglion. *Neuroscience* **66**, 655–662 (1995). Medline doi:10.1016/0306-4522(94)00595-V

16. A. Kuntz, R. L. Moseley, An experimental analysis of the pelvic autonomic ganglia in the cat. *J. Comp. Neurol.* **64**, 63–75 (1936). doi:10.1002/cne.900640104

17. W. C. De Groat, A. M. Booth, J. Krier, in *Integrative Functions of the Autonomic Nervous System*, C. M. Brooks, K. Koizumi, A. Sato, Eds. (University of Tokyo Press, Tokyo, 1979), pp. 234–245.

18. U. Ernsberger, H. Rohrer, Development of the cholinergic neurotransmitter phenotype in postganglionic sympathetic neurons. *Cell Tissue Res.* **297**, 339–361 (1999). Medline doi:10.1007/s004410051363

19. K. Huber, P. Narasimhan, S. Shtukmaster, D. Pfeifer, S. M. Evans, Y. Sun, The LIM-Homeodomain transcription factor Islet-1 is required for the development of sympathetic neurons and adrenal chromaffin cells. *Dev. Biol.* **380**, 286–298 (2013). Medline doi:10.1016/j.ydbio.2013.04.027

20. K. Tsarovina, A. Pattyn, J. Stubbusch, F. Müller, J. van der Wees, C. Schneider, J. F. Brunet, H. Rohrer, Essential role of Gata transcription factors in sympathetic neuron development. *Development* **131**, 4775–4786 (2004). Medline doi:10.1242/dev.01370

21. E. Doxakis, L. Howard, H. Rohrer, A. M. Davies, HAND transcription factors are required for neonatal sympathetic neuron survival. *EMBO Rep.* **9**, 1041–1047 (2008). Medline doi:10.1038/embor.2008.161

22. L. Huber, M. Ferdin, J. Holzmann, J. Stubbusch, H. Rohrer, HoxB8 in noradrenergic specification and differentiation of the autonomic nervous system. *Dev. Biol.* **363**, 219–233 (2012). Medline doi:10.1016/j.ydbio.2011.12.026

23. C. L. Yntema, W. S. Hammond, Experiments on the origin and development of the sacral autonomic nerves in the chick embryo. *J. Exp. Zool.* **129**, 375–413 (1955). doi:10.1002/jez.1401290210

24. V. Dyachuk, A. Furlan, M. K. Shahidi, M. Giovenco, N. Kaukua, C. Konstantinidou, V. Pachnis, F. Memic, U. Marklund, T. Müller, C. Birchmeier, K. Fried, P. Ernfors, I. Adameyko, Parasympathetic neurons originate from nerve-associated peripheral glial progenitors. *Science* **345**, 82–87 (2014). Medline doi:10.1126/science.1253281

25. I. Espinosa-Medina, E. Outin, C. A. Picard, Z. Chettouh, S. Dymecki, G. G. Consalez, E. Coppola, J. F. Brunet, Parasympathetic ganglia derive from Schwann cell precursors. *Science* **345**, 87–90 (2014). Medline doi:10.1126/science.1253286

26. S. Nilsson, in *Autonomic Nerve Function in the Vertebrates, Zoophysiology*, vol. 13, D. S. Farner, Ed. (Springer-Verlag, New York, 1983), chap. 2.

27. C. Olsson, B. N. Chen, S. Jones, T. K. Chataway, M. Costa, S. J. Brookes, Comparison of extrinsic efferent innervation of guinea pig distal colon and rectum. *J. Comp. Neurol.* **496**, 787–801 (2006). Medline doi:10.1002/cne.20965

28. K. Fukai, H. Fukuda, Three serial neurones in the innervation of the colon by the sacral parasympathetic nerve of the dog. *J. Physiol.* **362**, 69–78 (1985). Medline doi:10.1113/jphysiol.1985.sp015663

29. W. Jänig, *The Integrative Action of the Autonomic Nervous System: Neurobiology of Homeostatis* (Cambridge Univ. Press, Cambridge, UK, 2006).

30. W. C. de Groat, W. R. Saum, Sympathetic inhibition of the urinary bladder and of pelvic ganglionic transmission in the cat. *J. Physiol.* **220**, 297–314 (1972). Medline doi:10.1113/jphysiol.1972.sp009708

31. A. Pattyn, X. Morin, H. Cremer, C. Goridis, J. F. Brunet, The homeobox gene *Phox2b* is essential for the development of autonomic neural crest derivatives. *Nature* **399**, 366–370 (1999). Medline doi:10.1038/20700

32. E. Coppola, M. Rallu, J. Richard, S. Dufour, D. Riethmacher, F. Guillemot, C. Goridis, J. F. Brunet, Epibranchial ganglia orchestrate the development of the cranial neurogenic crest. *Proc. Natl. Acad. Sci. U.S.A.* **107**, 2066–2071 (2010). Medline doi:10.1073/pnas.0910213107

33. M. R. Elphick, in *Methods in Molecular Biology: Neurotransmitter Methods*, Vol 72, R. C. Rayne, Ed. (Humana Press, 1997), pp. 153–158.

34. A. Ertürk, K. Becker, N. Jährling, C. P. Mauch, C. D. Hojer, J. G. Egen, F. Hellal, F. Bradke, M. Sheng, H. U. Dodt, Three-dimensional imaging of solvent-cleared organs using 3DISCO. *Nat. Protoc.* **7**, 1983–1995 (2012). Medline doi:10.1038/nprot.2012.119

35. A. Pattyn, X. Morin, H. Cremer, C. Goridis, J. F. Brunet, Expression and interactions of the two closely related homeobox genes *Phox2a* and *Phox2b* during neurogenesis. *Development* **124**, 4065–4075 (1997). Medline

36. V. Dubreuil, M. Thoby-Brisson, M. Rallu, K. Persson, A. Pattyn, C. Birchmeier, J. F. Brunet, G. Fortin, C. Goridis, Defective respiratory rhythmogenesis and loss of central chemosensitivity in Phox2b mutants targeting retrotrapezoid nucleus neurons. *J. Neurosci.* **29**, 14836–14846 (2009). Medline doi:10.1523/JNEUROSCI.2623-09.2009

37. M. C. Tiveron, M. R. Hirsch, J. F. Brunet, The expression pattern of the transcription factor Phox2 delineates synaptic pathways of the autonomic nervous system. *J. Neurosci.* **16**, 7649–7660 (1996). Medline

38. H. D. Dufour, Z. Chettouh, C. Deyts, R. de Rosa, C. Goridis, J. S. Joly, J. F. Brunet, Precraniate origin of cranial motoneurons. *Proc. Natl. Acad. Sci. U.S.A.* **103**, 8727–8732 (2006). Medline doi:10.1073/pnas.0600805103

39. F. D'Autréaux, E. Coppola, M.-R. Hirsch, C. Birchmeier, J.-F. Brunet, Homeoprotein Phox2b commands a somatic-to-visceral switch in cranial sensory pathways. *Proc. Natl. Acad. Sci. U.S.A.* **108**, 20018–20023 (2011). Medline doi:10.1073/pnas.1110416108

40. L. Madisen, T. A. Zwingman, S. M. Sunkin, S. W. Oh, H. A. Zariwala, H. Gu, L. L. Ng, R. D. Palmiter, M. J. Hawrylycz, A. R. Jones, E. S. Lein, H. Zeng, A robust and high-throughput Cre reporting and characterization system for the whole mouse brain. *Nat. Neurosci.* **13**, 133–140 (2010). Medline doi:10.1038/nn.2467

41. M. Zawadzka, L. E. Rivers, S. P. Fancy, C. Zhao, R. Tripathi, F. Jamen, K. Young, A. Goncharevich, H. Pohl, M. Rizzi, D. H. Rowitch, N. Kessaris, U. Suter, W. D. Richardson, R. J. Franklin, CNS-resident glial progenitor/stem cells produce Schwann cells as well as oligodendrocytes during repair of CNS demyelination. *Cell Stem Cell* **6**, 578–590 (2010). Medline doi:10.1016/j.stem.2010.04.002

42. C. Sommer, C. Straehle, U. Köthe, F. A. Hamprecht, ilastik: Interactive learning and segmentation toolkit. 2011 8th IEEE International Symposium on Biomedical Imaging (ISBI 2011) 230–233 (2011). doi:10.1109/ISBI.2011.5872394

43. A. El-Badawi, E. A. Schenk, The peripheral adrenergic innervation apparatus. I. Intraganglionic and extraganglionic adrenergic ganglion cells. *Z. Zellforsch. Mikrosk. Anat.* **87**, 218–225 (1968). Medline doi:10.1007/BF00319721

Article 2

Dual Origin of Enteric Neurons in Vagal Schwann Cell Precursors and the Sympathetic Neural Crest

Espinosa-Medina I., Jevans B., Boismoreau F., Chettouh Z., Enomoto H., Müller T., Birchmeier C., Burns A., Brunet J.-F.

PNAS, 2017

Dual origin of enteric neurons in vagal Schwann cell precursors and the sympathetic neural crest

Isabel Espinosa-Medina[a,1], Ben Jevans[b,2], Franck Boismoreau[a,2], Zoubida Chettouh[a], Hideki Enomoto[c], Thomas Müller[d], Carmen Birchmeier[d], Alan J. Burns[b,e,3], and Jean-François Brunet[a,4]

[a]Institut de Biologie de l'École Normale Supérieure (IBENS), École Normale Supérieure, CNRS, INSERM, PSL Research University, 75005 Paris, France; [b]Stem Cells and Regenerative Medicine, Birth Defects Research Centre, University College London Great Ormond Street Institute of Child Health, WC1N 1EH London, United Kingdom; [c]Laboratory for Neural Differentiation and Regeneration, Graduate School of Medicine, Kobe University, 650-0017 Kobe City, Japan; [d]Max-Delbrück-Center for Molecular Medicine in the Helmholtz-Association, 13125 Berlin, Germany; and [e]Department of Clinical Genetics, Erasmus Medical Center, 3015 CE Rotterdam, The Netherlands

Edited by Marianne Bronner, California Institute of Technology, Pasadena, CA, and approved September 29, 2017 (received for review June 7, 2017)

Most of the enteric nervous system derives from the "vagal" neural crest, lying at the level of somites 1–7, which invades the digestive tract rostro-caudally from the foregut to the hindgut. Little is known about the initial phase of this colonization, which brings enteric precursors into the foregut. Here we show that the "vagal crest" subsumes two populations of enteric precursors with contrasted origins, initial modes of migration, and destinations. Crest cells adjacent to somites 1 and 2 produce Schwann cell precursors that colonize the vagus nerve, which in turn guides them into the esophagus and stomach. Crest cells adjacent to somites 3–7 belong to the crest streams contributing to sympathetic chains: they migrate ventrally, seed the sympathetic chains, and colonize the entire digestive tract thence. Accordingly, enteric ganglia, like sympathetic ones, are atrophic when deprived of signaling through the tyrosine kinase receptor ErbB3, while half of the esophageal ganglia require, like parasympathetic ones, the nerve-associated form of the ErbB3 ligand, Neuregulin-1. These dependencies might bear relevance to Hirschsprung disease, with which alleles of *Neuregulin-1* are associated.

enteric nervous system | neural crest | chicken | mouse | Neuregulin1

The enteric nervous system (ENS) is, for the most part, formed by one rostro-caudal wave of migrating neural crest-derived precursors that originate in the "vagal neural crest," lying from the levels of somites 1–7 (refs. 1 and 2 and references therein). The progression of enteric precursors through the postgastric digestive tract has been extensively studied (3, 4), in particular with respect to its dependency on Glial-derived neurotrophic-factor (GDNF) signaling through the tyrosine kinase receptor Ret and its dimerization partner GFRα1. In contrast, the inception of the invasive process (i.e., the events that bring the vagal neural crest in the walls of the esophagus) remain controversial. Early observations inspired the hypothesis that enteric precursors were nerve-associated cells that followed the vagus (Xth) cranial nerve (which provides extrinsic innervation to the gut) (5). However, these studies ignored the neural crest as such and were evinced from the corpus of accepted knowledge once the neural crest origin of enteric neurons was firmly established (6, 7) and are now long forgotten. Moreover, enteric precursors were later spotted ahead of the incipient vagus nerve, which has thus been viewed as following and "overtaking" them (8). An ensuing paradox is that the adjective "vagal" has stuck to the enteric crest after the vagus nerve was no longer assigned any role. In mouse embryos, it was proposed that the vagal crest, defined as spanning somites 1–5 (9), colonizes most of the gut in addition to forming the superior cervical ganglion (and was hence called "sympatho-enteric"), while an adjacent "anterior trunk" (cervical) crest would populate the esophagus exclusively. This dichotomy, however, was never fully integrated in the canonical narrative of ENS development (e.g., ref. 10) and remains at odds with the situation in chicken, where the most-caudal vagal crest (corresponding to the anterior trunk crest of ref. 9) colonizes not the most rostral but the most caudal part of the digestive tract (11). More recently, the vagal crest was proposed as a transitional entity between the cranial and trunk region, where both a dorsal and a ventral migration pathway would take place in temporal succession (12). Finally, several mutations, while they completely block the rostro-caudal invasion of the gut mesenchyme by enteric precursors past the stomach, respect, to an extent or for a while, the colonization of the esophagus and stomach (see below). Altogether, this slim body of data, some of them contradictory, shows that foregut colonization by enteric precursors obeys rules different from the rest of the digestive tract, and is still poorly understood.

Results

Schwann Cell Precursors of the Vagus Nerve Contribute Neurons to the Foregut. Null mutations in the genes for GDNF, its receptor GFRα1, its coreceptor Ret (9, 13–16), and for the pan-autonomic homeodomain transcription factor *Phox2b* (17), partially spare enteric neuronal precursors in a region that, strikingly, is coextensive with the stretch of the vagus nerve that travels alongside the digestive tract (Fig. S1): from the larynx down to the stomach, where the left vagus arborizes terminally and the right vagus veers off to join the prevertebral sympathetic plexi. This suggests that the vagus nerve itself could guide enteric precursors to the esophagus and

Significance

The enteric nervous system of vertebrates arises mostly from a rostral portion of the neural crest, encapsulated by the term "vagal." We show that the "vagal crest" is in fact a juxtaposition of two completely different types of cells: Schwann cell precursors associated with the vagus nerve, which provide esophageal neurons, and the rostral-most trunk crest, which also forms sympathetic ganglia and locally overshoots the aorta to colonize most of the gut. Moreover, in line with the known dependency of both Schwann cell precursors and trunk crest on the ErbB3 tyrosine receptor kinase and its ligand Neuregulin1, we discover that the enteric nervous system is also atrophic in *ErbB3* mutants, with potential relevance to Hirschsprung disease, a congenital hypoganglionosis.

Author contributions: J.-F.B. designed research; I.E.-M., B.J., F.B., and Z.C. performed research; H.E., T.M., C.B., and A.J.B. contributed new reagents/analytic tools; I.E.-M. and F.B. analyzed data; and I.E.-M. and J.-F.B. wrote the paper.

The authors declare no conflict of interest.

This article is a PNAS Direct Submission.

[1]Present address: Janelia Research Campus, Howard Hughes Medical Institute, Ashburn, VA 20147.

[2]B.J. and F.B. contributed equally to this work.

[3]Present address: Gastrointestinal Drug Discovery Unit, Takeda Pharmaceuticals International Co., Cambridge, MA 02139.

[4]To whom correspondence should be addressed. Email: jfbrunet@biologie.ens.fr.

This article contains supporting information online at www.pnas.org/lookup/suppl/doi:10.1073/pnas.1710308114/-/DCSupplemental.

stomach, independently of Phox2b or GDNF signaling, as it guides—and other cranial nerves guide—parasympathetic ganglionic precursors (18, 19). Evocative of such a mechanism was the fact that, at embryonic day (E) 11.5, the vagus nerve was covered with Sox10$^+$, Phox2b$^+$ cells coexpressing the Schwann cell precursor markers PLP-1 and Cadherin 19 (Fig. S2).

We investigated a role for the vagus nerve in the formation of esophageal ganglia in two ways. First, we prevented the formation of the nerve by deleting most neurons that project into it: viscerosensory neurons born in epibranchial placodes, as well as branchial and visceral motor neurons of the hindbrain were killed using a toxic variant of the sodium channel ASIC2a conditionally expressed from the promoter of *Phox2a* (18), the paralogue of *Phox2b* expressed in all these cell types (20). In *Pgk:Cre;Phox2a^{ASIC2a}* embryos, where Cre-mediated recombination occurs in the egg—thus where all Phox2a$^+$ cells are killed by *ASIC2a*—the vagus nerve was reduced to a vestigial ramus, most likely composed of somatosensory fibers emanating from its proximal ganglion (Fig. 1*A*). Consequently, Sox10$^+$ cells in the esophageal region were fewer at E11.5 (Fig. 1*A*) and, 2 days later, 36% of Phox2b$^+$ neuronal precursors were missing in the wall of the esophagus (Fig. 1*B*). Second, we hampered signaling by the vagus nerve to its Schwann cell precursors through the epidermal growth factor family protein Neuregulin-1 (Nrg1) (21) by partnering a floxed allele of *Nrg1* with a Cre recombinase driven by the *Phox2b* promoter, thus expressed in all cranial visceral sensory and motor neurons (20). *Phox2b::Cre;Nrg1$^{lox/lox}$* embryos lacked Schwann cell precursors associated with the facial and glossopharyngeal nerves, which moreover appeared defasciculated (Fig. S3). Concordantly all parasympathetic ganglia appended to these nerves were missing 2 days later (Fig. S3), phenocopying the constitutive knockouts for the receptor of Nrg1, the tyrosine kinase receptor *ErbB3*, which has been documented after birth (19). Similarly, the vagus nerve was depleted of Schwann cell precursors and, concomitantly, the esophageal ganglia were atrophic by 46% (Fig. 1 *C* and *D*). The effect was noncell-autonomous, as shown by the lack of phenotype of *Wnt1::Cre;Nrg1$^{lox/lox}$* embryos (Fig. 1*D*) and the lack of expression of Nrg1 by enteric precursors (Fig. S5). Thus, about half of the esophageal nervous system (or more if compensatory mechanisms take place in the mutants) derives from Schwann cell precursors of the vagus nerve.

The Cervical Sympathetic Crest Contributes Most of the ENS. In contrast, the postgastric ENS was not affected in *Pgk:Cre;Phox2a^{ASIC2a}* and only mildly so in *Phox2b::Cre;Nrg1$^{lox/lox}$* mutants (Fig. S4).

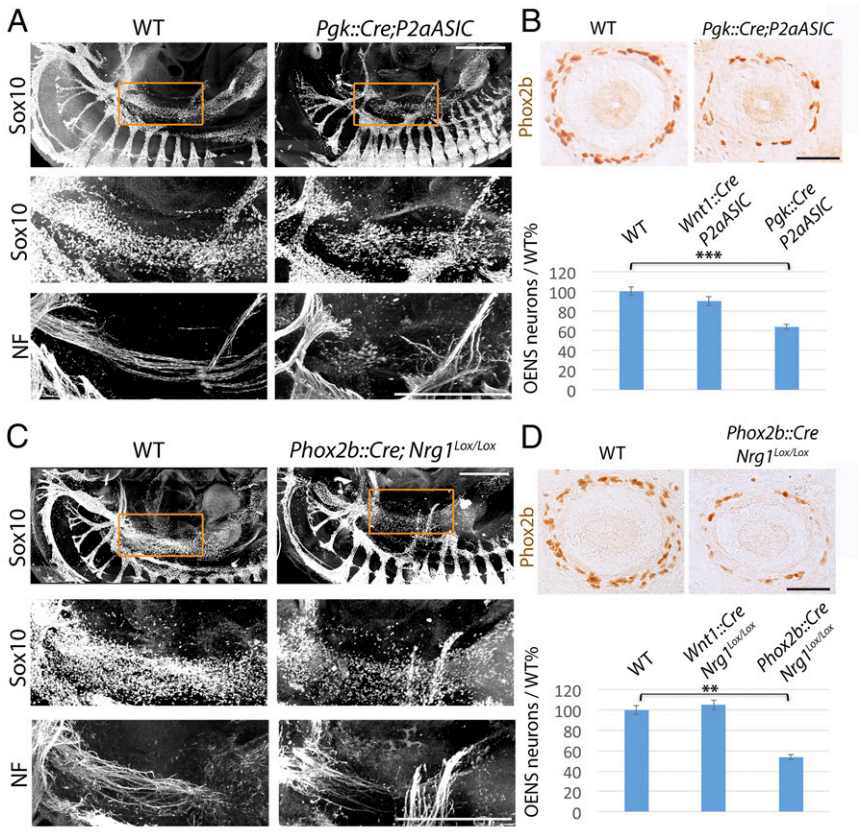

Fig. 1. Genetic damage to the vagus nerve depletes the esophageal nervous system. (*A* and *C*) Lateral views of whole-mount E11.5 (*A*) or E10.5 (*C*) embryos stained for Sox10 and Neurofilament, in the indicated genotypes. For each genotype, the *Middle* and *Bottom* panels are a magnified view of the area boxed in the *Top* panel. Atrophy of the vagus nerve (*A*), or deletion of *Neuregulin-1* from vagal fibers (*C*), leads to depletion of the pool of Sox10$^+$ cells (*Middle*) along the vagus path (*Bottom*) and defasciculation of the nerve (*C*). (*B* and *D*) (*Upper*) Cross-sections through the esophagus at E13.5 in the indicated genotypes, stained for Phox2b. (*Lower*) Count of Phox2b$^+$ neuronal precursors in the esophagus at E13.5, in the indicated genotypes. Esophageal precursors were depleted in *Pgk:Cre;Phox2a^{ASIC2a}* (64 ± 1.6%/wild-type; $P = 0.001$, $n = 4$) and *Phox2b::Cre;Nrg1$^{lox/lox}$* (54 ± 2.6%/wild-type; $P = 0.004$, $n = 3$) embryos, but were not significantly affected in *Wnt1::Cre;Phox2a$^{ASIC2\ a}$* (90 ± 4.2%/wild-type; $P = 0.898$, $n = 4$) or in *Wnt1::Cre;Nrg1$^{lox/lox}$* (105 ± 4.77%/wild-type; $P = 0.842$, $n = 3$) embryos. Error bars indicate SEM. $^{**}P < 0.005$, $^{***}P < 0.001$. The *Wnt1::Cre;Phox2a^{ASIC2a}* and *Wnt1::Cre;Nrg1$^{lox/lox}$* genetic backgrounds serve as controls, in which the expression of *ASIC2a* or the recombination of *Nrg1* respectively, is targeted to the neural-crest derived enteric precursors, rather than all Phox2a$^+$ or Phox2b$^+$ cells. The lack of phenotype—most likely because only a small subset of enteric precursors express Phox2a (20), and none express Nrg1 at this stage (Fig. S5)—ensures that in *Pgk:Cre;Phox2a^{ASIC2a}*and *Phox2b::Cre;Nrg1$^{lox/lox}$* embryos the enteric phenotype is noncell-autonomous, and due to the damage of the Phox2a- or Phox2b-expressing components of the vagus nerve. (Scale bars: *A* and *B*, 500 μm; *B* and *D*, 50 μm.)

Therefore, either a compensatory mechanism acts during the migration of enteric precursors to mitigate cell loss downstream of the stomach, or a second, nerve-independent population of cells invades the postgastric digestive tract (as well as the esophagus, since only half of its resident neurons are missing when the vagus nerve is damaged). Consistent with the latter hypothesis, we spotted a contingent of Sox10$^+$ cells at E10 in continuity with the incipient cervical sympathetic chain at the level of the esophagus (red arrowhead in Fig. 2 *A* and *D* and Movie S1). On transverse sections (Fig. 2 *B* and *C*), these cells formed a stream that followed the ventral neural crest pathway (Fig. 2*C*, sections 3, 4, and compatible images in refs. 9, 12, and 22), passed by the lateral edges of the dorsal aortas, overshot them, and invaded the walls of the digestive tract (red arrowhead in Fig. 2*C*, section 4). The bulk of these "postvagal" (i.e., cervical) cells were mostly segregated from the rostrally situated vagus-associated ones (Fig. 2 *A* and *D*, white arrowhead), both populations mingling only at a narrow junction (white asterisk in Fig. 2*C*, section 3).

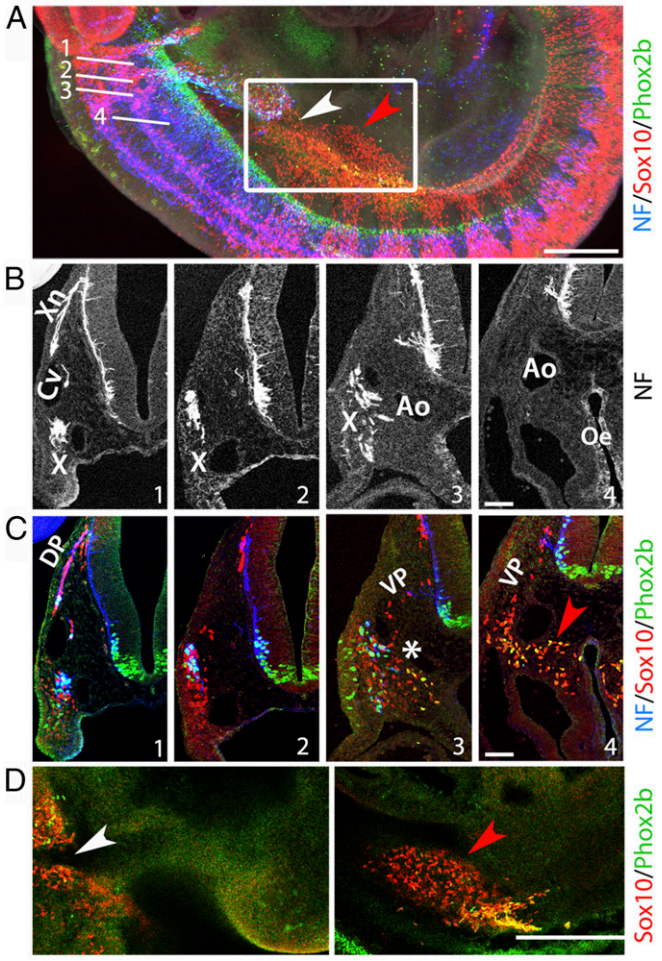

Fig. 2. Two distinct streams of cells migrate to the esophagus in mouse embryos. (*A*) Lateral view of a whole mount at E10 stained with the indicated markers and showing the four planes of sections displayed in *B* and *C* and a boxed area enlarged in *D*. (*B*) Oblique transverse sections through an E10 wild-type mouse embryo along the four planes indicated in *A*, stained for neurofilament (NF, the signal in the lining of the esophagus is due to cross-reactivity of the secondary antibody), with indications of anatomical landmarks: Ao, dorsal aorta; Cv, cardinal vein; X, nodose ganglion; Xn, vagus nerve. (*C*) Same sections as in *B* costained for Phox2b, NF, and Sox10. At the more rostral levels (sections 1, 2) Sox10$^+$ cells migrate along a dorsal pathway (DP), following the nascent vagus nerve, lateral to the anterior cardinal vein, and joining the forming nodose ganglion; at more caudal levels (sections 3, 4), a stream of Sox10$^+$ cells follows the ventral migratory pathway (VP) and colonizes the sides of the dorsal aortas and the lateral walls of the esophagus (red arrowhead, also in *A* and *D*). The two populations are connected only at a narrow junction (white asterisk in section 3). (*D*) Sagittal optical sections at the level of the boxed area in *A*, along a lateral (*Left*) and more medial (*Right*) plane. The white arrowhead marks the discontinuity between the vagal-associated cell population and the postvagal one (red arrowhead). (Scale bars: *A* and *D*, 500 μm; *B* and *C*, 50 μm.)

To directly demonstrate the contrasting migratory behavior of the two types of enteric crest—vagal proper and postvagal—we turned to the chicken embryo, where enteric neurons develop in a similar manner as in mouse (1, 2). We performed isotopic grafts of neural tubes from GFP transgenic chicken embryos into wild-type hosts. Grafts of neural tubes adjacent to somites 1 and 2 produced—in addition to the circumpharyngeal crest (marked Cc in Fig. 3*A*) that contributes to the heart and third branchial arch (23)—a neural crest that was intimately associated with the fibers of the vagus nerve at E3.5 (Fig. 3*A*). These cells correspond to the contingent of enteric precursors previously described as following a "dorsolateral" migration path (ref. 23 and references therein). At E7, these grafts had seeded mostly the esophagus and stomach, although a few cells could be found all of the way to the colon (Fig. 3*C*). In contrast, grafts adjacent to somites 3–7 produced exclusively a neural crest that followed the ventral path and invaded the digestive tract ahead of, and at a right angle to, the descending vagus nerve and its associated cells (Fig. 3*B*). At E7, cells arising from such grafts had contributed to the entire ENS (Fig. 3*D*). These different rostrocaudal extents of enteric colonization are compatible with previous reports using grafts with different limits, which blurred the sharp dichotomy (24).

An additional contrast between the vagal grafts (facing somites 1–2) and postvagal, cervical grafts (facing somites 3–7), is that the latter colonized the sympathetic chain (Fig. 3*F* and Fig. S6), while the former did not (Fig. 3*E* and Fig. S6). Even grafts restricted to the level of somite 3 or 4 contributed many cells to the superior cervical ganglia, mostly glia [as was previously observed with S1–S3 grafts (25)] and an occasional Th$^+$ cell in the case of S4 grafts (Fig. S6). Thus, the sympathetic and enteric crest overlap, not only between somites 5 and 7, as previously recognized (26), but all of the way to somite 3 (but no further rostrally), and nothing distinguishes their ventral migratory paths toward the aorta.

Nrg1/ErbB3 Signaling Is Required for the Formation of the ENS. Schwann cell precursors colonize nerves by responding to axonal Nrg1 (21) (Fig. 1 and Fig. S3) through the tyrosine kinase receptor ErbB3. Sympathetic precursors also express *ErbB3*, through which they respond to mesenchymal Nrg1 that directs their ventral migration toward the aorta (27, 28). Consequently, the sympathetic chains are massively atrophic in *ErbB3* knockouts (28) (white arrowheads in Fig. S7). Because at cervical levels the sympathetic crest is also the source of most of the ENS, we surmised that the latter should likewise depend on *Erbb3*. Following deletion of *ErbB3* from the neural crest—in a *Wnt1::Cre;ErbB3$^{lox/lox}$* background—the cervical sympatho-enteric population was depleted at E10 (red arrowheads in Fig. S7) and the corresponding region of the foregut contained fewer Sox10$^+$ cells at E10.5 (Fig. 4*A*). At E13.5, the esophageal ganglia were atrophic by 68% (Fig. 4*B*) [i.e., more than in *Phox2b::Cre;Nrg1$^{lox/lox}$* embryos (Fig. 1), likely due to the depletion of both the vagal and cervical contributions]. In addition, the postgastric ENS displayed a gradient of atrophy, from 76% just caudal to the stomach to 68% rostral to the cecum (Fig. 4*B*). To test whether the atrophy also affects the rectal aspect of the digestive tube (typically aganglionic in Hirschsprung disease), we examined the ENS at E17.5 and found a 51% atrophy in *Wnt1::Cre;ErbB3$^{lox/lox}$* embryos (Fig. 4*C*). The diminishing rostro-caudal gradient of atrophy of the ENS suggests that the digestive tract provides compensatory proliferative signals.

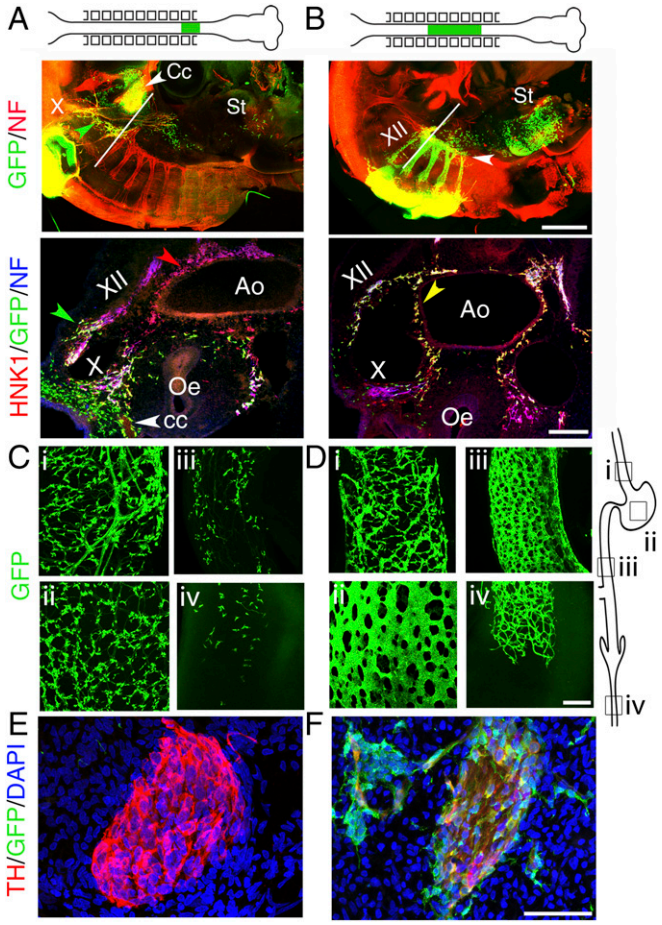

Fig. 3. Two distinct streams of cells migrate into the esophagus in chicken embryos. (*A*) E3.5 chicken embryo after a stage 10 isotopic graft of the neural tube facing somites 1 and 2, from a GFP transgenic donor to a wild-type host. (*Upper*) Whole-mount lateral view showing that the graft has produced circumpharyngeal crest (Cc) and cells associated with fibers, mostly in the vagus nerve (X) but also in a connecting meshwork between the hypoglossal nerve and the nodose ganglion (green arrowhead); a few cells have migrated ahead of the vagus nerve, all of the way to the stomach (St). (*Lower*) Transverse section at the level indicated on the *Upper* panel, showing that the crest produced by the graft reaches the esophagus (Oe) by following the vagus, not the sides of the aorta (Ao) which is populated only by HNK1^{+};GFP^{-} cells (red arrowhead). (*B*, *Upper*) Same as above but with a graft facing somites 3–7. The graft has produced cells associated with spinal nerves—and the hypoglossal (XII)—the nascent sympathetic chain (white arrowhead), a few cells in the esophagus and many more cells in the stomach than for the somite1-2 grafts. (*Lower*) Transverse section at the level indicated on the *Upper* panel, showing that the crest from the graft, apart from colonizing the hypoglossal (XII), follows the ventral path and reaches the esophagus by circumnavigating the dorsal aorta (yellow arrowhead), not by following the vagus. (*C* and *D*) Whole-mount views of the digestive tube at E7 showing the presence of graft-derived cells, after somite1–2 grafts (*C*) versus somite 3–7 grafts (*D*), at the rostro-caudal levels indicated in the schematic on the right: (*i*) esophagus; (*ii*) gizzard; (*iii*) preumbilical intestine; (*iv*) colon. At this stage the colon is still incompletely colonized (level *iv*). (*E* and *F*) Sagittal sections through the superior cervical ganglion at E5.5, stained with the indicated markers. [Scale bars: *A* and *B* (*Upper*), 500 μm; *A* and *B* (*Lower*), 100 μm; *C–F*, 50 μm.]

Discussion

In sum, our data substantiate the proposal that the vagal crest is a pseudo or "hybrid" entity (12, 23). More precisely, we show that it is a juxtaposition of three radically different cell populations, two of them precursors for the ENS: on the one hand, emerging from somites 1 and 2, (*i*) the circumpharyngeal crest (destined to the heart and third branchial arch) and (*ii*) Schwann-cell precursors of the vagus nerve; on the other hand, emerging from somites 3–7, (*iii*) the cervical (upper cervical in chicken) region of the trunk crest.

Schwann cell precursors destined to the ENS behave like parasympathetic precursors (18): they migrate along a nerve and form autonomic ganglia at their final destination, here, enteric ganglia in the walls of esophagus and stomach. They derive from a crest that is vagal indeed, and more literally than the original term intended, since it populates the vagus nerve. Of note, vagus nerve-derived enteric precursors have been proposed back in the 1910s based on histological descriptions (5), but have been overlooked since then.

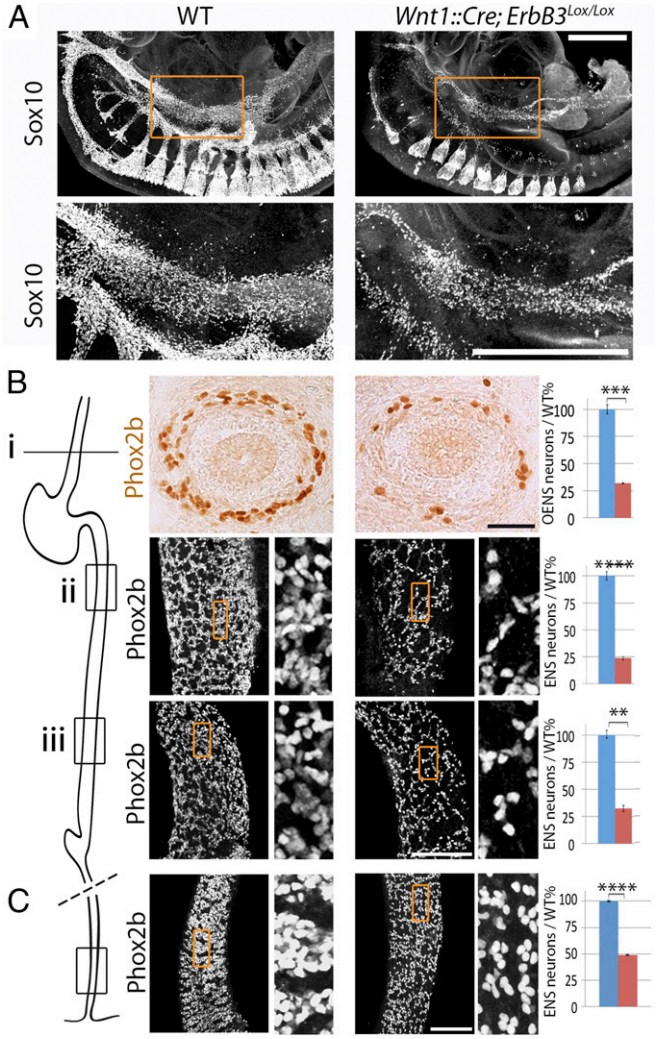

Fig. 4. The ENS is atrophic in the absence of the tyrosine kinase receptor ErbB3. (*A*) Lateral views of wholemount E10.5 embryos stained for Sox10, in the indicated genotypes. In mutants where *ErbB3* is deleted from the neural crest, Sox10^{+} cells are partially depleted in the foregut. (*Lower*) Magnified views of the area boxed in the *Upper* panels. (*B*) Sections through the esophagus (*Upper*) and whole mounts of the midgut at two rostro-caudal levels [(*Lower*) low magnifications at *Left*, enlarged views (7× zoom) of the boxed area at *Right*] indicated on the schematic on the *Left*, in E13.5 wild-type (*Left* column) and conditional *ErbB3* mutants (*Right* column), stained for Phox2b. The atrophy of the enteric ganglia is quantified on the graphs. *Wnt1::Cre;ErbB3$^{lox/lox}$* mutants showed fewer esophageal precursors (level *i*: 32 ± 0.6%/wild-type; $P = 0.003$, $n = 3$) and postgastric precursors (level *ii*: 24 ± 1.3%/wild-type; $P = 0.0001$, $n = 4$; level *iii*: 32 ± 2.8%/wild type; $P = 0.007$, $n = 4$). (*C*). Whole mounts of the distal hindgut (enlarged views of the boxed area on the *Right*), in E17.5 wild-type (*Left* column) and conditional *ErbB3* mutants (*Right* column) stained for Phox2b (49 ± 0.41%; $P = 0{,}00001$, $n = 5$. (Scale bars: *A*, 500 μm; *B* and *C*, 100 μm.). Error bars indicate SEM. $^{**}P < 0.01$, $^{***}P < 0.005$, $^{****}P < 0.0005$.

DEVELOPMENTAL BIOLOGY

In contrast, the cervical crest migrates along the classically described ventral pathway toward the dorsal aorta—where it contributes to the sympathetic chain—and part of it, possibly the major part at that level, overshoots the dorsal aorta to invade the nearby esophageal mesenchyme. It remains to be explored what determines some cells to home close to the aorta and others to continue their voyage to the gut. This crest is thus sympatho-enteric and has nothing vagal about it, not even a registration with the vagal motor roots, as evidenced by the failure of isotopic grafts of the neural tube at that level to contribute fibers to the vagus nerve (Fig. 3*B*). [The term sympatho-enteric, which we repurpose, was originally coined to describe the crest from somites 1–5 (9), which straddles the two populations that we identify here, and therefore obscures their contrasted nature].

A third source of enteric precursors is the sacral crest, which contributes 20% of the neurons in the descending colon and rectum (29, 30). Since the major contribution of the sacral crest to the autonomic nervous system, the pelvic ganglion, is entirely sympathetic (31), the trunk crest is sympatho-enteric at both ends (Fig. 5). Given that thoracic crest will produce enteric neurons when transposed rostrally (32) and, more generally, that neural crest cells are not specified before migration (33, 34), the restriction of the dual sympatho-enteric fate to the cervical and sacral levels of the trunk crest is likely to stem, less from cell-intrinsic fate restriction than from topological factors, such as the continuity of the peri-aortic and foregut mesenchymes at one end, and the contiguity of the pelvic ganglion—a "staging site" for the enteric sacral crest (30, 35)—to the rectum at the other end.

A fourth, recently discovered source of enteric neurons are Schwann cell precursors at a later differentiation stage than the vagal ones we describe here, which travel along the mesenteric and pelvic nerves and become enteric neurons after birth (36). Many of them are presumably born in the thoracolumbar neural crest and it thus appears that the trunk crest has been co-opted in all of its regions (cervical, thoracolumbar, and sacral) to invade the gut, but at different stages of development, according to a variety of mechanisms and intermediates, in a seemingly opportunistic fashion. It will be interesting to explore the evolutionary history of this complicated and presumably stepwise assemblage. A recent study in lamprey (37) showed a contribution of the trunk crest but not of the vagal crest to the ENS. Since agnathans are suggested to have no sympathetic neural crest derivative (38), the absence of vagal contribution to the ENS fits with our data that the formerly called "vagal" crest of gnathostomes is for the most part cervical and sympathetic; but it also entails the surprising notion that the vagus nerve itself does not carry Schwann cell precursors-like enteroblasts to the gut of lampreys, when trunk nerves do.

Finally, after an early suggestion (39), we conclusively demonstrate a role for ErbB-mediated signaling during the embryonic development of the ENS. Better than the previous implication of ErbB/Nrg1 signaling in postnatal enteric ganglia in vivo (40) or in vitro (41), it could explain that common variants of *Neuregulin-1*, the ErbB3 ligand, are associated with Hirschsprung's disease, which results from a partial agenesis of enteric ganglia (42). Given the missing heritability in Hirschprung disease, our results are also a suggestion to look for *ErbB3* variants. Another possible clinical relevance is to neuropathic cases of chronic intestinal pseudo-obstruction (43).

Materials and Methods

In situ hybridization and immunochemistry have been described previously (44). Immunofluorescence on cryostat or vibratome sections was performed as previously described (18). Whole-mount immunofluorescent staining using the 3DISCO method was adapted from ref. 45, as previously described (31). Whole mounts of chicken embryos were treated as described in *SI Materials and Methods*. Transgenic chicken expressing the GFP reporter ubiquitously (46) were obtained from the Roslin Institut (University of Edinburgh). Chicken chimeras were generated via transplantation of discrete segments of the neural tube, including the neural crest, from GFP^{+} donors to wild-type hosts, as previously described (47). References for all antibodies and mouse lines are in *SI Materials and Methods*. Quantification of esophageal neurons and measurements of the

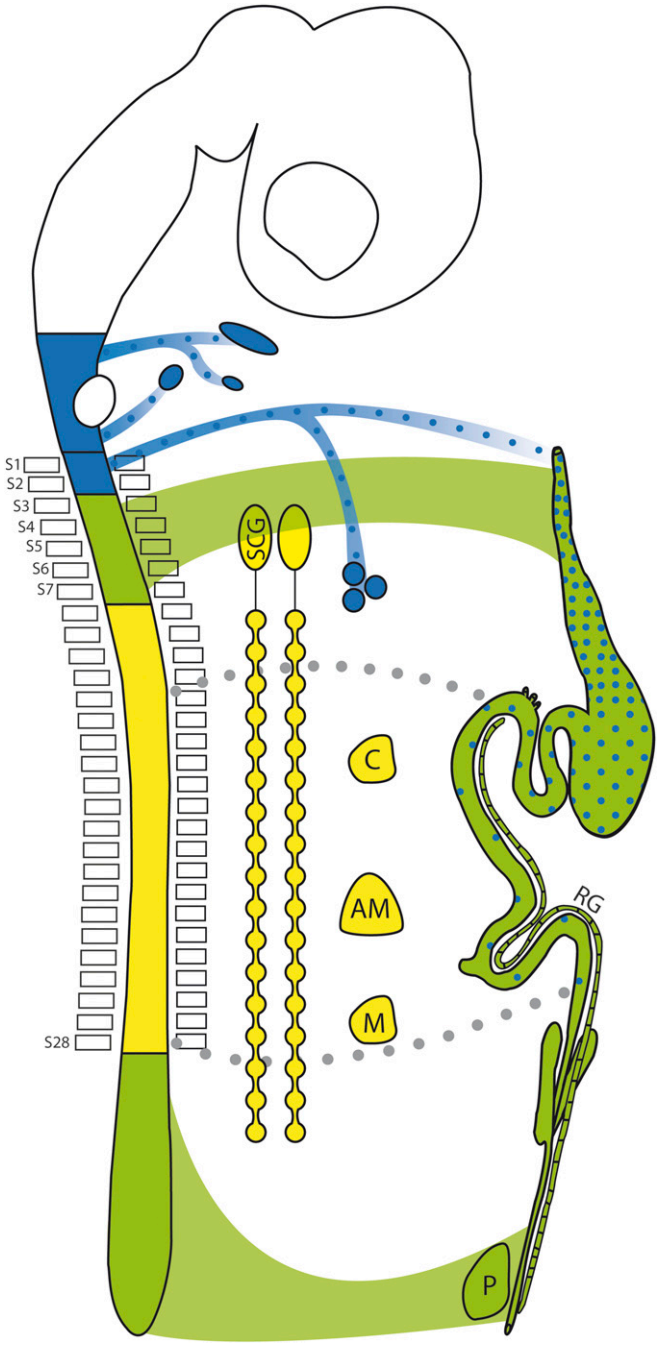

Fig. 5. Rostro-caudal levels of the neural crest contribution to the ENS. Schematic of the central and autonomic nervous systems of a tetrapod showing the three types of neural crest cells that can be distinguished according to their fates: (*i*) sympathetic and sympathoadrenal (yellow) from somite 8–28, that contributes to most para- and prevertebral sympathetic ganglia (C: celiac; M: mesenteric) and the adrenal medulla (AM); (*ii*) sympatho-enteric (green) from somite 3–7 and caudal to somite 28, that contributes to the superior cervical ganglion (SCG) and forms the pelvic ganglion (P) [as well as the ganglion of Remak in chicken (RG)], and most of the ENS; and (*iii*) parasympatho-enteric (blue), from preotic levels to somite 2, that forms parasympathetic ganglia and contributes to the foregut nervous system. Gray dots represent postnatal contribution of Schwann cell precursors of enteric extrinsic nerves to the ENS (36).

surface occupied by enteric neuron nuclei in the postgastric ENS were performed by use of FIJI software, as described in more details in *SI Materials and Methods*. All animal studies were done in accordance with the guidelines issued by the French Ministry of Agriculture and have been approved by the Direction Départementale des Services Vétérinaires de Paris.

ACKNOWLEDGMENTS. We thank the Imaging Facility of Institut de Biologie de l'École Normale Supèrieure (IBENS); the animal facility of IBENS; C. Goridis for helpful comments on the manuscript; and all the members of the J.-F.B. laboratory for discussions. The imaging facility of IBENS is supported by grants from the Fédération pour la Recherche sur le Cerveau, Région Ile de France DIM NeRF 2009 and 2011 and France-BioImaging. This study was supported by the CNRS, the Ecole normale supérieure, INSERM, Agence Nationale de la Recherche Award ANR-12-BSV4-0007-01 (to J.-F.B.), Fondation pour la Recherche Médicale Award DEQ2000326472 (to J.-F.B.), the 'Investissements d'Avenir' program of the French Government implemented by the Agence Nationale de la Recherche (referenced ANR-10-LABX-54 MEMO LIFE and ANR-11-IDEX-0001-02 PSL* Research University). I.E.-M. received a fellowship from the French Ministry of Higher Education and Research and from the Fondation pour la Recherche Médicale (FDT20160435297).

1. Uesaka T, Young HM, Pachnis V, Enomoto H (2016) Development of the intrinsic and extrinsic innervation of the gut. *Dev Biol* 417:158–167.
2. Heanue TA, Shepherd IT, Burns AJ (2016) Enteric nervous system development in avian and zebrafish models. *Dev Biol* 417:129–138.
3. Sasselli V, Pachnis V, Burns AJ (2012) The enteric nervous system. *Dev Biol* 366:64–73.
4. Lake JI, Heuckeroth RO (2013) Enteric nervous system development: Migration, differentiation, and disease. *Am J Physiol Gastrointest Liver Physiol* 305:G1–G24.
5. Kuntz A (1910) The development of the sympathetic nervous system in mammals. *J Comp Neurol Psychol* 20:211–258.
6. Yntema CL, Hammond WS (1954) The origin of intrinsic ganglia of trunk viscera from vagal neural crest in the chick embryo. *J Comp Neurol* 101:515–541.
7. Le Douarin NM, Teillet MA (1973) The migration of neural crest cells to the wall of the digestive tract in avian embryo. *J Embryol Exp Morphol* 30:31–48.
8. Baetge G, Gershon MD (1989) Transient catecholaminergic (TC) cells in the vagus nerves and bowel of fetal mice: Relationship to the development of enteric neurons. *Dev Biol* 132:189–211.
9. Durbec PL, Larsson-Blomberg LB, Schuchardt A, Costantini F, Pachnis V (1996) Common origin and developmental dependence on c-ret of subsets of enteric and sympathetic neuroblasts. *Development* 122:349–358.
10. Nagy N, Goldstein AM (2017) Enteric nervous system development: A crest cell's journey from neural tube to colon. *Semin Cell Dev Biol* 66:94–106.
11. Burns AJ, Delalande J-MM, Le Douarin NM (2002) In ovo transplantation of enteric nervous system precursors from vagal to sacral neural crest results in extensive hindgut colonisation. *Development* 129:2785–2796.
12. Kuo BR, Erickson CA (2011) Vagal neural crest cell migratory behavior: A transition between the cranial and trunk crest. *Dev Dyn* 240:2084–2100.
13. Yan H, et al. (2004) Neural cells in the esophagus respond to glial cell line-derived neurotrophic factor and neurturin, and are RET-dependent. *Dev Biol* 272:118–133.
14. Cacalano G, et al. (1998) GFRalpha1 is an essential receptor component for GDNF in the developing nervous system and kidney. *Neuron* 21:53–62.
15. Sánchez MP, et al. (1996) Renal agenesis and the absence of enteric neurons in mice lacking GDNF. *Nature* 382:70–73.
16. Heanue TA, Pachnis V (2007) Enteric nervous system development and Hirschsprung's disease: Advances in genetic and stem cell studies. *Nat Rev Neurosci* 8:466–479.
17. Pattyn A, Morin X, Cremer H, Goridis C, Brunet JF (1999) The homeobox gene Phox2b is essential for the development of autonomic neural crest derivatives. *Nature* 399:366–370.
18. Espinosa-Medina I, et al. (2014) Neurodevelopment. Parasympathetic ganglia derive from Schwann cell precursors. *Science* 345:87–90.
19. Dyachuk V, et al. (2014) Neurodevelopment. Parasympathetic neurons originate from nerve-associated peripheral glial progenitors. *Science* 345:82–87.
20. Pattyn A, Morin X, Cremer H, Goridis C, Brunet JF (1997) Expression and interactions of the two closely related homeobox genes Phox2a and Phox2b during neurogenesis. *Development* 124:4065–4075.
21. Newbern J, Birchmeier C (2010) Nrg1/ErbB signaling networks in Schwann cell development and myelination. *Semin Cell Dev Biol* 21:922–928.
22. Anderson RB, Stewart AL, Young HM (2006) Phenotypes of neural-crest-derived cells in vagal and sacral pathways. *Cell Tissue Res* 323:11–25.
23. Kuratani SC, Kirby ML (1991) Initial migration and distribution of the cardiac neural crest in the avian embryo: An introduction to the concept of the circumpharyngeal crest. *Am J Anat* 191:215–227.
24. Burns AJ, Champeval D, Le Douarin NM (2000) Sacral neural crest cells colonise aganglionic hindgut in vivo but fail to compensate for lack of enteric ganglia. *Dev Biol* 219:30–43.
25. Verberne ME, Gittenberger-De Groot AC, Van Iperen L, Poelmann RE (1999) Contribution of the cervical sympathetic ganglia to the innervation of the pharyngeal arch arteries and the heart in the chick embryo. *Anat Rec* 255:407–419.
26. Le Douarin N, Kalcheim C (1999) *The Neural Crest* (Cambridge Univ Press, Cambridge, UK).
27. Saito D, Takase Y, Murai H, Takahashi Y (2012) The dorsal aorta initiates a molecular cascade that instructs sympatho-adrenal specification. *Science* 336:1578–1581.
28. Britsch S, et al. (1998) The ErbB2 and ErbB3 receptors and their ligand, neuregulin-1, are essential for development of the sympathetic nervous system. *Genes Dev* 12:1825–1836.
29. Burns AJ, Douarin NM (1998) The sacral neural crest contributes neurons and glia to the post-umbilical gut: Spatiotemporal analysis of the development of the enteric nervous system. *Development* 125:4335–4347.
30. Kapur RP (2000) Colonization of the murine hindgut by sacral crest-derived neural precursors: Experimental support for an evolutionarily conserved model. *Dev Biol* 227:146–155.
31. Espinosa-Medina I, et al. (2016) The sacral autonomic outflow is sympathetic. *Science* 354:893–897.
32. Le Douarin NM, Teillet MA (1974) Experimental analysis of the migration and differentiation of neuroblasts of the autonomic nervous system and of neurectodermal mesenchymal derivatives, using a biological cell marking technique. *Dev Biol* 41:162–184.
33. Baggiolini A, et al. (2015) Premigratory and migratory neural crest cells are multipotent in vivo. *Cell Stem Cell* 16:314–322.
34. Bronner-Fraser M, Fraser SE (1988) Cell lineage analysis reveals multipotency of some avian neural crest cells. *Nature* 335:161–164.
35. Nagy N, Brewer KC, Mwizerwa O, Goldstein AM (2007) Pelvic plexus contributes ganglion cells to the hindgut enteric nervous system. *Dev Dyn* 236:73–83.
36. Uesaka T, Nagashimada M, Enomoto H (2015) Neuronal differentiation in Schwann cell lineage underlies postnatal neurogenesis in the enteric nervous system. *J Neurosci* 35:9879–9888.
37. Green SA, Uy BR, Bronner ME (2017) Ancient evolutionary origin of vertebrate enteric neurons from trunk-derived neural crest. *Nature* 544:88–91.
38. Häming D, et al. (2011) Expression of sympathetic nervous system genes in lamprey suggests their recruitment for specification of a new vertebrate feature. *PLoS One* 6:e26543.
39. Erickson SL, et al. (1997) ErbB3 is required for normal cerebellar and cardiac development: A comparison with ErbB2-and heregulin-deficient mice. *Development* 124:4999–5011.
40. Crone SA, Negro A, Trumpp A, Giovannini M, Lee K-F (2003) Colonic epithelial expression of ErbB2 is required for postnatal maintenance of the enteric nervous system. *Neuron* 37:29–40.
41. Barrenschee M, et al. (2015) Expression and function of Neuregulin 1 and its signaling system ERBB2/3 in the enteric nervous system. *Front Cell Neurosci* 9:360.
42. Tang CS-M, et al. (2016) Trans-ethnic meta-analysis of genome-wide association studies for Hirschsprung disease. *Hum Mol Genet* 25:5265–5275.
43. Burns AJ, et al. (2016) White paper on guidelines concerning enteric nervous system stem cell therapy for enteric neuropathies. *Dev Biol* 417:229–251.
44. Coppola E, et al. (2010) Epibranchial ganglia orchestrate the development of the cranial neurogenic crest. *Proc Natl Acad Sci USA* 107:2066–2071.
45. Ertürk A, et al. (2012) Three-dimensional imaging of solvent-cleared organs using 3DISCO. *Nat Protoc* 7:1983–1995.
46. McGrew MJ, et al. (2004) Efficient production of germline transgenic chickens using lentiviral vectors. *EMBO Rep* 5:728–733.
47. Delalande J-M, Thapar N, Burns AJ (2015) Dual labeling of neural crest cells and blood vessels within chicken embryos using Chick(GFP) neural tube grafting and carbocyanine dye DiI injection. *J Vis Exp* 99:e52514.
48. Hama H, et al. (2011) Scale: A chemical approach for fluorescence imaging and reconstruction of transparent mouse brain. *Nat Neurosci* 14:1481–1488.
49. Dubreuil V, et al. (2009) Defective respiratory rhythmogenesis and loss of central chemosensitivity in Phox2b mutants targeting retrotrapezoid nucleus neurons. *J Neurosci* 29:14836–14846.
50. D'Autréaux F, Coppola E, Hirsch M-R, Birchmeier C, Brunet J-F (2011) Homeoprotein Phox2b commands a somatic-to-visceral switch in cranial sensory pathways. *Proc Natl Acad Sci USA* 108:20018–20023.
51. Nagashimada M, et al. (2012) Autonomic neurocristopathy-associated mutations in PHOX2B dysregulate Sox10 expression. *J Clin Invest* 122:3145–3158.
52. Danielian PS, Muccino D, Rowitch DH, Michael SK, McMahon AP (1998) Modification of gene activity in mouse embryos in utero by a tamoxifen-inducible form of Cre recombinase. *Curr Biol* 8:1323–1326.
53. Lallemand Y, Luria V, Haffner-Krausz R, Lonai P (1998) Maternally expressed PGK-Cre transgene as a tool for early and uniform activation of the Cre site-specific recombinase. *Transgenic Res* 7:105–112.
54. Sheean ME, et al. (2014) Activation of MAPK overrides the termination of myelin growth and replaces Nrg1/ErbB3 signals during Schwann cell development and myelination. *Genes Dev* 28:290–303.
55. Riethmacher D, et al. (1997) Severe neuropathies in mice with targeted mutations in the ErbB3 receptor. *Nature* 389:725–730.
56. Li L, et al. (2002) The breast proto-oncogene, HRGalpha regulates epithelial proliferation and lobuloalveolar development in the mouse mammary gland. *Oncogene* 21:4900–4907.
57. Meyer D, Birchmeier C (1995) Multiple essential functions of neuregulin in development. *Nature* 378:386–390.
58. Meyer D, et al. (1997) Isoform-specific expression and function of neuregulin. *Development* 124:3575–3586.

Supporting Information

Espinosa-Medina et al. 10.1073/pnas.1710308114

SI Materials and Methods

Histology. Whole chicken and mice guts were fixed for 1 h in 4% paraformaldehyde (in PBS), permeabilized in 1% Triton (in PBS) for 30 min and incubated over night at 4 °C with primary antibodies in blocking solution (1% DMSO, 0.1% Triton in PBS, 20% FCS). After extensive washes in blocking solution, whole guts were incubated over night at 4 °C, with secondary antibodies in blocking solution. After several washes in 0.1% Triton in PBS, samples were cleared in Glycerol 80% in PBS.

Whole chicken chimeras were cleared using ScaleA2 solution as previously described (48). Samples were imaged using a SP8 or SP5 confocal microscope (Leica). Three-dimensional reconstructions and videos were obtained using the IMARIS imaging software. In situ hybridization and immunochemistry have been described previously (44). Immunofluorescence on cryostat sections was performed as previously described (18). Whole-mount immunofluorescent staining using the 3DISCO method was performed as previously described (31).

Image Generation and Processing. Samples were imaged using a SP8 or SP5 confocal microscope (Leica). Whole-embryo images were obtained by tile-scanning with a 20×-immersion objective and automatic stitching on a Leica SP8 confocal. Three-dimensional reconstructions and videos were obtained using the IMARIS imaging software. Note that the rendering process in IMARIS sometimes leads to the appearance of horizontal or vertical splices in the final whole-embryo images, which are processing artifacts. GFP/TH overlap panels in Fig. S6 are binary masks generated using the ImageJ software. Each .lif confocal file was first converted into .tiff, then run through a customized Macro involving the following processing steps: (*i*) background subtraction of the whole image; (*ii*) "despeckling"; (*iii*) "autothresholding"; (*iv*) binary mask generation (selection of the area of interest exclusively, i.e. the ganglion area); and (*v*) image calculator: calculates final binary image of the colocalized GFP/TH surfaces.

Antibodies and Probes. Antibodies and probes were as follows:

α-2H3 (NF), mouse, 1:500, Hybridoma Bank (#2H3);

α-bIII Tubulin (Tuj1), mouse, 1:500, Covance (#MMS-435P);

α-Phox2b, rabbit, 1:500 (20);

α-Phox2b, guinea pig, 1:500 (48);

α-Sox10, goat, 1:250, Santa Cruz (#SC-17342);

α-βgal, rabbit, 1:400, Cappel (#55976);

α-HuC/D mouse, 1:200, Invitrogen (MABN153);

α-GFP, chicken, 1:500, Aveslab (#GFP-1020);

α-HNK-1, mouse, 1:50, Hybridoma Bank (#3H5);

α-TH, rabbit, 1:800, Merck (#AB152);

α-rabbit Cy3, 1:500, Jackson Immunoresearch Laboratories (#711–165-152);

α-rabbit A488, 1:500, Jackson Immunoresearch Laboratories (#711–545-152);

α-goat Cy3, 1:500, Jackson Immunoresearch Laboratories (#705–166-147);

α-goat A647, 1:500, Jackson Immunoresearch Laboratories (#705–606-147);

α-mouse Cy3, 1:500, Jackson Immunoresearch Laboratories (#715–165-150);

α-mouse A488, 1:500, Invitrogen (#A-21202);

α-guinea pig Cy3, 1:500, Invitrogen (#A-11073);

α-chicken A488, 1:500, Jackson Immunoresearch Laboratories (#103–545-155).

Immunohistochemical reactions were processed with the Vectastain Elite ABC kits (PK-6101 and PK-6012; Vector Laboratories) as indicated by the manufacturer and color development was performed using DAB.

The probes for Cadherin19 and PLP-1 (cDNA from Source Bioscience, clones #IRCKp5014H0217Q and #IRAVp968G0365D, respectively) were synthesized following the distributor's information. The other probe used was *Peripherin* (obtained from M. M. Portier, Collège de France, Paris).

Transgenic Mouse Lines. Mouse lines used were as follows:

Phox2b::Cre(50): BAC transgenic line expressing Cre under the control of the Phox2b promoter.

Phox2b$^{LacZ/+}$ (17): Knockin line expressing the reporter gene *LacZ* from the second exon of the *Phox2b* locus, which is disrupted and lead to a null phenotype in *Phox2b*$^{LacZ/LacZ}$ embryos.

Ret$^{fl\text{-}CFP/+}$ (51): Knockin line comprising floxed human *Ret9* cDNA and CFP reporter in the first exon of the mouse *Ret* locus. Activation of Cre recombinase results in the removal of floxed *Ret9*, generating a CFP-knockin (*Ret*-null) allele.

Wnt1::Cre(52): Transgenic line expressing Cre under the control of the 3′ enhancer of Wnt1.

Pgk::Cre (53): Transgenic line expressing Cre in the germ line.

Phox2a^{ASIC2a} (*P2aASIC*) (18): Knockin line expressing the toxic G430 mutant of the ASIC2a cation channel upon Cre recombination under the control of *Phox2a* promoter.

ErbB3^{f} (*ErbB3*$^{Lox/Lox}$) (54): Activation of Cre recombinase results in the removal of floxed *ERBB3*, generating a *ErbB3*-null allele, which lacks the same coding sequences as the previously described ErbB3Δallele (55).

Nrg1^{tm3Cbm} (*Nrg1*$^{Lox/Lox}$) (56): A floxed allele of the *Nrg-1* gene containing loxP sites flanking exons 7 (containing sequence alterations), 8 and 9 was generated. Activation of Cre recombinase results in the removal of floxed *Nrg1*, generating a *Nrg-1* null allele.

Neuregulin$^{\Delta EGF\text{-}lacZ}$ (*Nrg* $^{LacZ/+}$) (57, 58): Knock in line expressing the reporter gene *LacZ* from the exon of the *Neuregulin1* locus.

All animal studies were done in accordance with the guidelines issued by the French Ministry of Agriculture and have been approved by the Direction Départementale des Services Vétérinaires de Paris.

Statistical Analyses. For esophageal neuronal counting, transverse sections of whole E13.5 embryos where immunostained for Phox2b and one section of three was selected. The total number of Phox2b^{+} cells in the esophageal walls was recorded using FIJI Cell Counter.

For postgastric neuronal countings, whole E13.5 guts were dissected and immunostained for Phox2b. The surface occupied by Phox2b^{+} enteric neurons was measured in three regions up to the cecum (at equal distances from the stomach for both wild-type and mutant embryos). First, stacked confocal images were transformed into Binary images, with a threshold restricted to the Phox2b^{+} cell surfaces. The total surface was then measured automatically by the FIJI Measuring tool applied to a specific perimeter of the total image (this perimeter was created to avoid areas of the image empty of gut tissue). Then the relation between total surface area/perimeter per region was recorded.

The similarity of variances between each group of data were tested using the *F* test. Statistical analysis was performed using unpaired two-tailed *t* test. Results are expressed as mean ±SEM %/wild-type.

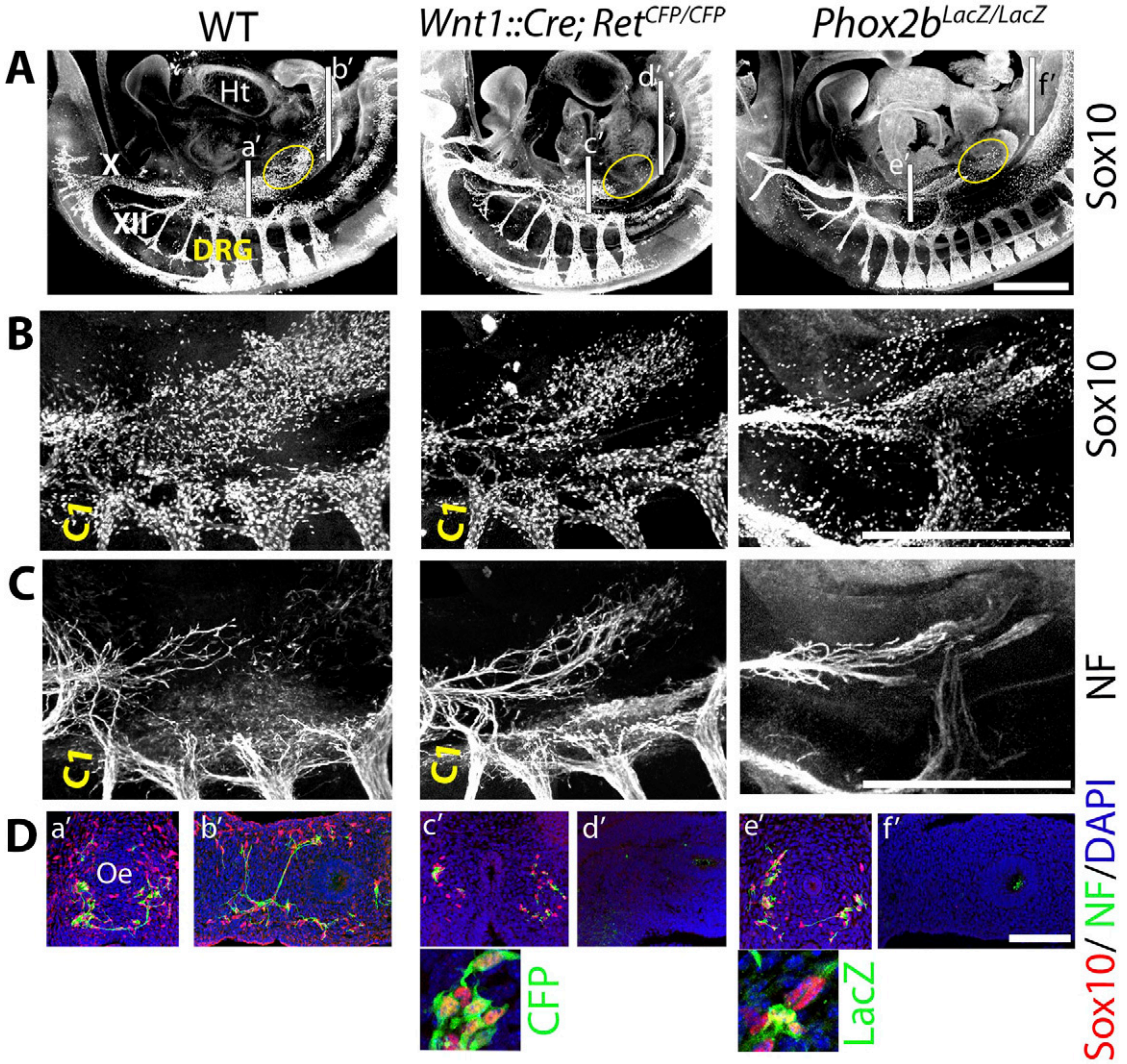

Fig. S1. Presence of enteric precursors associated with vagal nerve fibers in *Ret* and *Phox2b* mutants. (*A*) Lateral views of whole-mount E10.5 embryos of the indicated genotypes stained with the indicated markers. A yellow circle indicates the position of the stomach primordium. (*B*) Close-ups of the esophageal region stained with Sox10. (*C*) Close-ups on the esophageal region stained with Neurofilament. In *Wnt1::Cre;Ret*$^{CFP/CFP}$ and *Phox2b*$^{LacZ/LacZ}$ mice Sox10^{+} (thus neural crest-derived) cells are mostly confined to the fibers of the vagus nerve, unlike in the wild-type. (*D*, *Upper*) Transverse sections through the gut at the positions indicated in *A*, stained for the indicated markers. (*Lower*) Higher magnifications of groups of cells costained for Sox10 and DAPI and either the reporter Ret-CFP or Phox2b-LacZ. NCC are absent from the postgastric ENS in both *Wnt1::Cre;Ret*$^{CFP/CFP}$ and *Phox2b*$^{LacZ/LacZ}$ mutants (*D*, sections *d′* and *f′*). C1: first cervical spinal nerve. DRG, dorsal root ganglia; Oe, esophagus; X, vagus nerve; XII, hypoglossal nerve. (Scale bars: *A–C,* 500 μm; *D* 50 μm.)

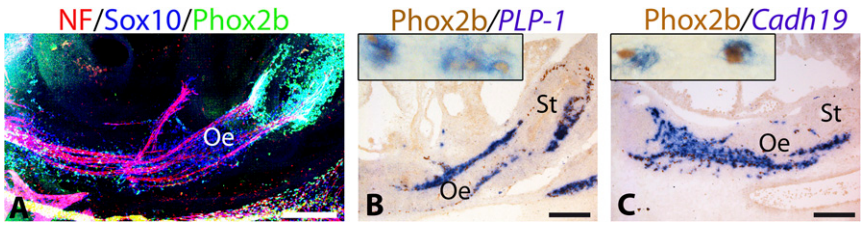

Fig. S2. Vagal-associated enteric precursors share their molecular signature with Schwann cell precursors. (*A*–*C*) Sagittal sections through the foregut of an E11.5 wild-type embryo, stained with the indicated antibodies and probes. Phox2b^{+} enteric precursors alongside the esophagus express the Schwann cell precursor markers *PLP-1* (*B*) and *Cadh19* (*C*). *Insets* show higher magnifications of double-positive enteric precursors scattered in the esophageal wall. Oe, esophagus; St, stomach. (Scale bars, 100 μm.)

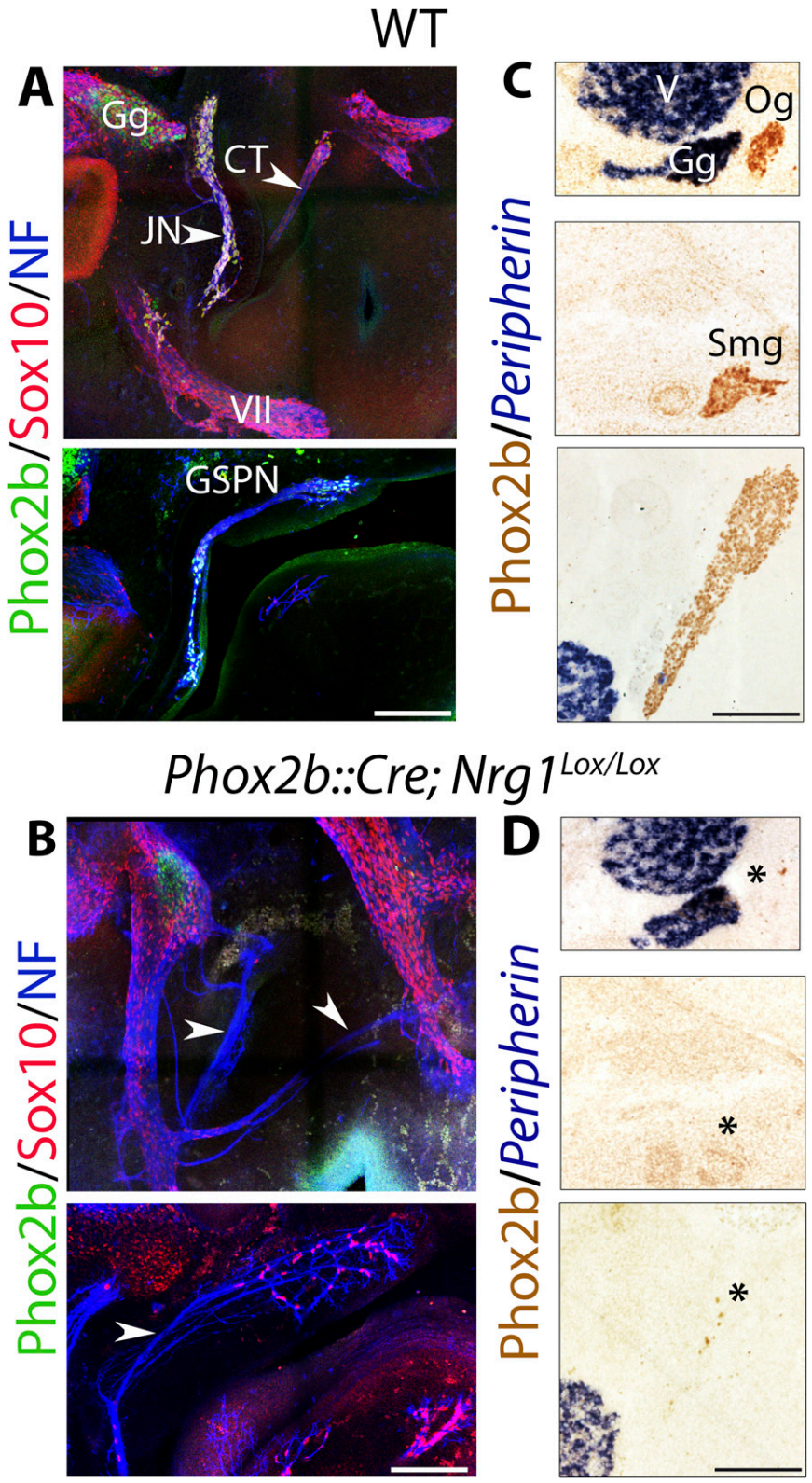

Fig. S3. Axonal Nrg1 is required for the migration of parasympathetic precursors along cranial nerves. (*A* and *B*) Lateral views of the head of whole-mount embryos at E11.5 of the indicated genotypes, immunostained with the indicated markers, showing the facial nerve (VII), Jacobson's nerve (JN), the corda tympani (CT), and the greater petrosal nerve (GSPN), covered with Sox10^{+} neural crest-derived cells (some of them coexpressing Phox2b) in the wild-type (*A*), but naked in the *Nrg1* mutant (white arrowheads in *B*). (*C* and *D*) Parasagittal sections at E13.5 showing parasympathetic ganglia associated with these nerves in the wild-type embryo (*C*)—the otic ganglion (Og), the submandibular ganglion (Smg), and the Sphenopalatine ganglion (Spg)—but absent in the *Nrg1* mutant (asterisks in *D*). Gg, geniculate ganglion; V, trigeminal ganglion. (Scale bars: *A* and *B*, 200 μm; *C* and *D*, 100 μm.)

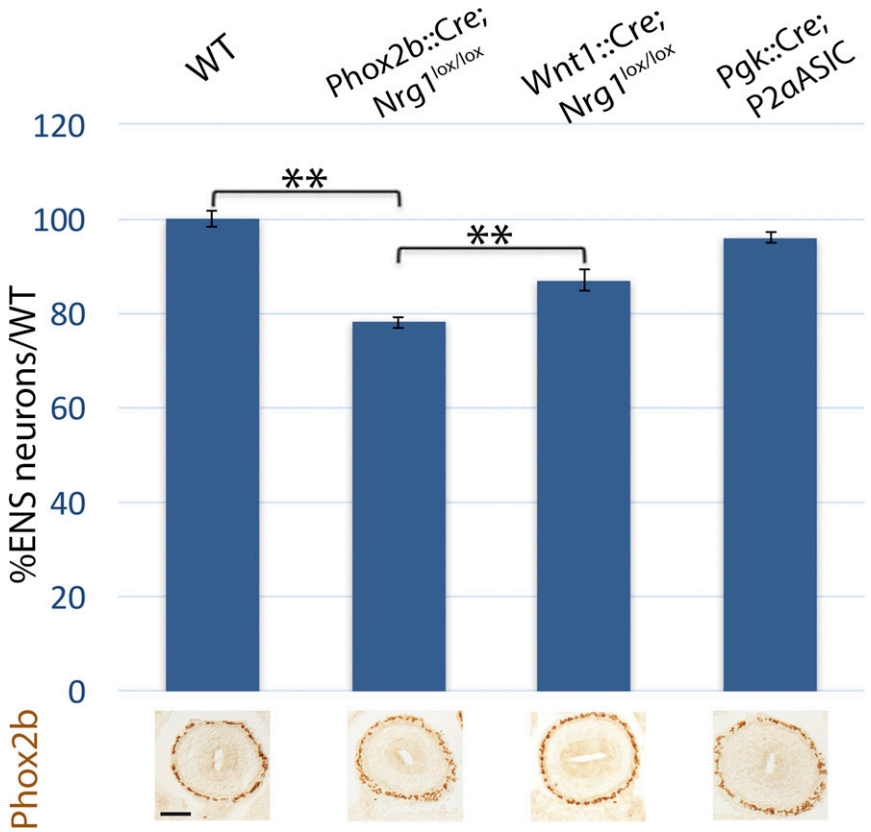

Fig. S4. Consequences on the postgastric ENS of the deletion of the vagus nerve or abrogation of its expression of *Nrg1*. (*Upper*) Quantitative analysis (see *Methods*) of the surface occupied by Phox2b^{+} ENS neurons in the indicated mutant backgrounds. *Phox2b::Cre;Nrg1$^{lox/lox}$* embryos have a mild atrophy of the postgastric ENS (79 ± 1.1%/wild-type, $P = 0.0047$; $n = 9$; and 90 ± 2%/*Wnt1::CreNrg1$^{lox/lox}$*, $P = 0.0040$; $n = 5$), due to loss of *Nrg1* expression by the vagus nerve, and not by enteric precursors, as shown by the lack of phenotype in *Wnt1::Cre;Nrg1$^{lox/lox}$* (87 ± 2.3%/wild-type, $P = 0.237$; $n = 5$). *Pgk::Cre;P2a^{ASIC}* have no phenotype (93 ± 1.2%/wild-type, $P = 0.283$; $n = 4$), presumably because genetic deletion of the nerve is less efficient or occurs later than abrogation of its expression of *Nrg1* (and in line with a weaker phenotype in the esophagus) (Fig. 1*B*). (*Lower*) Representative transverse sections through the postgastric ENS of the indicated mutant backgrounds, immunostained for Phox2b. (Scale bar: 50 μm.) Error bars indicate SEM; $^{**}P < 0.005$.

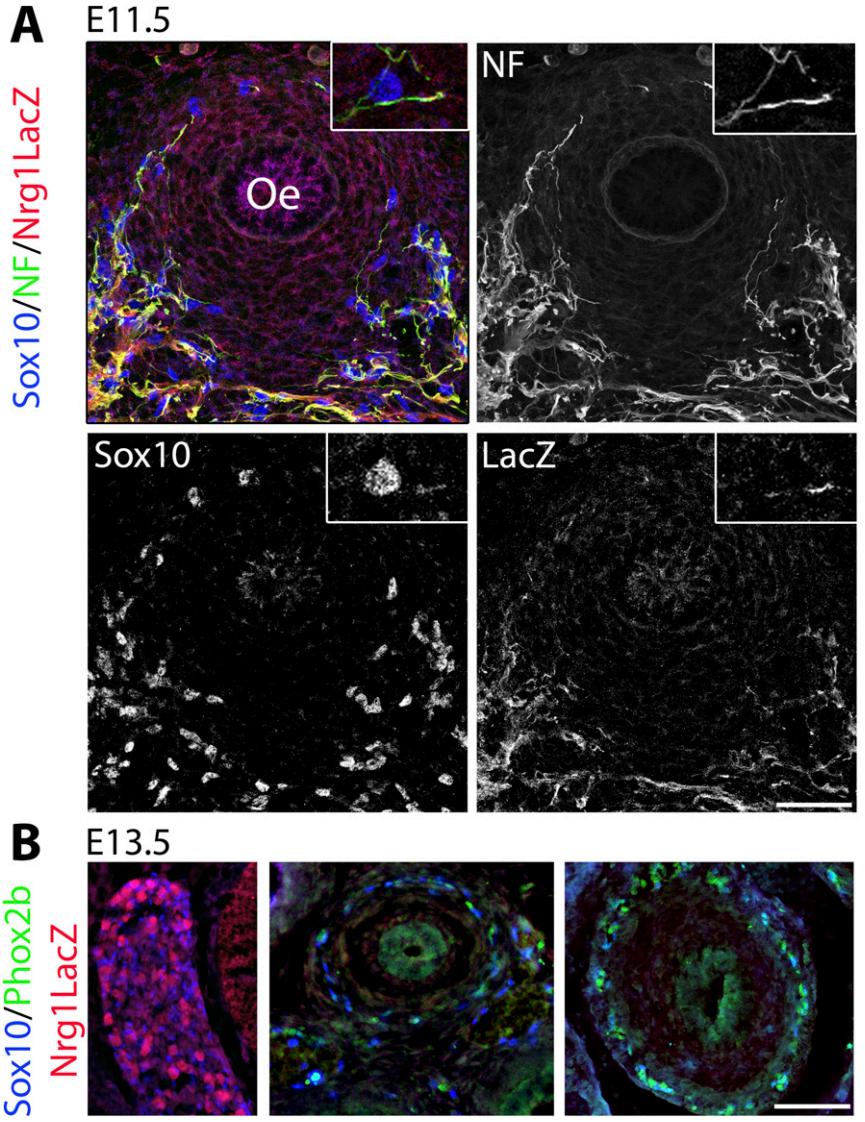

Fig. S5. Esophageal neuronal precursors do not express *Nrg1*. (*A*) Transverse sections through the esophagus of E11.5 *Nrg1*$^{LacZ/+}$ embryos, immunostained for Sox10 (which labels all enteric precursors at this stage), NF (neurofilament, which labels fibers of the vagus nerve), and β-galactosidase (which labels cells that express the *Nrg1* reporter LacZ). Vagus nerve fibers are LacZ^{+}, whereas enteric precursors are LacZ^{-}. (*Insets*) Close up (3× zoom of a cell in the lower magnification image) of a representative enteric precursor. (*B*) Transverse section through an E13.5 embryo at the level of a dorsal root ganglion (*Left*), the esophagus (*Center*), and an intestinal loop (*Right*). Dorsal root ganglionic cells serve as a LacZ^{+} control, Sox10^{+}/Phox2b^{+} esophageal and enteric precursors are LacZ^{-}. (Scale bars: *A*, 50 μm; *B*, 100μm.)

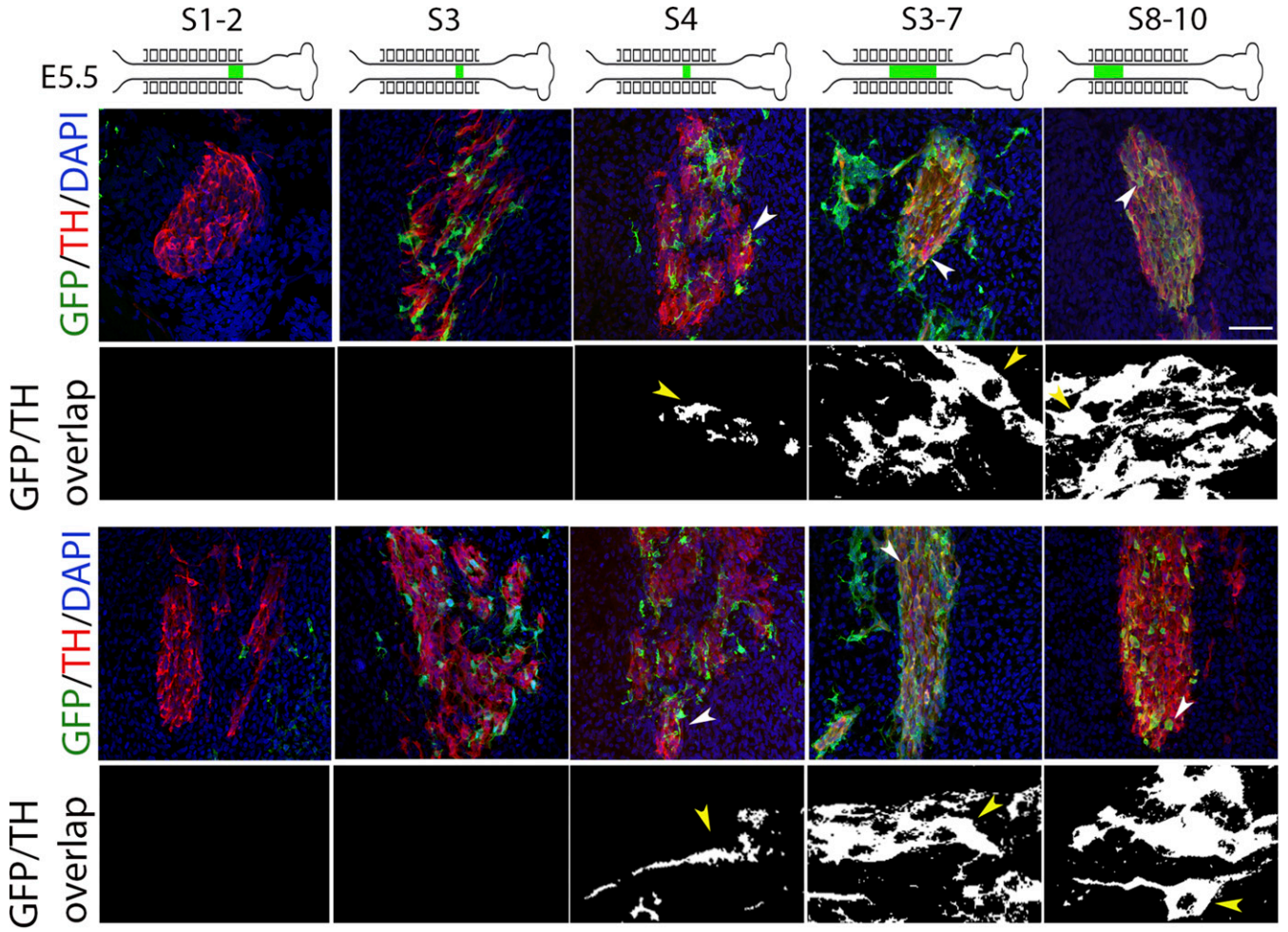

Fig. S6. The superior cervical ganglion receives contribution of the neural crest from level S3 to S10. Sections through the rostral pole of cervical sympathetic chain of chicken embryos at E5.5, after they received an isotopic graft of the neural tube from a GFP-transgenic donor at stage 10, at the indicated levels, stained with the indicated antibodies. Two sections from two embryos are shown for each type of graft. GFP/TH overlap panels show higher-magnification (*Insets*) of a GFP^+/TH^+ neuron or group of neurons (indicated by white arrowheads, *Upper*, corresponding to yellow arrowheads, *Lower*). S1–2 grafts do not contribute any cell to the SCG, S3 only glia, S4 glia, and an occasional neuron, S5–S10 many neurons and glia. (Scale bar, 50 μm.)

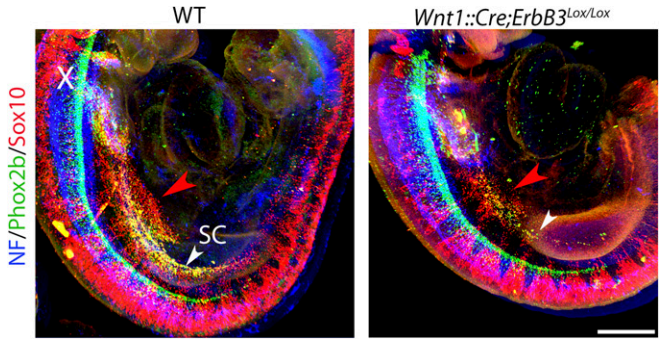

Fig. S7. Atrophy of the sympathetic chain in *Wnt1Cre;ErbB3$^{lox/lox}$* mutants. Whole-mount views of E10 embryos of the indicated genotypes, immunostained with the indicated antibodies. White arrowhead: sympathetic chain (SC); red arrowhead: cervical contingent of sympatho-enteric cells; X, vagus nerve. (Scale bar, 500 μm.)

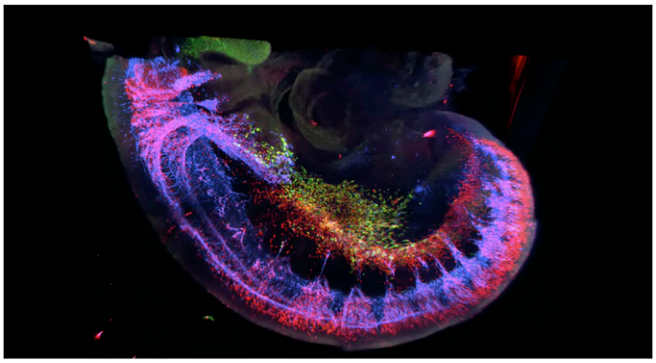

Movie S1. Two distinct streams of cells migrate to the esophagus in an E10 mouse embryo. Three-dimensional reconstruction of an E10 *Wnt1::Cre ;Ret*$^{CFP/+}$ embryo. The vagus nerve (NF^{+}, blue) projects dorsolaterally from the hindbrain to the foregut accompanied by neural crest cells (Sox10^{+}, red). Ahead of the vagus nerve and medially to it, a swarm of neural crest cells emerge from the incipient sympathetic chain toward the foregut. Enteric precursors at the level of the future esophagus express the reporter CFP (green) from the *Ret* promoter. The images were captured with a 20× objective on a SP8 confocal microscope.

Movie S1

Unpublished Results

I. Genetic interaction between *ErbB3* and *Ret*

The role of the *ErbB3/Nrg1* signaling pathway in the development of the ENS has been previously established (Espinosa-Medina et al., 2017), its abrogation entailing a deficit in neuron numbers, according to a gradient from esophagus to rectum, from 75 to 50%. On the other hand, in large Genome Wide Associated Studies of Hirschsprung disease, whose major causative gene is *RET*, variants of *NRG1* have been statistically associated with variants of *RET,* making *NRG1* a modifier of *RET* (Tang et al., 2016). Given the novel role discovered for *Erbb3* (a coreceptor for *Nrg1*) in the development of the ENS, I explored the possibility that it could interact with *Ret* in mouse, more precisely whether a heterozygous null mutation in *Ret* (asymptomatic in mice) could worsen the neuronal deficit of a homozygous null mutation in *Erbb3* and lead to a more pronounced hypoganglionosis, or even possibly a partial aganglionosis of the distal colon, pathognomonic of Hirschsprung disease. To do so, I generated an *ErbB3$^{lox/lox}$; Ret$^{lox/lox}$* line that I crossed with a *Wnt1::Cre; ErbB3$^{lox/+}$* line to generate, from a same litter, double *Wnt1::Cre; ErbB3$^{lox/lox}$; Ret$^{lox/+}$* mutants, and control *Wnt1::Cre; ErbB3$^{lox/lox}$* embryos, at E17.5.

I immunostained flatmounts of the gut for Phox2b and estimated the surface occupied by nuclei of enteric neurons. In the context of a homozygous null *ErbB3* background, the loss of one allele of *Ret* caused a loss of 20% of enteric neurons. Compared to the WT condition, the effect of the double *Wnt1::Cre; ErbB3$^{lox/lox}$; Ret$^{lox/+}$* mutation was thus a reduction by 60% of the number of neurons in the rectum at E17.5 (**Fig. 1**). Therefore, a null *Erbb3* mutation unmasks a haploinsufficiency of *Ret*. On the other hand, I did not detect aganglionosis of the rectum, so that this double mutation is not a *bona fide* model of Hirschsprung disease. However, a caveat to this conclusion is that there was a large variation in the effect of the double mutation from animal to animal, and one of the 8 *Wnt1::Cre; ErbB3$^{lox/lox}$; Ret$^{lox/+}$* mutants had a 80% deficit in rectal enteric neurons (**Fig. 2**). It remains thus possible that a *bona fide* Hirschsprung-like deficit occurs at low penetrance, and would be found in a larger cohort of mutants.

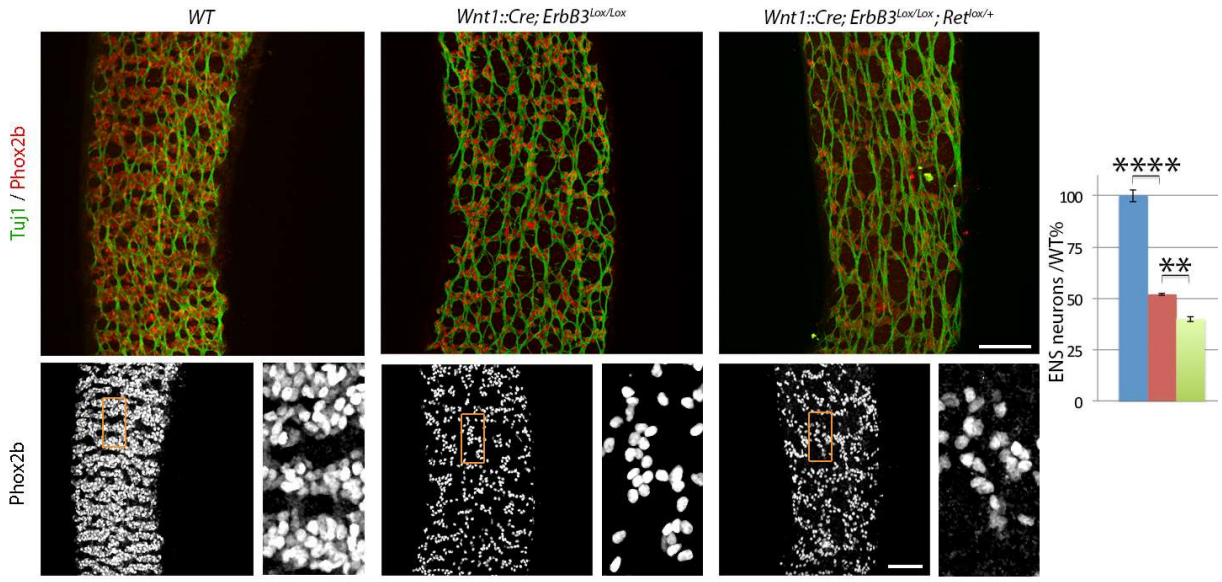

Figure 1: The reduction in *Ret* dosage worsens the ENS phenotype of the ErbB3 null mutation. Whole mounts of dissected rectum at E17.5 in WT (left), *Wnt1::Cre; ErbB3$^{lox/lox}$* (middle) and *Wnt1::Cre; ErbB3$^{lox/lox}$; Ret$^{lox/+}$* (right) stained for Tuj1 (green) and Phox2b (red) in upper panels and Phox2b on the close ups (4x zoom) in the lower panels. The atrophy of the enteric ganglia is quantified on the graph. *Wnt1::Cre; ErbB3$^{lox/lox}$* (red) showed fewer neurons than WT (49 ± 0.41%; P = 0,00001, n=4)(red), and *Wnt1::Cre; ErbB3$^{lox/lox}$; Ret$^{lox/+}$* (green) even fewer (61 ± 1,22% ; P = 0,0085, n=8). Scale bars are 100µm. Error bars indicate SEM. ***P<0.01, ****P<0.0005.

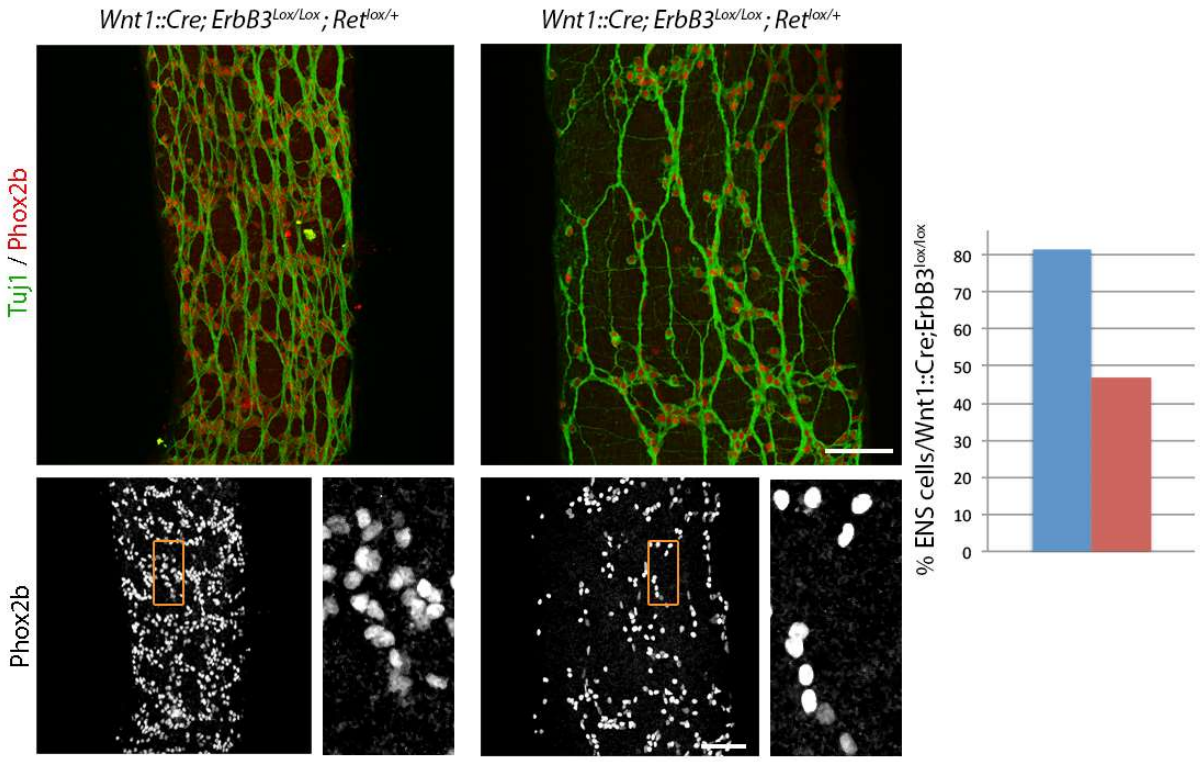

Figure 2: Large variations in the effect of Ret mutation in the context of the ErbB3 mutation. Whole mount of dissected rectum at E17.5 of two *Wnt1::Cre; ErbB3$^{lox/lox}$; Ret$^{lox/+}$* animals, stained for Tuj1 (green) and Phox2b (red) in upper panels and Phox2b in the lower panels (4x zoom) where the boxed area corresponds to the inset on the right hand of each panel. The atrophy of the enteric ganglia is quantified on the graph relative to the single *Erbb3* mutant (respectively 47% and 81% of *Wnt1::Cre; ErbB3$^{lox/lox}$*). Scale bars are 100µm.

II. *Hmx2* and *Hmx3* knockouts

II.A. Construction

The two paralogues *Hmx2* and *Hmx3* are expressed in the parasympathetic ganglia (Espinosa-Medina et al., 2016), and in the ENS (Heanue and Pachnis, 2006), where a potential effect of their mutation was never analyzed. As it happens the *Hmx2* mutant and the *Hmx2/3* double mutants that had been generated in the lab of Thomas Lufkin (Wang et al., 2001, 2004) were lost and the *Hmx3* mutant generated by Eva Bober (Hadrys et al., 1998) exists only in the form of frozen sperm. I thus set out to recreate these mutants, which meant generating independently 3 knockout line (*Hmx2*, *Hmx3* and *Hmx2/3*), because the similar expression of both paralogues in the ENS makes redundancy likely, and their extreme genetic linkage precludes the production of a double mutant by intercrosses of the single ones.

I opted for the use of the CRISPR/Cas9, a technique which was becoming standard. Despite the very preliminary, and thus far inconclusive, phenotypic analysis of the mutants (and moreover their possibly loss because of the COVID crisis), I will report here the process of their production, which proved much less straightforward than one could have surmised from the literature.

Two single guide RNAs (sgRNA) were designed and assayed on in vitro culture for their efficiency by J.P. Concordet (Muséum National d'Histoire Naturelle). These two sgRNA were conceived so that, in theory, they could produce a single cut followed by repair in the first exon of *Hmx2*, a single cut followed by repair in the first exon of *Hmx3*, a cut followed by repair in both *Hmx2* and *Hmx3* and a large deletion of the whole segment in between the cuts (**Fig. 3A**). To maximize the odds of creating null mutations, I designed a matrix that could be used to repair the sequence of *Hmx2* and/or *Hmx3* after the cut: the matrix was composed of two arms of 40bp of *Hmx2* or *Hmx3* that surround the cut site, 3 STOP codons that insured the production of a truncated protein in case of in-phase repair, and 2 restriction sites to facilitate the future genotyping of the animals.

Eggs were injected with 100ng/µl of *Cas9* RNA, 50ng/µl of each sgRNA and 100µl of each matrix by F. El Marjou (Genetic Platform of Institut Curie). In the following weeks, 12 pups were born, most of whom had a strong circling behavior, previously described in double *Hmx2/3* homozygous knockouts (Wang et al., 2004) due to a massive defect of the inner ear. As expected from their previous description, they all died before they could be crossed. A genotyping test on their tail tissue, by PCR followed by restriction digestion of the amplicon, revealed no integration of the repair matrix. The conclusion was i)

that repair occurred without integration of the matrix and ii) that the cuts were too efficient and presumably occurred systematically on the 4 alleles of *Hmx2/3*. A second injection was thus planned with reduced amounts of *Cas9* RNA and sg RNA, to diminish the efficiency of the system: one batch of eggs was injected with 50ng/µl of *Cas9* RNA and 20ng/µl of each sgRNA and a second batch with 20ng/µl of *Cas9* RNA and 10ng/µl of each sgRNA. Because the matrix did not seem to integrate well, it was omitted altogether to reduce DNA toxicity. From this second round of injections, 50 pups were born, a fraction of them presenting with a circling phenotype of various intensity. PCR analysis revealed a complex landscape of cases:

-First, many animals were clearly mosaic suggesting that the cut and non-homologous end junction event occurred after the first cell division. For example, some animals produced more than two bands for *Hmx3* after PCR (**Fig. 3B**). Another sign of mosaicism was when none of the two or three bands amplified for *Hmx2* or *Hmx3* corresponded to the wild type band, yet the animal presented no vestibular phenotype. Another animal appeared by PCR as a double homozygous *Hmx2/3* null yet had no vestibular phenotype and survived well beyond the classical maximum of 10 days for the double knockouts (Wang et al., 2004). One of the worst cases of mosaicism displayed 3 bands of the wrong size (thus with deletions) plus a large *Hmx2+Hmx3* deletion, meaning that 4 types of mutations affected the *Hmx3* locus.

- For the *Hmx3* knockouts some animals displayed two bands, one of which of the wild type size. The two bands were sequenced, the wild type band was confirmed, and one founder of that type was selected in which the mutated band displayed a deletion of 100 nucleotides, a frame shift and shortening the protein (**Fig. 3B**). It was outcrossed twice and its descendants were used to produce *Hmx3* KO animals.

-For the *Hmx2* knockouts all animals displayed a single band of the wild type size, yet several of them had a vestibular phenotype, thus were homozygous nulls. I therefore proceeded to sequence that band in an asymptomatic animal, and in a number of cases the sequence was double, with deletions of a few nucleotides in on the allele (**Fig. 3B,C**). Several of these individuals were selected and outcrossed twice, their offspring intercrossed, their progeny containing individuals with a vestibular phenotype but viable, as expected of *Hmx2* knockouts. The *Hmx2* PCR band was sequenced and one line was selected as the *Hmx2* knockout line: it has a 10 nucleotides-long deletion in the first exon, that changes the reading frame and shortens the protein and has lost a restriction site for *BsaH1* in the PCR fragment, which allowed relatively easy genotyping of WT, homozygous and heterozygous knockout.

-Finally, some animals had a large deletion encompassing the *Hmx2* and *Hmx3* loci (**Fig. 3B**). One of them was used to create the *Hmx2/3* double KO line. The deletion created an out-of-phase fusion of

the coding sequences of *Hmx2* and *Hmx3*. Genotyping could be achieved by a simple PCR using the forward primer of *Hmx3* with the reverse primer of *Hmx2*, which amplifies a band only in the mutants (the wild type band being too long). No living homozygote could be obtained at the moment of the genotyping (P21), which fits with the previously described death of double knockouts between P0 and P10 (Wang et al., 2004).

This whole process (from the design of the sgRNA to 3 established and unambiguously genotyped lines) took around two years, mosaicism (difficult to diagnose and entailing multiple outcrosses), and difficulties in genotyping representing major obstacles. Although it is possible that this technology is evolving and becoming more efficient, and that my first-hand experience is now slightly out of date, my conclusion was that this technique was too laborious and imprecise (amounting to what George Church once called “genetic vandalism”) to arrive in the end at a simple constitutive knockout, with none of the advantages made possible by homologous recombination (e.g. knockin of reporters, of Cre or Flp recombinases, of lox and FRT sites for conditionality).

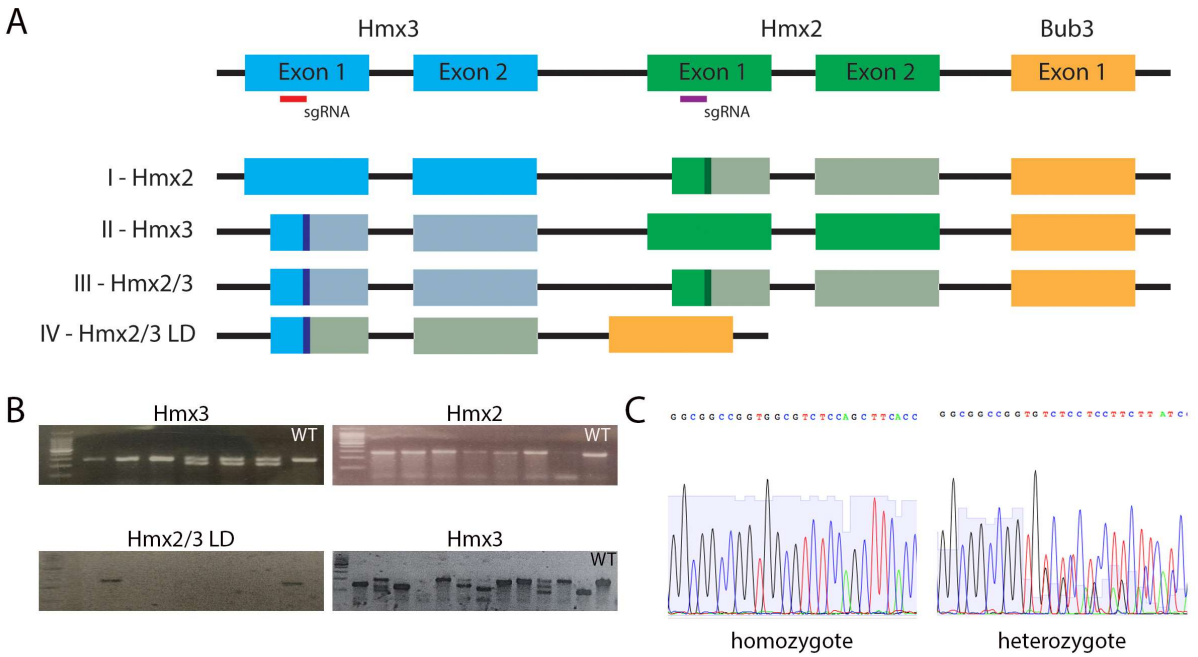

Figure 3: Strategy for the knockouts of *Hmx2*, *Hmx3* and *Hmx2/3*. (A) Position of the sg RNAs and expected consequences of the cuts: I, a single cut on *Hmx2* first exon; II, a single cut on *Hmx3* first exon; III, a cut of *Hmx2* and *Hmx3* first exons on the same chromosome; IV, a large deletion of the region between the two site of cut of *Hmx3* and *Hmx2*. Blue: endogen coding sequence of *Hmx3*, Dark blue: damage of the sequence of *Hmx3* due to the cut, Pale blue: modified non coding sequence of *Hmx3*, Green: endogen coding sequence of *Hmx2*, Dark green: damage of the sequence of *Hmx2* due to the cut, Pale green: modified non coding sequence of *Hmx2*, Orange: endogen coding sequence of *Bub3*. (B) Gels of PCR bands obtained after genotyping F0 animals showing a variety of patterns: two bands (*Hmx3* upper left), one band (*Hmx2*), a large deletion (*Hmx2/3* lower left) or mosaicism (*Hmx3* lower right). (C) Results of sequencing the single band for *Hmx2* to distinguish homozygote from heterozygote after the site of cut by Cas9.

II.B. Phenotype of the *Hmx* knockouts

Only a preliminary and superficial analysis of the mutant could be done so far: heterozygote animals for *Hmx3* and *Hmx2/3* lines were crossed and homozygous embryos were analyzed at E17.5. After a staining for Phox2b, the ENS of the mutants was detectable in both lines and did not present any gross anomaly (**Fig. 4**).

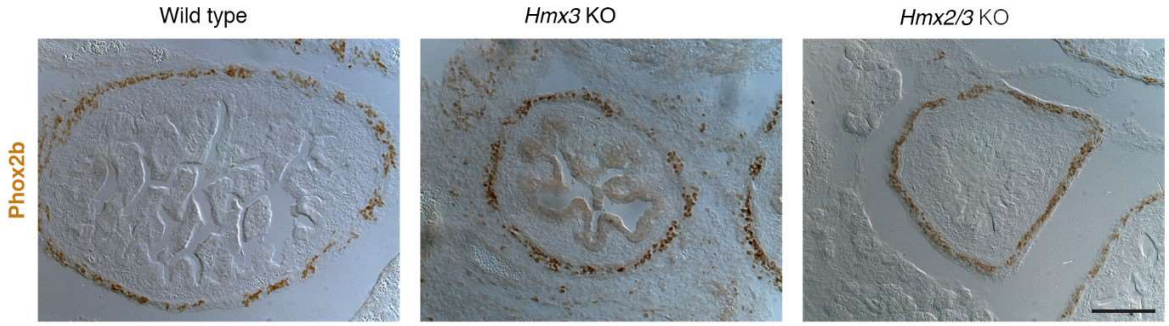

Figure 4: The ENS is present despite the inactivation of *Hmx3* or of *Hmx2/3*. Sagittal section of embryos at E17.5 WT (left), *Hmx3* KO (middle) or *Hmx2/3* KO (right) immunostained for Phox2b. The ENS is present and looks normal in all three conditions. Scale bar 100µm.

III. Role of *Tbx3* in the development of the ENS

III.A. Expression of *Tbx3* in the ENS

The transcription factor *Tbx3* has been reported to be expressed in the ENS (Heanue and Pachnis, 2006). There is also anecdotal evidence of expression in the medulla, in the region of the nucleus of the solitary tracts and/or dmnX (Eriksson and Mignot, 2009) and several years ago the Brunet lab found *Tbx3* in a screen for genes expressed in the epibranchial ganglia (unpublished results). Thus, the intriguing possibility arose that *Tbx3* would be expressed in most neurons innervating the gut, according to a circuit-wide logic (i.e. in the intrinsic as well as extrinsic sensorimotor circuits of the gut), similar, albeit on a smaller scale, to that of *Phox2b* throughout the sensorimotor circuits of the autonomic nervous system. I thus sought to verify this hypothesis by studying *Tbx3* expression in mouse embryos, by combining *in situ* hybridization for *Tbx3* and immunohistochemistry for Phox2b. I confirmed the expression of *Tbx3* in the ENS (**Fig. 5D**) and in addition detected expression in about half the neurons of the nodose ganglion (**Fig. 5A**), thus presumably corresponding to neuronal subtypes. This expression is not salt-and-pepper, but rather seems to define regions or lobes of the ganglion. Compatible with this non-ubiquitous expression pattern is the single cell transcriptomic study by Kupari et al. (2019) which finds *Tbx3* in several subtypes of one of the two large classes of nodose ganglion neurons, the polymodal nociceptors (but absent from the second large class, the mechanoreceptors). I also found expression in the dorsal motor nucleus of the vagus nerve (dmnX) (**Fig 5B**), again in a large fraction of cells but not ubiquitously. These two structures are the main component of the extrinsic innervation of the gut (apart from sympathetic neurons), containing respectively first order viscero-sensory neurons and preganglionic neurons for the ENS, i.e. the substrates of extrinsic enteric reflexes. In the CNS, expression of *Tbx3* was actually wider than the dmnX, and could be detected, at least transiently, in all branchial and visceromotor neurons: the salivary nucleus, nucleus ambiguus (nA) and migrating facial motoneurons (**Fig. 5C**).

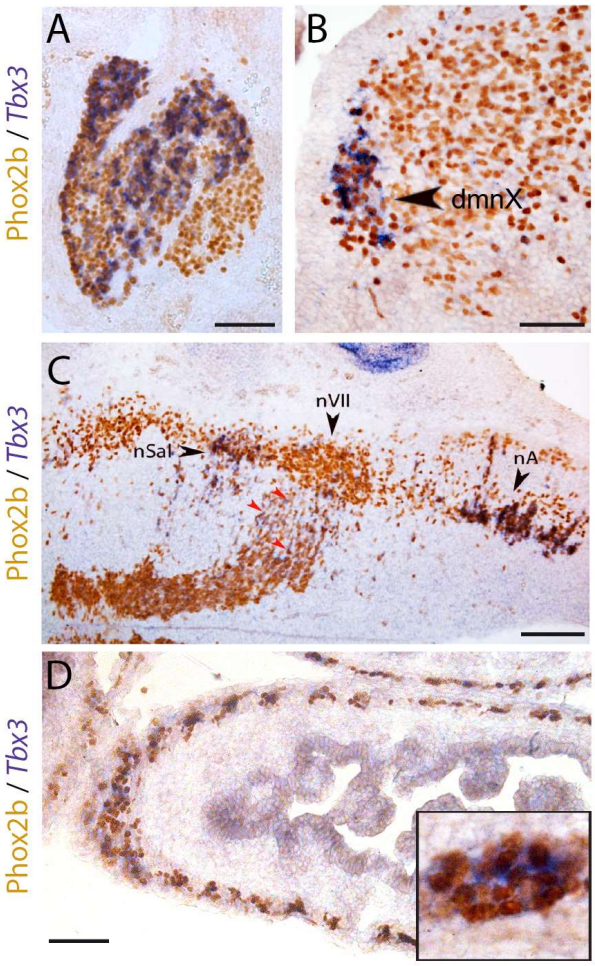

Figure 5: The extrinsic and intrinsic ENS express *Tbx3* during development. (A) Sagittal section of a WT embryo through the nodose ganglia at E13.5. (B) Coronal section through the dmnX at E13.5. (C) Transverse section through the medulla at E11.5. (D) Sagittal section through the gut at E16.5. All the sections are stained by *in situ* hybridization for *Tbx3* and immunohistochemistry against Phox2b. *Tbx3* is also expressed in a subset of migrating facial motoneuronal precursors (red arrowheads). dmnX: dorsal motor nucleus of the vagus nerve, nSal: salivatory nucleus, nVIII: facial nucleus, nA: nucleus ambiguus. Scale bars are 100µm (A, B, D) and 200µm (C).

To guide future functional explorations, I explored the dynamic of *Tbx3* expression during development of the ENS by immunofluorescence on wholemounts of the gut at several developmental stages (**Figure 6**). At E11.5 cells started expressing *Tbx3* in a salt-and-pepper pattern compared to *Phox2b* which was used as a general marker of the ENS cells, in the duodenum and ileum; expression in the ileum appeared sparser, presumably because the cells are younger; two days later, at E13.5, in these same regions, expression of *Tbx3* was still salt-and-pepper, and this pattern persisted until P15 at least. (**Fig 6**). Although *Tbx3* expression is strongly heterogeneous, it did not appear to occur in an all-or-none fashion: there was strong expression in some cells, and in many others, it was very weak and close to the background, and it was completely undetectable in only a few cells (see insets in the lower panels of **Figure 6**). Thus, *Tbx3* seems to be switched on by most enteric neuronal precursors during colonization of the gut, but at vastly different levels. Thus, these data could suggest some neuron-type specific functions, without excluding a role in most neurons.

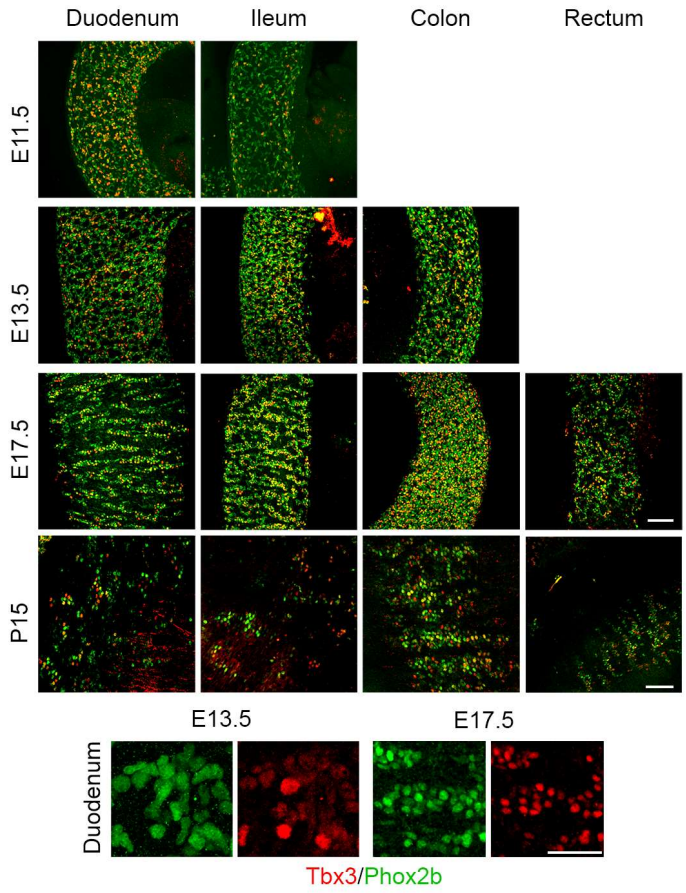

Figure 6: Dynamic of Tbx3 expression during ENS development. Whole mount of guts at E11.5, E13.5, E17.5 and P15, at the level of the duodenum, ileum, colon and rectum, co-stained for Tbx3 and Phox2b. Scale bars are 100µm (full pictures) and 50µm (insets).

III.B. Gross phenotype of a *Tbx3* conditional KO

To explore the function of *Tbx3* I first crossed a mouse line in which the 1st exon of *Tbx3* is floxed (Frank et al., 2013) with a *Pgk::Cre* line — in which *Cre* is under the promoter of *Phosphoglycerate kinase*, thus active in the zygote and producing the equivalent of a constitutive knockout. Because *Tbx3* is involved in the development of the pacemaker of the heart (Frank et al., 2012), the embryos could not be obtained later than E12.5. At this stage, staining by *in situ* hybridization for *Peripherin* and immunohistochemistry for Phox2b, revealed that all Phox2b-expressing neuronal groups that co-express *Tbx3* (epibranchial ganglia, dmnX and other branchio-visceral nuclei, and the ENS) are still present (**Fig. 7**), although subtle deficits are not ruled out.

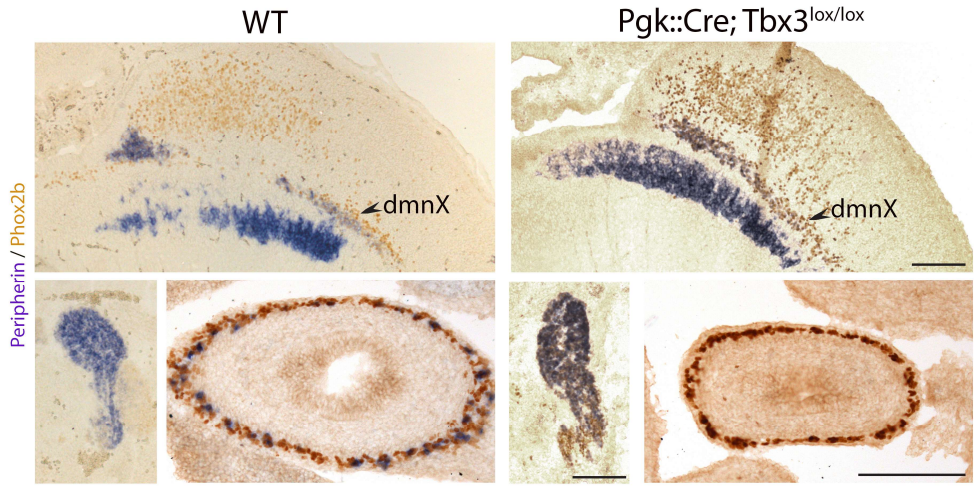

Figure 7: Presence of neurons innervating the gut in *Tbx3* KO. Sagittal sections through WT or *Pgk::Cre, Tbx3$^{lox/lox}$* embryos at E12.5 stained by *in situ* hybridization for *Peripherin* and immunohistochemistry against Phox2b. The dmnX (upper panel), the nodose ganglia (bottom left) and ENS (bottom right) develop in the absence of expression of *Tbx3*. dmnX: dorsal motor nucleus of the vagus nerve. Scale bars are 100µm.

To explore the possibility of a later role of *Tbx3*, and bypass the heart failure and embryonic death of constitutive knockouts (Frank et al., 2013), I crossed the *Tbx3$^{lox/lox}$* into a *Phox2b::Cre* background. This combination proved fortunate, since the alternative strategy that was available, which was to recombine the same floxed *Tbx3* allele in the neural crest with a *Wnt1::Cre*, was undertaken simultaneously in another lab, and turned out to cause a cleft palate and consequent neonatal death (López et al., 2018). *Phox2b::Cre*; *Tbx3$^{lox/lox}$* animals were born in a Mendelian proportion, and were indistinguishable from wild types for the first two weeks. However, out of 15 *Phox2b::Cre*; *Tbx3$^{lox/lox}$* pups from 7 litters, none survived after P27. A closer monitoring of two subsequent litters revealed that the mutant pups develop normally and thrived at the same rate than their control littermates until P18, at which stage (which roughly correspond to weaning) they suddenly stopped gaining weight and even started to lose some, leading to their death in the 3-5 following days (**Fig. 8B**). To avoid suffering of the animals, the rest of the experiments were conducted at P15.

Gross histological examination of the gut at P15 showed an incompletely penetrant but frequent malformation of the cecum, sometimes longer and more twisted than the wild type, sometimes enlarged, and sometimes filled with air (**Fig. 8A**). No obvious morphological anomaly was apparent in other

segments of the gut. I tested the intestinal transit of the mutants: the animals were fasted for 2 hours, then force-fed a non-absorbable charcoal tracer and sacrificed 2 hours later. In all animals, irrespective of genotype, the charcoal pellets had passed the cecum and had reached the colon (**Fig. 8C**). Thus, I could not detect any impairment of intestinal transit.

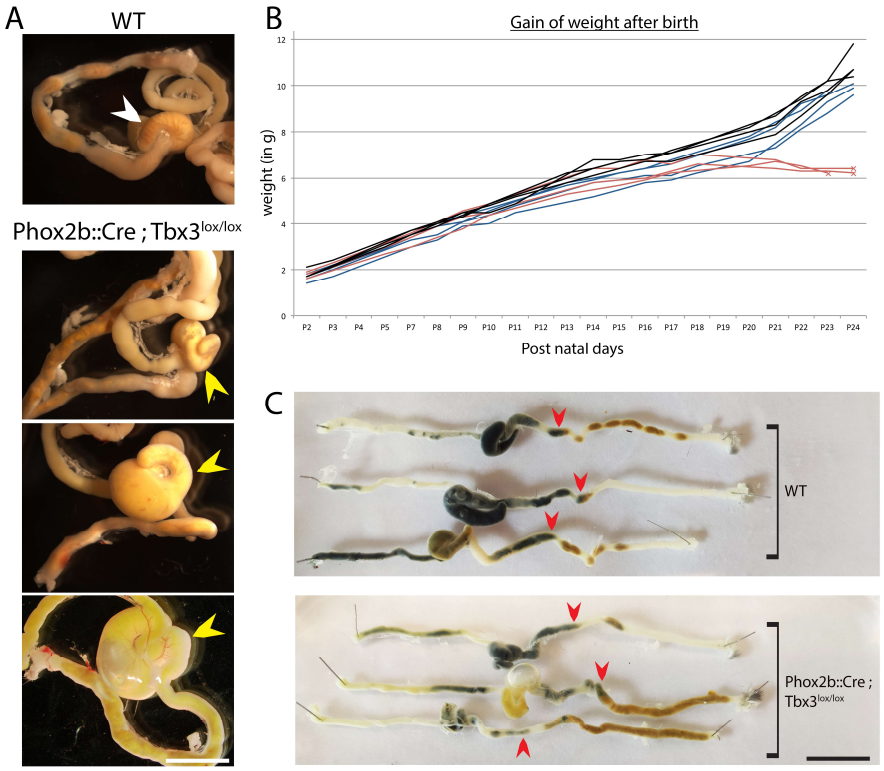

Figure 8: Animals lacking *Tbx3* in the autonomic nervous system die at weaning and have a malformed cecum. (A) Cecum from animals at P15, either WT (white arrowhead) or from Phox2b::Cre; $Tbx3^{lox/lox}$ pups (yellow arrowheads) and exhibiting a twist, or an enlarged base, or being longer and full of air. (B) Weight of animal from P2 to P24, either WT (black), *Phox2b::Cre;Tbx3*$^{lox/+}$ (blue) or *Phox2b::Cre; Tbx3*$^{lox/lox}$ (red). (C) Intestinal transit assays for WT (upper) or *Phox2b::Cre;Tbx3*$^{lox/lox}$ (bottom) animals force-fed with charcoal , which reaches the colon (red arrowheads) after two hours. The guts are oro-anally oriented from left to right. Scale bars are 0,5cm (A) and 1cm (C).

III.C. Histological analysis of the enteric nervous system of *Phox2b::Cre;Tbx3$^{lox/lox}$* mutants

To explore a potential histological defect in the ENS of *Tbx3* mutants, I first evaluated the number of enteric neurons at P15, when the thriving phenotype is already apparent, and about to precipitate death within a few days. Cryosections of the gut at 4 levels (duodenum, ileum, colon and rectum) were immunostained for Phox2b. The myenteric and submucosal plexi were readily detectable in the *Phox2b::Cre;Tbx3$^{lox/lox}$* mutants, but in most places appeared formed by a monolayer of neurons, as opposed to two or three layers of neurons in wild type animals, suggesting a decrease in neuronal numbers. Counting *Phox2b*+ nuclei on three sections per region of the gut revealed a decrease in the mutants relative to wild type, by 35% in the duodenum, 48% in the ileum, 50% in the colon and 16% in the rectum (**Fig. 9**). The cecum of the mutants contained neurons, but due to its massive enlargement and misshape, it was not possible to quantify neurons there (**Fig 10**).

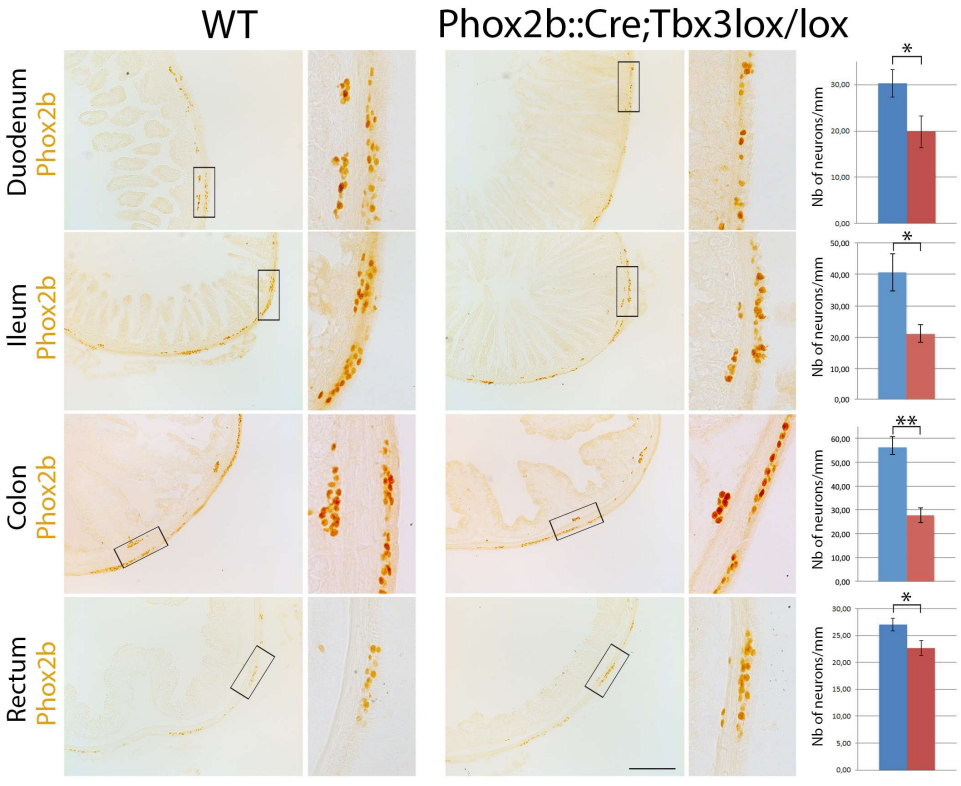

Figure 9: The ENS is atrophic at P15 in *Tbx3* knockouts. Transverse section of the gut at the level of the duodenum, ileum, colon and rectum at P15 in WT (left) or *Phox2b::Cre;Tbx3$^{lox/lox}$* (right) stained for Phox2b, with an enlarged view (4x zoom) of the boxed area. The atrophy of the enteric ganglia is quantified on the graph. *Phox2b::Cre;Tbx3$^{lox/lox}$* (red) showed fewer neurons (in the duodenum 19,82 ± 3,4 neurons/mm versus 30,32 ± 2,9 ; p = 0,037, n=4; in the ileum 21,18 ± 2,7 neurons/mm versus 40,59 ± 5,9; p = 0,035, n=4; in the colon 27,72 ± 3,1 neurons/mm versus 56,37 ± 4,6; p = 0,009, n=3; in the rectum 22,66 ± 1,3 neurons/mm versus 27,03 ± 1,2 ; p = 0,034, n=4). Scale bar is 100µm. Error bars indicate SEM. *P<0.05, **P<0.01.

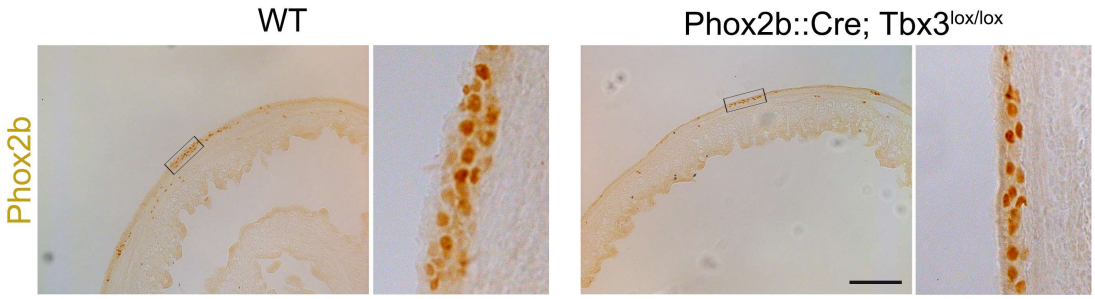

Figure 10: The cecum is misshape but still has neurons in Tbx3 knockouts. Sections through the cecum at P15 in WT (left) or *Phox2b::Cre;Tbx3$^{lox/lox}$* (right) stained for Phox2b, with an enlarged view (4x zoom) of the boxed area. Scale bar is 200µm.

To detect at which stage the deficit of neuronal numbers becomes manifest, I counted Phox2b+ nuclei at E17.5 and E15.5. At E17.5, a loss of neurons was already happening, by 27% in the duodenum, 31% in the ileum, 37% in the colon and 38% in the rectum (**Fig. 11**). On the other hand, neuron numbers at E15.5 were not statistically different from wild type (**Fig. 12**).

Thus, the absence of *Tbx3* during development of the ENS leads to a quantitatively normal development of the system until E15.5, followed by a significant loss of neurons at E17.5 which worsens postnatally.

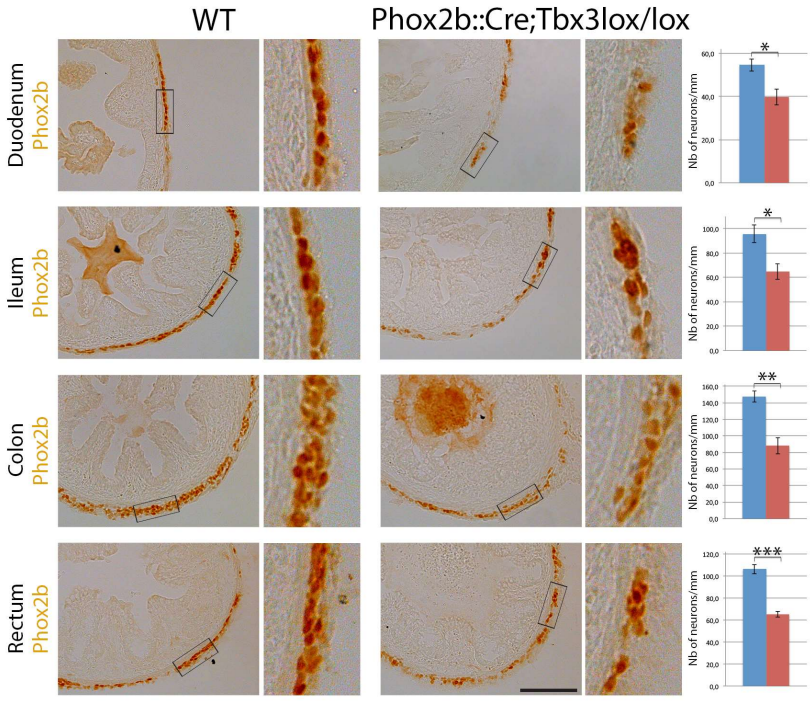

Figure 11: The ENS is atrophic at E17.5 in *Tbx3* knockouts. Transverse section of the gut at the level of the duodenum, ileum, colon and rectum at E17.5 of WT (left) or *Phox2b::Cre;Tbx3$^{lox/lox}$* (right) stained for Phox2b, with an enlarged view (4x zoom) of the boxed area. The atrophy of the enteric ganglia is quantified on the graph. *Phox2b::Cre;Tbx3$^{lox/lox}$* (red) showed fewer neurons (in the duodenum 39,6 ± 3,6 neurons/mm versus 54,6 ± 2,8 ; p = 0,034, n=3; in the ileum 64,7 ± 6,8 neurons/mm versus 95,4 ± 7,8; p = 0,042, n=3; in the colon 88,2 ± 9,9 neurons/mm versus 147,4 ± 6,5; p = 0,010, n=3; in the rectum 65,3 ± 2,6 neurons/mm versus 106,2 ± 4,1 ; P = 0,002, n=3). Scale bars are 100µm. Error bars indicate SEM. *P<0.05, **P<0.01, ***P<0,005

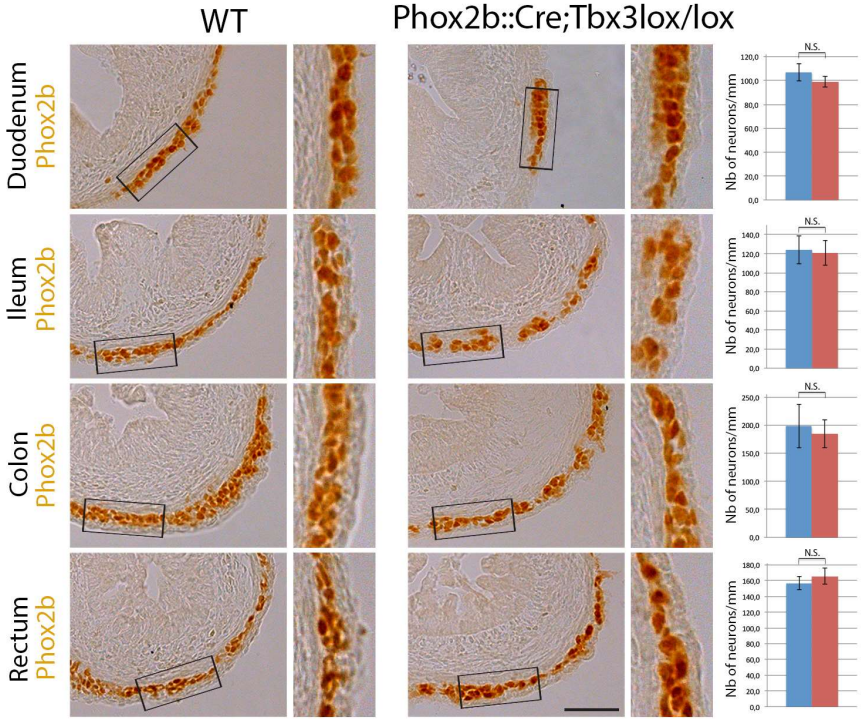

Figure 12: The ENS is quantitatively normal at E15.5 in *Tbx3* knockouts. Transverse sections of the gut at the level of the duodenum, ileum, colon and rectum at E15.5 of WT (left) or Phox2b::Cre; $Tbx3^{lox/lox}$ (right) stained against Phox2b, with an enlarged view (4x zoom) of the boxed area. The number of the enteric neurons is quantified on the graph. *Phox2b::Cre;*$Tbx3^{lox/lox}$ (red) had as many neurons as the WT (in the duodenum 98,9 ± 4,4 neurons/mm vs 107,0 ± 7,3 ; P = 0,29, n=3; in the ileum 120,8 ± 12,9 neurons/mm vs 123,8 ± 14,7; P = 0,85, n=3; in the colon 184,6 ± 24,9 neurons/mm vs 198,2 ± 39,2; P = 0,72, n=3; in the rectum 165,7 ± 9,9 neurons/mm vs 156,9 ± 8,5 ; P = 0,43, n=3). Scale bars are 50µm. Error bars indicate SEM.

As the expression of *Tbx3* is heterogeneous among ENS neurons, and even absent of some, I explored the possibility that *Tbx3* has neuron-type specific roles and that one or several subtypes of neurons are missing at P15, using classical markers of neurotransmitter phenotype.

First, I examined the expression of VIP, that characterizes inhibitory motor neurons of the myenteric plexus and secretomor neurons of the submucosal plexus, and by simple immunofluorescence is detectable mostly in fibers (as opposed to cell somas). In both wild types and *Tbx3* KO, I could detect VIP+ fibers inside the myenteric plexus, in the circular muscle (oriented parallel to the plane of section), and in the core of the intestinal villi, projecting to the mucosa (**Fig. 13**). Essentially the same result was obtained for *SP* (which characterizes excitatory motor neurons and sensory neurons), although the reduction in projections to the circular muscle seemed dramatically reduced in the mutants at the level of the colon (**Fig. 13**). Then, I tested the calcium binding molecule *CalB*, expressed in the cytoplasm and fibers of sensory neurons, which was still present in the knockout (**Fig. 13**). Finally, I tested the Choline

Acetylfransferase (ChAT), expressed in the cytoplasm of all the neurons of the ENS, except the inhibitory motoneurons, which was as well still present in the knockout (**Fig. 13**). Expression in the fibers made it difficult to quantify the neurons expressing these three markers.

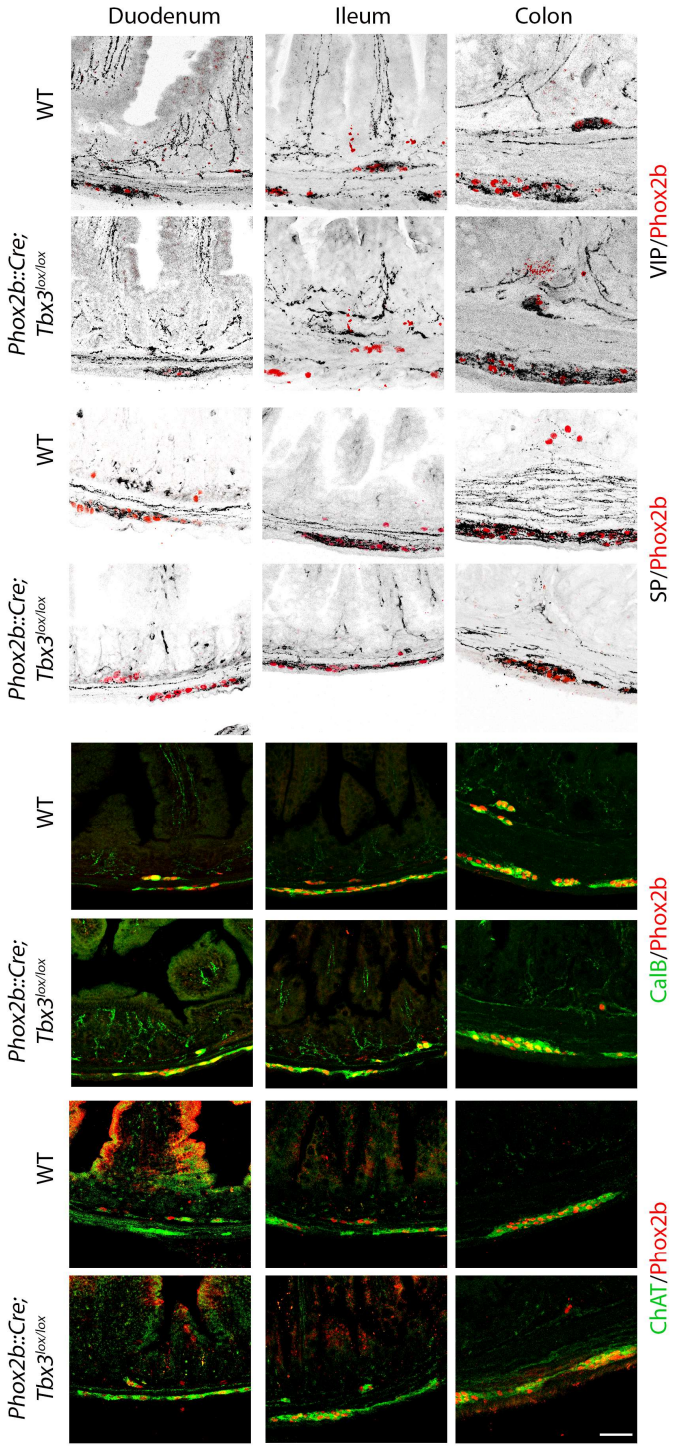

Figure 13: The neurotransmitters VIP, SP, CalB and ChAT are expressed in the ENS of *Tbx3* knockouts. Transverse section of the gut at the level of the duodenum (left), ileum (middle) and colon (right) at P15 in WT or *Phox2b::Cre;Tbx3$^{lox/lox}$* pups (as mentioned on the left) stained for Phox2b (red) and VIP (black, top), or SP (black, middle), or Calb (green, middle), or ChAT (green, bottom). Scale bar is 50µm.

Lastly, I examined the expression of NOS, which characterizes inhibitory motor neurons and descending interneurons. The staining for NOS activity by NADPH diaphorase allows precise delineation of the cell bodies surrounding Phox2b^{+} nuclei, which allowed counting them. There was a decrease of 54% of NOS neurons in the duodenum, 61% in the ileum and 40% in the colon (**Fig. 14**). At the level of the duodenum and the ileum, the loss was larger than the total loss of neurons, suggesting that *Tbx3* has a preferential (albeit not essential) role in the generation of NOS neurons. Concurrently to the loss of neurons, a massive loss of fibers in the circular muscle layer was evident at all the levels of the gut, but especially in the ileum. This suggests that inhibitory motor neurons rather than descending interneurons (which only projects within the plexus itself) are affected.

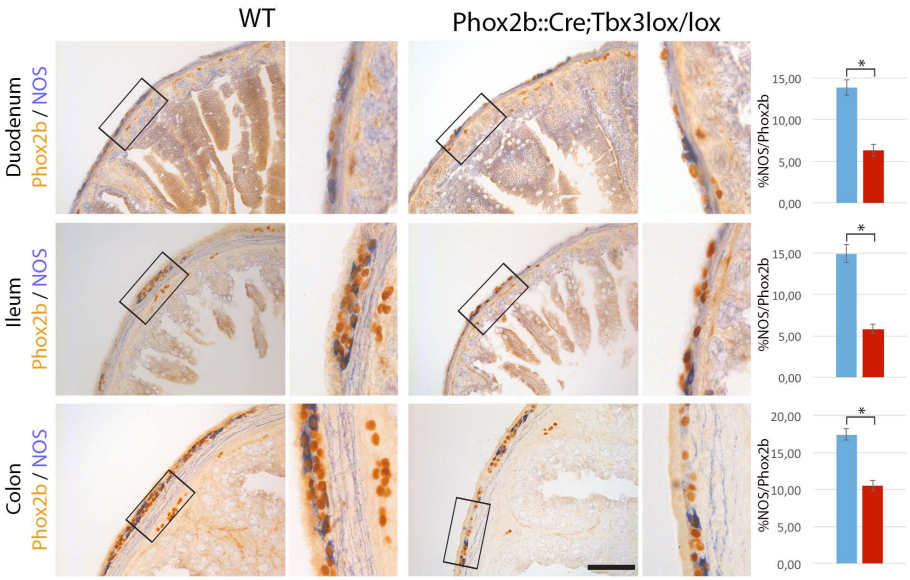

Figure 14: The number of nitrergic is decreased in *Tbx3* knockouts Transverse section of the gut at the level of the duodenum, ileum, and colon at P15 of WT (left) or *Phox2b::Cre;Tbx3$^{lox/lox}$* (middle) stained for NOS (blue) and Phox2b (brown), with an enlarged view (4x zoom) of the boxed area. The atrophy of the enteric ganglia is quantified on the graph. *Phox2b::Cre;Tbx3$^{lox/lox}$* pups (red) had fewer NOS neurons (in the duodenum 6,32 ± 0,77 % of NOS/Phox2b neurons vs 13,85 ± 0,95 ; p=0,023, n=3; in the ileum 5,83 ± 0,54 % of NOS/Phox2b neurons vs 14,93 ± 1,11; p=0,027, n=3; in the colon 10,48 ± 0,71 % of NOS/Phox2b neurons vs 17,43 ± 0,74; p= 0,021, n=3). Scale bars are 25µm. Error bars indicate SEM. *P<0.05.

Conclusion & Discussion

Conclusion & Discussion

I have characterized a role for *Tbx3* in the development of the nervous system, which had eluded the first study devoted to the subject (López et al., 2018). The total number of neurons is reduced by 15-50% depending on the region of the digestive tract, while the earlier study did not find any change. The reason for this discrepancy is unclear and could be related to the method of counting, on wholemounts in (López et al., 2018) and on section in the current study. The second phenotype (failure to thrive after P15 and death before P21) could be observed only by restricting the *Tbx3* mutation to *Phox2b* neurons, because restriction to the neural crest entailed a cleft palate, precluding feeding altogether and leading to neonatal death. It is of note however, that in my study, restriction to *Phox2b+* neurons does not completely ensure that the cause of neonatal death resides in the ENS, since two other populations of neurons co-express *Phox2b* and *Tbx3*: the dmnX and the nodose ganglion (gX), both involved in innervating the gut: the dmnX contains preganglionic neurons to enteric motor neurons and gX contains extrinsic sensory primary neurons for the gut. This circuit-wide expression was actually one reason to study this gene in the first place. My preliminary assessment rules out a massive impairment in the development of gX and dmnX, which are both present in E12.5 *Pgk::Cre;Tbx3*$^{lox/lox}$ embryos; but the dmnX is still present without apparent abnormalities at P15 (**Fig. 15**). However, the phenotype in the ENS proper is not massive either in terms of total cell counts. Thus, it is not excluded that the dmnX and/or gX, either are smaller or lack some neuron subtype that could explain neonatal death, by itself or in combination with the deficit in the ENS.

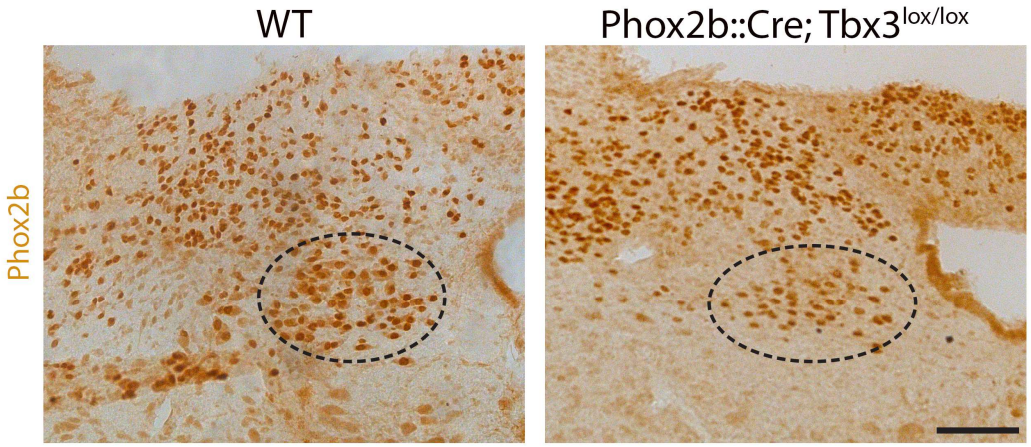

Figure 15: The Dorsal motor nucleus of the vagus nerve (dmnX) is present in *Tbx3* knockouts. Coronal section of a brain at P15 in a WT or *Phox2b::Cre;Tbx3*$^{lox/lox}$ animal stained for Phox2b. The dmnX (dashed circle) is present irrespective of the genotype. Scale bar is 50µm.

I attempted at ruling out a role for gX by creating a *Foxg1::Cre;Tbx3*$^{lox/lox}$ mouse in which *Tbx3* is removed selectively from the three placode-derived cranial ganglia (geniculate (gVII), petrose (gIX) and gX). The *Foxg1::Cre;Tbx3*$^{lox/lox}$ animals turned out fully viable and fertile. However, I found that deletion of *Phox2b* in the epibranchial placodes, in *Foxg1::Cre;Phox2b*$^{lox/lox}$, were also viable and fertile, which is surprising since *Phox2b* is a well-established determinant of epibranchial ganglia, its abrogation leading to massive loss of neurons (Dauger et al., 2003), those that remain having switched identity to that of somatic sensory neurons and projected to the spinal nucleus of the trigeminal nerve, instead of the nTS (d'Autréaux et al., 2011). I have not yet examined the state of epibranchial ganglia in *Foxg1::Cre;Tbx3*$^{lox/lox}$ or *Foxg1::Cre;Phox2b*$^{lox/lox}$ but the absence of a clear phenotype could be due to a mosaicism of the recombination by *Foxg1::Cre*. Indeed, such a mosaicism was evident from the expression pattern of the dual FREPE reporter gene in *Foxg1::Cre;Phox2bFlpo;FREPE* embryos (**Fig. 16**).

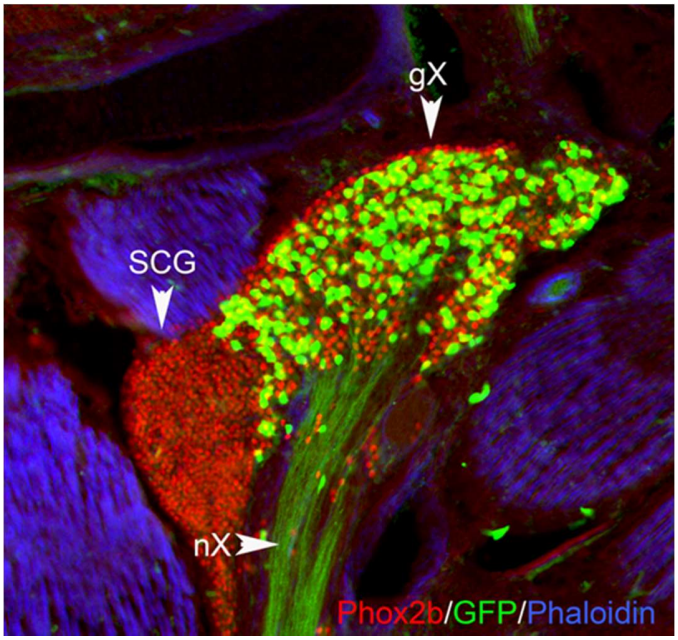

Figure 16: Mosaicism of recombination by Foxg1::Cre. Sagittal section through the nodose (gX) and superior cervical (SCG) ganglia at E15.5 in a *Foxg1::Cre;Phox2bFlpo;Ai65* mouse embryo where *GFP* is triggered by the dual recombination by *Foxg1::Cre* and *Phox2b::Flpo*. In the nodose ganglion, only a fraction of the Phox2b^{+} neurons are doubly recombined, despite the fact that all their placodal precursors express endogenous *Foxg1* (not shown). The mosaicism is most likely due to the *Foxg1::Cre*, since none were found with the *Phox2b::Flpo* (Hirsch et al., 2013) (and data not shown).

To rule out the role of the dmnX in the lethality of *Phox2b::Cre;Tbx3*$^{lox/lox}$ mutants, a similar experiment could be attempted by removing *Tbx3* from the dmnX only in *Brn4::Cre;Phox2b*$^{lox/lox}$ where *Cre* is expressed from the *Brn4* promoter (Zechner et al., 2003), thus exclusively in the central nervous system. However, both experiments would fail to be informative if death results from a combined ENS/gX or ENS/CNS lesion. A better way of incriminating the ENS alone would be restrict the *Tbx3*

deletion to this structure. However, I am not aware of *Cre*-driver that would be specific for early enteric precursors. In collaboration with the laboratory of Carmen Birchmeier we are currently engineering a *Hmx3::Cre*, but it is possible that *Hmx3* is switched on too late (e.g. post-mitotically) to completely prevent the action of *Tbx3*.

Tbx3 inactivation leads to a deficit in enteric neuron numbers. We do not know at this moment whether this is due to a decrease in proliferation or in cell survival. A deficit of proliferation could result from a role of *Tbx3* akin to that in stem cells (Carlson et al., 2002; Niwa et al., 2009). However, such a role will be difficult to demonstrate in vivo: a minor deficit of proliferation has the potential to cause significant cell loss after several days of development. Moreover, enteric cells are embedded in a mesenchymal which also undergoes massive proliferation (**Fig. 17**). Thus, it does not appear practical or even possible to detect this deficit with conventional markers of cell proliferation.

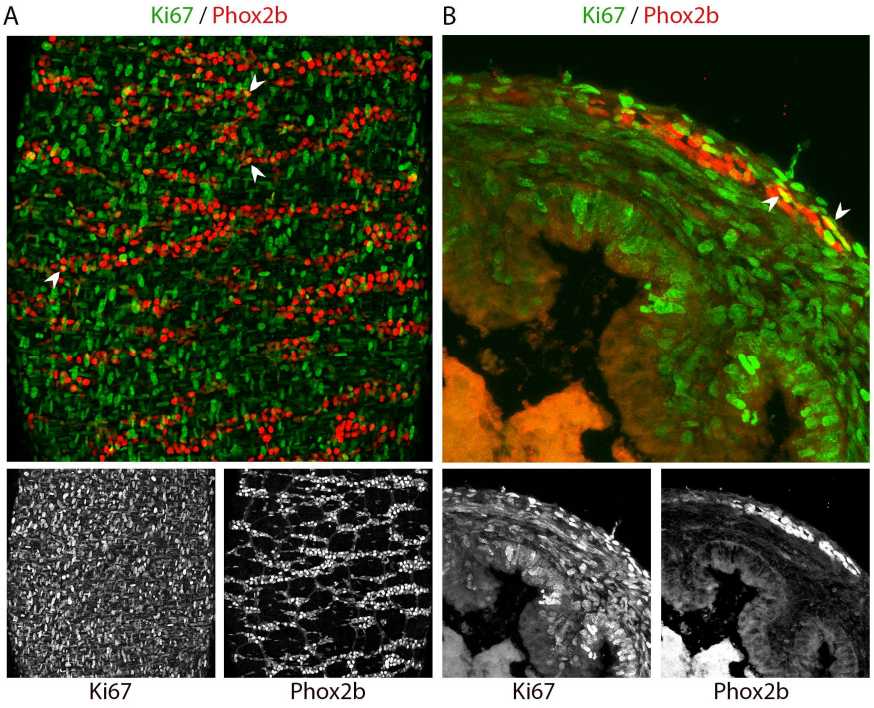

Figure 17: Detection of proliferative neurons in the ENS at E17.5. Whole mount (A) and transverse section (B) of a gut at E17.5 at the level of the ileum stained for Ki67 (green) and Phox2b (red) (top) and each channel separated (bottom) to visualize double positive cells (white arrowheads). Scale bars are 100µm (A) and 50µm (B).

Like all TFs studied, to this date, for their role in the development of the ENS, *Tbx3* does not seem to be a neuron type-specific determinant. The closest candidate for that role so far is *Sox6*, but even in this case, the specified cell type, dopaminergic neurons, is only reduced, not abolished (Memic et al., 2018). The role of *Tbx3* could be reminiscent of *Ascl1*, which does affect selectively some neuron

types, but several of them, and only partially (Memic et al., 2016). This conclusion though, must be qualified by the fact that no single marker tested so far, for any knockout including that of *Tbx3*, is specific for one cell type. A more informative survey of the conditional *Tbx3* KO could be inspired by some of the markers discovered in (Morarach et al., 2020).

Tbx3 knockouts die at the time of weaning, with a complete penetrance. The proximal cause for death likely involves energy metabolism since it is preceded for a few days, by a dramatic arrest of gain weight. It is of note that weaning is a critical survival period for a number of knockouts, including in the ENS. For example, mice in which *ChAT* has been inactivated in the ENS (in a *Wnt1::Cre;ChAT$^{lox/lox}$* background) also thrive for 2 weeks after birth but stop gaining weight during the third week and die around P30 (Johnson et al., 2018). It is likely that the drastic change of diet, from maternal milk to solid food (pellets in captivity), unmasks or decompensates a digestion defect which was latent until then. In the case of *ChAT* knockouts, a reduction of intestinal transit and impacted fecal content were diagnosed in the days before death, as well as dysbiosis (modification of the intestinal flora). For the *Tbx3* knockout, I ruled out the most intuitive mechanism, which is an arrest in intestinal transit, in agreement with (López et al., 2018), and with more complete evidence than in the latter paper, since the authors were limited by neonatal death to exploring the transport of the alimentary bolus to the duodenum. On the other hand, it could be that the failure to thrive is due to an arrest in food intake (which is observed in *ChAT* knockouts), which I did not assess yet. Since weaning entails changes in bacterial flora, and that several mutant pups had a cecum distended with gas, I tried to explore a role for bacteria in death, and to produce axenic pups by treating the mother with antibiotics. However, the mother failed to deliver and I abandoned this line of research, which lacks, so far, concrete preliminary evidence (such as dysbiosis, which should be explored) while entailing a lot of animal suffering. The proximal cause of death, probably digestive but mysterious so far, could be a very indirect consequence of the neuronal lesion caused by the abrogation of *Tbx3* (such as a deficit in nutrient absorption, anorexia from pain or other digestive cause, disruption of the intestinal epithelial barrier and consequent sepsis, etc.), and might not model any human pathology. Thus, it might be less interesting to pursue than a more fine-grained analysis of the neuronal lesion in the ENS due to loss of *Tbx3* function, using newly discovered markers for cell types (Morarach et al., 2020).

Material & Methods

Materials and Methods

Histology

Embryos

Mouse embryos of different stages (E11.5, E12.5, E13.5, E15.5, E16.5, and E17.5) were fixed in 4% Paraformaldehyde (PFA). For cryostat sections, tissues were embedded in OCT after a cryoprotection of 30% Sucrose in PBS and then stocked at -80°C, then sectioned at 20µm in the appropriated plan.

Guts

Mouse embryos or pups of different stages (E11.5, E13.5, E15.5, E17.5, and P15) were taken and the gut were freshly dissected and fixed in 4% PFA overnight. They were cryoprotected in 30% Sucrose in PBS and segments of interest were cut and oriented oro-anally in OCT before being frozen, and then stocked at -80°C. In the case of P15, the guts were segmented and flushed by PBS and then PFA. The blocs were then cut at 20µm on a transverse plan. For wholemount immunofluorescence, the guts were dissected, fixed in 4% PFA overnight, washed in PBS 1X before staining.

Brains

Mouse pup at P15 were injected with Pentobarbital (30mg/kg) and perfused with 4%PFA, the brains were then dissected out of the skull and fixed by immersion in 4%PFA overnight. For cryostat sections, tissues were embedded in OCT after a cryoprotection of 30% Sucrose in PBS and then stocked at -80°C, then sectioned at 20µm on a coronal plan.

In Situ Hybridization, Immunohistochemistry, Immunofluorescence

In situ hybridization and immunohistochemistry were performed as described in (Coppola et al., 2010), while immunofluorescence was performed as described in (Espinosa-Medina et al., 2014). The wholemount of gut was performed as described in (Espinosa-Medina et al., 2017).

Diaphorase Staining

Diaphorase staining on cryostat sections was performed as described in (Elphick et al., 1997)

Probes

The used probes were the following:

Tbx3 (gift of V.M. Christoffels)

Peripherin (gift of F. Guillemot)

Antibodies

The primary antibodies used in this study were the following:

α-Phox2b, Rabbit, 1:500 (Pattyn et al., 1997)

α-Phox2b, Goat, 1:100, R&D (#AF4940)

α-Tuj1, Mouse, 1:500, BioLegend (#801201)

α-Tbx3, Goat, 1:250, Santa Cruz (#SC-17871)

α-VIP, Rabbit, 1:500, Immunostar (#20077)

α-Calbindin, Rabbit, 1:1000, Swant (#CB-38a)

α-Sub.P, Rat, 1:400, Milipore (#MAB356)

α-Ki67, Rabbit, 1:500, Abcam (ab15580)

α-GFP, Chicken, 1:400, Aves Lab (GFP-1010)

The secondary antibodies were the following:

α-rabbit A488, Jackson Immunoresearch Laboratories (# 711-545-152)

α-rabbit Cy3, Jackson Immunoresearch Laboratories (#711-165-152)

α-goat A647, Jackson Immunoresearch Laboratories (# 705-605-147)

α-mouse 488, Jackson Immunoresearch Laboratories (# 715-545-150)

α-rat Cy3, Jackson Immunoresearch Laboratories (# 712-165-153)

α-chicken 488, Jackson Immunoresearch Laboratories (# 703-545-155)

α-phalloidin 647, Thermofisher (A22287)

For Immunohistochemistry, the secondary antibodies were α-Rabbit, and α-Goat respectively PK-6101 and PK-4005 from Vector Laboratories ; the color development was performed using DAB (3,3'-Diaminobenzidine, Sigma-Aldrich, D4293).

Transgenic Mouse Line

Phox2b::Cre (D'Autreaux et al., 2011): BAC transgenic line expressing Cre under the control of the Phox2b promoter.

Tbx3$^{lox/+}$ (Frank et al., 2013): Lox insertion around the first exon of *Tbx3*.

Pgk::Cre (Lallemand et al., 1998) : Transgenic line expressing Cre in the germ line.

Wnt1::Cre (Danielian et al., 1998): transgenic line expressing Cre under the control of the 3' enhancer of *Wnt1*.

ErbB3Lox/Lox (Sheean et al., 2014): Knock in line comprising floxed human *ErbB3* cDNA in the exon 12 of the mouse *ErbB3* locus.

Retfl-CFP/+ (Uesaka et al., 2008): Knock in line comprising floxed human *Ret9* cDNA and CFP reporter in the first exon of the *Ret* locus.

Phox2b::FLPo (Hirsch et al., 2013): BAC transgenic line expressing FLP under the control of the Phox2b promoter.

Foxg1::Cre (Kawagachi et al., 2016): Knock in of a transgenic construct integrating an internal ribosomal entry site (IRES) fused to Cre Recombinase after the sequence of FoxG1.

RC::FREPE (Bang et al., 2012): Dual-recombinase responsive fluorescent indicator allele has a *frt*-flanked STOP and *loxP*-flanked mCherry::STOP preventing transcription of an eGFP sequence in the ROSA locus.

Gut Motility

Mouse pups at P15 were removed from their mother and fasted 2h before the experiments. Each animal received a 0.1ml of 10% charcoal, 5% gum acacia in PBS directly in the stomach, adapted from Pol et al, 1996. The animals were sacrificed after 2h by cervical elongation.

Imaging

Tissues processed by *in situ* hybridization, immunohistochemistry, and diaphorase staining were photographed on bright field at 10X or 20X objective. Tissues processed by fluorescence were photographed on confocal microscope SP5 at 25X objective.

Statistics

Measurements of the surface occupied by enteric neurons, counting of the number of neurons and periphery of the gut were performed by use of FIJI software.

The similarity of variances between each group of data was tested using the F test. Statistical analysis was performed using unpaired two tailed t test. Results are expressed as %mean/WT ±SEM or number of neurons/mm±SEM.

References

References

Agulnik, S. I., Garvey, N., Hancock, S., Ruvinsky, I., Chapman, D. L., Agulnik, I., Bollag, R., Papaioannou, V., & Silver, L. M. (1996). Evolution of Mouse T-box Genes by Tandem Duplication and Cluster Dispersion. *Genetics*, *144*(1), 249–254.

Alaynick, W. A., Jessell, T. M., & Pfaff, S. L. (2011). SnapShot: Spinal cord development. *Cell*, *146*(1), 178–178.e1.

Aliwaini, S., Lubbad, A. M., Shourfa, A., Hamada, H. A. A., Ayesh, B., Abu Tayem, H. E. M., Abu Mustafa, A., Abu Rouk, F., Redwan, M. M., & Al-Najjar, M. (2019). Overexpression of TBX3 transcription factor as a potential diagnostic marker for breast cancer. *Molecular and Clinical Oncology*, *10*(1), 105–112. https://doi.org/10.3892/mco.2018.1761

Allan, I. J., & Newgreen, D. F. (1980). The origin and differentiation of enteric neurons of the intestine of the fowl embryo. *The American Journal of Anatomy*, *157*(2), 137–154. https://doi.org/10.1002/aja.1001570203

Altman, J., & Das, G. D. (1965). Autoradiographic and histological evidence of postnatal hippocampal neurogenesis in rats. *Journal of Comparative Neurology*, *124*(3), 319–335. https://doi.org/10.1002/cne.901240303

Amiel, J., Dubreuil, V., Ramanantsoa, N., Fortin, G., Gallego, J., Brunet, J.-F., & Goridis, C. (2009). PHOX2B in respiratory control: Lessons from congenital central hypoventilation syndrome and its mouse models. *Respiratory physiology & neurobiology*, *168*(1–2), 125–132.

Amiel, J., Laudier, B., Attié-Bitach, T., Trang, H., de Pontual, L., Gener, B., Trochet, D., Etchevers, H., Ray, P., Simonneau, M., Vekemans, M., Munnich, A., Gaultier, C., & Lyonnet, S. (2003). Polyalanine expansion and frameshift mutations of the paired-like homeobox gene PHOX2B in congenital central hypoventilation syndrome. *Nature genetics*, *33*(4), 459–461.

Anderson, R. B., Stewart, A. L., & Young, H. M. (2006). Phenotypes of neural-crest-derived cells in vagal and sacral pathways. *Cell and Tissue Research*, *323*(1), 11–25. https://doi.org/10.1007/s00441-005-0047-6

Anetsberger, D., Kürten, S., Jabari, S., & Brehmer, A. (2018). Morphological and Immunohistochemical Characterization of Human Intrinsic Gastric Neurons. *Cells Tissues Organs*, *206*(4–5), 183–195. https://doi.org/10.1159/000500566

Aoki, T., Jusuf, A. A., Iitsuka, Y., Isono, K., Tokuhisa, T., & Hatano, M. (2007). Ncx (Enx, Hox11L.1) is required for neuronal cell death in enteric ganglia of mice. *Journal of Pediatric Surgery*, *42*(6), 1081–1088. https://doi.org/10.1016/j.jpedsurg.2007.01.064

Baetge, G., & Gershon, M. D. (1989). Transient catecholaminergic (TC) cells in the vagus nerves and bowel of fetal mice: Relationship to the development of enteric neurons. *Developmental Biology*, *132*(1), 189–211. https://doi.org/10.1016/0012-1606(89)90217-0

Baetge, Greg, & Gershon, M. D. (1986). GABA in the PNS: Demonstration in enteric neurons. *Brain Research Bulletin*, *16*(3), 421–424. https://doi.org/10.1016/0361-9230(86)90066-3

Bamshad, M., Lin, R. C., Law, D. J., Watkins, W. S., Krakowiak, P. A., Moore, M. E., Franceschini, P., Lala, R., Holmes, L. B., Gebuhr, T. C., Bruneau, B. G., Schinzel, A., Seidman, J. G., Seidman, C. E., & Jorde, L. B. (1997). Mutations in human TBX3 alter limb, apocrine and genital development in ulnar-mammary syndrome. *Nature Genetics*, *16*(3), 311–315. https://doi.org/10.1038/ng0797-311

Bang, S. J., Jensen, P., Dymecki, S. M., & Commons, K. G. (2012). Projections and interconnections of genetically defined serotonin neurons in mice. *The European Journal of Neuroscience*, *35*(1), 85–96. https://doi.org/10.1111/j.1460-9568.2011.07936.x

Barlow, A. J., Wallace, A. S., Thapar, N., & Burns, A. J. (2008). Critical numbers of neural crest cells are required in the pathways from the neural tube to the foregut to ensure complete enteric

nervous system formation. *Development*, *135*(9), 1681–1691. https://doi.org/10.1242/dev.017418

Bartel, D. P. (2004). MicroRNAs: Genomics, Biogenesis, Mechanism, and Function. *Cell*, *116*(2), 281–297. https://doi.org/10.1016/S0092-8674(04)00045-5

Baynash, A. G., Hosoda, K., Giaid, A., Richardson, J. A., Emoto, N., Hammer, R. E., & Yanagisawa, M. (1994). Interaction of endothelin-3 with endothelin-B receptor is essential for development of epidermal melanocytes and enteric neurons. *Cell*, *79*(7), 1277–1285. https://doi.org/10.1016/0092-8674(94)90018-3

Bergner, A. J., Stamp, L. A., Gonsalvez, D. G., Allison, M. B., Olson, D. P., Myers, M. G., Anderson, C. R., & Young, H. M. (2014). Birthdating of myenteric neuron subtypes in the small intestine of the mouse. *Journal of Comparative Neurology*, *522*(3), 514–527. https://doi.org/10.1002/cne.23423

Birchmeier, C. (2009). ErbB receptors and the development of the nervous system. *Experimental Cell Research*, *315*(4), 611–618. https://doi.org/10.1016/j.yexcr.2008.10.035

Birchmeier, C., & Nave, K.-A. (2008). Neuregulin-1, a key axonal signal that drives Schwann cell growth and differentiation. *Glia*, *56*(14), 1491–1497. https://doi.org/10.1002/glia.20753

Blaugrund, E., Pham, T. D., Tennyson, V. M., Lo, L., Sommer, L., Anderson, D. J., & Gershon, M. D. (1996). Distinct subpopulations of enteric neuronal progenitors defined by time of development, sympathoadrenal lineage markers and Mash-1-dependence. *Development (Cambridge, England)*, *122*(1), 309–320.

Bober, E., Baum, C., Braun, T., & Arnold, H.-H. (1994). A Novel NK-Related Mouse Homeobox Gene: Expression in Central and Peripheral Nervous Structures during Embryonic Development. *Developmental Biology*, *162*(1), 288–303. https://doi.org/10.1006/dbio.1994.1086

Boesmans, W., Lasrado, R., Berghe, P. V., & Pachnis, V. (2015). Heterogeneity and phenotypic plasticity of glial cells in the mammalian enteric nervous system. *Glia*, *63*(2), 229–241. https://doi.org/10.1002/glia.22746

Bondurand, N., Dufour, S., & Pingault, V. (2018). News from the endothelin-3/EDNRB signaling pathway: Role during enteric nervous system development and involvement in neural crest-associated disorders. *Developmental Biology*, *444*, S156–S169. https://doi.org/10.1016/j.ydbio.2018.08.014

Bondurand, N., & Sham, M. H. (2013). The role of SOX10 during enteric nervous system development. *Developmental Biology*, *382*(1), 330–343. https://doi.org/10.1016/j.ydbio.2013.04.024

Boyer, L. A., Lee, T. I., Cole, M. F., Johnstone, S. E., Levine, S. S., Zucker, J. P., Guenther, M. G., Kumar, R. M., Murray, H. L., Jenner, R. G., Gifford, D. K., Melton, D. A., Jaenisch, R., & Young, R. A. (2005). Core Transcriptional Regulatory Circuitry in Human Embryonic Stem Cells. *Cell*, *122*(6), 947–956. https://doi.org/10.1016/j.cell.2005.08.020

Branchek, T. A., & Gershon, M. D. (1989). Time course of expression of neuropeptide Y, calcitonin gene-related peptide, and NADPH diaphorase activity in neurons of the developing murine bowel and the appearance of 5-hydroxytryptamine in mucosal enterochromaffin cells. *Journal of Comparative Neurology*, *285*(2), 262–273. https://doi.org/10.1002/cne.902850208

Brehmer, A., Schrödl, F., & Neuhuber, W. (1999). Morphological classifications of enteric neurons—100 years after Dogiel. *Anatomy and Embryology*, *200*(2), 125–135. https://doi.org/10.1007/s004290050267

Britsch, S., Goerich, D. E., Riethmacher, D., Peirano, R. I., Rossner, M., Nave, K.-A., Birchmeier, C., & Wegner, M. (2001). The transcription factor Sox10 is a key regulator of peripheral glial development. *Genes & Development*, *15*(1), 66–78. https://doi.org/10.1101/gad.186601

Britsch, S., Li, L., Kirchhoff, S., Theuring, F., Brinkmann, V., Birchmeier, C., & Riethmacher, D. (1998). The ErbB2 and ErbB3 receptors and their ligand, neuregulin-1, are essential for development of the sympathetic nervous system. *Genes & Development*, *12*(12), 1825–1836. https://doi.org/10.1101/gad.12.12.1825

Brookes, S. J. H. (2001). Classes of enteric nerve cells in the guinea-pig small intestine. *The Anatomical Record*, *262*(1), 58–70. https://doi.org/10.1002/1097-0185(20010101)262:1<58::AID-AR1011>3.0.CO;2-V

Brookes, S. J., Steele, P. A., & Costa, M. (1991). Identification and immunohistochemistry of cholinergic and non-cholinergic circular muscle motor neurons in the guinea-pig small intestine. *Neuroscience*, *42*(3), 863–878. https://doi.org/10.1016/0306-4522(91)90050-x

Brummelkamp, T. R., Kortlever, R. M., Lingbeek, M., Trettel, F., MacDonald, M. E., Lohuizen, M. van, & Bernards, R. (2002). TBX-3, the Gene Mutated in Ulnar-Mammary Syndrome, Is a Negative Regulator of p19 ARF and Inhibits Senescence. *Journal of Biological Chemistry*, *277*(8), 6567–6572. https://doi.org/10.1074/jbc.M110492200

Brunet, J.-F., & Pattyn, A. (2002). Phox2 genes—From patterning to connectivity. *Current opinion in genetics & development*, *12*(4), 435–440.

Burdon, T., Smith, A., & Savatier, P. (2002). Signalling, cell cycle and pluripotency in embryonic stem cells. *Trends in Cell Biology*, *12*(9), 432–438. https://doi.org/10.1016/S0962-8924(02)02352-8

Burgucu, D., Guney, K., Sahinturk, D., Ozbudak, I. H., Ozel, D., Ozbilim, G., & Yavuzer, U. (2012). Tbx3 represses PTEN and is over-expressed in head and neck squamous cell carcinoma. *BMC Cancer*, *12*(1), 481. https://doi.org/10.1186/1471-2407-12-481

Burns, A. J., Champeval, D., & Le Douarin, N. M. (2000). Sacral Neural Crest Cells Colonise Aganglionic Hindgut in Vivo but Fail to Compensate for Lack of Enteric Ganglia. *Developmental Biology*, *219*(1), 30–43. https://doi.org/10.1006/dbio.1999.9592

Burns, A. J., & Douarin, N. M. L. (1998). The sacral neural crest contributes neurons and glia to the post-umbilical gut: Spatiotemporal analysis of the development of the enteric nervous system. *Development*, *125*(21), 4335–4347.

Burns, A. J., Pasricha, P. J., & Young, H. M. (2004). Enteric neural crest-derived cells and neural stem cells: Biology and therapeutic potential. *Neurogastroenterology and Motility: The Official Journal of the European Gastrointestinal Motility Society*, *16 Suppl 1*, 3–7. https://doi.org/10.1111/j.1743-3150.2004.00466.x

Carlson, H., Ota, S., Song, Y., Chen, Y., & Hurlin, P. J. (2002). Tbx3 impinges on the p53 pathway to suppress apoptosis, facilitate cell transformation and block myogenic differentiation. *Oncogene*, *21*(24), 3827–3835. https://doi.org/10.1038/sj.onc.1205476

Chapman, D. L., Garvey, N., Hancock, S., Alexiou, M., Agulnik, S. I., Gibson-Brown, J. J., Cebra-Thomas, J., Bollag, R. J., Silver, L. M., & Papaioannou, V. E. (1996). Expression of the T-box family genes, Tbx1–Tbx5, during early mouse development. *Developmental Dynamics*, *206*(4), 379–390. https://doi.org/10.1002/(SICI)1097-0177(199608)206:4<379::AID-AJA4>3.0.CO;2-F

Chen, H. (2017). Ulnar-Mammary Syndrome. In H. Chen, *Atlas of Genetic Diagnosis and Counseling* (bll 2931–2936). Springer New York. https://doi.org/10.1007/978-1-4939-2401-1_240

Coppola, E., Rallu, M., Richard, J., Dufour, S., Riethmacher, D., Guillemot, F., Goridis, C., & Brunet, J.-F. (2010). Epibranchial ganglia orchestrate the development of the cranial neurogenic crest. *Proceedings of the National Academy of Sciences of the United States of America*, *107*(5), 2066–2071.

Costa, M., Furness, J. B., Franco, R., Llewellyn-Smith, I., Murphy, R., & Beardsley, A. M. (1982). Substance P in nerve tissue in the gut. *Ciba Foundation Symposium*, *91*, 129–144. https://doi.org/10.1002/9780470720738.ch8

Costa, M., Furness, J. B., Pullin, C. O., & Bornstein, J. (1985). Substance P enteric neurons mediate non-cholinergic transmission to the circular muscle of the guinea-pig intestine. *Naunyn-Schmiedeberg's Archives of Pharmacology*, *328*(4), 446–453. https://doi.org/10.1007/BF00692914

Danielian, P. S., Muccino, D., Rowitch, D. H., Michael, S. K., & McMahon, A. P. (1998). Modification of gene activity in mouse embryos in utero by a tamoxifen-inducible form of Cre recombinase. *Current Biology: CB*, *8*(24), 1323–1326. https://doi.org/10.1016/s0960-9822(07)00562-3

Dauger, S., Pattyn, A., Lofaso, F., Gaultier, C., Goridis, C., Gallego, J., & Brunet, J.-F. (2003). Phox2b controls the development of peripheral chemoreceptors and afferent visceral pathways. *Development (Cambridge, England)*, *130*(26), 6635–6642. https://doi.org/10.1242/dev.00866

D'Autréaux, F., Coppola, E., Hirsch, M.-R., Birchmeier, C., & Brunet, J.-F. (2011). Homeoprotein Phox2b commands a somatic-to-visceral switch in cranial sensory pathways. *Proceedings of the National Academy of Sciences*, *108*(50), 20018–20023. https://doi.org/10.1073/pnas.1110416108

D'Autréaux, F., Morikawa, Y., Cserjesi, P., & Gershon, M. D. (2007). Hand2 is necessary for terminal differentiation of enteric neurons from crest-derived precursors but not for their migration into the gut or for formation of glia. *Development*, *134*(12), 2237–2249. https://doi.org/10.1242/dev.003814

Davenport, T. G., Jerome-Majewska, L. A., & Papaioannou, V. E. (2003). Mammary gland, limb and yolk sac defects in mice lacking Tbx3, the gene mutated in human ulnar mammary syndrome. *Development*, *130*(10), 2263–2273. https://doi.org/10.1242/dev.00431

Dogiel, A. (1895a). Zur Frage über den feineren Bau des sympa-thischen Nervensystems bei den Säugethieren. *Arch Mikrosk Anat*, *46*, 305–344.

Dogiel, A. (1895b). Zur Frage über die Ganglien der Darm-geflechte bei den Säugetieren. *Anat Anz*, *10*, 517–528.

Dogiel, A. (1896). Zwei Arten sympathischer Nervenzellen. *Anat Anz*, *11*, 679–687.

Dogiel, A. (1899). Ueber den Bau der Ganglien in den Geflechtendes Darmes und der Gallenblase des Menschen und der Säuge-thiere. *Arch Anat Physiol Leip Anat Abt*, 130–158.

Douarin, N. M. L., & Teillet, M.-A. (1973). The migration of neural crest cells to the wall of the digestive tract in avian embryo. *Development*, *30*(1), 31–48.

Douglas, N. C., & Papaioannou, V. E. (2013). The T-box Transcription Factors TBX2 and TBX3 in Mammary Gland Development and Breast Cancer. *Journal of Mammary Gland Biology and Neoplasia*, *18*(2), 143–147. https://doi.org/10.1007/s10911-013-9282-8

Druckenbrod, N. R., & Epstein, M. L. (2005). The pattern of neural crest advance in the cecum and colon. *Developmental Biology*, *287*(1), 125–133. https://doi.org/10.1016/j.ydbio.2005.08.040

Du, H. F., Ou, L. P., Yang, X., Song, X. D., Fan, Y. R., Tan, B., Luo, C. L., & Wu, X. H. (2014). A new PKCα/β/TBX3/E-cadherin pathway is involved in PLCε-regulated invasion and migration in human bladder cancer cells. *Cellular Signalling*, *26*(3), 580–593. https://doi.org/10.1016/j.cellsig.2013.11.015

Dyachuk, V., Furlan, A., Shahidi, M. K., Giovenco, M., Kaukua, N., Konstantinidou, C., Pachnis, V., Memic, F., Marklund, U., Müller, T., Birchmeier, C., Fried, K., Ernfors, P., & Adameyko, I. (2014). Parasympathetic neurons originate from nerve-associated peripheral glial progenitors. *Science*, *345*(6192), 82–87. https://doi.org/10.1126/science.1253281

Elphick, M. R. (1997). Localization of nitric oxide synthase using NADPH diaphorase histochemistry. *Methods in Molecular Biology (Clifton, N.J.)*, *72*, 153–158. https://doi.org/10.1385/0-89603-394-5:153

Enomoto, H., Araki, T., Jackman, A., Heuckeroth, R. O., Snider, W. D., Johnson, E. M., & Milbrandt, J. (1998). GFRα1-Deficient Mice Have Deficits in the Enteric Nervous System and Kidneys. *Neuron*, *21*(2), 317–324. https://doi.org/10.1016/S0896-6273(00)80541-3

Eriksson, K. S., & Mignot, E. (2009). T-box 3 is expressed in the adult mouse hypothalamus and medulla. *Brain Research*, *1302*, 233–239. https://doi.org/10.1016/j.brainres.2009.08.101

Esmailpour, T., & Huang, T. (2012). TBX3 Promotes Human Embryonic Stem Cell Proliferation and Neuroepithelial Differentiation in a Differentiation Stage-dependent Manner. *STEM CELLS*, *30*(10), 2152–2163. https://doi.org/10.1002/stem.1187

Espinosa-Medina, I, Outin, E., Picard, C. A., Chettouh, Z., Dymecki, S., Consalez, G. G., Coppola, E., & Brunet, J. F. (2014). Neurodevelopment. Parasympathetic ganglia derive from Schwann cell precursors. *Science*, *345*(6192), 87–90.

Espinosa-Medina, I., Saha, O., Boismoreau, F., Chettouh, Z., Rossi, F., Richardson, W. D., & Brunet, J.-F. (2016a). The sacral autonomic outflow is sympathetic. *Science*, *354*(6314), 893–897. https://doi.org/10.1126/science.aah5454

Espinosa-Medina, Isabel, Jevans, B., Boismoreau, F., Chettouh, Z., Enomoto, H., Müller, T., Birchmeier, C., Burns, A. J., & Brunet, J.-F. (2017b). Dual origin of enteric neurons in vagal Schwann cell precursors and the sympathetic neural crest. *Proceedings of the National Academy of Sciences*, *114*(45), 11980–11985. https://doi.org/10.1073/pnas.1710308114

Etcheverry, A., Aubry, M., Tayrac, M. de, Vauleon, E., Boniface, R., Guenot, F., Saikali, S., Hamlat, A., Riffaud, L., Menei, P., Quillien, V., & Mosser, J. (2010). DNA methylation in glioblastoma: Impact on gene expression and clinical outcome. *BMC Genomics*, *11*(1), 701. https://doi.org/10.1186/1471-2164-11-701

Fan, W., Huang, X., Chen, C., Gray, J., & Huang, T. (2004). TBX3 and Its Isoform TBX3+2a Are Functionally Distinctive in Inhibition of Senescence and Are Overexpressed in a Subset of Breast Cancer Cell Lines. *Cancer Research*, *64*(15), 5132–5139. https://doi.org/10.1158/0008-5472.CAN-04-0615

Fasano, A., Visanji, N. P., Liu, L. W. C., Lang, A. E., & Pfeiffer, R. F. (2015). Gastrointestinal dysfunction in Parkinson's disease. *The Lancet. Neurology*, *14*(6), 625–639. https://doi.org/10.1016/S1474-4422(15)00007-1

Frank, D. U., Carter, K. L., Thomas, K. R., Burr, R. M., Bakker, M. L., Coetzee, W. A., Tristani-Firouzi, M., Bamshad, M. J., Christoffels, V. M., & Moon, A. M. (2012). Lethal arrhythmias in Tbx3-deficient mice reveal extreme dosage sensitivity of cardiac conduction system function and homeostasis. *Proceedings of the National Academy of Sciences*, *109*(3), E154–E163. https://doi.org/10.1073/pnas.1115165109

Frank, D. U., Emechebe, U., Thomas, K. R., & Moon, A. M. (2013). Mouse Tbx3 Mutants Suggest Novel Molecular Mechanisms for Ulnar-Mammary Syndrome. *PLOS ONE*, *8*(7), e67841. https://doi.org/10.1371/journal.pone.0067841

Furness, I. B., Johnson, P. J., Pompolo, S., & Bornstein, J. C. (1995). Evidence that enteric motility reflexes can be initiated through entirely intrinsic mechanisms in the guinea-pig small intestine. *Neurogastroenterology & Motility*, *7*(2), 89–96. https://doi.org/10.1111/j.1365-2982.1995.tb00213.x

Furness, J. B. (2000). Types of neurons in the enteric nervous system. *Journal of the Autonomic Nervous System*, *81*(1), 87–96. https://doi.org/10.1016/S0165-1838(00)00127-2

Furness, J. B., Costa, M., Emson, P. C., Håkanson, R., Moghimzadeh, E., Sundler, F., Taylor, I. L., & Chance, R. E. (1983). Distribution, pathways and reactions to drug treatment of nerves with neuropeptide Y- and pancreatic polypeptide-like immunoreactivity in the guinea-pig digestive tract. *Cell and Tissue Research*, *234*(1), 71–92. https://doi.org/10.1007/BF00217403

Furness, J. B., Costa, M., & Miller, R. J. (1983). Distribution and projections of nerves with enkephalin-like immunoreactivity in the guinea-pig small intestine. *Neuroscience*, *8*(4), 653–664. https://doi.org/10.1016/0306-4522(83)90001-5

Furness, John B. (2003). Intestinofugal neurons and sympathetic reflexes that bypass the central nervous system. *Journal of Comparative Neurology*, *455*(3), 281–284. https://doi.org/10.1002/cne.10415

Furness, John B., Callaghan, B. P., Rivera, L. R., & Cho, H.-J. (2014). The Enteric Nervous System and Gastrointestinal Innervation: Integrated Local and Central Control. In M. Lyte & J. F. Cryan (Reds), *Microbial Endocrinology: The Microbiota-Gut-Brain Axis in Health and Disease* (bll 39–71). Springer. https://doi.org/10.1007/978-1-4939-0897-4_3

Furness, John B., Nguyen, T. V., Nurgali, K., & Shimizu, Y. (2009). The Enteric Nervous System and Its Extrinsic Connections. In *Textbook of Gastroenterology* (bll 15–39). John Wiley & Sons, Ltd. https://doi.org/10.1002/9781444303254.ch2

Furness, John Barton. (2006). *The enteric nervous system*. Blackwell Pub.

Gabella, G. (1971). Neuron size and number in the myenteric plexus of the newborn and adult rat. *Journal of Anatomy*, *109*(Pt 1), 81–95.

Gabella, G., & Trigg, P. (1984). Size of neurons and glial cells in the enteric ganglia of mice, guinea-pigs, rabbits and sheep. *Journal of Neurocytology*, *13*(1), 49–71. https://doi.org/10.1007/BF01148318

Ganz, J. (2018). Gut feelings: Studying enteric nervous system development, function, and disease in the zebrafish model system. *Developmental Dynamics*, *247*(2), 268–278. https://doi.org/10.1002/dvdy.24597

Gelman, D., Griveau, A., Dehorter, N., Teissier, A., Varela, C., Pla, R., Pierani, A., & Marín, O. (2011). A wide diversity of cortical GABAergic interneurons derives from the embryonic preoptic area. *The Journal of Neuroscience: The Official Journal of the Society for Neuroscience*, *31*(46), 16570–16580. https://doi.org/10.1523/JNEUROSCI.4068-11.2011

Gelman, D. M., Martini, F. J., Nóbrega-Pereira, S., Pierani, A., Kessaris, N., & Marín, O. (2009). The embryonic preoptic area is a novel source of cortical GABAergic interneurons. *The Journal of Neuroscience: The Official Journal of the Society for Neuroscience*, *29*(29), 9380–9389. https://doi.org/10.1523/JNEUROSCI.0604-09.2009

Geuna, S., Borrione, P., & Filogamo, G. (2002). Postnatal histogenesis in the peripheral nervous system. *International Journal of Developmental Neuroscience*, *20*(6), 475–479. https://doi.org/10.1016/S0736-5748(02)00059-X

Gianino, S., Grider, J. R., Cresswell, J., Enomoto, H., & Heuckeroth, R. O. (2003). GDNF availability determines enteric neuron number by controlling precursor proliferation. *Development*, *130*(10), 2187–2198. https://doi.org/10.1242/dev.00433

Grider, J. R. (1994). CGRP as a transmitter in the sensory pathway mediating peristaltic reflex. *American Journal of Physiology-Gastrointestinal and Liver Physiology*, *266*(6), G1139–G1145. https://doi.org/10.1152/ajpgi.1994.266.6.G1139

Grundmann, D., Loris, E., Maas-Omlor, S., Huang, W., Scheller, A., Kirchhoff, F., & Schäfer, K.-H. (2019). Enteric Glia: S100, GFAP, and Beyond. *The Anatomical Record*, *302*(8), 1333–1344. https://doi.org/10.1002/ar.24128

Guillemot, F., Lo, L. C., Johnson, J. E., Auerbach, A., Anderson, D. J., & Joyner, A. L. (1993). Mammalian achaete-scute homolog 1 is required for the early development of olfactory and autonomic neurons. *Cell*, *75*(3), 463–476. https://doi.org/10.1016/0092-8674(93)90381-y

Gulbransen, B. D., & Sharkey, K. A. (2012). Novel functional roles for enteric glia in the gastrointestinal tract. *Nature Reviews Gastroenterology & Hepatology*, *9*(11), 625–632. https://doi.org/10.1038/nrgastro.2012.138

Hadrys, T., Braun, T., Rinkwitz-Brandt, S., Arnold, H. H., & Bober, E. (1998). Nkx5-1 controls semicircular canal formation in the mouse inner ear. *Development (Cambridge, England)*, *125*(1), 33–39.

Han, J., Yuan, P., Yang, H., Zhang, J., Soh, B. S., Li, P., Lim, S. L., Cao, S., Tay, J., Orlov, Y. L., Lufkin, T., Ng, H.-H., Tam, W.-L., & Lim, B. (2010). Tbx3 improves the germ-line competency of induced pluripotent stem cells. *Nature*, *463*(7284), 1096–1100. https://doi.org/10.1038/nature08735

Hao, M. M., Moore, R. E., Roberts, R. R., Nguyen, T., Furness, J. B., Anderson, R. B., & Young, H. M. (2010). The role of neural activity in the migration and differentiation of enteric neuron precursors. *Neurogastroenterology & Motility*, *22*(5), e127–e137. https://doi.org/10.1111/j.1365-2982.2009.01462.x

Häring, M., Zeisel, A., Hochgerner, H., Rinwa, P., Jakobsson, J. E. T., Lönnerberg, P., La Manno, G., Sharma, N., Borgius, L., Kiehn, O., Lagerström, M. C., Linnarsson, S., & Ernfors, P. (2018). Neuronal atlas of the dorsal horn defines its architecture and links sensory input to transcriptional cell types. *Nature Neuroscience*, *21*(6), 869–880. https://doi.org/10.1038/s41593-018-0141-1

Hatano, M., Aoki, T., Dezawa, M., Yusa, S., Iitsuka, Y., Koseki, H., Taniguchi, M., & Tokuhisa, T. (1997). A novel pathogenesis of megacolon in Ncx/Hox11L.1 deficient mice. *The Journal of Clinical Investigation*, *100*(4), 795–801. https://doi.org/10.1172/JCI119593

Hatano, M., Iitsuka, Y., Yamamoto, H., Dezawa, M., Yusa, S., Kohno, Y., & Tokuhisa, T. (1997). Ncx, a Hox11 related gene, is expressed in a variety of tissues derived from neural crest cells. *Anatomy and Embryology*, *195*(5), 419–425. https://doi.org/10.1007/s004290050061

Heanue, T. A., & Pachnis, V. (2006b). Expression profiling the developing mammalian enteric nervous system identifies marker and candidate Hirschsprung disease genes. *Proceedings of the National Academy of Sciences of the United States of America*, *103*(18), 6919–6924.

Hearn, C. J., Murphy, M., & Newgreen, D. (1998). GDNF and ET-3 Differentially Modulate the Numbers of Avian Enteric Neural Crest Cells and Enteric Neuronsin Vitro. *Developmental Biology*, *197*(1), 93–105. https://doi.org/10.1006/dbio.1998.8876

Hirsch, M.-R., d'Autréaux, F., Dymecki, S. M., Brunet, J.-F., & Goridis, C. (2013). A Phox2b::FLPo transgenic mouse line suitable for intersectional genetics. *Genesis (New York, N.Y.: 2000)*, *51*(7), 506–514. https://doi.org/10.1002/dvg.22393

Hoek, K., Rimm, D. L., Williams, K. R., Zhao, H., Ariyan, S., Lin, A., Kluger, H. M., Berger, A. J., Cheng, E., Trombetta, E. S., Wu, T., Niinobe, M., Yoshikawa, K., Hannigan, G. E., & Halaban, R. (2004). Expression Profiling Reveals Novel Pathways in the Transformation of Melanocytes to Melanomas. *Cancer Research*, *64*(15), 5270–5282. https://doi.org/10.1158/0008-5472.CAN-04-0731

Holmberg, A., Schwerte, T., Fritsche, R., Pelster, B., & Holmgren, S. (2003). Ontogeny of intestinal motility in correlation to neuronal development in zebrafish embryos and larvae. *Journal of Fish Biology*, *63*(2), 318–331. https://doi.org/10.1046/j.1095-8649.2003.00149.x

Holst, M. C., Kelly, J. B., & Powley, T. L. (1997). Vagal preganglionic projections to the enteric nervous system characterized with Phaseolus vulgaris-leucoagglutinin. *The Journal of Comparative Neurology*, *381*(1), 81–100. https://doi.org/10.1002/(sici)1096-9861(19970428)381:1<81::aid-cne7>3.0.co;2-g

Holzer, P., Lippe, I. Th., Barthó, L., & Saria, A. (1987). Neuropeptide Y inhibits excitatory enteric neurons supplying the circular muscle of the guinea pig small intestine. *Gastroenterology*, *92*(6), 1944–1950. https://doi.org/10.1016/0016-5085(87)90628-7

Hoogaars, W. M. H., Barnett, P., Moorman, A. F. M., & Christoffels, V. M. (2007). T-box factors determine cardiac design. *Cellular and Molecular Life Sciences*, *64*(6), 646. https://doi.org/10.1007/s00018-007-6518-z

Hoogaars, Willem M. H., Barnett, P., Rodriguez, M., Clout, D. E., Moorman, A. F. M., Goding, C. R., & Christoffels, V. M. (2008). TBX3 and its splice variant TBX3 + exon 2a are functionally similar. *Pigment Cell & Melanoma Research*, *21*(3), 379–387. https://doi.org/10.1111/j.1755-148X.2008.00461.x

Hoogaars, Willem M. H., Engel, A., Brons, J. F., Verkerk, A. O., Lange, F. J. de, Wong, L. Y. E., Bakker, M. L., Clout, D. E., Wakker, V., Barnett, P., Ravesloot, J. H., Moorman, A. F. M., Verheijck, E. E., & Christoffels, V. M. (2007). Tbx3 controls the sinoatrial node gene program and imposes pacemaker function on the atria. *Genes & Development*, *21*(9), 1098–1112. https://doi.org/10.1101/gad.416007

Horn, J. P. (2018). The sacral autonomic outflow is parasympathetic: Langley got it right. *Clin Auton Res*, *28*(2), 181–185.

Hosoda, K., Hammer, R. E., Richardson, J. A., Baynash, A. G., Cheung, J. C., Giaid, A., & Yanagisawa, M. (1994). Targeted and natural (piebald-lethal) mutations of endothelin-B receptor gene produce megacolon associated with spotted coat color in mice. *Cell*, *79*(7), 1267–1276. https://doi.org/10.1016/0092-8674(94)90017-5

Humtsoe, J. O., Koya, E., Pham, E., Aramoto, T., Zuo, J., Ishikawa, T., & Kramer, R. H. (2012). Transcriptional profiling identifies upregulated genes following induction of epithelial-mesenchymal transition in squamous carcinoma cells. *Experimental Cell Research*, *318*(4), 379–390. https://doi.org/10.1016/j.yexcr.2011.11.011

Ivanova, N., Dobrin, R., Lu, R., Kotenko, I., Levorse, J., DeCoste, C., Schafer, X., Lun, Y., & Lemischka, I. R. (2006). Dissecting self-renewal in stem cells with RNA interference. *Nature*, *442*(7102), 533–538. https://doi.org/10.1038/nature04915

Jessen, K. R. (1981). GABA and the enteric nervous system. A neurotransmitter function? *Molecular and Cellular Biochemistry*, *38 Spec No*(Pt 1), 69–76. https://doi.org/10.1007/BF00235689

Jiang, K., Ren, C., & Nair, V. D. (2013). MicroRNA-137 represses Klf4 and Tbx3 during differentiation of mouse embryonic stem cells. *Stem Cell Research*, *11*(3), 1299–1313. https://doi.org/10.1016/j.scr.2013.09.001

Johnson, C. D., Barlow-Anacker, A. J., Pierre, J. F., Touw, K., Erickson, C. S., Furness, J. B., Epstein, M. L., & Gosain, A. (2018). Deletion of choline acetyltransferase in enteric neurons results in postnatal intestinal dysmotility and dysbiosis. *FASEB Journal: Official Publication of the Federation of American Societies for Experimental Biology*, *32*(9), 4744–4752. https://doi.org/10.1096/fj.201701474RR

Joseph, N. M., He, S., Quintana, E., Kim, Y.-G., Núñez, G., & Morrison, S. J. (2011). Enteric glia are multipotent in culture but primarily form glia in the adult rodent gut. *The Journal of Clinical Investigation*, *121*(9), 3398–3411. https://doi.org/10.1172/JCI58186

Kamijo, T., Zindy, F., Roussel, M. F., Quelle, D. E., Downing, J. R., Ashmun, R. A., Grosveld, G., & Sherr, C. J. (1997). Tumor Suppression at the Mouse INK4a Locus Mediated by the Alternative Reading Frame Product p19 ARF. *Cell*, *91*(5), 649–659. https://doi.org/10.1016/S0092-8674(00)80452-3

Kandimalla, R., van Tilborg, A. A. G., Kompier, L. C., Stumpel, D. J. P. M., Stam, R. W., Bangma, C. H., & Zwarthoff, E. C. (2012). Genome-wide Analysis of CpG Island Methylation in Bladder Cancer Identified TBX2, TBX3, GATA2, and ZIC4 as pTa-Specific Prognostic Markers. *European Urology*, *61*(6), 1245–1256. https://doi.org/10.1016/j.eururo.2012.01.011

Kawaguchi, D., Sahara, S., Zembrzycki, A., & O'Leary, D. D. M. (2016). Generation and analysis of an improved Foxg1-IRES-Cre driver mouse line. *Developmental Biology*, *412*(1), 139–147. https://doi.org/10.1016/j.ydbio.2016.02.011

Keast, J. R., Furness, J. B., & Costa, M. (1985). Distribution of certain peptide-containing nerve fibres and endocrine cells in the gastrointestinal mucosa in five mammalian species. *The Journal of Comparative Neurology*, *236*(3), 403–422. https://doi.org/10.1002/cne.902360308

Krantis, A. (2000). GABA in the Mammalian Enteric Nervous System. *News in Physiological Sciences: An International Journal of Physiology Produced Jointly by the International Union of Physiological Sciences and the American Physiological Society*, *15*, 284–290. https://doi.org/10.1152/physiologyonline.2000.15.6.284

Kruger, G. M., Mosher, J. T., Bixby, S., Joseph, N., Iwashita, T., & Morrison, S. J. (2002). Neural crest stem cells persist in the adult gut but undergo changes in self-renewal, neuronal subtype potential, and factor responsiveness. *Neuron*, *35*(4), 657–669. https://doi.org/10.1016/s0896-6273(02)00827-9

Kulaberoglu, Y., Gundogdu, R., & Hergovich, A. (2016). Chapter 15—The Role of p53/p21/p16 in DNA-Damage Signaling and DNA Repair. In I. Kovalchuk & O. Kovalchuk (Reds), *Genome Stability* (bll 243–256). Academic Press. https://doi.org/10.1016/B978-0-12-803309-8.00015-X

Kulis, M., & Esteller, M. (2010). 2—DNA Methylation and Cancer. In Z. Herceg & T. Ushijima (Reds), *Advances in Genetics* (Vol 70, bll 27–56). Academic Press. https://doi.org/10.1016/B978-0-12-380866-0.60002-2

Kulkarni, S., Micci, M.-A., Leser, J., Shin, C., Tang, S.-C., Fu, Y.-Y., Liu, L., Li, Q., Saha, M., Li, C., Enikolopov, G., Becker, L., Rakhilin, N., Anderson, M., Shen, X., Dong, X., Butte, M. J., Song, H., Southard-Smith, E. M., … Pasricha, P. J. (2017a). Adult enteric nervous system in health is maintained by a dynamic balance between neuronal apoptosis and neurogenesis. *Proceedings of the National Academy of Sciences*, *114*(18), E3709–E3718. https://doi.org/10.1073/pnas.1619406114

Kumar P., P., Franklin, S., Emechebe, U., Hu, H., Moore, B., Lehman, C., Yandell, M., & Moon, A. M. (2014). TBX3 Regulates Splicing In Vivo: A Novel Molecular Mechanism for Ulnar-Mammary Syndrome. *PLoS Genetics*, *10*(3), e1004247. https://doi.org/10.1371/journal.pgen.1004247

Kupari, J., Häring, M., Agirre, E., Castelo-Branco, G., & Ernfors, P. (2019). An Atlas of Vagal Sensory Neurons and Their Molecular Specialization. *Cell Reports*, *27*(8), 2508-2523.e4. https://doi.org/10.1016/j.celrep.2019.04.096

Kuwahara, A., Kuwahara, Y., Kato, I., Kawaguchi, K., Harata, D., Asano, S., Inui, T., & Marunaka, Y. (2019). Xenin-25 induces anion secretion by activating noncholinergic secretomotor neurons in the rat ileum. *American Journal of Physiology-Gastrointestinal and Liver Physiology*, *316*(6), G785–G796. https://doi.org/10.1152/ajpgi.00333.2018

Kuwahara, M., Ogaeri, T., Matsuura, R., Kogo, H., Fujimoto, T., & Torihashi, S. (2004). In vitro organogenesis of gut-like structures from mouse embryonic stem cells. *Neurogastroenterology and Motility: The Official Journal of the European Gastrointestinal Motility Society*, *16 Suppl 1*, 14–18. https://doi.org/10.1111/j.1743-3150.2004.00468.x

Lahav, R., Dupin, E., Lecoin, L., Glavieux, C., Champeval, D., Ziller, C., & Douarin, N. M. L. (1998). Endothelin 3 selectively promotes survival and proliferation of neural crest-derived glial and melanocytic precursors in vitro. *Proceedings of the National Academy of Sciences*, *95*(24), 14214–14219. https://doi.org/10.1073/pnas.95.24.14214

Lallemand, Y., Luria, V., Haffner-Krausz, R., & Lonai, P. (1998). Maternally expressed PGK-Cre transgene as a tool for early and uniform activation of the Cre site-specific recombinase. *Transgenic Research*, *7*(2), 105–112. https://doi.org/10.1023/a:1008868325009

Landman, K. A., Simpson, M. J., & Newgreen, D. F. (2007). Mathematical and experimental insights into the development of the enteric nervous system and Hirschsprung's Disease. *Development, Growth & Differentiation*, *49*(4), 277–286. https://doi.org/10.1111/j.1440-169X.2007.00929.x

Lang, D., Chen, F., Milewski, R., Li, J., Lu, M. M., & Epstein, J. A. (2000). Pax3 is required for enteric ganglia formation and functions with Sox10 to modulate expression of c-ret. *The Journal of Clinical Investigation*, *106*(8), 963–971. https://doi.org/10.1172/JCI10828

Langley, J. N., & Magnus, R. (1905). Some observations of the movements of the intestine before and after degenerative section of the mesenteric nerves. *The Journal of Physiology*, *33*(1), 34–51. https://doi.org/10.1113/jphysiol.1905.sp001108

Laranjeira, C., Sandgren, K., Kessaris, N., Richardson, W., Potocnik, A., Berghe, P. V., & Pachnis, V. (2011). Glial cells in the mouse enteric nervous system can undergo neurogenesis in response to injury. *The Journal of Clinical Investigation*, *121*(9), 3412–3424. https://doi.org/10.1172/JCI58200

Larsson, L. I., Fahrenkrug, J., Schaffalitzky De Muckadell, O., Sundler, F., Håkanson, R., & Rehfeld, J. R. (1976). Localization of vasoactive intestinal polypeptide (VIP) to central and peripheral neurons. *Proceedings of the National Academy of Sciences of the United States of America*, *73*(9), 3197–3200. https://doi.org/10.1073/pnas.73.9.3197

Lasrado, R., Boesmans, W., Kleinjung, J., Pin, C., Bell, D., Bhaw, L., McCallum, S., Zong, H., Luo, L., Clevers, H., Vanden Berghe, P., & Pachnis, V. (2017). Lineage-dependent spatial and functional organization of the mammalian enteric nervous system. *Science*, *356*(6339), 722–726. https://doi.org/10.1126/science.aam7511

Le Douarin, N. M., Smith, J., & Le Lievre, C. S. (1981). From the Neural Crest to the Ganglia of the Peripheral Nervous System. *Annual Review of Physiology*, *43*(1), 653–671. https://doi.org/10.1146/annurev.ph.43.030181.003253

Lei, J., & Howard, M. J. (2011). Targeted deletion of Hand2 in enteric neural precursor cells affects its functions in neurogenesis, neurotransmitter specification and gangliogenesis, causing functional aganglionosis. *Development*, *138*(21), 4789–4800. https://doi.org/10.1242/dev.060053

Leibl, M. A., Ota, T., Woodward, M. N., Kenny, S. E., Lloyd, D. A., Vaillant, C. R., & Edgar, D. H. (1999). Expression of endothelin 3 by mesenchymal cells of embryonic mouse caecum. *Gut*, *44*(2), 246–252. https://doi.org/10.1136/gut.44.2.246

Lelievre, V., Favrais, G., Abad, C., Adle-Biassette, H., Lu, Y., Germano, P. M., Cheung-Lau, G., Pisegna, J. R., Gressens, P., Lawson, G., & Waschek, J. A. (2007). Gastrointestinal dysfunction in mice

with a targeted mutation in the gene encoding vasoactive intestinal polypeptide: A model for the study of intestinal ileus and Hirschsprung's disease. *Peptides*, *28*(9), 1688–1699. https://doi.org/10.1016/j.peptides.2007.05.006

Li, Z., Chalazonitis, A., Huang, Y., Mann, J. J., Margolis, K. G., Yang, Q. M., Kim, D. O., Côté, F., Mallet, J., & Gershon, M. D. (2011). Essential Roles of Enteric Neuronal Serotonin in Gastrointestinal Motility and the Development/Survival of Enteric Dopaminergic Neurons. *Journal of Neuroscience*, *31*(24), 8998–9009. https://doi.org/10.1523/JNEUROSCI.6684-10.2011

Lingbeek, M. E., Jacobs, J. J. L., & Lohuizen, M. van. (2002). The T-box Repressors TBX2 and TBX3Specifically Regulate the Tumor Suppressor Genep14 ARF via a Variant T-site in the Initiator. *Journal of Biological Chemistry*, *277*(29), 26120–26127. https://doi.org/10.1074/jbc.M200403200

Liu, J. A.-J., Lai, F. P.-L., Gui, H.-S., Sham, M.-H., Tam, P. K.-H., Garcia-Barcelo, M.-M., Hui, C.-C., & Ngan, E. S.-W. (2015). Identification of GLI Mutations in Patients With Hirschsprung Disease That Disrupt Enteric Nervous System Development in Mice. *Gastroenterology*, *149*(7), 1837-1848.e5. https://doi.org/10.1053/j.gastro.2015.07.060

Liu, M.-T., Kuan, Y.-H., Wang, J., Hen, R., & Gershon, M. D. (2009). 5-HT4 Receptor-Mediated Neuroprotection and Neurogenesis in the Enteric Nervous System of Adult Mice. *Journal of Neuroscience*, *29*(31), 9683–9699. https://doi.org/10.1523/JNEUROSCI.1145-09.2009

Liu, N., Dong, Q.-Z., & Wang, E.-H. (2012). Expression of TBX3 Is Correlated with Tumor Proliferation and Invasion in Non-small Cell Lung Cancer—《Journal of China Medical University》2012 年 04 期. *Journal of China Medical University*, *41*, 360–363.

Lomnytska, M., Dubrovska, A., Hellman, U., Volodko, N., & Souchelnytskyi, S. (2006). Increased expression of cSHMT, Tbx3 and utrophin in plasma of ovarian and breast cancer patients. *International Journal of Cancer*, *118*(2), 412–421. https://doi.org/10.1002/ijc.21332

López, S. H., Avetisyan, M., Wright, C. M., Mesbah, K., Kelly, R. G., Moon, A. M., & Heuckeroth, R. O. (2018). Loss of Tbx3 in murine neural crest reduces enteric glia and causes cleft palate, but does not influence heart development or bowel transit. *Developmental biology*.

Lowe, S. W. (1999). Activation of p53 by oncogenes. *Endocrine-Related Cancer*, *6*(1), 45–48. https://doi.org/10.1677/erc.0.0060045

Lüdtke, T. H., Rudat, C., Wojahn, I., Weiss, A.-C., Kleppa, M.-J., Kurz, J., Farin, H. F., Moon, A., Christoffels, V. M., & Kispert, A. (2016). Tbx2 and Tbx3 Act Downstream of Shh to Maintain Canonical Wnt Signaling during Branching Morphogenesis of the Murine Lung. *Developmental Cell*, *39*(2), 239–253. https://doi.org/10.1016/j.devcel.2016.08.007

Lui, V. C. H., Cheng, W. W. C., Leon, T. Y. Y., Lau, D. K. C., Garcia-Barcelo, M.-M., Garcia-Bareclo, M.-M., Miao, X. P., Kam, M. K. M., So, M. T., Chen, Y., Wall, N. A., Sham, M. H., & Tam, P. K. H. (2008). Perturbation of hoxb5 signaling in vagal neural crests down-regulates ret leading to intestinal hypoganglionosis in mice. *Gastroenterology*, *134*(4), 1104–1115. https://doi.org/10.1053/j.gastro.2008.01.028

Marese, A. C. M., de Freitas, P., & Natali, M. R. M. (2007). Alterations of the number and the profile of myenteric neurons of Wistar rats promoted by age. *Autonomic Neuroscience*, *137*(1), 10–18. https://doi.org/10.1016/j.autneu.2007.05.003

Mashimo, H., He, X. D., Huang, P. L., Fishman, M. C., & Goyal, R. K. (1996). Neuronal constitutive nitric oxide synthase is involved in murine enteric inhibitory neurotransmission. *The Journal of Clinical Investigation*, *98*(1), 8–13. https://doi.org/10.1172/JCI118781

McCallion, A. S., Stames, E., Conlon, R. A., & Chakravarti, A. (2003). Phenotype variation in two-locus mouse models of Hirschsprung disease: Tissue-specific interaction between Ret and Ednrb. *Proceedings of the National Academy of Sciences*, *100*(4), 1826–1831. https://doi.org/10.1073/pnas.0337540100

McKeown, S. J., Chow, C. W., & Young, H. M. (2001). Development of the submucous plexus in the large intestine of the mouse. *Cell and Tissue Research*, *303*(2), 301–305. https://doi.org/10.1007/s004410000303

Memic, F., Knoflach, V., Morarach, K., Sadler, R., Laranjeira, C., Hjerling-Leffler, J., Sundström, E., Pachnis, V., & Marklund, U. (2018). Transcription and Signaling Regulators in Developing Neuronal Subtypes of Mouse and Human Enteric Nervous System. *Gastroenterology*, *154*(3), 624–636. https://doi.org/10.1053/j.gastro.2017.10.005

Memic, F., Knoflach, V., Sadler, R., Tegerstedt, G., Sundström, E., Guillemot, F., Pachnis, V., & Marklund, U. (2016). Ascl1 Is Required for the Development of Specific Neuronal Subtypes in the Enteric Nervous System. *The Journal of Neuroscience*, *36*(15), 4339–4350. https://doi.org/10.1523/JNEUROSCI.0202-16.2016

Mesbah, K., Harrelson, Z., Théveniau-Ruissy, M., Papaioannou, V. E., & Kelly, R. G. (2008). Tbx3 Is Required for Outflow Tract Development. *Circulation Research*, *103*(7), 743–750. https://doi.org/10.1161/CIRCRESAHA.108.172858

Mohan, R. A., Mommersteeg, M. T. M., Domínguez, J. N., Choquet, C., Wakker, V., de Gier-de Vries, C., Boink, G. J. J., Boukens, B. J., Miquerol, L., Verkerk, A. O., & Christoffels, V. M. (2018). Embryonic Tbx3 $^{+}$ cardiomyocytes form the mature cardiac conduction system by progressive fate restriction. *Development*, *145*(17), dev167361. https://doi.org/10.1242/dev.167361

Mongardi Fantaguzzi, C., Thacker, M., Chiocchetti, R., & Furness, J. B. (2009). Identification of neuron types in the submucosal ganglia of the mouse ileum. *Cell and Tissue Research*, *336*(2), 179–189. https://doi.org/10.1007/s00441-009-0773-2

Moore, M. W., Klein, R. D., Fariñas, I., Sauer, H., Armanini, M., Phillips, H., Reichardt, L. F., Ryan, A. M., Carver-Moore, K., & Rosenthal, A. (1996). Renal and neuronal abnormalities in mice lacking GDNF. *Nature*, *382*(6586), 76–79. https://doi.org/10.1038/382076a0

Morarach, K., Mikhailova, A., Knoflach, V., Memic, F., Kumar, R., Li, W., Ernfors, P., & Marklund, U. (2020b). *Diversification of molecularly defined myenteric neuron classes revealed by single cell RNA-sequencing* [Preprint]. Neuroscience. https://doi.org/10.1101/2020.03.02.955757

Mosher, J. T., Yeager, K. J., Kruger, G. M., Joseph, N. M., Hutchin, M. E., Dlugosz, A. A., & Morrison, S. J. (2007). Intrinsic differences among spatially distinct neural crest stem cells in terms of migratory properties, fate determination, and ability to colonize the enteric nervous system. *Developmental Biology*, *303*(1), 1–15. https://doi.org/10.1016/j.ydbio.2006.10.026

Mourad, F. H., Barada, K. A., Abdel-Malak, N., Rached, N. A. B., Khoury, C. I., Saadé, N. E., & Nassar, C. F. (2003). Interplay between Nitric Oxide and Vasoactive Intestinal Polypeptide in Inducing Fluid Secretion in Rat Jejunum. *The Journal of Physiology*, *550*(3), 863–871. https://doi.org/10.1113/jphysiol.2003.043737

Mowla, S., Pinnock, R., Leaner, V. D., Goding, C. R., & Prince, S. (2011). PMA-induced up-regulation of TBX3 is mediated by AP-1 and contributes to breast cancer cell migration. *Biochemical Journal*, *433*(1), 145–153. https://doi.org/10.1042/BJ20100886

Mundell, N. A., Plank, J. L., LeGrone, A. W., Frist, A. Y., Zhu, L., Shin, M. K., Southard-Smith, E. M., & Labosky, P. A. (2012). Enteric nervous system specific deletion of Foxd3 disrupts glial cell differentiation and activates compensatory enteric progenitors. *Developmental Biology*, *363*(2), 373–387. https://doi.org/10.1016/j.ydbio.2012.01.003

Nagy, N., & Goldstein, A. M. (2017). Enteric nervous system development: A crest cell's journey from neural tube to colon. *Seminars in Cell & Developmental Biology*, *66*, 94–106. https://doi.org/10.1016/j.semcdb.2017.01.006

Nakanishi, A., Kitagishi, Y., Ogura, Y., & Matsuda, S. (2014). The tumor suppressor PTEN interacts with p53 in hereditary cancer (Review). *International Journal of Oncology*, *44*(6), 1813–1819. https://doi.org/10.3892/ijo.2014.2377

Nataf, V., Amemiya, A., Yanagisawa, M., & Le Douarin, N. M. (1998). The expression pattern of endothelin 3 in the avian embryo. *Mechanisms of Development*, *73*(2), 217–220. https://doi.org/10.1016/S0925-4773(98)00048-3

Nataf, V., Lecoin, L., Eichmann, A., & Douarin, N. M. L. (1996). Endothelin-B receptor is expressed by neural crest cells in the avian embryo. *Proceedings of the National Academy of Sciences*, *93*(18), 9645–9650. https://doi.org/10.1073/pnas.93.18.9645

Natarajan, D., Marcos-Gutierrez, C., Pachnis, V., & Graaff, E. de. (2002). Requirement of signalling by receptor tyrosine kinase RET for the directed migration of enteric nervous system progenitor cells during mammalian embryogenesis. *Development*, *129*(22), 5151–5160.

Neuhuber, WI, M, A., Jm, P., W, B.-K., L, A., & Gl, F. (1993, September). *Rectospinal neurons: Cell bodies, pathways, immunocytochemistry and ultrastructure*. Neuroscience; Neuroscience. https://doi.org/10.1016/0306-4522(93)90338-g

Neuhuber, Winfried, Mclachlan, E., & Jänig, W. (2017). The Sacral Autonomic Outflow Is Spinal, but Not "Sympathetic". *Anatomical Record (Hoboken, N.J.: 2007)*, *300*(8), 1369–1370. https://doi.org/10.1002/ar.23600

Niquille, M., Limoni, G., Markopoulos, F., Cadilhac, C., Prados, J., Holtmaat, A., & Dayer, A. (2018). Neurogliaform cortical interneurons derive from cells in the preoptic area. *ELife*, *7*, e32017. https://doi.org/10.7554/eLife.32017

Nishiyama, C., Uesaka, T., Manabe, T., Yonekura, Y., Nagasawa, T., Newgreen, D. F., Young, H. M., & Enomoto, H. (2012). Trans-mesenteric neural crest cells are the principal source of the colonic enteric nervous system. *Nature Neuroscience*, *15*(9), 1211. https://doi.org/10.1038/nn.3184

Niwa, H., Ogawa, K., Shimosato, D., & Adachi, K. (2009). A parallel circuit of LIF signalling pathways maintains pluripotency of mouse ES cells. *Nature*, *460*(7251), 118–122. https://doi.org/10.1038/nature08113

Nurgali, K., Stebbing, M. J., & Furness, J. B. (2004). Correlation of electrophysiological and morphological characteristics of enteric neurons in the mouse colon. *Journal of Comparative Neurology*, *468*(1), 112–124. https://doi.org/10.1002/cne.10948

Obata, Y., & Pachnis, V. (2016). The Effect of Microbiota and the Immune System on the Development and Organization of the Enteric Nervous System. *Gastroenterology*, *151*(5), 836–844. https://doi.org/10.1053/j.gastro.2016.07.044

Pachnis, V., Mankoo, B., & Costantini, F. (1993). Expression of the c-ret proto-oncogene during mouse embryogenesis. *Development*, *119*(4), 1005–1017.

Papaioannou, V. E. (2014). The T-box gene family: Emerging roles in development, stem cells and cancer. *Development*, *141*(20), 3819–3833. https://doi.org/10.1242/dev.104471

Pattyn, A, Morin, X., Cremer, H., Goridis, C., & Brunet, J. F. (1999). The homeobox gene Phox2b is essential for the development of autonomic neural crest derivatives. *Nature*, *399*(6734), 366–370.

Pattyn, Alexandre, Guillemot, F., & Brunet, J.-F. (2006). Delays in neuronal differentiation in Mash1/Ascl1 mutants. *Developmental Biology*, *295*(1), 67–75. https://doi.org/10.1016/j.ydbio.2006.03.008

Pattyn, Alexandre, Simplicio, N., van Doorninck, J. H., Goridis, C., Guillemot, F., & Brunet, J.-F. (2004). Ascl1/Mash1 is required for the development of central serotonergic neurons. *Nature Neuroscience*, *7*(6), 589–595. https://doi.org/10.1038/nn1247

Peres, J., Davis, E., Mowla, S., Bennett, D. C., Li, J. A., Wansleben, S., & Prince, S. (2010). The Highly Homologous T-Box Transcription Factors, TBX2 and TBX3, Have Distinct Roles in the Oncogenic Process. *Genes & Cancer*, *1*(3), 272–282. https://doi.org/10.1177/1947601910365160

Peres, J., & Prince, S. (2013). The T-box transcription factor, TBX3, is sufficient to promote melanoma formation and invasion. *Molecular Cancer*, *12*(1), 117. https://doi.org/10.1186/1476-4598-12-117

Perlin, J. R., Lush, M. E., Stephens, W. Z., Piotrowski, T., & Talbot, W. S. (2011). Neuronal Neuregulin 1 type III directs Schwann cell migration. *Development*, *138*(21), 4639–4648. https://doi.org/10.1242/dev.068072

Pham, T. D., Gershon, M. D., & Rothman, T. P. (1991). Time of origin of neurons in the murine enteric nervous system: Sequence in relation to phenotype. *The Journal of Comparative Neurology*, *314*(4), 789–798. https://doi.org/10.1002/cne.903140411

Plageman, T. F., & Yutzey, K. E. (2005). T-box genes and heart development: Putting the “T” in heart. *Developmental Dynamics*, *232*(1), 11–20. https://doi.org/10.1002/dvdy.20201

Pontecorvi, M., Goding, C. R., Richardson, W. D., & Kessaris, N. (2008). Expression of Tbx2 and Tbx3 in the developing hypothalamic–pituitary axis. *Gene Expression Patterns*, *8*(6), 411–417. https://doi.org/10.1016/j.gep.2008.04.006

Qiu, M., Bulfone, A., Martinez, S., Meneses, J. J., Shimamura, K., Pedersen, R. A., & Rubenstein, J. L. (1995). Null mutation of Dlx-2 results in abnormal morphogenesis of proximal first and second branchial arch derivatives and abnormal differentiation in the forebrain. *Genes & Development*, *9*(20), 2523–2538. https://doi.org/10.1101/gad.9.20.2523

Qu, Z.-D., Thacker, M., Castelucci, P., Bagyánszki, M., Epstein, M. L., & Furness, J. B. (2008). Immunohistochemical analysis of neuron types in the mouse small intestine. *Cell and Tissue Research*, *334*(2), 147–161. https://doi.org/10.1007/s00441-008-0684-7

Quarta, C., Fisette, A., Xu, Y., Colldén, G., Legutko, B., Tseng, Y.-T., Reim, A., Wierer, M., De Rosa, M. C., Klaus, V., Rausch, R., Thaker, V. V., Graf, E., Strom, T. M., Poher, A.-L., Gruber, T., Le Thuc, O., Cebrian-Serrano, A., Kabra, D., … Tschöp, M. H. (2019). Functional identity of hypothalamic melanocortin neurons depends on Tbx3. *Nature Metabolism*, *1*(2), 222–235. https://doi.org/10.1038/s42255-018-0028-1

Ramirez, R. N., & Kozin, S. H. (2014). Ulnar Mammary Syndrome. *The Journal of Hand Surgery*, *39*(4), 803–805. https://doi.org/10.1016/j.jhsa.2014.01.024

Rancourt, D. E., Tsuzuki, T., & Capecchi, M. R. (1995). Genetic interaction between hoxb-5 and hoxb-6 is revealed by nonallelic noncomplementation. *Genes & Development*, *9*(1), 108–122. https://doi.org/10.1101/gad.9.1.108

Rao, M., & Gershon, M. D. (2018). Enteric nervous system development: What could possibly go wrong? *Nat Rev Neurosci*, *19*(9), 552–565.

Renard, C.-A., Labalette, C., Armengol, C., Cougot, D., Wei, Y., Cairo, S., Pineau, P., Neuveut, C., Reyniès, A. de, Dejean, A., Perret, C., & Buendia, M.-A. (2007). Tbx3 Is a Downstream Target of the Wnt/β-Catenin Pathway and a Critical Mediator of β-Catenin Survival Functions in Liver Cancer. *Cancer Research*, *67*(3), 901–910. https://doi.org/10.1158/0008-5472.CAN-06-2344

Rinkwitz-Brandt, S., Arnold, H. H., & Bober, E. (1996). Regionalized expression of Nkx5-1, Nkx5-2, Pax2 and sek genes during mouse inner ear development. *Hearing Research*, *99*(1–2), 129–138. https://doi.org/10.1016/s0378-5955(96)00093-7

Robertson, K., & Mason, I. (1997). The GDNF-RET signalling partnership. *Trends in Genetics: TIG*, *13*(1), 1–3. https://doi.org/10.1016/s0168-9525(96)30113-3

Rodriguez, M., Aladowicz, E., Lanfrancone, L., & Goding, C. R. (2008). Tbx3 Represses E-Cadherin Expression and Enhances Melanoma Invasiveness. *Cancer Research*, *68*(19), 7872–7881. https://doi.org/10.1158/0008-5472.CAN-08-0301

Rothman, T. P., Nilaver, G., & Gershon, M. D. (1984). Colonization of the developing murine enteric nervous system and subsequent phenotypic expression by the precursors of peptidergic neurons. *Journal of Comparative Neurology*, *225*(1), 13–23. https://doi.org/10.1002/cne.902250103

Rowley, M., Grothey, E., & Couch, F. J. (2004). The Role of Tbx2 and Tbx3 in Mammary Development and Tumorigenesis. *Journal of Mammary Gland Biology and Neoplasia*, *9*(2), 109–118. https://doi.org/10.1023/B:JOMG.0000037156.64331.3f

Sanders, K. M., & Ward, S. M. (1992). Nitric oxide as a mediator of nonadrenergic noncholinergic neurotransmission. *American Journal of Physiology-Gastrointestinal and Liver Physiology*, *262*(3), G379–G392. https://doi.org/10.1152/ajpgi.1992.262.3.G379

Sanders, Kenton M. (2016). Enteric Inhibitory Neurotransmission, Starting Down Under. In S. Brierley & M. Costa (Reds), *The Enteric Nervous System: 30 Years Later* (bll 21–29). Springer International Publishing. https://doi.org/10.1007/978-3-319-27592-5_3

Sang, Q., Ciampoli, D., Greferath, U., Sommer, L., & Young, H. M. (1999). Innervation of the esophagus in mice that lack MASH1. *Journal of Comparative Neurology*, *408*(1), 1–10. https://doi.org/10.1002/(SICI)1096-9861(19990524)408:1<1::AID-CNE1>3.0.CO;2-4

Sang, Q., WILLIAMSON, S., & YOUNG, H. M. (1997). Projections of chemically identified myenteric neurons of the small and large intestine of the mouse. *Journal of Anatomy*, *190*(Pt 2), 209–222. https://doi.org/10.1046/j.1469-7580.1997.19020209.x

Sang, Q., & Young, H. M. (1996). Chemical coding of neurons in the myenteric plexus and external muscle of the small and large intestine of the mouse. *Cell and Tissue Research*, *284*(1), 39–53. https://doi.org/10.1007/s004410050565

Sebé-Pedrós, A., & Ruiz-Trillo, I. (2017). Evolution and Classification of the T-Box Transcription Factor Family. In M. Frasch (Red), *Current Topics in Developmental Biology* (Vol 122, bll 1–26). Academic Press. https://doi.org/10.1016/bs.ctdb.2016.06.004

Serbedzija, G. N., Burgan, S., Fraser, S. E., & Bronner-Fraser, M. (1991). Vital dye labelling demonstrates a sacral neural crest contribution to the enteric nervous system of chick and mouse embryos. *Development*, *111*(4), 857–866.

Sheean, M. E., McShane, E., Cheret, C., Walcher, J., Müller, T., Wulf-Goldenberg, A., Hoelper, S., Garratt, A. N., Krüger, M., Rajewsky, K., Meijer, D., Birchmeier, W., Lewin, G. R., Selbach, M., & Birchmeier, C. (2014). Activation of MAPK overrides the termination of myelin growth and replaces Nrg1/ErbB3 signals during Schwann cell development and myelination. *Genes & Development*, *28*(3), 290–303. https://doi.org/10.1101/gad.230045.113

Sheeba, C. J., & Logan, M. P. O. (2017). Chapter Twelve—The Roles of T-Box Genes in Vertebrate Limb Development. In M. Frasch (Red), *Current Topics in Developmental Biology* (Vol 122, bll 355–381). Academic Press. https://doi.org/10.1016/bs.ctdb.2016.08.009

Shirasawa, S., Arata, A., Onimaru, H., Roth, K. A., Brown, G. A., Horning, S., Arata, S., Okumura, K., Sasazuki, T., & Korsmeyer, S. J. (2000). Rnx deficiency results in congenital central hypoventilation. *Nature Genetics*, *24*(3), 287–290. https://doi.org/10.1038/73516

Stadler, H. S., Murray, J. C., Leysens, N. J., Goodfellow, P. J., & Solursh, M. (1995). Phylogenetic conservation and physical mapping of members of the H6 homeobox gene family. *Mammalian Genome: Official Journal of the International Mammalian Genome Society*, *6*(6), 383–388. https://doi.org/10.1007/BF00355637

Stadler, H. S., Padanilam, B. J., Buetow, K., Murray, J. C., & Solursh, M. (1992). Identification and genetic mapping of a homeobox gene to the 4p16.1 region of human chromosome 4. *Proceedings of the National Academy of Sciences of the United States of America*, *89*(23), 11579–11583. https://doi.org/10.1073/pnas.89.23.11579

Takahashi, K., & Yamanaka, S. (2006). Induction of Pluripotent Stem Cells from Mouse Embryonic and Adult Fibroblast Cultures by Defined Factors. *Cell*, *126*(4), 663–676. https://doi.org/10.1016/j.cell.2006.07.024

Takaki, M., Nakayama, S., Misawa, H., Nakagawa, T., & Kuniyasu, H. (2006). In vitro formation of enteric neural network structure in a gut-like organ differentiated from mouse embryonic stem cells. *Stem Cells (Dayton, Ohio)*, *24*(6), 1414–1422. https://doi.org/10.1634/stemcells.2005-0394

Talbot, J., Hahn, P., Kroehling, L., Nguyen, H., Li, D., & Littman, D. R. (2020). Feeding-dependent VIP neuron–ILC3 circuit regulates the intestinal barrier. *Nature*, *579*(7800), 575–580. https://doi.org/10.1038/s41586-020-2039-9

Tang, C. S., Gui, H., Kapoor, A., Kim, J.-H., Luzón-Toro, B., Pelet, A., Burzynski, G., Lantieri, F., So, M., Berrios, C., Shin, H. D., Fernández, R. M., Le, T.-L., Verheij, J. B. G. M., Matera, I., Cherny, S. S., Nandakumar, P., Cheong, H. S., Antiñolo, G., … Garcia-Barceló, M.-M. (2016). Trans-ethnic meta-analysis of genome-wide association studies for Hirschsprung disease. *Human Molecular Genetics*, *25*(23), 5265–5275. https://doi.org/10.1093/hmg/ddw333

Theveneau, E., & Mayor, R. (2011). Can mesenchymal cells undergo collective cell migration? The case of the neural crest. *Cell Adhesion & Migration*, *5*(6), 490–498. https://doi.org/10.4161/cam.5.6.18623

Thrasivoulou, C., Soubeyre, V., Ridha, H., Giuliani, D., Giaroni, C., Michael, G. J., Saffrey, M. J., & Cowen, T. (2006). Reactive oxygen species, dietary restriction and neurotrophic factors in age-related loss of myenteric neurons. *Aging Cell*, *5*(3), 247–257. https://doi.org/10.1111/j.1474-9726.2006.00214.x

Timmermans, J. P., Adriaensen, D., Cornelissen, W., & Scheuermann, D. W. (1997). Structural organization and neuropeptide distribution in the mammalian enteric nervous system, with special attention to those components involved in mucosal reflexes. *Comparative Biochemistry and Physiology. Part A, Physiology*, *118*(2), 331–340. https://doi.org/10.1016/s0300-9629(96)00314-3

Trowe, M.-O., Zhao, L., Weiss, A.-C., Christoffels, V., Epstein, D. J., & Kispert, A. (2013). Inhibition of Sox2-dependent activation of Shh in the ventral diencephalon by Tbx3 is required for formation of the neurohypophysis. *Development*, *140*(11), 2299–2309. https://doi.org/10.1242/dev.094524

Trupp, M., Rydén, M., Jörnvall, H., Funakoshi, H., Timmusk, T., Arenas, E., & Ibáñez, C. F. (1995). Peripheral expression and biological activities of GDNF, a new neurotrophic factor for avian and mammalian peripheral neurons. *Journal of Cell Biology*, *130*(1), 137–148. https://doi.org/10.1083/jcb.130.1.137

Tümpel, S., Sanz-Ezquerro, J. J., Isaac, A., Eblaghie, M. C., Dobson, J., & Tickle, C. (2002). Regulation of Tbx3 Expression by Anteroposterior Signalling in Vertebrate Limb Development. *Developmental Biology*, *250*(2), 251–262. https://doi.org/10.1006/dbio.2002.0762

Uesaka, T., Nagashimada, M., & Enomoto, H. (2015). Neuronal Differentiation in Schwann Cell Lineage Underlies Postnatal Neurogenesis in the Enteric Nervous System. *Journal of Neuroscience*, *35*(27), 9879–9888. https://doi.org/10.1523/JNEUROSCI.1239-15.2015

Uesaka, T., Nagashimada, M., Yonemura, S., & Enomoto, H. (2008). Diminished Ret expression compromises neuronal survival in the colon and causes intestinal aganglionosis in mice. *The Journal of Clinical Investigation*, *118*(5), 1890–1898. https://doi.org/10.1172/JCI34425

Viader, A., Wright-Jin, E. C., Vohra, B. P. S., Heuckeroth, R. O., & Milbrandt, J. (2011). Differential Regional and Subtype-Specific Vulnerability of Enteric Neurons to Mitochondrial Dysfunction. *PLoS ONE*, *6*(11), e27727. https://doi.org/10.1371/journal.pone.0027727

Waghray, A., Saiz, N., Jayaprakash, A. D., Freire, A. G., Papatsenko, D., Pereira, C.-F., Lee, D.-F., Brosh, R., Chang, B., Darr, H., Gingold, J., Kelley, K., Schaniel, C., Hadjantonakis, A.-K., & Lemischka, I. R. (2015). Tbx3 Controls Dppa3 Levels and Exit from Pluripotency toward Mesoderm. *Stem Cell Reports*, *5*(1), 97–110. https://doi.org/10.1016/j.stemcr.2015.05.009

Wallace, A. S., Barlow, A. J., Navaratne, L., Delalande, J. -m, Tauszig-delamasure, S., Corset, V., Thapar, N., & Burns, A. J. (2009). Inhibition of cell death results in hyperganglionosis: Implications for enteric nervous system development. *Neurogastroenterology & Motility*, *21*(7), 768-e49. https://doi.org/10.1111/j.1365-2982.2009.01309.x

Wang, H., Hughes, I., Planer, W., Parsadanian, A., Grider, J. R., Vohra, B. P. S., Keller-Peck, C., & Heuckeroth, R. O. (2010). The Timing and Location of Glial Cell Line-Derived Neurotrophic Factor Expression Determine Enteric Nervous System Structure and Function. *Journal of Neuroscience*, *30*(4), 1523–1538. https://doi.org/10.1523/JNEUROSCI.3861-09.2010

Wang, W., & Lufkin, T. (1997). Assignment of the murine Hmx2 and Hmx3 homeobox genes to the distal region of mouse chromosome 7. *Chromosome Research: An International Journal on the Molecular, Supramolecular and Evolutionary Aspects of Chromosome Biology*, *5*(7), 501–502. https://doi.org/10.1023/a:1018429316424

Wang, W., Water, T. V. D., & Lufkin, T. (1998). Inner ear and maternal reproductive defects in mice lacking the Hmx3 homeobox gene. *Development*, *125*(4), 621–634.

Wang, Weidong, Chan, E. K., Baron, S., Water, T. V. D., & Lufkin, T. (2001). Hmx2 homeobox gene control of murine vestibular morphogenesis. *Development*, *128*(24), 5017–5029.

Wang, Weidong, Grimmer, J. F., Van De Water, T. R., & Lufkin, T. (2004). Hmx2 and Hmx3 Homeobox Genes Direct Development of the Murine Inner Ear and Hypothalamus and Can Be

Functionally Replaced by Drosophila Hmx. *Developmental Cell*, *7*(3), 439–453. https://doi.org/10.1016/j.devcel.2004.06.016

Wang, Weidong, Lo, P., Frasch, M., & Lufkin, T. (2000). Hmx: An evolutionary conserved homeobox gene family expressed in the developing nervous system in mice and Drosophila. *Mechanisms of Development*, *99*(1–2), 123–137. https://doi.org/10.1016/S0925-4773(00)00488-3

Wang, X., Chan, A. K. K., Sham, M. H., Burns, A. J., & Chan, W. Y. (2011). Analysis of the Sacral Neural Crest Cell Contribution to the Hindgut Enteric Nervous System in the Mouse Embryo. *Gastroenterology*, *141*(3), 992-1002.e6. https://doi.org/10.1053/j.gastro.2011.06.002

Wansleben, S., Peres, J., Hare, S., Goding, C. R., & Prince, S. (2014). T-box transcription factors in cancer biology. *Biochimica et Biophysica Acta (BBA) - Reviews on Cancer*, *1846*(2), 380–391. https://doi.org/10.1016/j.bbcan.2014.08.004

Willmer, T., Hare, S., Peres, J., & Prince, S. (2016). The T-box transcription factor TBX3 drives proliferation by direct repression of the p21 WAF1 cyclin-dependent kinase inhibitor. *Cell Division*, *11*(1), 1–13. https://doi.org/10.1186/s13008-016-0019-0

Wu, J. J., Chen, J. X., Rothman, T. P., & Gershon, M. D. (1999). Inhibition of in vitro enteric neuronal development by endothelin-3: Mediation by endothelin B receptors. *Development*, *126*(6), 1161–1173.

Yamashita, S., Tsujino, Y., Moriguchi, K., Tatematsu, M., & Ushijima, T. (2006). Chemical genomic screening for methylation-silenced genes in gastric cancer cell lines using 5-aza-2'-deoxycytidine treatment and oligonucleotide microarray. *Cancer Science*, *97*(1), 64–71. https://doi.org/10.1111/j.1349-7006.2006.00136.x

Yntema, C. L., & Hammond, W. S. (1954). The origin of intrinsic ganglia of trunk viscera from vagal neural crest in the chick embryo. *Journal of Comparative Neurology*, *101*(2), 515–541. https://doi.org/10.1002/cne.901010212

Young, H. M., Bergner, A. J., Anderson, R. B., Enomoto, H., Milbrandt, J., Newgreen, D. F., & Whitington, P. M. (2004). Dynamics of neural crest-derived cell migration in the embryonic mouse gut. *Developmental Biology*, *270*(2), 455–473. https://doi.org/10.1016/j.ydbio.2004.03.015

Young, H. M., Hearn, C. J., Farlie, P. G., Canty, A. J., Thomas, P. Q., & Newgreen, D. F. (2001). GDNF Is a Chemoattractant for Enteric Neural Cells. *Developmental Biology*, *229*(2), 503–516. https://doi.org/10.1006/dbio.2000.0100

Young, H. M., Turner, K. N., & Bergner, A. J. (2005). The location and phenotype of proliferating neural-crest-derived cells in the developing mouse gut. *Cell and Tissue Research*, *320*(1), 1–9. https://doi.org/10.1007/s00441-004-1057-5

Zechner, D., Fujita, Y., Hülsken, J., Müller, T., Walther, I., Taketo, M. M., Crenshaw, E. B., Birchmeier, W., & Birchmeier, C. (2003). Beta-Catenin signals regulate cell growth and the balance between progenitor cell expansion and differentiation in the nervous system. *Developmental Biology*, *258*(2), 406–418. https://doi.org/10.1016/s0012-1606(03)00123-4

Zeisel, A., Hochgerner, H., Lönnerberg, P., Johnsson, A., Memic, F., van der Zwan, J., Häring, M., Braun, E., Borm, L. E., La Manno, G., Codeluppi, S., Furlan, A., Lee, K., Skene, N., Harris, K. D., Hjerling-Leffler, J., Arenas, E., Ernfors, P., Marklund, U., & Linnarsson, S. (2018). Molecular Architecture of the Mouse Nervous System. *Cell*, *174*(4), 999-1014.e22. https://doi.org/10.1016/j.cell.2018.06.021

Zhao, D., Wu, Y., & Chen, K. (2014). Tbx3 isoforms are involved in pluripotency maintaining through distinct regulation of Nanog transcriptional activity. *Biochemical and Biophysical Research Communications*, *444*(3), 411–414. https://doi.org/10.1016/j.bbrc.2014.01.093

Zirzow, S., Lüdtke, T. H.-W., Brons, J. F., Petry, M., Christoffels, V. M., & Kispert, A. (2009). Expression and requirement of T-box transcription factors Tbx2 and Tbx3 during secondary palate development in the mouse. *Developmental Biology*, *336*(2), 145–155. https://doi.org/10.1016/j.ydbio.2009.09.020

RÉSUMÉ

Le système nerveux entérique qui occupe la paroi du tube digestif et contient autant de neurones que la moelle épinière, contrôle les mouvements de l'intestin et la sécrétion d'hormone permettant la digestion. Son développement est un processus lent et complexe commençant vers le milieu de la gestation et se terminant durant les premières semaines de vie. Il est contrôlé par de nombreux paramètres dont des signaux des guidages de la migration des neurones, mais peu d'éléments sont connus quant à la génétique du développement des nombreux types de neurones qui composent ce système. Durant ma thèse j'ai montré que le facteur de transcription *Tbx3* est essentiel au bon développement du système nerveux entérique puisque son absence provoque la mort des animaux avec une perte d'environ la moitié des neurones, cependant l'identification d'un sous-type particulier manquant est difficile en l'état actuel des connaissances. J'ai aussi montré que l'inactivation de facteurs de transcription *Hmx2* et *Hmx3*, malgré leur expression pendant les phases de différenciation, n'engendre pas de perte neuronal massive dans les systèmes entérique ni parasympathique.

MOTS CLÉS

Système nerveux entérique – Développement – Ontogénie – Tbx – Souris

ABSTRACT

The enteric nervous system which is present in the wall of the digestive tract, and contains as many neurons as the spinal cord, controls the gut mouvement and the secretion of hormones allowing the digestion. Its development is a slow and complex process starting at mi-gestation and ending during the first week after birth. It is controlled by many parameters among them guidance signals for the neuronal migration but few is known about the genetics of the development of the multiple neuronal types present in it. During my thesis, I showed that the transcription factor Tbx3 is essential for the well development of the enteric nervous system because its absence leads to the death of the animals with a loss of half of the neurons, however the identification of a precise missing subtype is difficult with nowadays knowledge. I also showed that the inactivation of the transcription factors Hmx2 and Hmx3, despite their expression during the differentiation phases, do not lead to a massive loss of neurons in the enteric nor parasympathetic systems.

KEYWORDS

Enteric nervous system – Development, - Ontogeny – Tbx – Mice